

NATURAL KILLER CELLS AS IMMUNOTHERAPY TO TARGET RAPIDLY  
EVOLVING NON-SMALL CELL LUNG CARCINOMA

by

Sarah Schwartz

Submitted in partial fulfillment of the requirements  
for the degree of Master of Science

at

Dalhousie University

Halifax, Nova Scotia

June, 2021

©Copyright by Sarah Schwartz, 2021

## **DEDICATION PAGE**

This thesis is dedicated to my best friend, Cassidy Bradley. Your kindness, support, and encouragement made this possible.

## TABLE OF CONTENTS

<b>LIST OF TABLES</b> .....	vii
<b>LIST OF FIGURES</b> .....	viii
<b>ABSTRACT</b> .....	xi
<b>LIST OF ABBREVIATIONS AND SYMBOLS USED</b> .....	xii
<b>ACKNOWLEDGEMENTS</b> .....	xiv
<b>CHAPTER 1: INTRODUCTION</b> .....	1
<b>1.1 Non-small cell lung carcinoma</b> .....	1
<i>1.1.1 NSCLC standard of care treatments</i> .....	2
<i>1.1.2 NSCLC upcoming promising treatments</i> .....	4
<b>1.2 Natural killer cells</b> .....	5
<i>1.2.1 NK cell activation</i> .....	8
<i>1.2.2 NK cell receptors</i> .....	11
<i>1.2.3 NK cell education</i> .....	15
<i>1.2.4 NK cell role in cancer</i> .....	15
<b>1.3 Lung cancer immunotherapy</b> .....	17
<i>1.3.1 Immune-checkpoint blockade</i> .....	17
<i>1.3.2 NK cell role in ICB</i> .....	19
<i>1.3.3 Cellular therapies</i> .....	22
<b>1.4 Tumor evolution</b> .....	22
<b>1.5 Rationale and hypothesis</b> .....	24
<i>1.5.1 Rationale</i> .....	24
<i>1.5.2 Hypothesis</i> .....	24
<i>1.5.3 Objectives</i> .....	25
<b>CHAPTER 2: MATERIALS AND METHODS</b> .....	26
<b>2.1 Cell isolations and culturing</b> .....	26
<i>2.1.1 Peripheral blood mononuclear cells (PBMC)</i> .....	26
<i>2.1.2 Natural killer cells</i> .....	26

2.1.3 Tumor cell lines .....	27
<b>2.2 Monitoring tumor evolution by phenotyping following stimulations.....</b>	<b>27</b>
2.2.1 Stimulation of A549 Cells with IFN- $\gamma$ .....	27
2.2.2 Stimulation of A549 cells with PBMCs.....	27
2.2.3 Stimulation of A549 cells with NK cell effectors .....	28
2.2.4 Stimulation of A549 cells with chemotherapeutic agents .....	28
2.2.5 Treatment of A549 cells with irradiation .....	29
2.3.1 PBMC co-culture post-HLA ligand blockade.....	31
2.3.2 PBMC co-culture post-anti-PD-1/PD-L1 blockade .....	31
2.3.3 PBMC co-culture post-chemotherapy treatment .....	33
2.3.4 PBMC co-culture post-irradiation .....	33
2.3.5 PBMC co-culture post-chemotherapy treatment with inhibitory ligand blockade.....	33
2.3.6 PBMC co-culture post-irradiation with inhibitory ligand blockade .....	33
2.4.1 Flow cytometry staining protocol.....	35
2.4.2 Flow cytometry staining panels .....	35
2.4.3 Flow cytometry analysis .....	37
<b>CHAPTER 3: Results .....</b>	<b>40</b>
<b>3.1 Monitoring tumor evolution by phenotyping following stimulation .....</b>	<b>40</b>
3.1.1 Exposure to IFN- $\gamma$ induces rapid evolution of death receptors and activating and inhibitory ligands on A549 cells.....	40
3.1.2 PBMC pressure induces rapid evolution of death receptors and activating and inhibitory ligands on A549 cells.....	43
3.1.3 NK cell pressure induces rapid evolution of MIC-A/B and HLA-G on A549 cells.....	48
3.1.4 Palbociclib and trametinib chemotherapy induces death receptors and upregulation of activating and inhibitory ligands in dose- and time-dependent manners .....	52
3.1.5 Irradiation treatment induces death receptors and upregulation of activating and inhibitory ligands in a dose-dependent manner .....	58

<b>3.2 NK cell response is rescued with inhibitory ligand blockade.....</b>	<b>65</b>
3.2.1 <i>HLA ligands' blockade on A549 cells induces greater response of cognate receptor-positive NK cells .....</i>	<i>65</i>
3.2.2 <i>Blocking the PD-1/PD-L1 axis induces greater response of PD-1<sup>+</sup> NK cells..</i>	<i>67</i>
<b>3.3 NK cell response to tumors post-treatment .....</b>	<b>69</b>
3.3.1 <i>The subset of NK cells responding to a tumor can be predicted by the tumor cell phenotype post-chemotherapy .....</i>	<i>69</i>
3.3.2 <i>The subset of NK cells responding to a tumor can be predicted by the tumor cell phenotype after irradiation treatment.....</i>	<i>87</i>
<b>3.4 Impact of inhibitory ligand blockade on the NK cell response to tumors post-treatment.....</b>	<b>93</b>
3.4.1 <i>Inhibitory ligand blockade rescues the inhibitory receptor-positive NK cells against chemotherapy-treated A549 cells .....</i>	<i>93</i>
3.4.2 <i>Inhibitory ligand blockade rescues the inhibitory receptor-positive NK cells against irradiated A549 cells .....</i>	<i>97</i>
<b>CHAPTER 4: DISCUSSION .....</b>	<b>102</b>
<b>4.1 Phenotypic evolution of NSCLC death receptors and inhibitory and activating ligands within the TME .....</b>	<b>104</b>
4.1.1 <i>HLA class I regulation on tumor cells.....</i>	<i>104</i>
4.1.2 <i>Impact of IFN-<math>\gamma</math>.....</i>	<i>105</i>
4.1.3 <i>Effector cells .....</i>	<i>107</i>
<b>4.2 Impact of clinical treatments on NSCLC evolution and NK cell response ....</b>	<b>110</b>
4.2.1 <i>Chemotherapy-induced phenotypic changes on NSCLC.....</i>	<i>110</i>
4.2.2 <i>Irradiation-induced phenotypic changes on NSCLC.....</i>	<i>114</i>
4.2.3 <i>NK cell populations responding to NSCLC post-clinical therapy.....</i>	<i>116</i>
<b>4.3 Applications .....</b>	<b>120</b>
<b>4.5 Critique and Limitations .....</b>	<b>122</b>
<b>4.6 Future Directions.....</b>	<b>123</b>
<b>4.8 Concluding Remarks.....</b>	<b>124</b>

**REFERENCES..... 126**

## LIST OF TABLES

<b>Table 1.1 Cytokines acting on NK cells.....</b>	<b>9</b>
<b>Table 2.1 Experimental designs.....</b>	<b>34</b>
<b>Table 2.2 Flow cytometry antibodies and panels.....</b>	<b>36</b>

## LIST OF FIGURES

<b>Figure 1.1 NK cell attack against target cells .....</b>	<b>7</b>
<b>Figure 1.2 NK cell activation depends on the interactions of activating and inhibitory receptors with the cognate ligands.....</b>	<b>10</b>
<b>Figure 1.3 NK cell receptors bind specific, cognate ligands .....</b>	<b>14</b>
<b>Figure 1.4 Blocking PD-1 on NK cells or PD-L1 on cancer cells prevents NK cell inhibition by the immune checkpoint pathway.....</b>	<b>21</b>
<b>Figure 2.1 Experimental timelines for monitoring tumor evolution by phenotyping following stimulation.....</b>	<b>30</b>
<b>Figure 2.2 Experimental timelines for tumor co-cultures with PBMCs.....</b>	<b>32</b>
<b>Figure 2.3 Representative flow cytometry gating strategy for tumor cells (A) and NK cells (B).....</b>	<b>38</b>
<b>Figure 3.1 Inflammation by exposure to IFN-<math>\gamma</math> induces rapid upregulation of death receptor Fas and activating ligand HLA-F on A549 cells.....</b>	<b>41</b>
<b>Figure 3.2 Inflammation by exposure to IFN-<math>\gamma</math> induces rapid evolution of inhibitory ligands on A549 cells.....</b>	<b>42</b>
<b>Figure 3.3 PBMC pressure on A549 cells induces rapid evolution of death receptors and activating ligands, both with and without IFN-<math>\gamma</math> stimulation.....</b>	<b>45</b>
<b>Figure 3.4 PBMC pressure on A549 cells induces rapid evolution of inhibitory ligands, both with and without IFN-<math>\gamma</math> stimulation.....</b>	<b>46</b>
<b>Figure 3.5 NK cell activation increases with longer co-cultures with A549 cells treated with or without IFN-<math>\gamma</math>.....</b>	<b>47</b>
<b>Figure 3.6 NK cell pressure contributes to rapid MIC-A/B phenotypic evolution induced by PBMC co-cultures.....</b>	<b>50</b>
<b>Figure 3.7 NK cell pressure contributes to rapid inhibitory ligand phenotypic evolution induced by PBMC co-cultures.....</b>	<b>51</b>



<b>Figure 3.8 Palbociclib (P) and trametinib (T) chemotherapy treatments induce death receptor and activating ligand upregulation in a dose- and time-dependent manner.....</b>	<b>54</b>
<b>Figure 3.9 Palbociclib (P) and trametinib (T) chemotherapy treatments induce inhibitory ligand upregulation in a dose- and time-dependent manner..</b>	<b>55</b>
<b>Figure 3.10 Palbociclib and trametinib treatments slow A549 proliferation....</b>	<b>57</b>
<b>Figure 3.11 Irradiation treatment induces dose-dependent upregulation of death receptors and activating ligands.....</b>	<b>59</b>
<b>Figure 3.12 Irradiation treatment induces dose-dependent upregulation of inhibitory ligands.....</b>	<b>60</b>
<b>Figure 3.13 Death receptors and activating and inhibitory ligands on A549 cells rapidly evolve depending on different treatment pressures.....</b>	<b>63</b>
<b>Figure 3.14 Blocking HLA ligands on A549 cell surfaces induces greater response of cognate receptor-positive NK cells.....</b>	<b>66</b>
<b>Figure 3.15 Blocking the PD-1/PD-L1 axis induces greater response of PD-1<sup>+</sup> NK cells.....</b>	<b>68</b>
<b>Figure 3.16 Activation of KIR2DL2/L3<sup>+</sup> NK cells drops when chemotherapy treatment induces HLA-C upregulation.....</b>	<b>70</b>
<b>Figure 3.17 Activation of KIR3DL1<sup>+</sup> NK cells drops when chemotherapy treatment induces HLA-Bw4 upregulation.....</b>	<b>71</b>
<b>Figure 3.18 Activation of PD-1<sup>+</sup> NK cells increases against chemotherapy-treated A549 cells when excluding KIR<sup>+</sup> NK cells.....</b>	<b>72</b>
<b>Figure 3.19 Activation of TRAIL<sup>+</sup> NK cells increases against chemotherapy-treated A549 cells when excluding KIR<sup>+</sup> NK cells.....</b>	<b>73</b>
<b>Figure 3.20 Activation of NKG2D<sup>+</sup> NK cells increases against chemotherapy-treated A549 cells when excluding KIR<sup>+</sup> NK cells.....</b>	<b>75</b>
<b>Figure 3.21 Activation of Fas<sup>+</sup> NK cells increases when chemotherapy treatment induces Fas upregulation.....</b>	<b>76</b>

<b>Figure 3.22 Chemotherapy and PBMC co-cultures induce death receptor and activating ligand upregulation.....</b>	<b>79</b>
<b>Figure 3.23 Chemotherapy and PBMC co-cultures induce death receptor and activating ligand upregulation.....</b>	<b>81</b>
<b>Figure 3.24 Activation of NK cells against chemotherapy-treated tumor cells depends on the expression of inhibitory KIRs.....</b>	<b>85</b>
<b>Figure 3.25 Activation of PD-1<sup>+</sup> NK cells increases against irradiated A549 cells when excluding KIR<sup>+</sup> NK cells.....</b>	<b>88</b>
<b>Figure 3.26 Activation of FasL<sup>+</sup> NK cells increases as irradiation induces Fas upregulation on A549 cells.....</b>	<b>89</b>
<b>Figure 3.27 Activation of NKG2D<sup>+</sup> NK cells increases against irradiated A549 cells when excluding KIR<sup>+</sup> NK cells.....</b>	<b>90</b>
<b>Figure 3.28 Activation of TRAIL<sup>+</sup> NK cells increases against irradiated A549 cells when excluding KIR<sup>+</sup> NK cells.....</b>	<b>91</b>
<b>Figure 3.29 Blocking inhibitory interactions rescues the inhibitory receptor-positive NK cell response against chemotherapy-treated A549 cells.....</b>	<b>95</b>
<b>Figure 3.30 Blocking inhibitory interactions rescues the inhibitory receptor-positive NK against irradiated A549 cells, particularly after 5 days.....</b>	<b>99</b>
<b>Figure 3.31 Activation of educated activating receptor/ligand-positive NK cells increases against irradiated A549 cells as inhibitory interactions are blocked.....</b>	<b>100</b>
<b>Figure 3.32 FasL<sup>+</sup> NK cells were more activated against irradiated A549 cells than TRAIL<sup>+</sup> and NKG2D<sup>+</sup> NK cells.....</b>	<b>101</b>
<b>Figure 4.1 Summary of stimulation-induced phenotypic changes observed on A549 cells.....</b>	<b>103</b>

## ABSTRACT

Non-small cell lung carcinoma (NSCLC) is a hard-to-treat, high mortality cancer in need of more effective therapy options. Natural killer (NK) cells are innate lymphocytes that contribute to anti-tumor functions through direct cell lysis and cytokine release. NK cells may be adoptively transferred or recruited for therapy, but treatment-induced phenotypic evolution of tumor surface proteins challenge selection of the ideal cell subsets. We studied how surface proteins interacting with NK cells on A549 cells evolve in response to inflammation, interaction with immune cells, chemotherapy, and radiation. Our results revealed dynamic, transient changes that implicate different NK cell subsets as ideal tumor killers. Analysis of responding NK cell populations against treated A549 cells, and antibody-mediated blockade experiments revealed that inhibitory interactions dominantly suppress activation driven through activating receptor-ligand binding. We conclude understanding evolving tumor phenotypes allows for selection of ideal NK cell killers to complement existing and nascent treatment approaches.

## LIST OF ABBREVIATIONS AND SYMBOLS USED

ANOVA	Analysis of variance
APC	Antigen presenting cell
APM	Antigen processing and presentation machinery
CAR	Chimeric antigen receptor
CDK4/6	Cyclin-dependent kinase 4 and 6
CFRT	Conventionally fractionated radiation therapy
CRS	Cytokine release syndrome
DC	Dendritic cell
DDR	DNA damage response
ELISA	Enzyme-linked immunosorbent assay
FasL	Fas ligand
FBS	Fetal bovine serum
FSC	Forward scatter
GVHD	Graft-versus-host disease
Gy	Gray
ICB	Immune-checkpoint blockade
KIR	Killer immunoglobulin like receptor
LDR	Low-dose radiation
IDO	Indoleamine-2,3-dioxygenase
IFN	Interferon
IHC	Immunohistochemistry
IL	Interleukin
iPSC	Induced pluripotent stem cell
ITAM	Immunoreceptor tyrosine-based activating motif
ITIM	Immunoreceptor tyrosine-based inhibitory motif
MAPK	Mitogen-activated protein kinase
MDSC	Myeloid derived suppressor cell
MEK	MAPK kinase
MIC	MHC class I related proteins
MHC	Major histocompatibility complex
NCR	Natural cytotoxicity receptor
NKG2	Natural killer group 2
NK	Natural killer
NSCLC	Non-small cell lung carcinoma
OS	Overall survival
PBMC	Peripheral blood mononuclear cell
PBS	Phosphate buffer saline
PD-1	Programmed death receptor-1
PD-L1	Programmed death-ligand 1
PFS	Progression free survival
RM	Repeated measures
ROS	Reactive oxygen species
SBRT	Stereotactic body radiation therapy
SOC	Standard of care

SPOP	Speckle-type POZ protein
SSC	Side scatter
TCR	T cell receptor
TGF	Transforming growth factor
Th	T helper cell
TKI	Tyrosine kinase inhibitor
TMB	Tumor mutational burden
TME	Tumor microenvironment
TNF	Tumor necrosis factor
Treg	Regulatory T-cell
TPS	Tumor proportion score
QQ	Quantile-quantile
$\alpha$	Alpha
$\beta$	Beta
$\delta$	Delta
$\kappa$	Kappa
$\gamma$	Gamma
$^{\circ}\text{C}$	Degree Celsius
G	Gram
Gy	Gray
$\mu\text{g}$	Microgram
$\mu\text{L}$	Microliter
mL	Milliliter
IU	International units

## ACKNOWLEDGEMENTS

I would like to take this opportunity to thank my family, friends, and colleagues for the constant support and guidance throughout my degree.

I would firstly like to thank my committee, Drs. Jean Marshall and Zhaolin Xu, who guided this project and provided insightful feedback. I appreciate all the thoughtful suggestions and time you both spent reading my reports and attending my committee meetings.

I would like to thank all members of the Boudreau lab for the consistent encouragement and laughs, and who created a supportive, warm environment for me to grow as a scientist. I would especially like to thank Lauren Westhaver, who has kindly answered my countless questions since I began in the Boudreau lab three and a half years ago. Stacey Lee, thank you for your encouragements and always enthusiastically agreeing to run my flow cytometry samples for hours at a time. I am grateful for the friendships fostered in the Boudreau lab and I will appreciate this time forever!

Thank you to all members of Dalhousie's CORE flow cytometry facilities for their gracious help and support in running my samples. Derek Rowter, thank you for your patience and guidance in troubleshooting.

I would like to thank my generous funders for providing me opportunities to perform important research. Thank you to the Dalhousie Faculty of Medicine-Dalhousie Medical Research Foundation and CIBC for the Graduate Studentship in Cancer Immunotherapies; to the Nova Scotia Graduate Studies for the Master's Scholarship; and to Reserch Nova Scotia for the Scotia Scholar's Award. I'd also like to thank the Faculty of Graduate Studies at Dalhousie University for an honorary Killam Predoctoral Award.

Thank you to my parents for their unwavering support as I've continued my education halfway across the country. Though we could not be physically together much throughout my degree due to the pandemic, I am grateful for all the calls on the walk to the lab, encouraging messages, and for always reading my reports, even if they sounded like another language to you. Thank you to my friends for cheering me on, keeping me sane during pandemic lockdowns, and listening to me talk about NK cells one too many times.

Finally, I would like to extend an immense thank you to my supervisor, Dr. Jeanette Boudreau. I am very grateful for your unwavering support, guidance, and encouragement during the past three and a half years, especially with the challenges that came with completing a Master's degree during a pandemic. I am better for all the ways you've challenged me and helped me grow.

## **CHAPTER 1: INTRODUCTION**

### **1.1 Non-small cell lung carcinoma**

Lung cancer is the most commonly diagnosed cancer, and the most common cause of cancer death in Canada and worldwide (Brenner et al., 2020; Ferlay et al., 2019).

According to the Canadian Cancer Society, it is expected that lung cancer in Canada will cause more deaths in 2020 than colorectal, pancreatic and breast cancers combined (Canadian Cancer Statistics Advisory Committee, 2020). This high mortality (19% five-year survival) can be attributed to both the high incidence and low survival rates of lung cancer (Canadian Cancer Statistics Advisory Committee, 2020). There are an estimated 29,800 new cases of lung cancer in Canada for 2020 – 13% of all cancer diagnoses – and almost half (49%) of all lung cancer cases in Canada are diagnosed at stage 4 when tumors have become metastatic (Canadian Cancer Society, 2020; Canadian Cancer Statistics Advisory Committee, 2020). Modifiable risk factors, such as tobacco, radon gas, asbestos, and air pollution, are attributed to 86% of lung cancer cases. These carcinogenic exposures can directly or indirectly cause DNA damage, leading to genetic instability and cancer development (Barnes et al., 2018). This contributes to the tumor heterogeneity observed between individuals and the high mutational burden in lung cancer (De Sousa & Carvalho, 2018; Penault-Llorca & Radosevic-Robin, 2018).

Lung cancer is histologically categorized as either non-small cell lung carcinoma (NSCLC, approximately 88% of lung cancer cases), and small-cell lung carcinoma, (around 12%; Canadian Cancer Statistics Advisory Committee, 2020). NSCLC is further distinguished into three histological subtypes: adenocarcinoma (48%), squamous cell carcinoma (20%), and large cell carcinoma (1%; Canadian Cancer Statistics Advisory Committee, 2020). The trends in incidence rates of the histologic subtypes vary: adenocarcinoma, which is more commonly diagnosed among non-smokers, has been on the rise; squamous cell carcinoma, which is strongly associated with tobacco smoking, has been decreasing since 1992 (Canadian Cancer Statistics Advisory Committee, 2020). Overall, the development of lung cancer can be attributed to the exposure to exogenous and endogenous risk factors, however some cases are caused by bad luck mutations (Tomasetti & Vogelstein, 2015).



### *1.1.1 NSCLC standard of care treatments*

Standard of care (SOC) treatments are designed based on the characteristics of a patient's disease, and its underlying genetics. Potential treatments include surgery, radiation, target therapy, chemotherapy and/or immune checkpoint blockade (ICB; Canadian Cancer Society, 2021b). Surgery is employed when the tumor is sufficiently localized, the patient is healthy enough to withstand surgical intervention, and there is reasonable opportunity to safely remove the tumor (Canadian Cancer Society, 2021b). As an alternative to surgery, high dose radiation of typically 18 Gray (Gy) three times over 1.5-2 weeks can be used (termed stereotactic body radiation therapy [SBRT]; Sebastian et al., 2018). For advanced disease, radiation can be delivered at lower, fractionated doses of 1.8-2 Gy/day for a total of ~60 Gy (termed conventionally fractionated radiation therapy [CFRT]; Ohri, 2017). Targeted therapy is an individualized approach given for patients with targetable genetic mutations (Canadian Cancer Society, 2021b). The standard chemotherapy treatments are generally a combination of two platinum-based drugs, and can be employed before or after surgery, or as the main treatment if surgery is not an option (Canadian Cancer Society, 2021b). ICB aims to activate the immune system by blocking inhibitory interactions between tumor cells and immune cells, and is typically given to patients with advanced or metastatic disease (Canadian Cancer Society, 2021b; Ohri, 2017; Sebastian et al., 2018). SOC treatments are often combined with one another; for example, chemotherapy can be used before or after surgery, in combination with radiation (chemoradiation), or with immunotherapy.

The design of therapy for patients is informed by the histologic, molecular, and immunohistochemical subtypes of the cancer (Elkrief et al., 2020). For patients with stage IV disease, the histological subtype (squamous or non-squamous) helps determine the optimal chemotherapy regimen (Midthun, 2021). Driver mutations, which occur in genes involved with cell growth and survival, can be queried by molecular testing to determine if they have a targetable alteration for that individual patient (Elkrief et al., 2020). A study of 799 patients in Nova Scotia reported the frequencies of alterations among the population to be 24.9% *KRAS*, 6.96% *EGFR*, 1.2% *PIK3CA*, 1.08% *BRAF*, and 0.12% *ALK* rearrangements (Forsythe et al., 2020). The balance (66.15% of cases) had no driver mutations (Forsythe et al., 2020). For some molecular alterations, there are

effective targeted therapy options such as tyrosine kinase inhibitors (TKIs) for *EGFR* and *ALK* mutations, however others, including *KRAS*, still rely on more classical treatments (i.e. surgery, radiation, chemotherapy; Forsythe et al., 2020; Moore et al., 2021).

The *KRAS* oncogene constitutively activates the mitogen-activated protein kinase (MAPK) signalling pathway, which has been proven difficult to treat due to the inability of sustained inhibition on RAS-driven signaling (Ruscetti et al., 2018). The most frequently mutated RAS isoform is KRAS-G12C, and the only targeted therapy for patients with advanced KRAS-G12C NSCLC is Sotorasib, approved in May 2021 (Moore et al., 2021; Sequist & Neal, 2021). Furthermore, there are late stage clinical trials for KRAS-G12C NSCLC using allele-specific covalent inhibitors (NCT04303780, NCT04685135; Moore et al., 2021). Other potential therapy options for *KRAS*-mutant tumors are focused on immunotherapy; *KRAS*-mutant tumors are expected to incite immune reactions as they are associated with genetic instability and high levels of tumor mutation burden (TMB), which denotes total number of non-synonymous mutations in the coding regions of genes (C. Liu et al., 2020). Immunosuppression may be impeding the expected immune response; for patients with advanced disease without any targeted therapy options, the immunohistochemical testing for PD-L1 is used to determine the tumor proportion score (TPS; Midthun, 2021). The TPS determines whether the patient will receive ICB alone or in combination with chemotherapy (further discussed in 1.3.1; Elkrief et al., 2020).

Current SOC treatments are imperfect: platinum-based chemotherapies have high toxicities, and tumors can gain resistance to treatments, especially since NSCLC is a high TMB cancer (R. Chen et al., 2020; C. Lin et al., 2020; H.-X. Wu et al., 2019). High TMB is negatively associated with clinical outcomes for patients receiving targeted therapy and adjuvant chemotherapy, however it is a good indicator for immunotherapy (Devarakonda et al., 2018; C. Lin et al., 2020). Although tumors may be initially sensitive to therapy, when they are incompletely controlled, relapsing, treatment-resistant tumors may occur. As mortality rate remains high for advanced NSCLC, other treatment options are being investigated.

### *1.1.2 NSCLC upcoming promising treatments*

Radiation dose can have opposing impacts on immune function. While CFRT is given with curative intent, high doses of irradiation can induce the upregulation of inhibitory ligands such as major histocompatibility complex (MHC) class I molecules and PD-L1, which are known to interrupt antitumor activities of natural killer (NK) cells (Chiriva-Internati et al., 2006; Gong et al., 2017; Park et al., 2014; Reits et al., 2006). Numerous studies have identified the ability of low-dose radiation (LDR) to be “immunosenesitizing” (Zhou et al., 2018). Specifically, LDR stimulates proliferation and cell survival of normal cells and normal stem cells, without the same effects in cancer cells (Yang et al., 2016). LDR in tumor-bearing mice can induce an altered cytokine profile that involves increased secretion of immunostimulatory cytokines (ex. interferon [IFN]- $\gamma$ , interleukin [IL]-2, tumor necrosis factor [TNF]) and decreased secretion of immunosuppressive cytokines (ex. IL-10, transforming growth factor [TGF]- $\beta$ ; Yang et al., 2016). Consistent with this shift toward pro-inflammatory immunity, studies in mice have revealed that LDR can augment expansion and cytotoxicity of NK cells, enhance activation of dendritic cells (DCs) and T cells, and decrease immunosuppressive regulatory T-cell (Treg) populations (Zhou et al., 2018). Since radiation induces cancer cell death through DNA damage, the resultant stress ligands upregulated on the tumor cell surfaces may contribute to the NK cell activation (Gasser et al., 2005; Yang et al., 2014). Overall, LDR provides a promising approach of inducing an immunostimulatory environment and the upregulation of stress ligands that activate immune cells.

SOC for lung cancer may involve platinum-doublet chemotherapy, but there is increasing interest in alternative, non-platinum based chemotherapies. Platinum-based chemotherapies, particularly cisplatin, may result in extensive adverse effects such as neurotoxicity, hearing loss, nephrotoxicity, and severe emesis (Breglio et al., 2017; D’Addario et al., 2005). Alternative chemotherapies may afford more targeted treatment and some are already in use for subsets of lung cancer. For example, the MAPK signaling pathway, which promotes proliferation, differentiation, and survival in tumor cells, may be inhibited to impair cancer growth (Ruscetti et al., 2018). Inhibition of the MAPK pathway is beneficial for tumors with *EGFR* alterations because they depend on this downstream signaling cascade, however it is less effective with *KRAS*-mutant tumors

because there are other pathways that can be activated (Ruscetti et al., 2018; Samatar & Poulidakos, 2014). The inhibition of cyclin-dependent kinase 4 and 6 (CDK4/6) could abrogate signalling through the cell cycle progression, another major downstream RAS pathway (Sherr et al., 2016). In *KRAS*-mutant lung tumor models, the combination of trametinib, a MEK1/2 inhibitor, and palbociclib, a CDK4/6 inhibitor, resulted in tumor regression, cellular senescence, and increased NK cell activation (Ruscetti et al., 2018). These results suggest that combinatorial strategies aimed at RAS-driven signalling could be used to slow or even stop tumor growth, while concurrently activating NK cells to kill the tumors. The promising *in vitro* data in *KRAS*-mutant models demonstrates the ability to reduce resistance acquired from monotherapies when combining MEK inhibitors with CDK4/6 inhibitors (Haines et al., 2018). More research is required to understand the mechanism of NK cell activation and the safety of the combination therapy in patients (ongoing phase I/II clinical trial: NCT02065063).

Although good progress has been made toward treatment of NSCLC by studying its subsets and development of targeted therapies, additional work is needed to improve outcomes for all patients. Immunotherapy – strategies to activate the immune system – may be key to durable control of NSCLC. Presently, immunotherapy is limited to ICB for NSCLC, but in other cancers, cell-based treatments or specific monoclonal antibodies are able to redirect immune systems to support anti-tumor activities. Activation of NK cells is already a key feature in the success of many cancer treatment strategies, and we expect that approaches to specifically activate NK cells for control of lung cancer is both logical and highly promising.

## **1.2 Natural killer cells**

NK cells are lymphocytes of the innate immune system that function to mediate early defenses against cells which are malignant or virally infected, and respond to fungal and bacterial infections (Mody et al., 2019; Vivier et al., 2011). NK cell functions are carried out via secreted products and cell-cell interactions. NK cells engage first with the cytokine environment, then with target cells using receptor-ligand partnerships to form immunologic synapses (Orange, 2008). These synapses are stabilized by adhesion molecules (i.e. LFA-1 + ICAM) and facilitate interaction between receptor-ligand

partnerships on cell surfaces (Orange, 2008). NK cell receptors, activated through cell-to-cell contact or soluble factors, engage with adapter molecules to initiate intracellular signaling cascades (Orange, 2008). Those signals determine how the NK cell will respond by integrating and weighing the magnitude of incoming activating and inhibitory signals.

Activated NK cells induce target cells to die by apoptosis, which may be initiated by insertion of granzyme molecules, or activation of apoptotic pathways. Activated NK cells can perform direct cytotoxic attack on target cells by polarization of cytotoxic granules toward the immunological synapse, resulting in release of perforin and granzymes by degranulation (**Figure 1.1**; Kannan et al., 2017). Perforin, a pore-forming protein, inserts itself into the target cell membrane to allow entry into the cytosol for granzymes (serine proteases), which in turn induce apoptosis via direct activation of Caspase 3 (Kannan et al., 2017). NK cells can activate the death receptor pathways by engaging death receptors with the NK cell cognate ligands (**Figure 1.1**; Smyth et al., 2005). One pathway involves TNF-related apoptosis-inducing ligand (TRAIL; CD253) on NK cells, which interact with death receptors TRAIL-R1 (CD261) and TRAIL-R2 (CD262) on target cells to transduce an apoptotic signal (Smyth et al., 2005). Another pathway induces target cell death by Fas ligand on the NK cell binding the death receptor Fas (CD95) on the target cell (Smyth et al., 2005). The death domains for death receptors recruit adaptor proteins when bound to their ligands, which initiates a cascade that activates executioner caspases triggering apoptosis (Smyth et al., 2005). NK cells can recognize antibody-coated targets (signalling antigens as foreign and dangerous) via the activating receptor Fc $\gamma$ RIIIa (CD16; **Figure 1.1**; Lo Nigro et al., 2019). CD16 binds to the Fc portion of IgG<sub>1</sub> and IgG<sub>2</sub> antibodies, which leads to NK cell degranulation and cytokine secretion (Lo Nigro et al., 2019). NK cells release pro-inflammatory cytokines, such as IFN- $\gamma$  and chemokines, that signal for recruitment of immune cells to the inflamed tissues and tumor microenvironment (TME), promote activation of T cells and DCs, and stimulate B cell maturation (**Figure 1.1**; Kannan et al., 2017). The features of NK cells position them at the intersection of innate and adaptive immunity, both as early responders and polarizers of downstream immunity.

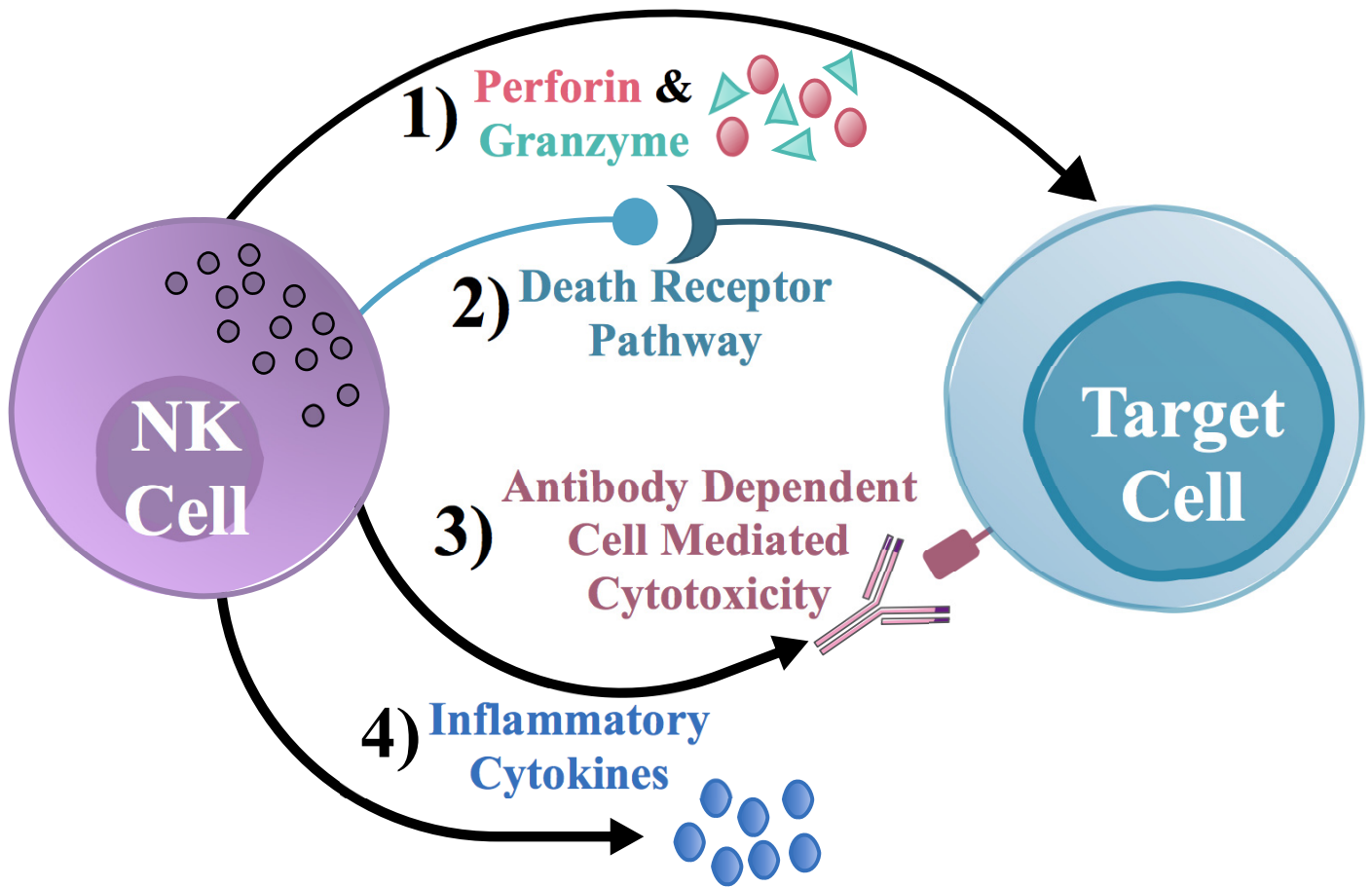


**Figure 1.1 NK cell attack against target cells.** Activated NK cells execute four pathways to promote killing of target cells. 1) NK cells release granules containing perforin and granzyme to induce apoptosis in target cells. 2) NK cell death ligands bind cognate death receptors on target cells to induce apoptosis. 3) NK cells bind antibody-coated target cells via CD16 and become activated (no prior activation required). 4) NK cells release inflammatory cytokines to promote innate and adaptive immune responses against target cells.

### *1.2.1 NK cell activation*

Cytokines released by non-immune and immune cells have direct impacts on NK cell proliferation, activation, and suppression (**Table 1.1**; Konjević et al., 2019; Lee & Ashkar, 2018). NK cells are recruited to sites of inflammation by stimulation of their chemokine receptors, including CCR2, CCR5, and CXCR3 (Grégoire et al., 2007). NK cells are activated by cytokines produced by innate cells, including IL-12 or IL-15, to produce IFN- $\gamma$  or proliferate, respectively (Konjević et al., 2019). The major hallmark cytokine produced by activated NK cells is IFN- $\gamma$ , which promotes the immune response by enhancing antigen presentation, increasing immune cell trafficking, reprogramming macrophages to an M1 proinflammatory phenotype, and promoting DC maturation (Jorgovanovic et al., 2020; Müller et al., 2017). NK cells also release TNF, which has both pro- and anti-tumor functions, such as promoting cancer cell death and activating immunoregulatory cells, such as Tregs and myeloid derived suppressor cells (MDSCs), respectively (Montfort et al., 2019).

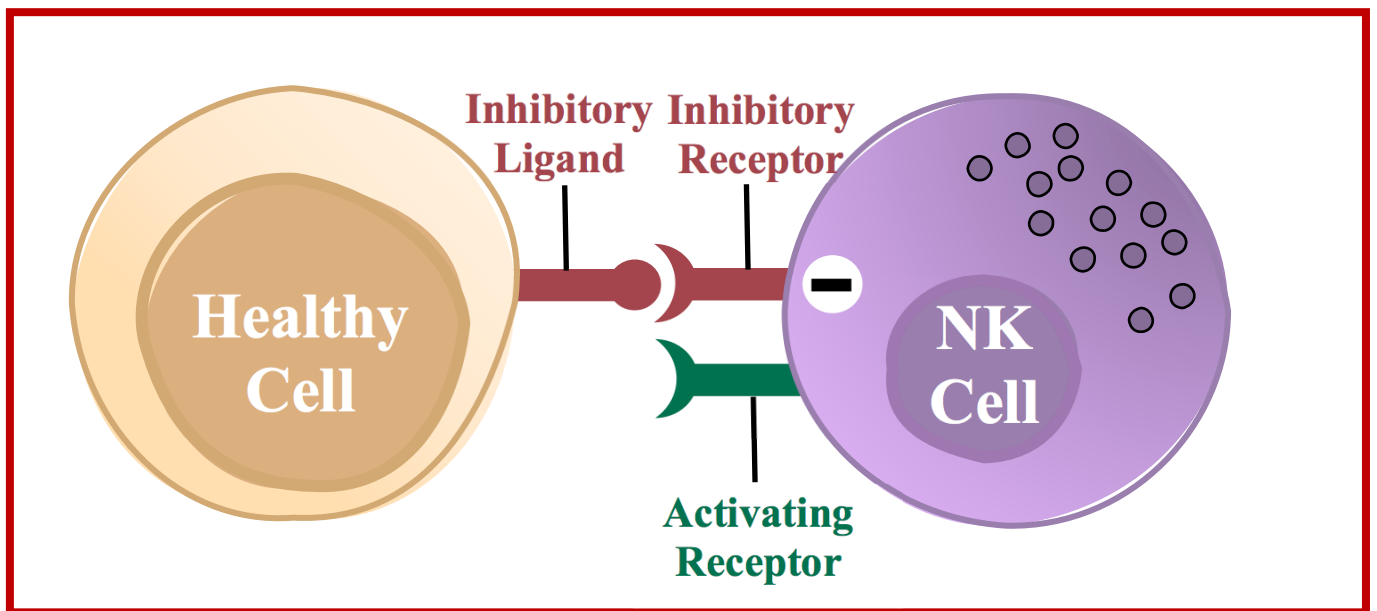
Alongside cytokine stimulation, NK cell activation is dependent on a variety of activating and inhibitory receptors. Inhibitory receptors ostensibly prevent autoimmunity and excessive reactivity during physiological conditions (Beldi-Ferchiou & Caillat-Zucman, 2017). When the inhibitory ligands on healthy cells interact with their cognate inhibitory receptors on NK cells, the NK cell receives an inhibitory signal that stops cytotoxic attacks (**Figure 1.2A**; Beldi-Ferchiou & Caillat-Zucman, 2017). There are various immune checkpoint pathways that keep the NK cell response under control, such as the interaction between PD-L1 and programmed cell death receptor-1 (PD-1) on NK cells (Beldi-Ferchiou & Caillat-Zucman, 2017). In addition, one of the main inhibitory receptor families, killer immunoglobulin like receptors (KIRs), bind MHC class I molecules with defined, conserved epitopes, which are known as human leukocyte antigens (HLA) in humans (Kannan et al., 2017). Healthy cells constitutively express HLA class I, therefore when KIRs bind to the conserved epitopes on their respective HLA molecules, the NK cells are prevented from killing healthy cells (Beldi-Ferchiou & Caillat-Zucman, 2017).

**Table 1.1 Cytokines acting on NK cells.**

<b>Cytokine</b>	<b>Released By</b>	<b>Function on NK Cells</b>
Type I IFN	Fibroblasts and monocytes	<ul style="list-style-type: none"><li>• Recruits to inflammatory site</li><li>• Promotes cytotoxicity and IFN-<math>\gamma</math> secretion</li></ul>
IL-2	CD4 <sup>+</sup> T cells	<ul style="list-style-type: none"><li>• Promotes expression of activation markers</li><li>• Enhances cytotoxicity</li></ul>
IL-12	Antigen presenting cells	<ul style="list-style-type: none"><li>• Promotes maturation</li><li>• Induces IFN-<math>\gamma</math> secretion</li></ul>
IL-15	DCs and macrophages	<ul style="list-style-type: none"><li>• Promotes and regulates proliferation, activation, survival, cytotoxicity</li></ul>
IL-18	Macrophages, DCs, fibroblasts, activated immune cells	<ul style="list-style-type: none"><li>• Promotes proliferation</li><li>• Induces chemokine receptor expression</li></ul>
IL-21	DCs and Th17 cells	<ul style="list-style-type: none"><li>• Positively and negatively impacts NK cell proliferation and activation</li></ul>
TGF- $\beta$	Tregs	<ul style="list-style-type: none"><li>• Regulates and limits NK cell cytotoxicity</li></ul>
IL-10	Macrophages, DCs, B cells, T cells	<ul style="list-style-type: none"><li>• Immunosuppressive and immunoregulatory</li></ul>



## A NK Cell Inhibition



## B NK Cell Activation

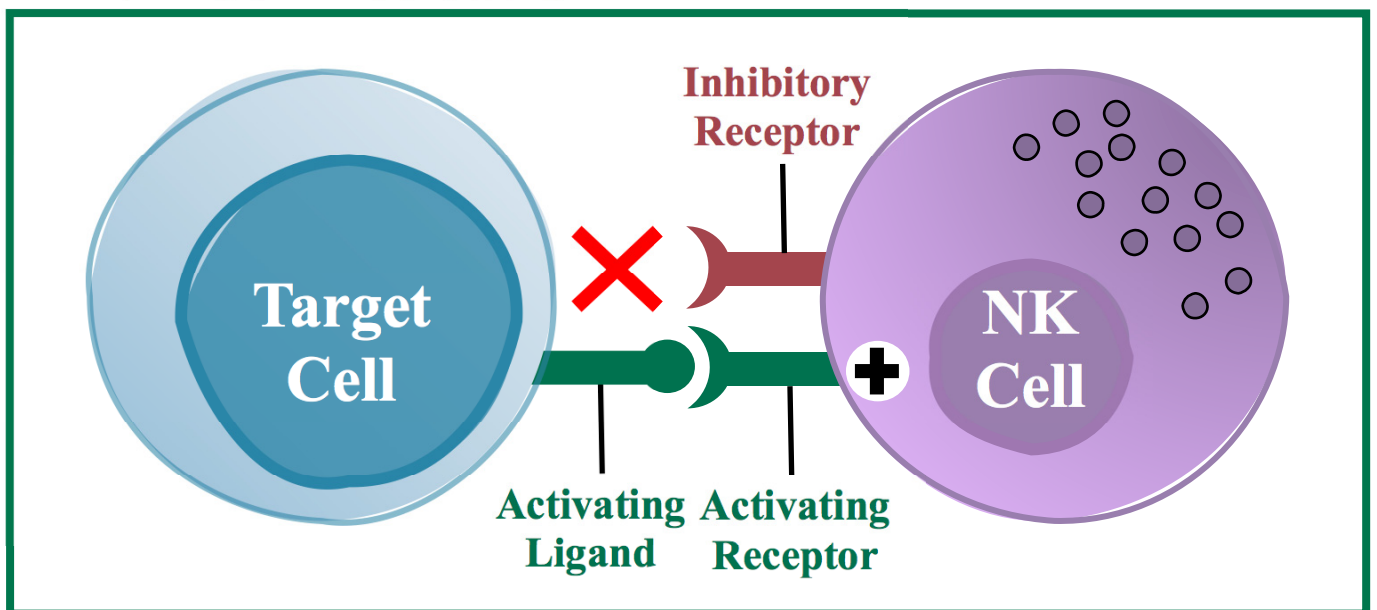


**Figure 1.2 NK cell activation depends on the interactions of activating and inhibitory receptors with the cognate ligands. (A)** When inhibitory receptors on NK cells interact with inhibitory ligands on healthy cells, the NK cells receive an inhibitory signal and do not attack that cell. **(B)** When the activating receptors on NK cells interact with activating ligands on target cells, the NK cells receive an activating signal to perform cytotoxic attack.

### 1.2.2 NK cell receptors

The three main receptor families for NK cells include KIRs, C-type lectin receptors, and natural cytotoxicity receptors (NCRs; Kannan et al., 2017). NCRs generally signal for activation, and recognize an array of abnormal or viral proteins and stress ligands, and include NKp30, NKp44, NKp46, NKp65, and NKp80 (Boudreau & Hsu, 2018; Kannan et al., 2017). KIR can be inhibitory or activating, depending on whether the cytoplasmic tails contain immunoreceptor tyrosine-based inhibitory motifs (ITIMs), or if the associated adapter proteins contain immunoreceptor tyrosine-based activating motifs (ITAMs; Kannan et al., 2017).

Within the human genome, there are 15 functional KIR genes which individuals inherit in diverse combinations (Hsu & Dupont, 2005). The four primary inhibitory KIRs that regulate the inhibition of NK cells against classical HLA class Ia-expressing cells include KIR2DL1 (binds HLA-C molecules encoding the HLA-C2 epitope), KIR3DL1 (binds HLA-B molecules encoding the HLA-Bw4 epitope), and KIR2DL2 and KIR2DL3 (binds HLA-C molecules encoding the HLA-C1 epitope; **Figure 1.3**; Kannan et al., 2017). The activating receptor KIR3DS1 binds to HLA-F in its open conformation (Garcia-Beltran et al., 2016). Two other activating KIRs, KIR2DS1 and KIR2DS2, weakly bind HLA-C2 and HLA-C1, respectively (Ivarsson et al., 2014). The *KIR* genes are divided into *KIR-A* and *KIR-B* haplotypes; an individual will either have an AA, AB or BB genotype (Middleton & Gonzelez, 2010). The A haplotype contains a fixed number of genes encoding inhibitory receptors (*KIR2DL1*, *KIR2DL3*, *KIR3DL1*, *KIR3DL2*, and *KIR2DL4*) and activating *KIR2DS4*; the B haplotype includes at least one of: *KIR2DS2*, *KIR2DL2*, *KIR2DL5B*, *KIR2DS3*, *KIR2DL5A*, *KIR2DS5* and *KIR2DS1* (Pende et al., 2019). Therefore, while each individual will encode the genes for inhibition by “self” HLA, the presence and copy numbers of the activating *KIR* genes differs between people.

Another important inhibitory receptor is natural killer group 2a (NKG2A), which forms a C-type lectin receptor as a heterodimer with CD94 (Kannan et al., 2017). When NKG2A binds peptide-loaded HLA-E, a nonclassical HLA class Ib molecule, an inhibitory signal is transduced through ITIMs (**Figure 1.3**; Kamiya et al., 2019). Other C-type lectin receptors, CD94/NKG2C and CD94/NKG2E, produce an activating signal

when bound to HLA-E through the ITAMs on the adapter molecule DAP10 (Kannan et al., 2017; Lanier et al., 1998). A final C-type lectin receptor, NKG2D, does not form a heterodimer with CD94, and interacts with adaptor molecule DAP10 to provide an activating signal to the NK cell (Kannan et al., 2017; Wu et al., 2000). NKG2D binds HLA class I chain-related proteins (MIC) A and B, and the UL16 binding proteins (ULBP) 1-6 (Raulet et al., 2013).

Target cells will lose their inhibitory ligands, such as the downregulation or loss of expression of HLA class I molecules (Paul & Lal, 2017). This tumor escape mechanism stops effector T cells from becoming activated, as they rely on interactions with antigens on HLA class I molecules (Waldman et al., 2020). However, this loss can promote NK cell activation as they are no longer receiving the inhibitory signal. NK cells primed for activation by cytokine stimulation can therefore be polarized for attack through activating receptor-ligand partnerships (Kannan et al., 2017).

DNA damage and cellular stress results in the upregulation of “stress ligands” on cell surfaces, also known as activating ligands (Rezvani & Rouce, 2015). When the activating ligands or death receptors interact with the activating receptors and ligands on NK cells, a positive signal is delivered to that cell to attack (**Figure 1.2B**; Rezvani & Rouce, 2015). For this research, we studied NKG2D/MIC-A and MIC-B, and the two death receptor pathways (**Figure 1.3**), which have each been associated with NK cell recognition of tumors. Previous studies have demonstrated their upregulation in response to irradiation (Cacan et al., 2015; Ifeadi & Garnett-Benson, 2012; Sheard et al., 1997) and chemotherapy (Elrod & Sun, 2008). Importantly, when both inhibitory and activating receptors on NK cells are engaged, the functional outcome is typically dominated by the inhibitory signals (Long et al., 2013).

Overall, the surface receptors on NK cells are extremely diverse and expand much farther than discussed here. Interestingly, a study using mass spectrometry revealed that within a healthy individual, there are between 6,000 and 30,000 distinct NK cell phenotypic populations (Horowitz et al., 2013). Among the analyzed population of 22 individuals, there were more than 100,000 subpopulations of NK cells (Horowitz et al., 2013). The authors concluded that the composition of inhibitory receptor expression patterns is predominantly influenced by genetic elements, whereas environmental factors

largely influenced the surface expression of activating and costimulatory receptors (Horowitz et al., 2013). This diversity of NK cell phenotypes creates a spectrum of functionality, and the process by which each NK cell function is calibrated is termed “NK cell education”.

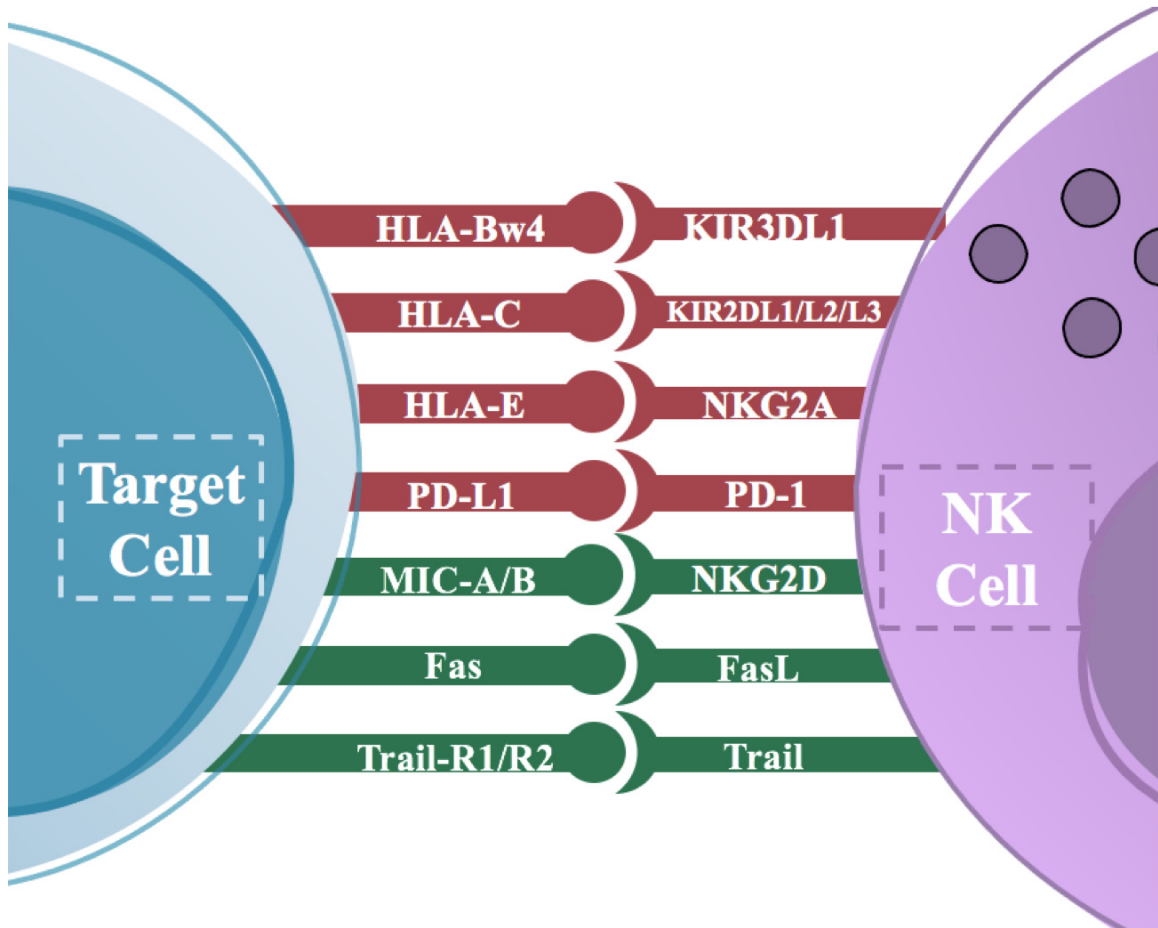


**Figure 1.3 NK cell receptors bind specific, cognate ligands.** Inhibitory pairings are shown in red; activating pairings are shown in green.

### 1.2.3 NK cell education

NK cell reactivity is programmed through cumulative interactions between the inhibitory receptors and self-HLA ligands on healthy cells (Boudreau & Hsu, 2018). HLA class I molecules are constitutively expressed on healthy cells, and the polymorphic loci important for NK cell recognition include *HLA-B* and *-C*, and to some extent *HLA-A* (Kannan et al., 2017; Moradi et al., 2021). KIR molecules bind to conserved regions – epitopes – that are found on groups of HLA molecules. HLA-C molecules, which are all KIR ligands, are classified into two main subgroups: HLA-C1 (asparagine 80) or HLA-C2 (lysine 80), which bind KIR2DL2/L3 and KIR2DL1, respectively (Gwozdowicz et al., 2019). All motifs within the HLA-Bw4 superfamily are recognized by KIR3DL1, which includes ~40% of the *HLA-B* alleles and a select few *HLA-A* alleles (Kannan et al., 2017). The other ~60% of the *HLA-B* alleles carry the HLA-Bw6 epitope, against which NK cells are nonreactive (Gwozdowicz et al., 2019). Based on their genotype, an individual will express two alleles for each of HLA-A, -B, and -C, and their expression, along with HLA-E, influences NK cell education (Kannan et al., 2017).

As NK cells interact with the expressed self-HLA ligands on healthy cells in an individual, they become “educated” and express the cognate KIRs (Boudreau & Hsu, 2018). Educated NK cells can therefore be inhibited by self-HLA, and are capable of detecting the downregulation of those HLA ligands (Boudreau & Hsu, 2018). Despite their sensitivity to inhibition, educated NK cells are strong killers in response to stimulation because they have a lower threshold for activation and a greater effector potential (Boudreau & Hsu, 2018). In contrast, uneducated NK cells are important effectors when HLA ligands remain expressed in disease states, however they require stronger stimuli for activation, which prevents inappropriate NK cell activation that might lead to tissue damage and autoimmunity (Boudreau & Hsu, 2018). Understanding the interactions between NK cells and cognate ligands on tumor cells has been crucial to identifying the role of NK cells in cancer treatment.

### 1.2.4 NK cell role in cancer

We recently completed a systematic review of 53 studies that revealed that NK cell infiltration into solid tumors was associated with a decreased risk of death (Nersesian,

Schwartz et al., 2021). The prognostic value was greater with intraepithelial infiltration compared to tumor-adjacent stromal infiltration (Nersesian, Schwartz et al., 2021). NK cells contribute not only by direct lysis of tumor cells, but also to recruitment and activation of other immune cells (Shaver et al., 2021).

The initial study of NK cells in cancer treatment was first noticed in mismatched hematopoietic stem cell transplants in patients with high risk acute myeloid leukemia (Ruggeri et al., 2002). The incompatibility of KIRs and HLA ligands between donors and recipients resulted in greater probability of survival due to lower rates of relapse, graft failure, and acute graft-versus-host disease (GVHD; Ruggeri et al., 2002). These promising results led to further work into NK cellular therapy in non-transplant settings. Initially, NK cell adoptive therapy had limited success because they relied on *ex vivo* expanded autologous NK cells (Hu et al., 2019). Although this approach could successfully increase the number of circulating NK cells in the patient, recognition (and inhibition) of educated NK cells by self-HLA on the tumor cells prevented their activation (Hu et al., 2019). The use of allogeneic NK cells may overcome this challenge by transplanting NK cells that are refractory to inhibition by the HLA presented on the tumor. This was proven to be safe in 2005, and NK cells were shown to persist and expand *in vivo* in cancer patients without generating GVHD (Miller et al., 2005). In 2010, *KIR-HLA* mismatched allogeneic adoptive transfer demonstrated significant NK cell expansion and may have reduced the risk of childhood acute myeloid leukemia relapse (Rubnitz et al., 2010). Hence, the use of allogeneic NK cell adoptive therapy is attractive in comparison to T cell therapy because it is practical, affordable and safe. NK cells do not need to be autologous, and because they only target cells bearing markers of stress, NK cells have been associated with little toxicity including GVHD or cytokine release syndrome (E. Liu et al., 2020; Shin et al., 2020). Donor NK cells can be obtained from umbilical cord blood, clonal cell lines such as NK-92, and from lymphapheresis of allogeneic peripheral blood mononuclear cells (PBMCs; Shin et al., 2020).

While allogeneic NK cell adoptive transfer has some promising results in hematological malignancies, it requires further investigation to promote its full potential in cancer treatment. It may be possible to leverage NK cells for even better tumor control by selecting for the populations that will be sensitive to the activating ligands and

refractory to the inhibitory ones. The developing field of immunotherapy continues to expand the possibilities of promoting NK cell anti-tumor killing within the NSCLC therapeutic landscape.

### **1.3 Lung cancer immunotherapy**

Cancer immunotherapy, which aims to promote anti-tumor functions of the immune system, has grown over the decades with numerous new approaches that have improved patient outcomes and survival. NSCLC is an especially high TMB cancer, which can be unfavourable as somatic mutations support tumor escape mechanisms to avoid targeted therapy (Devarakonda et al., 2018; C. Lin et al., 2020). However, a high TMB is generally favourable for immunotherapy because it generates tumor immunogenicity (Wang et al., 2020). The increased frequency of neoantigens derived from somatic mutations is thought to promote stronger T effector cell responses (Wang et al., 2020). Immunotherapy has made advancements in NSCLC patient survival, and understanding the immunological responses provides an understanding of how we can continue to improve outcomes.

#### *1.3.1 Immune-checkpoint blockade*

Immune checkpoint pathways tightly regulate the immune response by preventing effector cells from attacking cells indiscriminately. Immune-checkpoint blockade (ICB) interferes with immune checkpoint pathways, which are employed by cancer cells to inhibit immune cell activation and tumor killing (Elkrief et al., 2020). The first historical ICB clinical trial was in 2000 with ipilimumab, a T cell antigen receptor (CTLA-4) blocking antibody, which was approved for advanced melanoma treatment in 2011 (Dobosz & Dzieciatkowski, 2019). The next approved inhibitor was nivolumab (2014), an anti-PD-1 blocking antibody, which delivered promising results that led to further developments of ICB against PD-1, PD-L1 and PD-L2 (Dobosz & Dzieciatkowski, 2019). The role of ICB in NSCLC began with nivolumab in 2015, when two landmark clinical trials compared its efficacy against the chemotherapy docetaxel in patients with previously treated squamous (Brahmer et al., 2015) and non-squamous (Borghaei et al., 2015) NSCLC tumors. Nivolumab demonstrated unprecedented results, with 14% 4-year



OS, compared to only 5% 4-year OS with docetaxel (Antonia et al., 2019). Currently approved ICB treatment for NSCLC patients in Canada includes two anti-PD-1 inhibitors, pembrolizumab and nivolumab, and three anti-PD-L1 inhibitors, atezolizumab, cemiplimab, and durvalumab (Canadian Cancer Society, 2021a; Hellmann & West, 2021). There are NK cell specific ICB currently in clinical trials, including lirilumab, an anti-KIR blocking antibody, and monalizumab, an anti-NKG2A blocking antibody (Cohen et al., 2020; Vey et al., 2018).

The inclusion of ICB in the treatment plan for advanced NSCLC patients depends firstly on the TPS of PD-L1 (Elkrief et al., 2020). Greater PD-L1 expression has been generally associated with better patient outcomes in NSCLC and other cancer types when treated with PD-1/PD-L1 blockade (Daud et al., 2016; Herbst et al., 2014; Taube et al., 2014). Hence, tumors from advanced patients with NSCLC without targetable driver mutations are analyzed for the percentage of positive PD-L1 expressing neoplastic cells (Vigliar et al., 2019). The quantification of TPS scoring is crucial, as pembrolizumab or atezolizumab is typically given as a first-line monotherapy if PD-L1 expression is 50% or greater (Elkrief et al., 2020). If a patient's disease is rapidly progressing, their regiment will include pembrolizumab with platinum doublet chemotherapy (Hellmann & West, 2021). When PD-L1 expression is in the 1%-49% range, pembrolizumab has not demonstrated superior patient outcomes over SOC chemotherapy (Mok et al., 2019). Therefore, patients in this range with non-squamous or squamous NSCLC receive pembrolizumab in combination with various platinum-based chemotherapies, depending on the histological subgroup (Elkrief et al., 2020). For non-squamous, the preferred chemotherapy options are pemetrexed and carboplatin; for squamous, patients typically receive carboplatin with paclitaxel or nabpaclitaxel (Hellmann & West, 2021). Patients with less than 1% PD-L1 TPS receive chemotherapy with pembrolizumab, though promising results from clinical trials are revealing greater OS when treated with nivolumab (anti-PD-1) and ipilimumab (anti-CTLA-4; Elkrief et al., 2020; Hellmann et al., 2019). Overall, the guidelines for treating advanced NSCLC without targetable genetic alterations are constantly evolving as more clinical trials determine which treatments provide the greatest OS with the least toxicities.

T cells are important effectors that are supported by ICB; one study observed that patients with NSCLC positively responding to anti-PD-1/anti-PD-L1 therapy had an increase in proliferation and expansion of PD-1<sup>+</sup>CD8<sup>+</sup> effector T cells (Kamphorst et al., 2017). Cytotoxic T cell activation is antigen-dependent, therefore the tumor cell is required to present antigens on its surface via HLA class I molecules to activate the T cell attack (Waldman et al., 2020). However, tumors may evolve during and after treatment to evade immune recognition, which includes the downregulation of HLA molecules. A study of 90 patients with NSCLC observed 40% of tumors exhibited a loss of heterozygosity for HLA (McGranahan et al., 2017). As HLA expression is downregulated in NSCLC tumors, the number of cytotoxic T lymphocytes infiltrating the tumors significantly decreases (Perea et al., 2018). Tumors that have low HLA class I expression, such as Hodgkins lymphoma, still demonstrate significant clinical response to PD-1 blockade (Ansell et al., 2015). Furthermore, downregulation of HLA class I antigens was associated with improved survival in patients with NSCLC (Ramnath et al., 2006). Hence, ICB in NSCLC requires the collaboration of other immune cell populations when T cell activation is limited from HLA class I downregulation or loss.

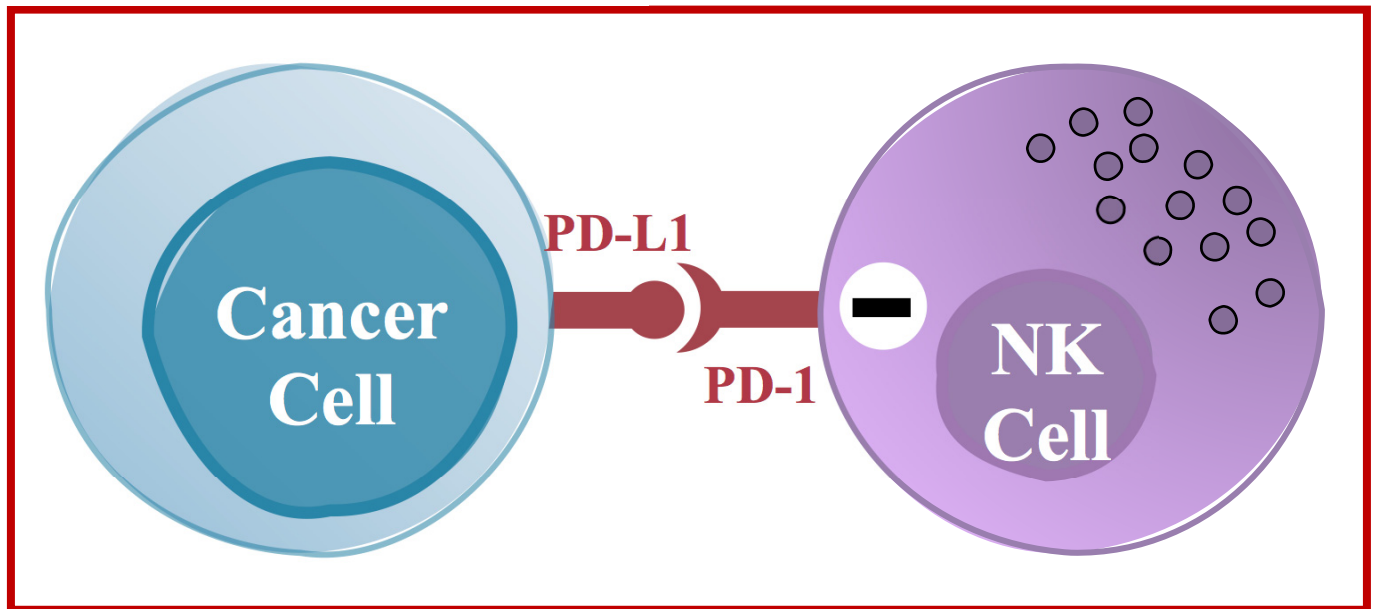
### *1.3.2 NK cell role in ICB*

Similar to T cells, NK cells express PD-1, and therefore can benefit from ICB that inhibits the PD-1/PD-L1 inhibitory interaction (**Figure 1.4**; M. Lin et al., 2020). The combination of pembrolizumab (anti-PD-1 blocking antibody) and allogeneic NK cells in patients with NSCLC resulted in a greater proportion of NK cells in the blood and overall immune function, and increased progression free survival (PFS) and OS (M. Lin et al., 2020). Patients receiving the combination compared to pembrolizumab alone had decreased numbers of circulating tumor cells, reflecting that NK cells prevented metastasis and alleviated the residual tumor load (M. Lin et al., 2020). These results suggest that NK cells contribute to the clinical benefit of ICB by directly killing tumor cells, as well as recruiting T cells to the TME. This finding has been supported in *in vivo* studies. PD-1 blockade enhanced NK cell anti-tumor function in an MHC class I-deficient lymphoma mouse model, in which NK cells were indispensable for tumor control (Hsu et al., 2018). An ovarian cancer mouse model treated with anti-PD-L1 and

particle expanded NK cells demonstrated NK cell persistence and augmented cytotoxic functions (Oyer et al., 2018).

There are currently three clinical trials assessing the use of ICB with NK cells: 1) a phase 2 study examining off-the-shelf CD16-targeted NK cells with IL-15 superagonist and an anti-PD-L1 inhibitor (avelumab) in Merkel cell carcinoma (NCT03853317); 2) a phase 1/2a assessing allogeneic NK cells with an anti-PD-1 inhibitor (pembrolizumab) in biliary tract cancer (NCT03937895); 3) a phase 1/2 study investigating DF1001, a molecule targeting NK cell activation to specific tumor cell receptors, with an anti-PD-1 inhibitory (pembrolizumab) in solid cancers (NCT04143711).

## A NK Cell Inhibition



## B NK Cell Activation

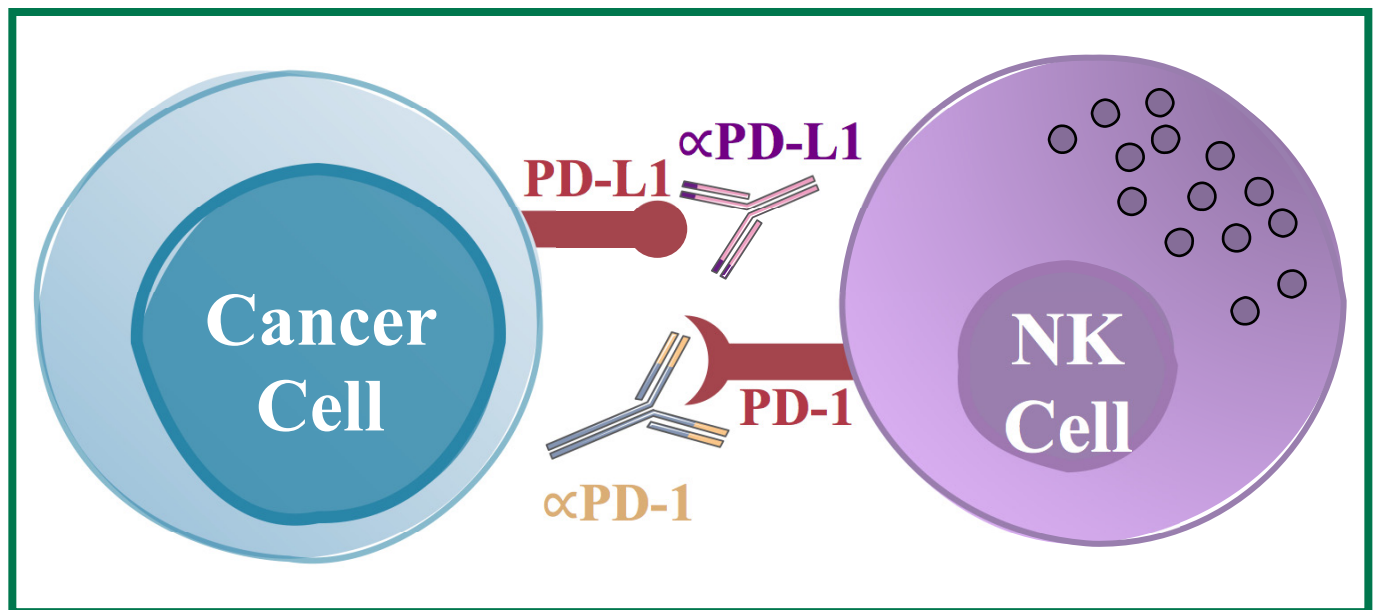


**Figure 1.4 Blocking PD-1 on NK cells or PD-L1 on cancer cells prevents NK cell inhibition by the immune checkpoint pathway.** (A) Inhibitory interactions between PD-1 and PD-L1 delivers an inhibitory signal to NK cells and stops NK cell antitumor killing. (B) ICB disrupts the PD-1/PD-L1 immune checkpoint pathway and allows for NK cell activation.

### 1.3.3 Cellular therapies

Current studies and clinical trials aim to improve outcomes by increasing trafficking of donor NK cells into the TME, and through combination treatment with ICB, cytokines, and immunomodulatory agents (Shin et al., 2020). Other NK cell-based immunotherapies include human induced pluripotent stem cells (iPSCs), which generate homogenous NK cells that can be expanded without the introduction of chromosomal abnormalities (which can occur with NK clonal cell lines; Shin et al., 2020). Currently, a phase I clinical trial (NCT03841110) is examining a master iPSC line-derived NK cell product, and other *in vitro* and *in vivo* studies are exploring the use of iPSC NK cells with customized KIR expression and in chimeric antigen receptor (CAR) therapy (Knorr et al., 2013; Li et al., 2018; Ueda et al., 2020). CAR therapy utilizes a genetically engineered immune cell that express CARs that target antigens on tumor cells, and CAR-T cells have proven to be extremely successful (Shin et al., 2020). However, CAR-T therapy is associated with toxicities such as cytokine release syndrome (CRS), while CAR-NK cells offer less adverse effects (Shin et al., 2020). A phase I/II clinical trial of HLA-mismatched anti-CD19 CAR-NK cells in B cell cancers revealed that 73% of the patients responded within 30 days of infusion, without any major toxicities (E. Liu et al., 2020). There are numerous ongoing clinical trials examining the safety and efficacy of CAR-NK therapy in solid tumors (NCT03941457, NCT03940820, NCT03692637, NCT03415100, NCT03383978, NCT02839954). Overall, NK-based immunotherapies have come a long way since the first use in mismatched hematopoietic stem cell transplants, and promising clinical trials suggest developments will continue for NK cells in cancer treatment. and solid cancers (Shin et al., 2020).

### 1.4 Tumor evolution

The interactions between the immune system and tumors lead to tumor development, progression, and suppression, and is termed immunoediting (Dunn et al., 2004). The three dynamic stages of this cancer immunosurveillance include elimination, equilibrium, and escape (Dunn et al., 2004). The elimination phase involves contributions from both innate and adaptive immune cells to kill tumor cells that are driven by cell-intrinsic mechanisms (Dunn et al., 2004; O'Donnell et al., 2019). When tumor cells are not completely

destroyed, their outgrowth as tumors is controlled in the equilibrium phase, where the immune system's killing of transformed cells suppresses the net tumor growth (Dunn et al., 2004). However, tumor cells can evolve to avoid immune recognition, leading to the escape phase in which the tumor growth outpaces the immune system's ability to maintain control (Dunn et al., 2004). This evolution can result from the selection of subclones with decreased immunogenicity, increased genetic instability, and acquired or selected features that enable immune escape (ODonnell et al., 2019).

One form of tumor evolution is termed adaptive immune resistance, in which the tumor cell phenotype changes to escape cytotoxic immune responses (Ribas, 2015). The activation of tumor antigen specific T cells and NK cells induces the release of IFN- $\gamma$  in an attempt to intensify the immune response against the tumor cells (Jorgovanovic et al., 2020). However, IFN- $\gamma$  can induce immunosuppressive factors such as the upregulation of PD-L1 on tumor cell surfaces (Ribas, 2015). Other TME-resident cytokines that have been observed to induce PD-L1 expression include IL-1a, IL-10, IL-27, and IL-32- $\gamma$  (S. Chen et al., 2019). This immune escape mechanism which inhibits PD-1<sup>+</sup> immune cells is especially detrimental for NK cell and T cell anti-tumor activity, since both immune populations express PD-1 in an activation-induced manner (Pesce et al., 2019; Ribas, 2015). PD-L1 can also be upregulated by innate immune resistance, which corresponds to *PDL1* gene amplification or genetic alterations of oncogenic signaling pathways, and thus PD-L1 is constitutively expressed (S. Chen et al., 2019).

As described in *1.3.1 Immune-checkpoint blockade*, HLA molecules can be downregulated or genetically lost, which results in reduced antigen presentation and therefore a diminished T cell response. Another defense mechanism of tumor cells to protect against cytotoxic immune attacks includes upregulation of inhibitory HLA class Ib molecules, such as HLA-E and HLA-G (Rodríguez, 2017). Type I and type II IFNs and TNF have also been observed to induce HLA class I molecules (Kersh et al., 2016). Moreover, they have been temporarily upregulated after the pressure of NK cells in neuroblastoma (Spel et al., 2015) and in colon carcinoma in rat models (Jonges et al., 2000); these trends are likely attributed to NK cell release of IFN- $\gamma$ . Overall, HLA class I upregulation versus loss/downregulation on tumor surfaces requires further studies, though evidence is emerging that it is likely due to the complex relationship between the

TME, immune system, and tumor cells (Campoli & Ferrone, 2011). The role of treatment in HLA class I expression is as well becoming more clear with ongoing studies; agents such as anti-EGFR antibodies, tyrosine kinase inhibitors (TKIs), and high dose irradiation have been shown to induce HLA class I expression (Chiriva-Internati et al., 2006; G. Garrido et al., 2017). Overall, tumor cells are constantly changing from the different pressures they are facing; the naïve tumor that is analyzed may appear quite differently after immune pressure or cancer treatment.

## **1.5 Rationale and hypothesis**

### *1.5.1 Rationale*

NK cells have critical anti-tumor functions that support tumor cell elimination or equilibrium. Their diversity of activating and inhibitory receptors make NK cells a unique effector cell that can be activated against the various tumor phenotypes that can evolve and occur during treatment and immune cell attack. Understanding the phenotype changes of NSCLC cells, especially those that change how the cancer interacts with NK cells, is critical to developing successful NK-centric therapies. By ensuring there will be as little inhibitory pairing and more activating pairing between NK cells and tumor cells, we expect to promote anti-tumor NK cell functions and encourage tumor elimination. The ideal NK cell adoptive transfer does not have to be a single NK cell population, but rather multiple distinct populations to support the killing of tumor cells as they continue to evolve as a defense mechanism and from cellular damage. Furthermore, opportunities exist to redirect the endogenous NK cell population by interfering with inhibition or amplifying activation. Here, we set out to define the characteristics of NK cells that enable response to NSCLC at rest and in response to the changes induced by treatment and tumor progression.

### *1.5.2 Hypothesis*

**We hypothesize that NK cells, as dynamic and durable effectors with phenotypic and functional diversity, can be selected against rapidly evolving NSCLC tumors.**

As treatment pressures induce temporary changes to the NSCLC phenotype, it is expected that NK cells sensitive to activating ligands and refractory to inhibitory ones

will be the most effective killers during the window of opportunity post-treatment. The applications of this research are not aimed at changing the current standard treatments for NSCLC, but rather determining how NK cell adoptive therapy can be added to promote more complete tumor control.

### *1.5.3 Objectives*

The objective of this project is to evaluate how NK cell adoptive therapy can be leveraged to challenge NSCLC tumors that have evolved due to treatment pressure. We divided our investigations into two main aims:

1. To understand how various treatment pressures induce NSCLC phenotypic evolution of the death receptors and activating and inhibitory ligands that interact with NK cells.
2. To understand how activating and inhibitory interactions feature in NK-mediated NSCLC targeting with a goal of designing prescriptive immunotherapies.



## **CHAPTER 2: MATERIALS AND METHODS**

### **2.1 Cell isolations and culturing**

#### *2.1.1 Peripheral blood mononuclear cells (PBMC)*

Healthy donor peripheral blood was collected from volunteers for blood transfusion by Canadian Blood Services. Lymphocyte-rich buffy coats are normally discarded, but through collaboration, the Boudreau laboratory claims these for research (approved Dalhousie REB 16-046, Canadian Blood Services REB 2016-016). Buffy coats were washed with 1x phosphate buffer saline (PBS) (Wisent) with 2% fetal bovine serum (FBS) (ThermoFisher) and layered onto 15 mL of Ficoll-Paque PLUS (VWR). The layered blood was centrifuged at 1,136 x g with the brake off to separate lymphocytes in a density gradient from the plasma and red blood cells. The lymphocytes were collected to be washed, resuspended in 50 mL 1x PBS 2% FBS, and centrifuged at 1528 x g for 5 minutes. The cells were resuspended in 10 mL of ACK Lysis Buffer (VWR) for 10 minutes, washed again with 1x PBS, and counted for cryopreservation. Peripheral blood mononuclear cells (PBMCs) were frozen in 90% FBS and 10% dimethyl sulfoxide (Sigma-Aldrich), cooled using a CoolCell freezing container, and stored in liquid nitrogen vapour phase or at -80°C. All PBMC donors were genotyped for *HLA* and *KIR* genes using established protocols (Hong et al., 2011; K. C. Hsu et al., 2002; Vilches et al., 2007).

For use in experiments, PBMCs were thawed and recovered at 37 °C and 5% CO<sub>2</sub> overnight in Roswell Park Memorial Institute-1640 (RPMI) (ThermoFisher) containing 1x penicillin and streptomycin (Wisent), 10% FBS, and 100 IU/mL IL-2 (Peprotech). To discourage clumping of cells, the PBMCs were cultured in 6-well plates at ~5x10<sup>6</sup> cells/well. If clumping still occurred, the cells were treated with 1.5uM EDTA (Invitrogen) per 15 mL media for 10 minutes, which was then washed off.

#### *2.1.2 Natural killer cells*

After thawing and overnight recovery, primary healthy human NK cells were isolated from PBMCs using the EasySep™ Human NK Cell Enrichment Kit according to the manufacturer's instructions (Stemcell Technologies). PBS containing 2% FBS and 1 mM EDTA was used to resuspend 5x10<sup>7</sup> PBMCs in 2 mL in a polystyrene round-bottom tube.

To the sample, 50  $\mu\text{L}/\text{mL}$  of the Isolation Cocktail (Stemcell Technologies) was added, mixed, and incubated at room temperature for five minutes. The magnetic particles (RapidSpheres™, Stemcell Technologies) were vortexed for 30 seconds, then 50  $\mu\text{L}$  was added for each mL of the sample. The tube was placed into the EasySep™ magnet and incubated at room temperature for three minutes. The unbound supernatant, which contained the NK cells, was poured off. NK cells were then counted, and used immediately in co-culture experiments.

### *2.1.3 Tumor cell lines*

Primary tumor cell lines were cultured at 37°C with 5% CO<sub>2</sub> in 75 cm<sup>2</sup> vented flasks containing 14 mL RPMI with 1% penicillin-streptomycin and 10% FBS. The NSCLC cell line, A549, and the leukemia cell line, K562, were obtained from the National Cancer Institute. The cells were split every 3-4 days as required to maintain a confluency between 60 and 90% (~4-5x10<sup>5</sup> cells/mL). To split the adherent A549 cells, the flasks were washed with PBS, then the cells were lifted with 3 mL of Trypsin with 0.05% EDTA (Wisent).

## **2.2 Monitoring tumor evolution by phenotyping following stimulations**

To monitor how tumors change in response to growth and treatment, we created a series of *in vitro* experiments to mimic the changes expected to occur during cancer growth, interaction with NK cells, and treatment. The concentrations and reagents are shown in **Table 2.1** (end of 2.3 and specific protocols are outlined below).

### *2.2.1 Stimulation of A549 Cells with IFN- $\gamma$*

A549 cells were treated with IFN- $\gamma$  at 1000 IU/mL once daily for either 1, 2, or 3 days. The cells were collected and stained for flow cytometry (see 2.4).

### *2.2.2 Stimulation of A549 cells with PBMCs*

A549 cells were treated with IFN- $\gamma$  at 1000 IU/mL once daily for three days, or left untreated but cultured simultaneously in parallel. The tumor cells were plated in a 48-well plate at 1x10<sup>6</sup> cell/mL (200  $\mu\text{L}/\text{well}$ ), and the effector PBMCs resuspended at 5x10<sup>6</sup>

cells/mL (100  $\mu$ L/well). For three experimental replicates, PBMCs were added to new wells containing A549 cells treated with or without IFN- $\gamma$  for either 1, 3, 5 or 10 hours (n=3). In one experiment replicate, PBMCs were added to a new well every hour for 5 hours (n=1). Immediately after PBMC addition, the plate was centrifuged at 20 xg for 30 seconds and incubated at 37°C. The cells were separated and stained for flow cytometry (see experimental timeline, **Figure 2.1A**).

### *2.2.3 Stimulation of A549 cells with NK cell effectors*

A549 cells were treated with IFN- $\gamma$  at 1000 IU/mL once daily for three days, or left untreated but cultured simultaneously in parallel, then plated in a 48-well plate at  $1 \times 10^6$  cell/mL (200  $\mu$ L/well). The effector PBMCs were counted and separated for either the co-culture as PBMCs ( $5 \times 10^5$  cells/mL, 100  $\mu$ L/well), or for NK cell isolation. After isolation with the EasySep™ Human NK Cell Enrichment Kit, NK cells were resuspended at  $5 \times 10^4$  cells/mL (100  $\mu$ L/well), which represented the expected number of NK cells in the PBMC fraction (~10%). The effector cells were co-cultured separately with tumor cells for five hours, then stained for flow cytometry.

### *2.2.4 Stimulation of A549 cells with chemotherapeutic agents*

A549 cells were treated with either low, middle or high doses of trametinib (5 nM, 25 nM, 125 nM; Cayman Biochemical) or palbociclib (100 nM, 500 nM, 1500 nM; Toronto Research Chemicals), or the middle dose of both drugs, every 2 days. The cells were treated for either 2, 4, 6 or 8 days, then stained for flow cytometry (see experimental timeline, **Figure 2.1B**). For two of the replicates, the A549 cells were first stained with CFSE to enable cell tracking. To do so, 5 mM stocks were first made by adding 18  $\mu$ L DMSO (Invitrogen) to a vial of CellTrace CFSE staining solution (Invitrogen) according to the manufacturer's instructions. A stock was diluted with 1 mL of warm PBS to make 5  $\mu$ M staining solution. Between  $1.5$  and  $2.0 \times 10^7$  A549 cells were resuspended per mL of staining solution, incubated at 37°C for 20 minutes, and rinsed twice with 50 mL PBS 5% FBS.

### *2.2.5 Treatment of A549 cells with irradiation*

Two irradiators were used in this project: the Gamma Cell Irradiator (Sir Charles Tupper Medical Building, Halifax, NS) and the Varian TrueBeam Linear Accelerator (Dickson Building, Halifax, NS; Varian Medical Systems, Palo Alto, USA). The dose rate of Varian TrueBeam Linear Accelerator was 600 cGy/min, and the Gamma Cell Irradiator was 428 cGy/min as of May 20<sup>th</sup>, 2021. The cells were resuspended in  $2-5 \times 10^6$  cells/mL in 1.5 mL microfuge tubes and irradiated at 0.5 Gy, 2 Gy, 5 Gy, and 10 Gy. The irradiated cells were left to rest in culture media at 37°C and 5% CO<sub>2</sub> for either 1, 3, or 5 days, then stained for flow cytometry (see experimental timeline, **Figure 2.1C**).

## 2.2 Experimental Timelines

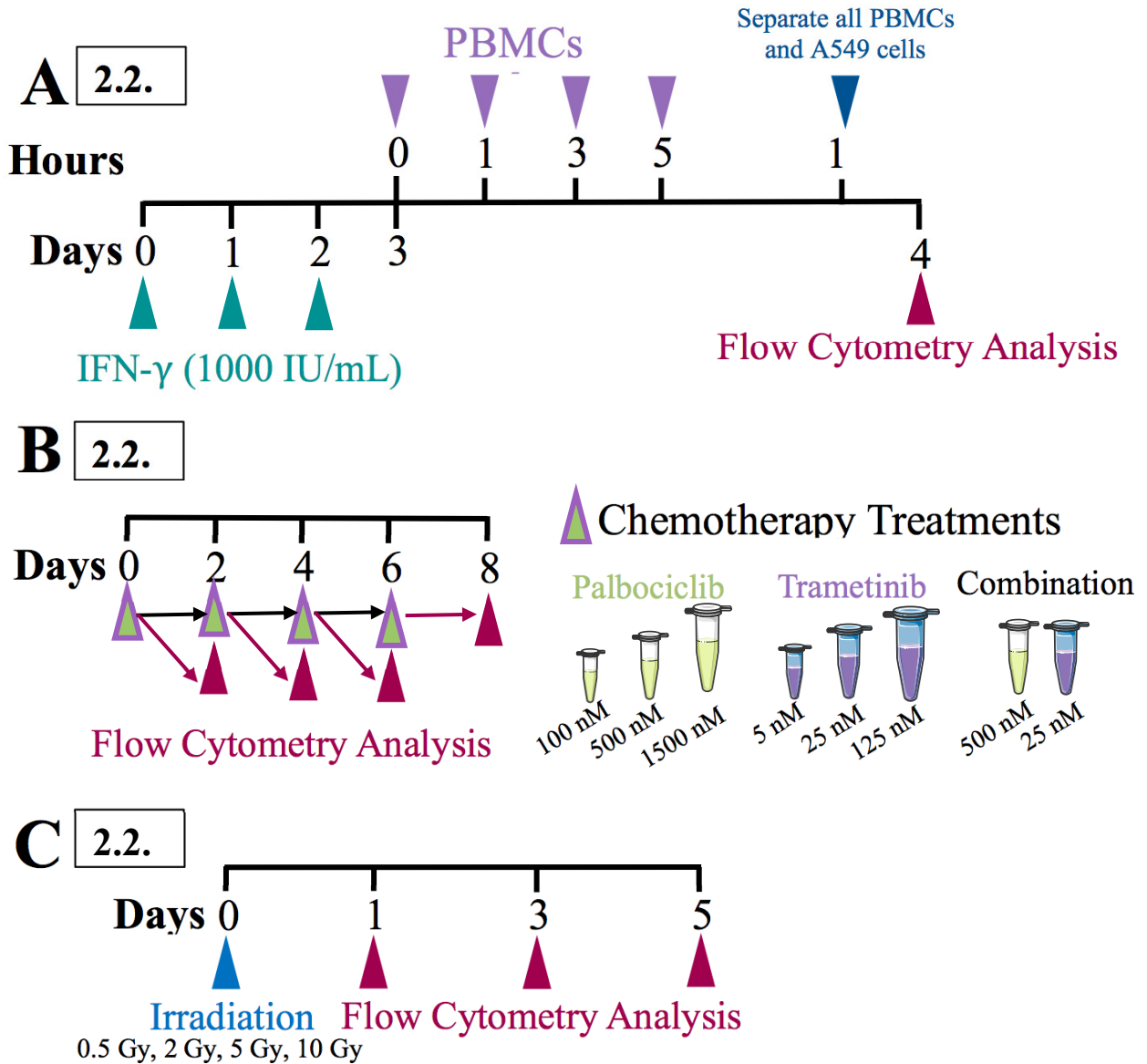


**Figure 2.1 Experimental timelines for monitoring tumor evolution by phenotyping following stimulation.** (A) A549 cells were treated with or without IFN- $\gamma$  once per day for three days. A549 cells were co-cultured with PBMCS for either 1, 3, 5, or 10 hours, then separated. The tumor cells were stained for flow cytometry. (B) A549 cells were treated with either low, middle or high doses of either Trametinib or Palbociclib, or the middle dose of both drugs every 2 days. The cells were treated for either 2, 4, 6 or 8 days, then stained for flow cytometry. (C) A549 cells were subjected to varying doses of radiation on either the Varian TrueBeam Linear Accelerator or the Gamma Cell Irradiator. The cells were left to rest for either 1, 3, or 5 days, then stained for flow cytometry.

## 2.3 Tumor co-cultures with PBMCs

To monitor how the NK cell responses changes as tumors evolve in response to growth and treatment, we trialled a number of protocols *in vitro*. The concentrations and reagents are continued in **Table 2.1** (end of 2.3) and specific protocols are outlined below.

### 2.3.1 PBMC co-culture post-HLA ligand blockade

A549 cells were treated with or without IFN- $\gamma$  at 1000 IU/mL once daily for 3 days, then plated on a 48-well plate at  $1 \times 10^6$  cell/mL (200  $\mu$ L/well). The cells were incubated for 30 minutes with either 2  $\mu$ g/ $\mu$ L per well of anti-HLA-C antibody, clone DT9 (MABF233, Millipore Sigma), or 2  $\mu$ g/ $\mu$ L per well of anti-HLA-ABC antibody, clone W6/32 (MA1-70111). W6/32 targets the heavy chains of HLA-A, -B, and -C (Parham et al., 1979), and has been observed to bind HLA-E (Tremante et al., 2015). With both blocking antibodies, 0.5  $\mu$ g/ $\mu$ L of Fc Block (564220, BD Biosciences) was added per well to limit ADCC. After the incubation, the cells were washed. For the co-culture, the effector PBMCs were resuspended at  $5 \times 10^5$  cells/mL and added to wells with the tumor cells (100  $\mu$ L/well). After 5 hours, the cells were separated and stained for their respective flow cytometry analysis (see experimental timeline, **Figure 2.2A**).

### 2.3.2 PBMC co-culture post-anti-PD-1/PD-L1 blockade

A549 cells were treated with or without IFN- $\gamma$  at 1000 IU/mL once daily for 3 days, then plated in 48-well plates at  $1 \times 10^6$  cell/mL (200  $\mu$ L/well). The cells were incubated for 30 minutes with 2  $\mu$ g/mL anti-hPD-L1-hIgG1 (N298A, InvivoGen), then washed. Anti-hPD-L1-hIgG1 was designed to limit ADCC via N298A, an engineered hIgG1 which eliminates the ability of the antibody to bind Fc $\gamma$  receptors (InvivoGen, n.d.). PBMCs were resuspended at  $5 \times 10^5$  cells/mL (100  $\mu$ L/well) and incubated for 30 minutes with 6  $\mu$ g/mL anti-PD1 [NAT105] (ab52587, Abcam), then washed. Anti-PD1 was empirically tested and determined to not induce ADCC against other NK cells. The tumor cells were co-cultured with PBMCs as explained in 2.3.1 (see experimental design, **Figure 2.2B**).

## 2.3 Experimental Timelines

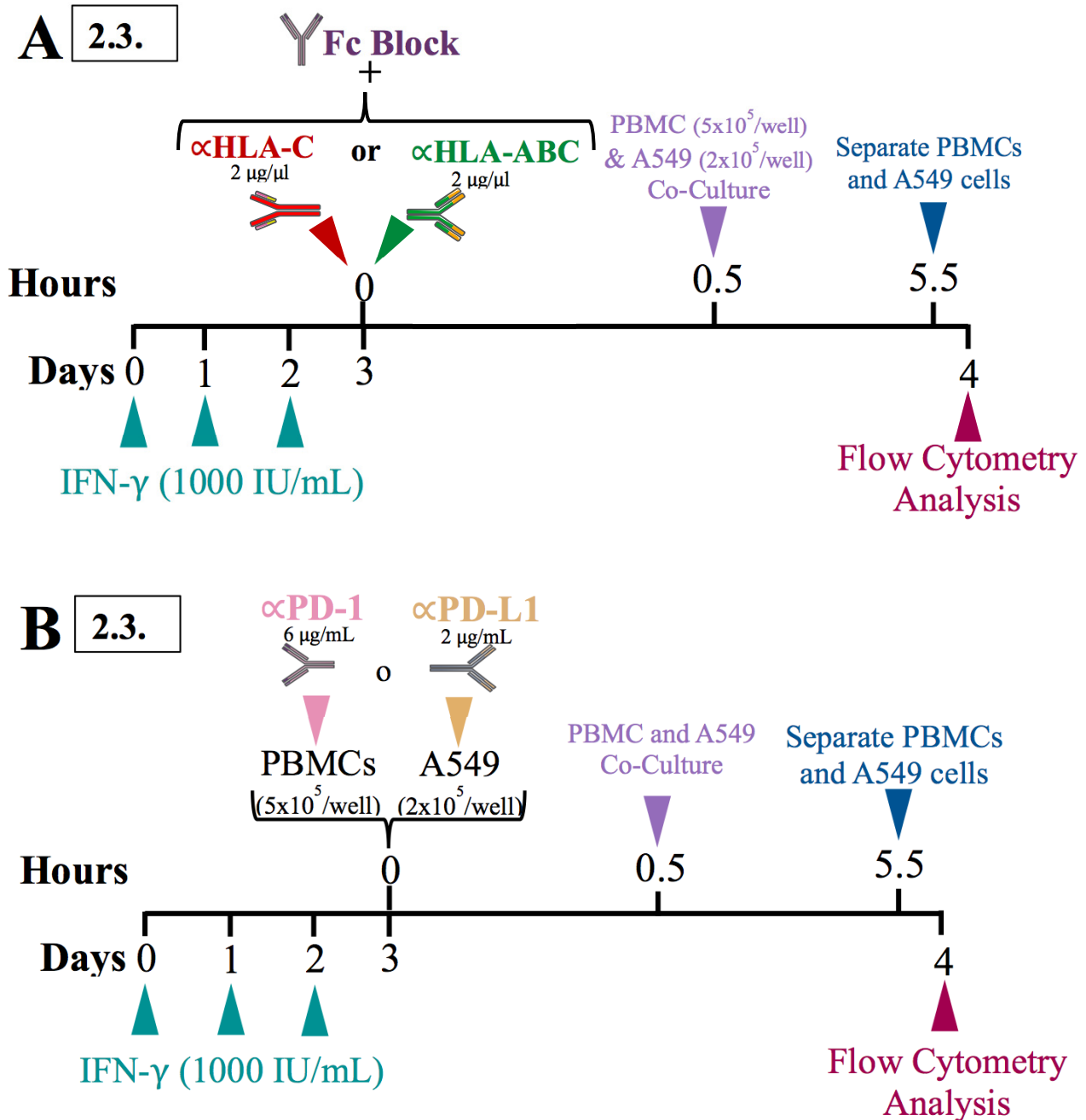


**Figure 2.2 Experimental timelines for tumor co-cultures with PBMCs.** (A) A549 cells were treated with or without IFN- $\gamma$  once per day for 3 days. A549 cells were incubated for 30 minutes with either an anti-HLA-C blocking antibody or a pan-HLA class I blocking antibody. The antibodies were washed off, then the cells were co-cultured with PBMCs for 5 hours, separated, and stained for flow cytometry. (B) A549 cells were treated with or without IFN- $\gamma$  once per day for 3 days. The A549 cells were incubated with an anti-PD-L1 blocking antibody and the PBMCs were incubated with an anti-PD-1 blocking antibody. After 30 minutes, the antibodies were washed off, then the cells were co-cultured for 5 hours, separated, and stained for flow cytometry.

### *2.3.3 PBMC co-culture post-chemotherapy treatment*

A549 cells were treated with either low, middle or high doses of trametinib or palbociclib, or the middle dose of both drugs as described in 2.2.4. The cells were resuspended and co-cultured as explained in 2.3.1).

### *2.3.4 PBMC co-culture post-irradiation*

A549 cells, resuspended in  $2-5 \times 10^6$  cells/mL in 1.5 mL microfuge tubes, were irradiated in the Gamma Cell at 0.5 Gy, 10 Gy, 100 Gy, 200 Gy, 400 Gy and 600 Gy. The cells were incubated for 72 hours, then co-cultured with PBMCs as explained in 2.3.1.

### *2.3.5 PBMC co-culture post-chemotherapy treatment with inhibitory ligand blockade*

A549 cells were treated with the middle dose of either trametinib (25 nM) or palbociclib (500 nM), or the middle dose of both drugs every 2 days for 8 days. The tumor cells were plated in 48-well plates at  $1 \times 10^6$  cell/mL (200  $\mu$ L/well), and incubated for 30 minutes with either 2  $\mu$ g/mL anti-hPD-L1-hIgG1, 2  $\mu$ g/ $\mu$ l per well of W6/32 or both, then washed off. The cells were co-cultured with PBMCs as explained in 2.3.1.

### *2.3.6 PBMC co-culture post-irradiation with inhibitory ligand blockade*

A549 cells were subjected to 5 Gy of irradiation on the Varian TrueBeam Linear Accelerator, then left to rest for either 1 or 5 days. PBMCs were resuspended at  $5 \times 10^5$  cells/mL (100  $\mu$ L/well) and incubated for 30 minutes with 6  $\mu$ g/mL anti-PD1. The tumor cells were plated in 48-well plates at  $1 \times 10^6$  cell/mL (200  $\mu$ L/well), and incubated with either 2  $\mu$ g/mL anti-hPD-L1-hIgG1, 2  $\mu$ l/well of anti-HLA-C antibody, 2  $\mu$ l/well of W6/32 or a combination of both PD-1/PD-L1 axis blocking antibodies and W6/32. With both HLA blocking antibodies, 1  $\mu$ L/well of Fc Block was added. After 30 minutes, the cells were washed, then co-cultured with PBMCs as explained in 2.3.1.



**Table 2.1 Experimental designs.**

Section	Title	Tumor Treatment	Effectors	Blocking Antibodies
2.2.1	<i>Stimulation of A549 Cells with IFN-<math>\gamma</math></i>	+/- IFN- $\gamma$ (1, 2, or 3 days)	N/A	N/A
2.2.2	<i>Stimulation of A549 cells with PBMCs</i>	+/- IFN- $\gamma$ (3 days)	PBMCs (1, 3, 5, or 10 hours)	N/A
2.2.3	<i>Stimulation of A549 cells with NK cell effectors</i>	+/- IFN- $\gamma$ (3 days)	PBMCs or NK cells (5 hours)	N/A
2.2.4	<i>Stimulation of A549 cells with chemotherapeutic agents</i>	2, 4, 6, or 8 days of: 1. Trametinib (5 nM, 25 nM, 125 nM) 2. Palbociclib (100 nM, 500 nM, 1500 nM) 3. Trametinib (25 nM) + Palbociclib (500 nM)	N/A	N/A
2.2.5	<i>Treatment of A549 cells with irradiation</i>	Irradiation (1, 3, or 5 days rest) - 0.5 Gy, 2 Gy, 5 Gy, or 10 Gy	N/A	N/A
2.3.1	<i>PBMC co-culture post-anti-PD-1/ anti-PD-L1 blockade</i>	+/- IFN- $\gamma$ (3 days)	PBMCs (5 hours)	1. anti-PD-L1 (2 $\mu$ g/mL) 2. anti-PD-1 (6 $\mu$ g/mL)
2.3.2	<i>PBMC co-culture post-HLA ligand blockade</i>	+/- IFN- $\gamma$ (3 days)	PBMCs (5 hours)	1. W6/32 (2 $\mu$ g/ $\mu$ L) 2. anti-HLA-C (2 $\mu$ g/ $\mu$ L)
2.3.3	<i>PBMC co-culture post-chemotherapy treatment</i>	8 days of: 1. Trametinib (5 nM, 25 nM, 125 nM) 2. Palbociclib (100 nM, 500 nM, 1500 nM) 3. Trametinib (25 nM) + Palbociclib (500 nM)	PBMCs (5 hours)	N/A
2.3.4	<i>PBMC co-culture post-irradiation</i>	Irradiation (3 days rest) - 0.5 Gy, 10 Gy, 100 Gy, 200 Gy, 400 Gy, or 600 Gy	PBMCs (5 hours)	N/A
2.3.5	<i>PBMC co-culture post-chemotherapy treatment with inhibitory ligand blockade</i>	8 days of: 1. Trametinib (25 nM) 2. Palbociclib (500 nM) 3. Trametinib (25 nM) + Palbociclib (500 nM)	PBMCs (5 hours)	1. anti-PD-L1 (2 $\mu$ g/mL) 2. W6/32 (2 $\mu$ g/ $\mu$ L) 3. anti-PD-L1 + W6/32
2.3.6	<i>PBMC co-culture post-irradiation with inhibitory ligand blockade</i>	Irradiation (1 or 5 days rest) - 0.5 Gy, 10 Gy, 100 Gy, 200 Gy, 400 Gy, or 600 Gy	PBMCs (5 hours)	1. anti-PD-L1 (2 $\mu$ g/mL) 2. anti-PD-1 (6 $\mu$ g/mL) 3. W6/32 (2 $\mu$ g/ $\mu$ L) 4. anti-HLA-C (2 $\mu$ g/ $\mu$ L) 5. anti-PD-L1 + anti-PD-1 + W6/32

## 2.4 Flow cytometry

### 2.4.1 Flow cytometry staining protocol

All spins were conducted at 300 x g for 5 minutes. The cells were transferred to v-bottom plates and spun to pellet. The Fixable Viability Dye eFluor 506 (ThermoFisher), aliquoted to 1  $\mu$ L in microfuge tubes, was resuspended in 1 mL of PBS according to the manufacturer's instructions. The Fixable Viability Dye eFluor 506 was added at 50  $\mu$ L to each well (1/1000), and the plate was incubated at room temperature in the dark. After 20 minutes, the wells were washed with 150  $\mu$ L PBS. Antibody cocktails specific for the tumor cells and effector cells were prepared in FACS buffer and added at 50  $\mu$ L to each well. The plate was incubated for 30 minutes at room temperature in the dark, followed by another wash with 150  $\mu$ L FACS buffer (PBS, 5% bovine serum albumin [Wisent], 1% sodium azide [EMD Millipore]) per well. The plate was centrifuged and resuspended in 50  $\mu$ L of 4% Paraformaldehyde (PFA, Sigma Aldrich) for 10 minutes. The cells were again washed and resuspended in 200  $\mu$ L FACS buffer.

### 2.4.2 Flow cytometry staining panels

To all the effector-stimulated wells in the experiments, 5  $\mu$ L (1/200) of anti-CD107a APC-H7 antibodies (H4A3) (BD Biosciences) was added before the co-incubation period of the effector and tumor cells. The effector cell flow cytometry panel is shown in **Table 2.2**. The tumor cells were stained with either an activating panel or an inhibitory panel (**Table 2.2**).

**Table 2.2 Flow cytometry antibodies and panels.**

Laser (excitation)	Fluoro-chrome	Marker	Biological Function	Clone	Dilution	Supplier	Panel
Violet 405 nm 100 mW	BV21	TRAIL (CD253)	Activating ligand	RIK-2	1/50	BD	1
	BV421	PD-L1	Inhibitory ligand	MIH1	1/150	BD	3
	eFluor506	Viability	/	/	1/1000	BD	1, 2, 3
	BV605	FasL	Activating ligand	NOK-1	1/30	BD	1
	BV650	CD3	T and NKT cell marker	UCHT1	1/400	BD	1
	PE-Cy5	HLA-ABC	Inhibitory ligand	G46-2.6	1/800	BD	3
	BV711	NKG2D (CD314)	Activating ligand	1D11	1/50	BD	1
	BV786	KIR3DL1 (CD158e)	NK cell KIR	DX9	1/200	BD	1
Blue 488 nm 60 mW	FITC	CFSE	Cell tracking	/	5 uM	ThermoFisher	2, 3
	AF-488	PD-1	Inhibitory receptor	913429	1/100	R&D	1
	PerCP-Vio700	KIR3DL1/S1 (CD158e1/e2)	NK cell KIR	REA293	1/200	Miltenyi	1
Green 532 nm 150 mW	PE	KIR2DL2/L3 (CD158b1/b2)	NK cell KIR	DX27	1/50	Miltenyi	1
	PE	HLA-F	Activating ligand	3D11	1/100	Cedarlane	2
	PE	HLA-C	Inhibitory ligand	DT9	1/100	BD	3
	ECD	CD56	NK cell marker	N901	1/50	Beckman	1
	PE-Vio615	Fas (CD95)	Death receptor	REA738	1/400	Miltenyi	2
	PE-Vio770	KIR2DL1 (CD158a)	NK cell KIR	REA284	1/100	Miltenyi	1
	PE-Vio770	TRAIL-R1 (CD261)	Death receptor	DJR1	1/200	Miltenyi	2
	PE-Vio770	HLA-E	Inhibitory ligand	3D12	1/50	Cedarlane	3
Red 628 nm 200 mW	APC	NKG2A (CD159a)	Inhibitory receptor	REA110	1/200	Miltenyi	1
	APC	TRAIL-R2 (CD262)	Death receptor	DR5	1/400	Cedarlane	2
	APC	HLA-Bw4	Inhibitory ligand	REA274	1/50	Miltenyi	3
	AF-700	CD69	Activation marker	FN50	1/80	BD	1
	APC-H7	CD107a	Degranulation marker	H4A3	1/200	BD	1
	APC-Vio770	MIC-A/B	Activating ligands	6D4	1/50	Miltenyi	2
	APC-Vio770	HLA-G	Inhibitory ligand	87G	1/50	Miltenyi	3

1 – effector cell panel; 2 – activating tumor panel; 3 – inhibitory tumor panel

### 2.4.3 Flow cytometry analysis

Stained cells were analyzed on the BD LSR Fortessa SORP using FACS Diva software to perform single-cell analysis (Dalhousie Faculty of Medicine CORE facility). To ensure consistency among geometric means, most experiments read on the Fortessa were preceded by Sphero™ 8 peak Rainbow Calibration Beads (Biolegend) and voltages were adjusted so that experimental measurements were consistent between calibration beads for each run. The fluorochromes were compensated to read the specific antibodies in the panel using compensation beads where possible, and stained cells when dyes were used (i.e. CFSE or live/dead). The compensation beads used were either anti-REA (Miltenyi Biotec) or anti-mouse (BD Biosciences), depending on the isotype of each antibody.

To prepare the compensation beads, one drop (~60 µL) of the positive and negative controls beads for the isotype of interest was added to create a mastermix (100 µL FACS buffer per sample). The mastermix was aliquoted and each sample was stained with 1 µL of a monoclonal antibody, then incubated for 10 minutes in the dark. The beads then were washed and resuspended in 400 µL of FACS buffer. On the Fortessa, the compensation beads for each antibody are used to ensure samples are on scale and correct for fluorescent spill from other fluorochrome channels.

Data were analyzed using FlowJo 10.7.1. Gating was performed by selecting for the tumor or effector cells based on the properties of forward scatter (FSC, size) and side scatter (SSC, complexity; **Figure 2.3**). Doublet cells were excluded from the analysis using FSC-height and -width, followed by SSC-height and -width. The dead cells were excluded through gating on the cell populations that were unstained with the Fixable Viability Dye eFluor 506. Fluorescence-minus-one (FMO) controls were included to validate staining and assist in gate placement. In some experiments, CFSE staining allowed monitoring of tumor cell proliferation of tumor cells following treatment; dilution would indicate that cells continued to proliferate (and may have died during culture), while non-proliferation in cells that remained viable would indicate the cells were prevented from dividing (**Figure 2.3A**). To identify NK cells, we gated CD3<sup>-</sup>CD56<sup>+</sup> cells (**Figure 2.3B**). Further gating to study single inhibitory receptor positive populations was subsequently carried out; a representative gating strategy is shown in **Figure 2.3B**.

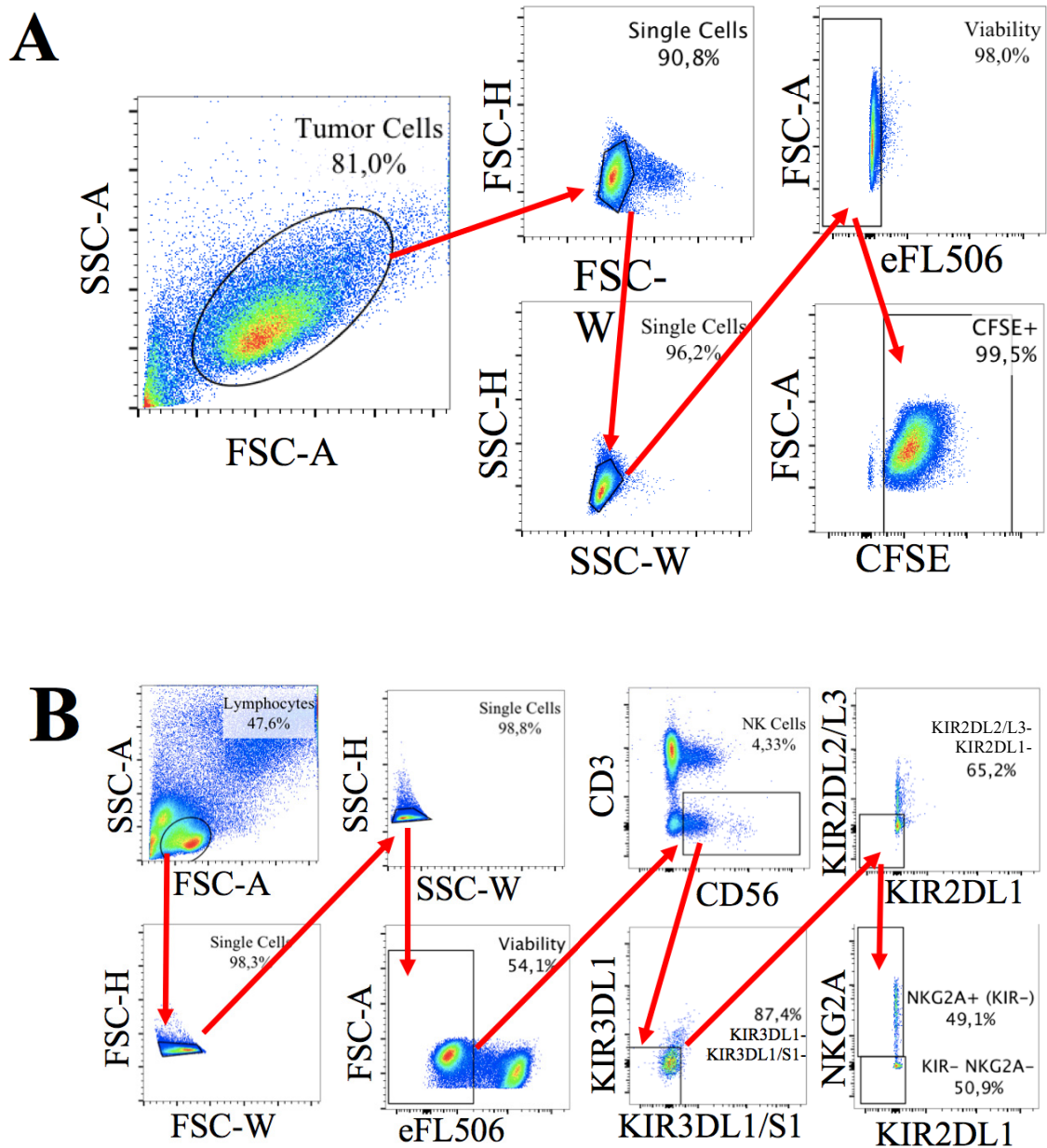


**Figure 2.3 Representative flow cytometry gating strategy for tumor cells (A) and NK cells (B).** Flow cytometry data was collected using a BD LSR Fortessa SORP and analysis was performed on FlowJo 10.7.1. Tumor cells (A) and lymphocytes (B) were gated based on their size and complexity through the forward scatter area (FSC-A) and side scatter area (SSC-A), respectively. Duplicate cells were excluded by gating the single cells using the forward scatter height (FSC-H) and forward scatter width (FSC-W), followed by the side scatter height (SSC-H) and side scatter width (SSC-W). The cells were stained with the Viability Dye eFl106, which allowed for the exclusion of stained dead cells. NK cells were gated on as CD3<sup>+</sup>CD56<sup>+</sup>, followed by representative gating for single inhibitory receptor positive NK cell populations (NKG2A<sup>+</sup> KIR<sup>-</sup>) and inhibitory receptor negative populations (KIR<sup>-</sup> NKG2A<sup>-</sup>).

## 2.5 Statistical analysis

Sample size requirements to power experiments at 80% (5% type I error rate) were determined using 1-Sample, 2-Sided Equality tests for tumor data, and 2-Sample, 2-Sided Equality tests for NK cell data (**Appendix Table 1; Appendix Table 2**). Samples were tested for normality with the Shapiro-Wilk normality test, and passed normality if  $\alpha=0.05$ . If one time point or condition within an experiment did not pass normality, but the rest of the conditions did, then the quantile-quantile (Q-Q) plots generated in GraphPad Prism (8.4.3) were analyzed visually. Q-Q plots are scatterplots that plot two sets of quantiles against one another; the theoretical quantiles (predicted values for Gaussian normal distribution) are plotted on the y-axis, and the actual quantiles are plotted on the x-axis (Ford, 2015). If the points form a straight line, then the quantiles came from the same distribution and we assumed normal distribution for that condition (Ford, 2015). We compiled a table including all graphs in this thesis that we assumed normal distribution for that had one condition not pass  $\alpha=0.05$  (**Appendix Table 3**). If the data passed normality, analysis of variance (ANOVA) and parametric matched ratio paired  $t$  tests were completed. If the data did not pass normality, paired non-parametric Wilcoxon  $t$  tests were performed.

## **CHAPTER 3: Results**

### **3.1 Monitoring tumor evolution by phenotyping following stimulation**

#### *3.1.1 Exposure to IFN- $\gamma$ induces rapid evolution of death receptors and activating and inhibitory ligands on A549 cells*

We hypothesized that changes would occur in the phenotype of tumors, and consequently their interactions with NK cells, in response to treatment and engagement with immune cells. To explore this possibility, we treated tumors with IFN- $\gamma$ , a hallmark cytokine of inflammation, and one frequently found in tumors undergoing treatment (Burke & Young, 2019). We treated A549 cells with 1000 IU/mL of IFN- $\gamma$  once per day for one, two, or three days, then analyzed the cells by flow cytometry. The impact of longer exposure and daily treatments with IFN- $\gamma$  was assessed by repeated measures (RM) 2-way ANOVA.

There was a significant interaction between time and IFN- $\gamma$  exposure inducing the upregulation of death receptor Fas (n=4, p=0.0018 [interaction]; **Figure 3.1B**), and inhibitory ligands HLA-ABC (n=4, p=0.0039 [interaction]), HLA-G (n=3, p=0.0349 [interaction]) and PD-L1 (n=4, p=0.0053 [interaction]; **Figure 3.2A, E, F**). Over three days with IFN- $\gamma$ , there was a non-significant upward trend of activating ligand HLA-F (n=4; **Figure 3.1C**) and inhibitory ligand and HLA-C (n=4; **Figure 3.2C**). Inhibitory HLA-Bw4 similarly trended upwards with longer IFN- $\gamma$  treatment (n=3; cannot assume normal distribution and requires larger sample size for Wilcoxon matched-pairs signed rank test; **Figure 3.2B**). The expression of HLA-C, determined through Sidak's multiple comparisons test, was significantly upregulated compared to untreated after 1 day of treatment (p=0.0320) and 2 days of treatment (p=0.0140). Compared with untreated cells, cells exposed to IFN- $\gamma$  exhibited significantly greater expression of activating ligand HLA-F (p=0.0417 [treatment]) and HLA-C (p=0.0002 [treatment]). Although most changes that occurred after one day remained high, we did observe a downward trend in expression of inhibitory ligand HLA-E after the initial upregulation compared to untreated (n=4, p=0.0061 [interaction]; **Figure 3.2D**). There was no clear trend for MIC-A/B (n=4), TRAIL-R1 (n=3) or TRAIL-R2 (n=4; **Figure 3.1A, D, E**). These results reflect the potential changes transpiring to tumor cells within the TME as inflammation occurs from therapy and incoming immune cells.

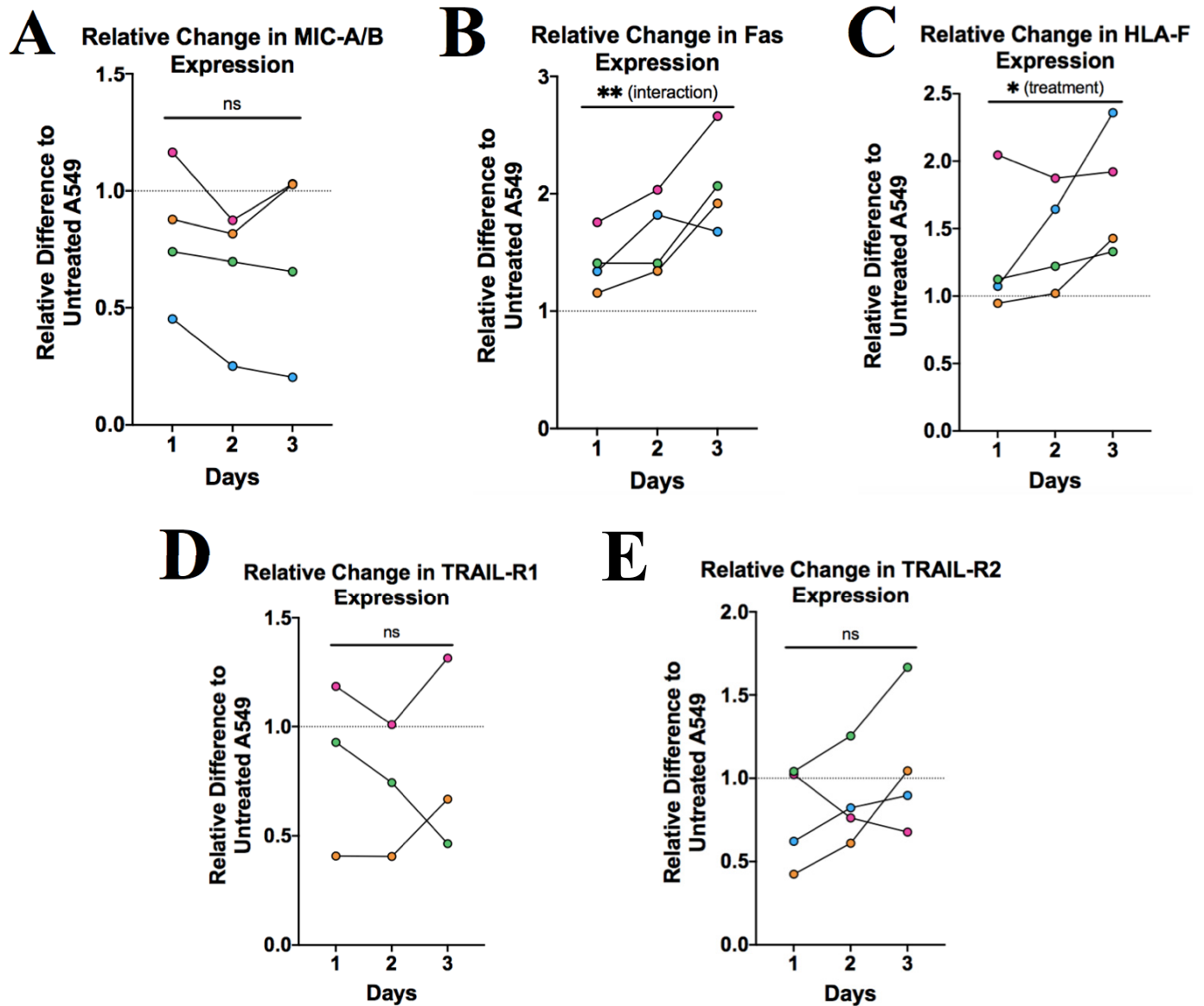


**Figure 3.1 Inflammation by exposure to IFN- $\gamma$  induces rapid upregulation of death receptor Fas and activating ligand HLA-F on A549 cells.** (A-E) A549 cells were treated with IFN- $\gamma$  (1000 IU/mL) once per day for 1, 2 or 3 days. The cells were stained for flow cytometry with Viability Dye eFl506, anti-MIC-A/B antibodies, anti-Fas antibodies, and anti-HLA-F antibodies, anti-TRAIL-R1 antibodies, and anti-TRAIL-R2 antibodies. The mean fluorescence intensities were normalized against untreated A549 cells to achieve the relative difference in tumor phenotypic evolution (n=3 or 4). RM 2-way ANOVA and Sidak's multiple comparisons test were performed comparing the tumor ligand changes with IFN- $\gamma$  stimulation at each time-point to untreated A549 cells. \* = significantly different from baseline as indicated by the line at y=1 (\*, p<0.05; \*\*, p<0.01; \*\*\*, p<0.001; \*\*\*\*, p<0.0001). Each colour represents a different experiment.



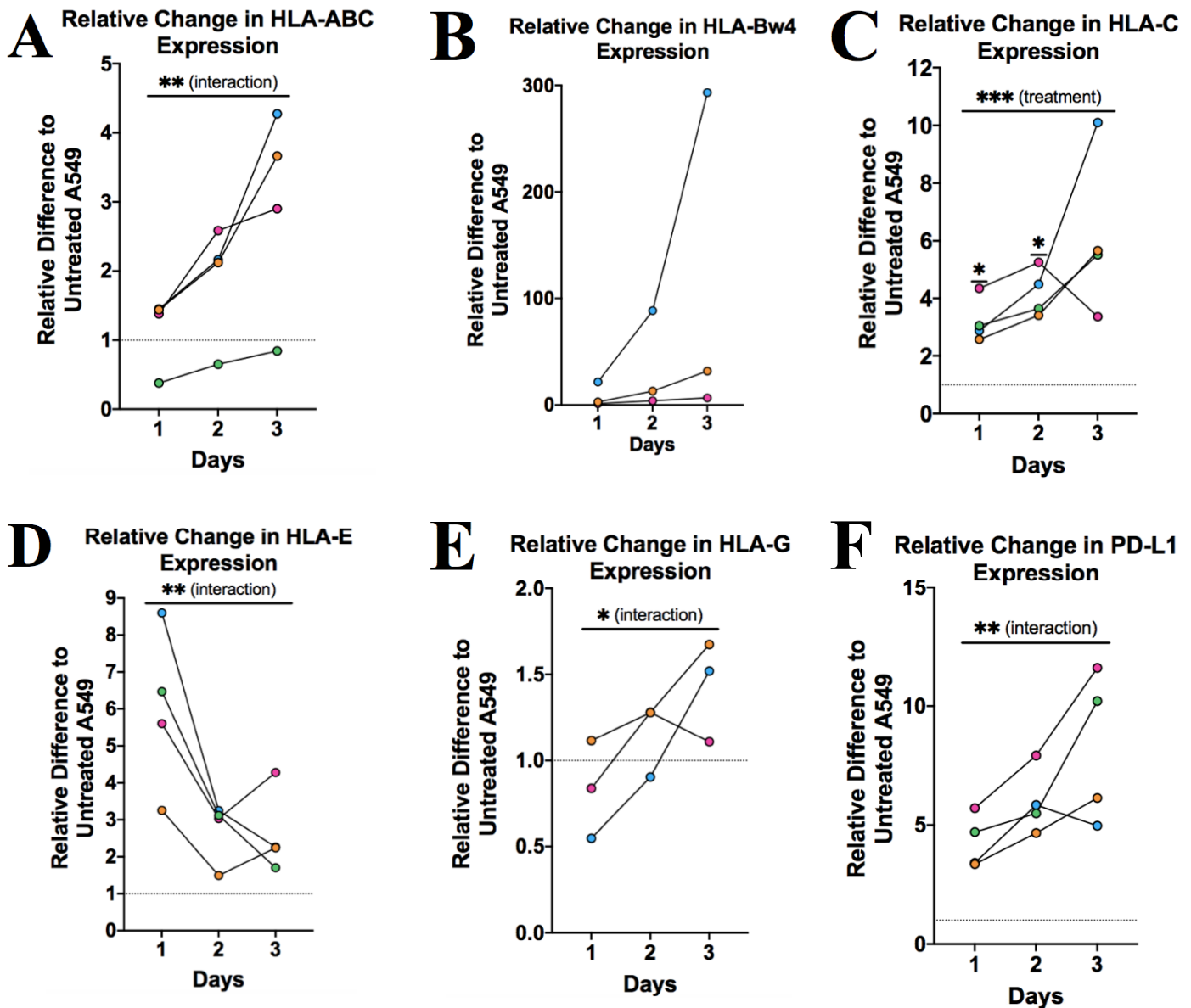


**Figure 3.2 Inflammation by exposure to IFN- $\gamma$  induces rapid evolution of inhibitory ligands on A549 cells.** (A-F) A549 cells were treated with IFN- $\gamma$  (1000 IU/mL) once per day for 1, 2 or 3 days. The cells were stained for flow cytometry with Viability Dye eF1506, anti-HLA-ABC antibodies, anti-HLA-Bw4 antibodies, anti-HLA-C antibodies, anti-HLA-E antibodies, anti-HLA-G antibodies, anti-PD-L1 antibodies. The mean fluorescence intensities were normalized against untreated A549 cells to achieve the relative difference in tumor phenotypic evolution ( $n=3$  or 4). RM 2-way ANOVA and Sidak's multiple comparisons test were performed comparing the tumor ligand changes with IFN- $\gamma$  stimulation at each time-point to untreated A549 cells. \* = significantly different from baseline as indicated by the line at  $y=1$  (\*,  $p<0.05$ ; \*\*,  $p<0.01$ ; \*\*\*,  $p<0.001$ ; \*\*\*\*,  $p<0.0001$ ). Each colour represents a different experiment.

### 3.1.2 PBMC pressure induces rapid evolution of death receptors and activating and inhibitory ligands on A549 cells

Lymphocytes engaging with tumor cells may produce IFN- $\gamma$ ; we therefore hypothesized that exposure to PBMC could change the phenotype of the tumor, including expression of activating and inhibitory ligands for NK cells, and therefore its sensitivity to immunotherapy. Hence, we next tested how PBMC pressure induces changes to tumor cells over time, when cocultured. We treated A549 cells with or without IFN- $\gamma$  for three days, then co-cultured the tumor cells with different PBMC donors for either 1, 3, 5, or 10 hours. The impact of longer exposure and PBMC treatment was assessed by separate RM 2-way ANOVAs with or without prior IFN- $\gamma$  treatment. Normal distribution could not be assumed for Fas (+ IFN- $\gamma$ ), HLA-F (+ IFN- $\gamma$ ) and TRAIL-R1 (+/- IFN- $\gamma$ ), and larger sample sizes are required to perform Wilcoxon matched-pairs signed rank test.

In the non-IFN- $\gamma$  treated conditions, there was a significant interaction between time and PBMC pressure inducing the upregulation of activating ligand MIC-A/B (n=3, p=0.0002 [interaction]), death receptor Fas (n=3, p=0.0100 [interaction]; **Figure 3.3A, B**), and the inhibitory ligands, HLA-ABC (n=3, p=0.0373 [interaction]), HLA-C (n=3, p<0.0001 [interaction]), HLA-E (n=3, p=0.0001 [interaction]), HLA-G (n=3, p<0.0001 [interaction]) and PD-L1 (n=3, p=0.0183 [interaction]; **Figure 3.4A, C, D, E, F**). A similar trend was observed for inhibitory ligand HLA-Bw4 (n=2; **Figure 3.4B**). Compared with untreated cells, PBMC pressure induced the significant upregulation of activating ligand HLA-F (n=3, p=0.0086 [treatment]). The death receptors TRAIL-R1 (n=3) and TRAIL-R2 (n=3) trended upwards for the first five hours compared to untreated A549 cells, and diminished after 10 hours, suggesting that these changes are acute and reversible under these conditions (**Figure 3.3D, E**). Alternatively, this could result from NK cells, increasingly activated in longer co-cultures, killing the TRAIL-R<sup>+</sup> tumor cells between hours five and 10 of the co-culture (n=4; **Figure 3.5**). This increase in NK cell activation was observed against both A549 cells treated with IFN- $\gamma$  and without.

In the IFN- $\gamma$  treated conditions, there was a significant interaction between time and PBMC pressure. We observed upregulation of the activating ligand MIC-A/B (n=3, p=0.0019 [interaction]; **Figure 3.3A**) and the inhibitory ligand HLA-G (n=3, p=0.0044

[interaction]; **Figure 3.4E**). We observed an initial upregulation from untreated cells (as expected with IFN- $\gamma$  treatment [**Figure 3.1, 3.2**]) at the 1 hour mark, which decreased over the subsequent 9 hours towards baseline levels for death receptor TRAIL-R2 (n=3, p=0.0386 [interaction]; **Figure 3.3F**) and inhibitory ligands HLA-ABC (n=3, p<0.0001 [interaction]), HLA-Bw4 (n=2), and HLA-E (n=3, p<0.0001 [interaction]; **Figure 3.4A, B, D**). PBMC pressure and IFN- $\gamma$  treatment induced significantly greater expression levels of inhibitory ligands HLA-C (n=3, p=0.0086 [treatment]) and PD-L1 (n=3, p=0.0023 [treatment]; **Figure 3.4C, F**), and non-significantly greater expression levels of activating ligand HLA-F (n=3) and death receptor Fas (n=3; **Figure 3.3B, C**). There were no significant differences in expression for TRAIL-R1 (n=3; **Figure 3.3D**). Overall, these results reflect that tumors are rapidly evolving phenotypically in the presence of IFN- $\gamma$  and PBMCs, which we hypothesized reflects the activity of NK cell-tumor interactions.

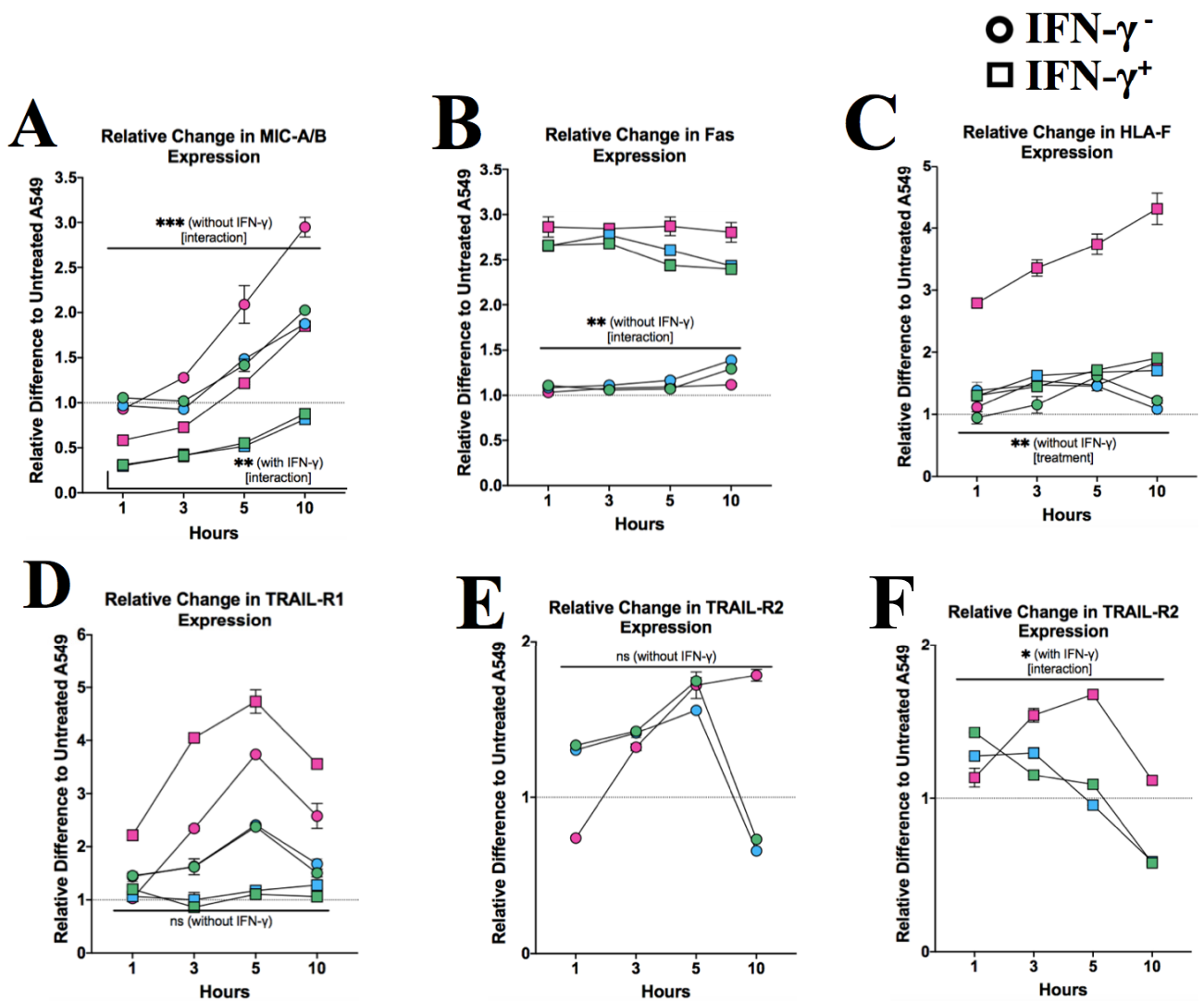


**Figure 3.3 PBMC pressure on A549 cells induces rapid evolution of death receptors and activating ligands, both with and without IFN- $\gamma$  stimulation.** (A-F) A549 cells were treated with or without IFN- $\gamma$  (1000 IU/mL) once per day for three days. The A549 cells were co-cultured with PBMCs for either 1, 3, 5, or 10 hours, then separated. The tumor cells were stained for flow cytometry with Viability Dye eF1506, anti-MIC-A/B antibodies, anti-Fas antibodies, and anti-HLA-F antibodies, anti-TRAIL-R1 antibodies, and anti-TRAIL-R2 antibodies. The mean fluorescence intensities were normalized against untreated A549 cells to achieve the relative difference in tumor phenotypic evolution (n=3). RM 2-way ANOVA were performed comparing the tumor ligand changes with PBMC pressure at each time-point to untreated A549 cells. The conditions were grouped as A549 cells treated with and without IFN- $\gamma$ . \* = significantly different from baseline as indicated by the line at y=1 (\*, p<0.05; \*\*, p<0.01; \*\*\*, p<0.001; \*\*\*\*, p<0.0001). Each colour represents a different experiment, circles represent A549 cells without IFN- $\gamma$ , and squares represent A549 cells treated with IFN- $\gamma$ . The experiments were completed in replicates, as indicated by the error bars.

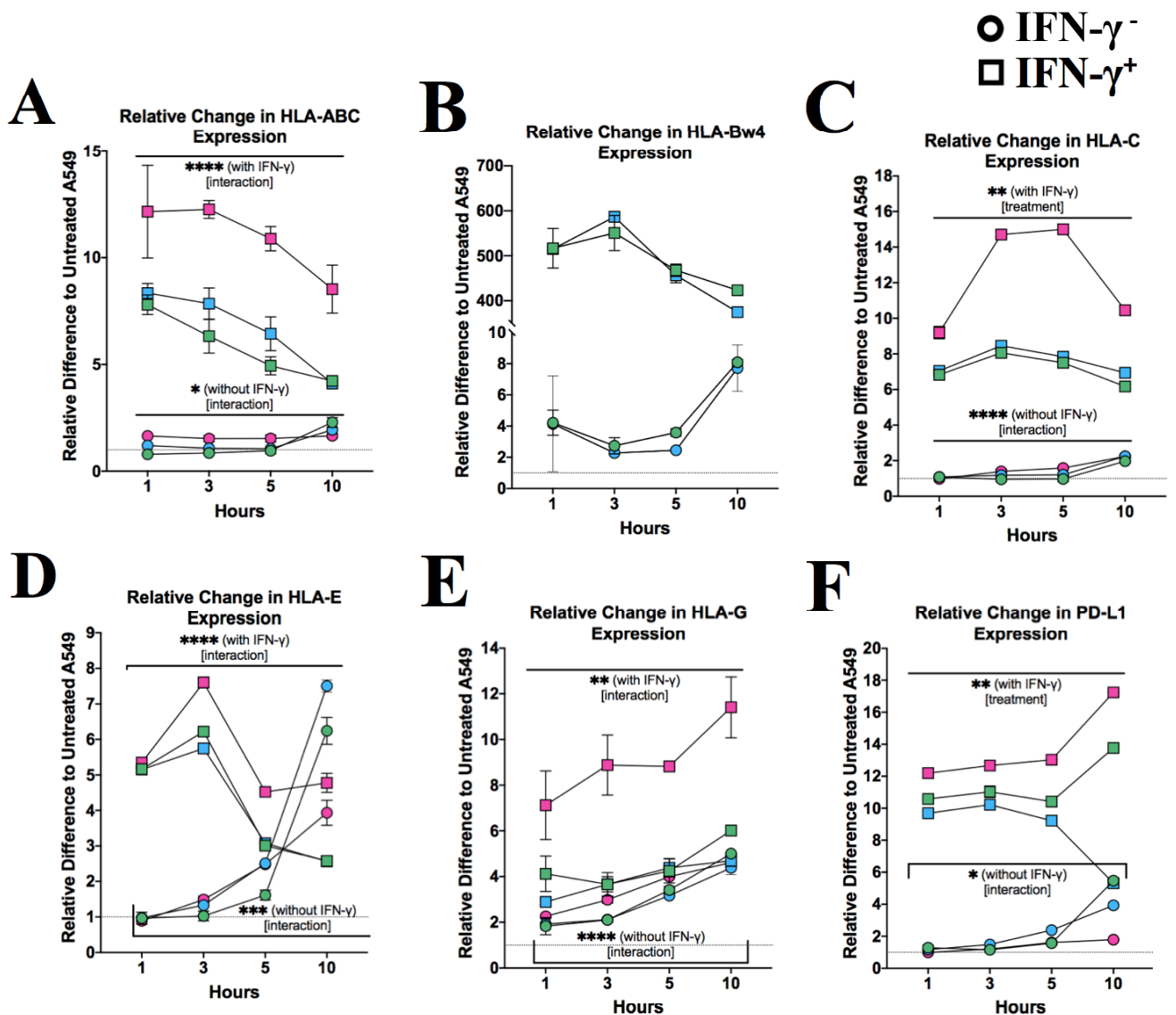


**Figure 3.4 PBMC pressure on A549 cells induces rapid evolution of inhibitory ligands, both with and without IFN- $\gamma$  stimulation.** (A-F) A549 cells were treated with or without IFN- $\gamma$  (1000 IU/mL) once per day for three days. The A549 cells were co-cultured with PBMCs for either 1, 3, 5, or 10 hours, then separated. The tumor cells were stained for flow cytometry with Viability Dye eFl506, anti-HLA-ABC antibodies, anti-HLA-Bw4 antibodies, anti-HLA-C antibodies, anti-HLA-E antibodies, anti-HLA-G antibodies, anti-PD-L1 antibodies. The mean fluorescence intensities were normalized against untreated A549 cells to achieve the relative difference in tumor phenotypic evolution (n=3). RM 2-way ANOVA were performed comparing the tumor ligand changes with PBMC pressure at each time-point to untreated A549 cells. The conditions were grouped as A549 cells treated with and without IFN- $\gamma$ . \* = significantly different from baseline as indicated by the line at y=1 (\*, p<0.05; \*\*, p<0.01; \*\*\*, p<0.001; \*\*\*\*, p<0.0001). Each colour represents a different experiment, circles represent A549 cells without IFN- $\gamma$ , and squares represent A549 cells treated with IFN- $\gamma$ . The experiments were completed in replicates, as indicated by the error bars.

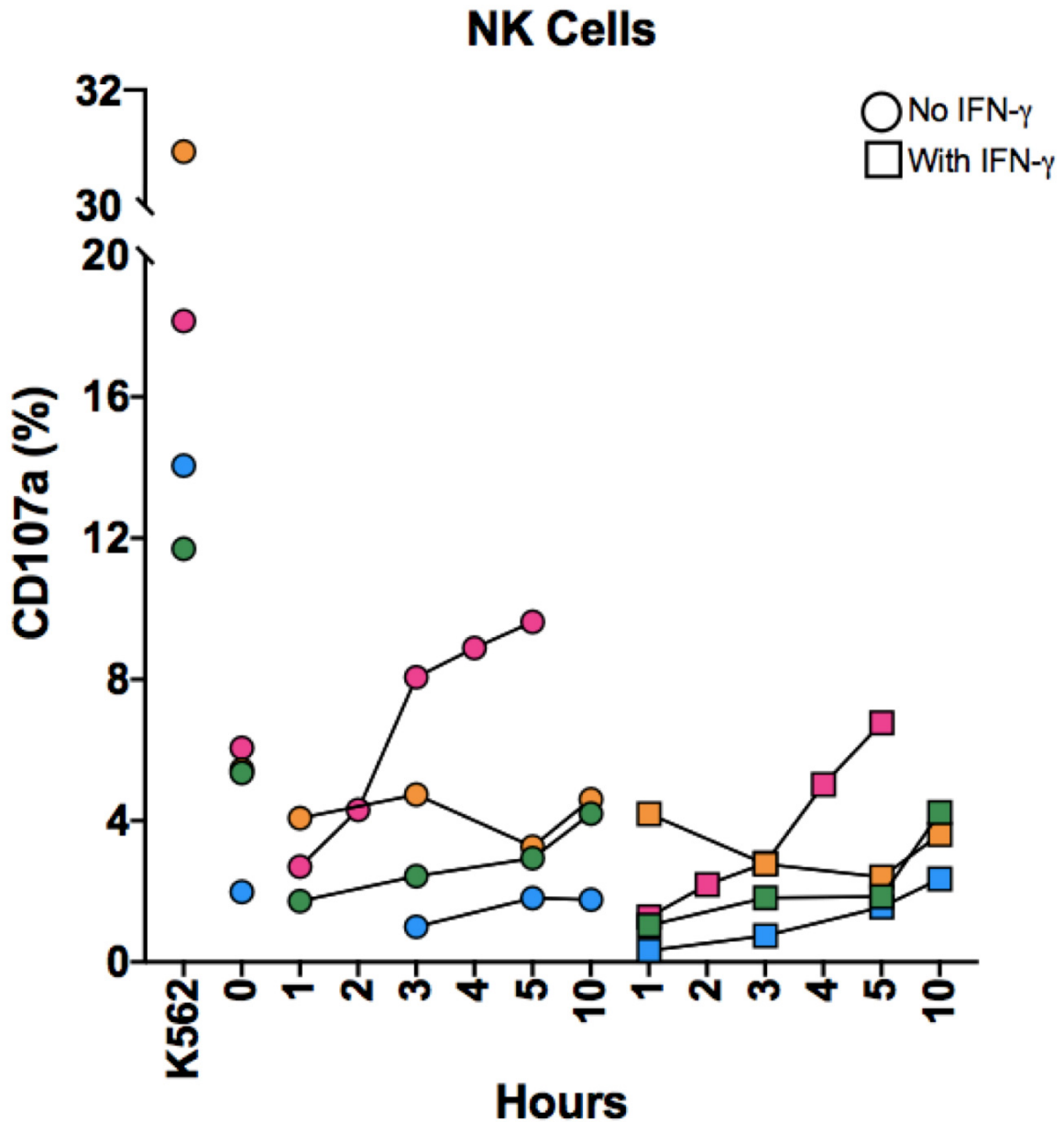


**Figure 3.5 NK cell activation increases with longer co-cultures with A549 cells treated with or without IFN- $\gamma$ .** A549 cells were treated with or without IFN- $\gamma$  (1000 IU/mL) once per day for 3 days. A549 cells were co-cultured with PBMCs for either 1, 2, 3, 4, 5, or 10 hours, then separated. PBMCs were co-culture for five hours with K562 cells as a positive control. PBMCs were stained for flow cytometry with Viability Dye eF1506, anti-CD3 antibodies, anti-CD56 antibodies, and anti-CD107a antibodies. NK cells (CD3<sup>-</sup> CD56<sup>+</sup>) were gated on, and the percent of responding cells was determined by the frequency of CD107a<sup>+</sup> cells in each population (min. 50 NK cells for analysis). Each colour represents a different PBMC donor.

### 3.1.3 NK cell pressure induces rapid evolution of MIC-A/B and HLA-G on A549 cells

We hypothesized that the phenotypic changes induced on A549 cells by PBMCs were mediated by NK cells. To test this, we compared the tumor expression changes on cells treated with or without IFN- $\gamma$  challenged with either total PBMCs, or the NK cells isolated from the same donors. The quantity of NK cells per well was calculated to match the number of NK cells in the PBMC fraction. The impact of IFN- $\gamma$  treatment and effector pressure was assessed by RM 2-way ANOVAs. Tukey's multiple comparisons tests were used to compare between effector types, and paired t-tests were used to compare IFN- $\gamma$ -treated tumor cells' expression levels between conditions with and without effector pressure. Normal distribution could not be assumed for Fas and TRAIL-R1, and larger sample sizes are required to perform Wilcoxon matched-pairs signed rank test.

Similar changes occurred when tumor cells were cultured with total PBMC or the isolated NK cell fraction. There was a significant interaction between IFN- $\gamma$  treatment and effector pressure inducing the upregulation of HLA-ABC (n=5, p=0.0001 [interaction]), HLA-C (n=4, p=0.0045 [interaction]), HLA-E (n=4, p=0.0009 [interaction]), and PD-L1 (n=5, p=0.0203 [interaction]; **Figure 3.7A, C, D, E, F**). Of the remaining ligands and receptors, the impact of IFN- $\gamma$  treatment independently induced a significant upregulation of HLA-F (n=4, p=0.0112 [IFN- $\gamma$ ]; **Figure 3.6C**), HLA-Bw4 (n=5, p=0.0314 [IFN- $\gamma$ ]; **Figure 3.7B**), and HLA-G (n=4, p=0.0403 [IFN- $\gamma$ ]; **Figure 3.7E**). The co-culture with effector cells induced a significant upregulation in comparison to untreated cells of MIC-A/B (n=4, p<0.0001 [effectors]; **Figure 3.6A**) and HLA-G (n=4, p<0.0001 [effectors]; **Figure 3.7E**). These results support our findings from 3.1.1 and 3.1.2 in that both IFN- $\gamma$  and immune cell pressure promote tumor evolution, either independently or potentially additively.

Our comparison between effector populations through Tukey's multiple comparison tests revealed similar results between PBMCs and isolated NK cells for inducing tumor evolution. In the conditions without IFN- $\gamma$  pre-treatment, we observed a significant upregulation compared with untreated A549 cells of MIC-A/B in the presence of PBMC or NK cells (n=4, p=0.0001 with PBMCs, p=0.0003 with NK cells) and HLA-

G (n=3, p=0.0004 with PBMCs, p=0.0009 with NK cells). These results suggest NK cells are the primary cells inducing changes in MIC-A/B and HLA-G expression.

In the conditions with pre-treatment of IFN- $\gamma$ , we observed a significant upregulation of MIC-A/B (n=4, p=0.0034 with PBMCs, p=0.0011 with NK cells), and paired t tests revealed that this upregulation in expression for both PBMCs and NK cells was significantly higher than IFN- $\gamma$  alone, without PBMCs or NK cells (p=0.0364 with PBMCs, p=0.0163 with NK cells). Of the other activating ligands and death receptors, Fas, HLA-F and TRAIL-R1 trended similarly, but more repeats are required to draw this conclusion. There were no clear trends in changing expression levels for TRAIL-R2. For the inhibitory ligands, we observed a significant upregulation with pressure from both effectors on HLA-ABC (n=5, p<0.0001 with PBMCs, p<0.0001 with NK cells), HLA-C (n=4, p=0.0001 with PBMCs, p=0.0002 with NK cells), HLA-E (n=4, p<0.0001 with PBMCs, p=0.0005 with NK cells), HLA-G (n=4, p<0.0001 with PBMCs, p<0.0001 with NK cells), and PD-L1 (n=5, p=0.0007 with PBMCs, p=0.00037 with NK cells). Of these, the only ligands that were significantly upregulated with effector pressure in comparison to the IFN- $\gamma$  control without effectors were HLA-ABC (p=0.0088 with PBMCs, p=0.0078) and HLA-G (p=0.0160 with PBMCs, p=0.0054). Overall, these results revealed that NK cells promote the upregulation of MIC-A/B and HLA-G independently, and contribute additively with prior IFN- $\gamma$  treatment to induce HLA-ABC upregulation. The phenotypic changes observed in the remaining ligands and death receptors require further experiments to confirm the role of NK cell pressure, as these results suggest these effectors are likely contributing to tumor evolution.



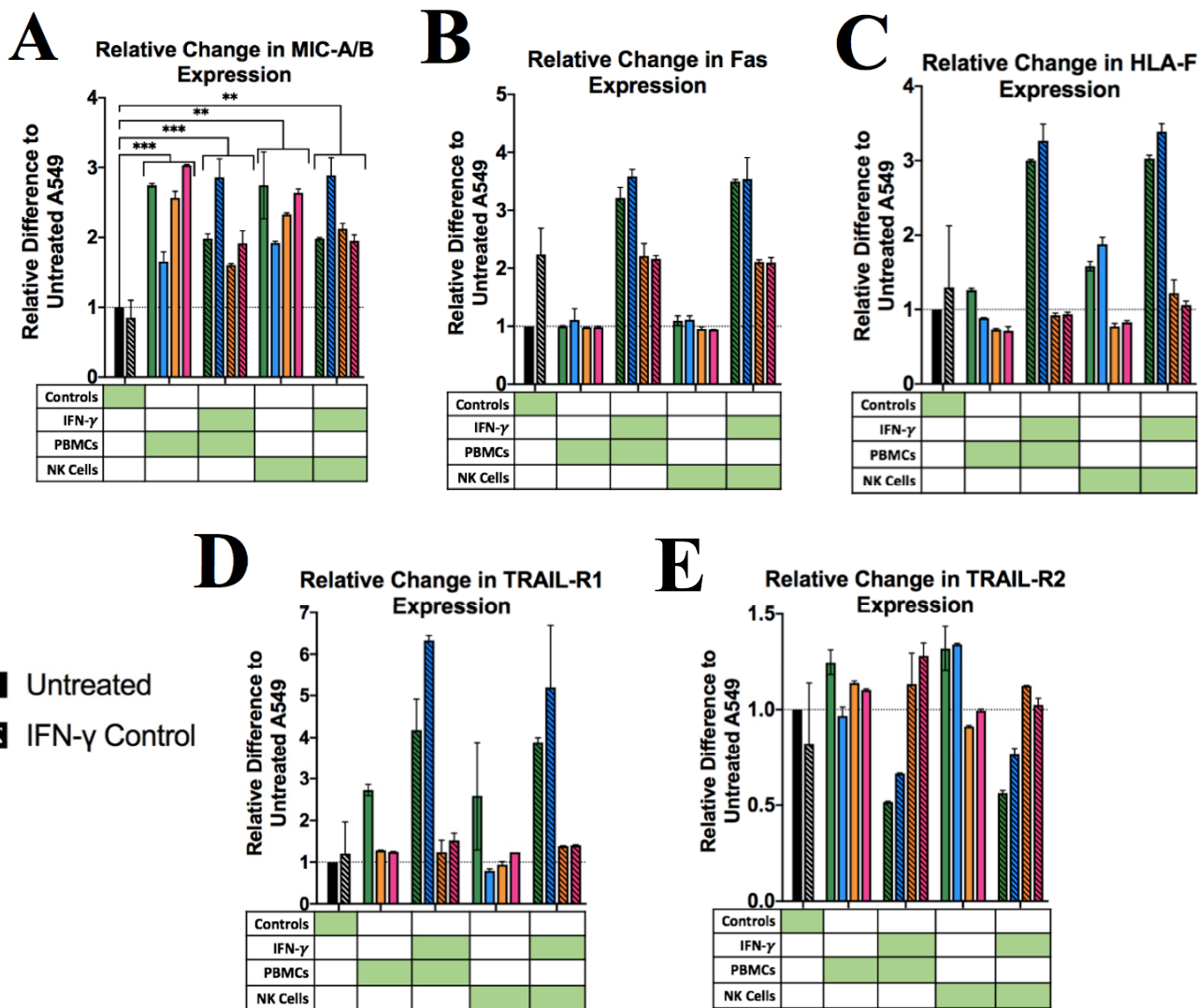


**Figure 3.6 NK cell pressure contributes to rapid MIC-A/B phenotypic evolution induced by PBMC co-cultures.** (A-E) A549 cells were treated with or without IFN- $\gamma$  (1000 IU/mL) once per day for 3 days. A549 cells were co-cultured separately with effector cells (either PBMCs or isolated NK cells) then separated. A549 cells were stained for flow cytometry with Viability Dye eF1506, anti-MIC-A/B antibodies, anti-Fas antibodies, and anti-HLA-F antibodies, anti-TRAIL-R1 antibodies, and anti-TRAIL-R2 antibodies. The mean fluorescence intensities were normalized against untreated A549 cells to achieve the relative difference in tumor phenotypic evolution (n=4). RM 2-way ANOVA and Tukey's multiple comparisons tests were performed comparing the tumor ligand changes with different effectors to untreated A549 cells. Two-tailed matched t tests were performed comparing the IFN- $\gamma$  control to the IFN- $\gamma$ -treated tumor cells with effector pressure. \* = significantly different from baseline as indicated by the line at y=1 (\*, p<0.05; \*\*, p<0.01; \*\*\*, p<0.001; \*\*\*\*, p<0.0001). The four clustered bars represent four experimental replicates. Each colour represents an experiment with a different effector donor, and the diagonal lines indicate tumor cells treated with IFN- $\gamma$ .

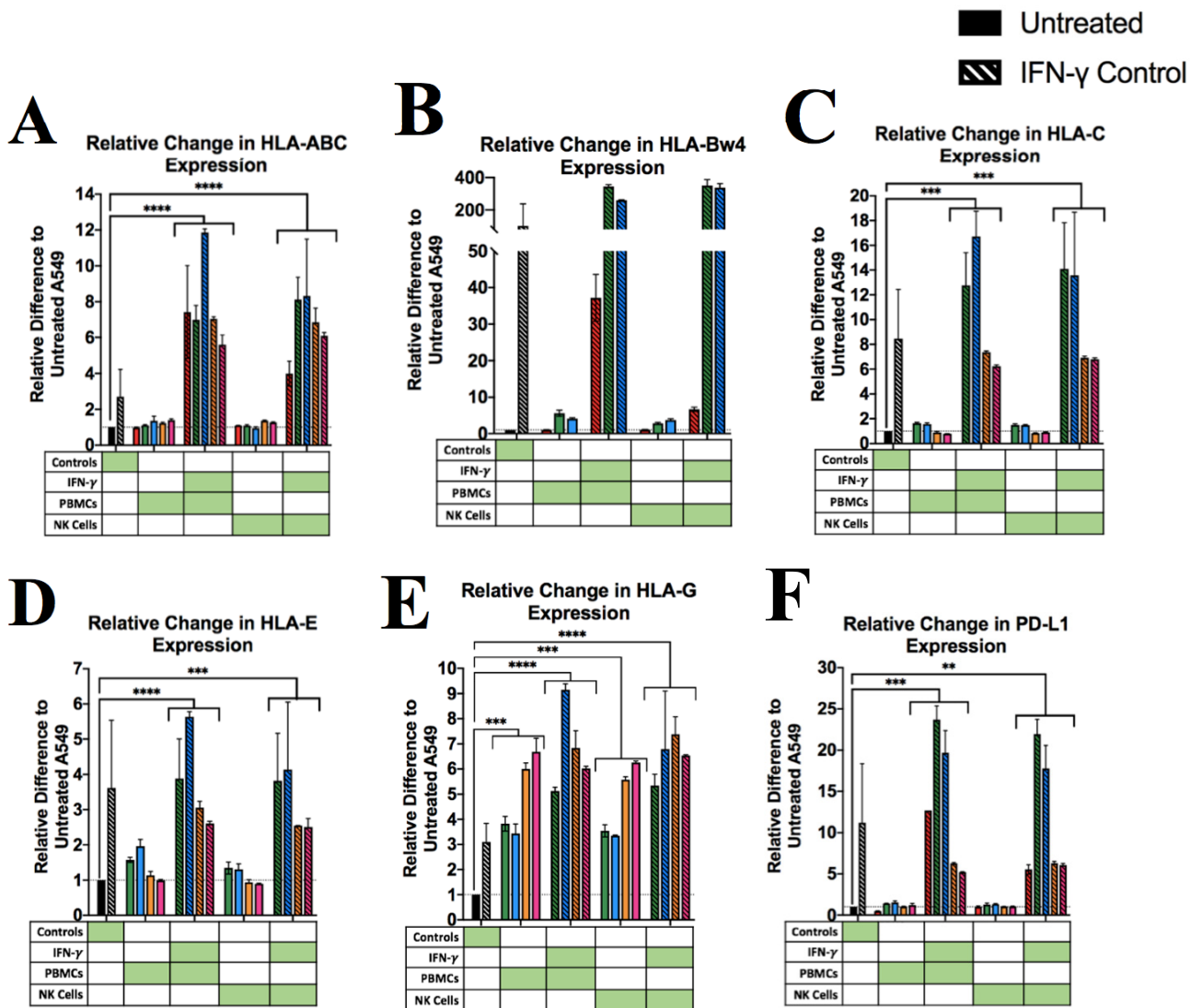


**Figure 3.7 NK cell pressure contributes to rapid inhibitory ligand phenotypic evolution induced by PBMC co-cultures.** (A-F) A549 cells were treated with or without IFN- $\gamma$  (1000 IU/mL) once per day for 3 days. A549 cells were co-cultured separately with effector cells (either PBMCs or isolated NK cells) then separated. A549 cells were stained for flow cytometry with Viability Dye eF1506, anti-HLA-ABC antibodies, anti-HLA-Bw4 antibodies, anti-HLA-C antibodies, anti-HLA-E antibodies, anti-HLA-G antibodies, anti-PD-L1 antibodies. The mean fluorescence intensities were normalized against untreated A549 cells to achieve the relative difference in tumor phenotypic evolution (n=4). RM 2-way ANOVA and Tukey's multiple comparisons tests were performed comparing the tumor ligand changes with different effectors to untreated A549 cells. Two-tailed matched t tests were performed comparing the IFN- $\gamma$  control to the IFN- $\gamma$ -treated tumor cells with effector pressure. \* = significantly different from baseline as indicated by the line at y=1 (\*, p<0.05; \*\*, p<0.01; \*\*\*, p<0.001; \*\*\*\*, p<0.0001). The four clustered bars represent four experimental replicates. Each colour represents an experiment with a different effector donor, and the diagonal lines indicate tumor cells treated with IFN- $\gamma$ . The red bars in HLA-ABC, HLA-Bw4 and PD-L1 were completed in my Undergrad Honours research.

### *3.1.4 Palbociclib and trametinib chemotherapy induces death receptors and upregulation of activating and inhibitory ligands in dose- and time-dependent manners*

Our data reveal an interaction between tumor and NK cells that may be exploited to support control of NSCLC, especially when it is incompletely controlled by therapeutic interventions. A combination of two cytostatic small molecules, palbociclib (a CDK4/6 inhibitor) and trametinib (a MEK1/2 inhibitor), have demonstrated to promote NK cell activity when given in combination to *KRAS*-mutant lung tumors (Ruscetti et al., 2018). We treated A549 cells with three doses of each drug and the middle dose of both, and examined the changes in expression of ligands for NK cell receptors at four time-points. The impact of longer exposure and chemotherapy treatments was assessed by RM 2-way ANOVA between all treatment groups, and individual tests within the palbociclib-treated cells, the trametinib-treated cells, and the combination-treated cells. Normal distribution could not be assumed for HLA-Bw4, and a larger sample size is required to perform Wilcoxon matched-pairs signed rank test.

Within all chemotherapy conditions, compared to untreated cells, the impact of longer exposure to the small molecules and the increasing dosing had a significant effect on the upregulation of Fas (n=3, p=0.0400 [interaction]; **Figure 3.8B**), and HLA-C (n=3, p=0.0002 [interaction]), HLA-E (n=2, p=0.0008 [time], p=0.0233 [treatment]), and PD-L1 (n=3, p=0.0142 [interaction]; **Figure 3.9C, E, F**). The ligands that were significantly upregulated by longer exposure to both small molecules include HLA-F (n=3, p=0.0002 [time]) and TRAIL-R2 (n=3, p=0.0008 [time]; **Figure 3.8C, E**), and HLA-G (n=3, p<0.0001 [time]; **Figure 3.9G**).

In comparison to untreated A549 cells, the palbociclib-treated cells demonstrated significant upregulation of HLA-C (n=3, p=0.0252 [time], p=0.0118 [treatment]) and HLA-G (n=3, p=0.0119 [time]). Our results revealed non-significant trends among all death receptors and activating and inhibitory ligands of greater expression with higher doses of palbociclib, particularly after 6 and 8 days. These expression change trends with palbociclib treatment generally resulted in greater expression compared to the untreated cells, predominantly at the high dose. Increasing doses of trametinib and later timepoints resulted in the significant upregulation of Fas (n=3, p=0.0322 [time]), HLA-F (n=3, p=0.0047 [time]), TRAIL-R2 (n=3, p=0.0440 [treatment], p=0.0010 [time]), HLA-C

(n=3, p=0.0051 [interaction]), HLA-E (n=3, p=0.0238 [time]), HLA-G (n=3, p=0.0112 [interaction]), and PD-L1 (n=3, p=0.0200 [time]). When comparing the two small molecules, our results reveal that trametinib treatments generally induce greater inhibitory ligand upregulation than palbociclib, but both small molecules similarly induced upregulation of activating ligands.

The combination treatment of both drugs induced similar levels of activating ligand upregulation as seen with the individual treatments, but lower inhibitory ligand upregulation than that is observed with high doses of trametinib (no significance from combination-treated only 2-way ANOVA). Through a 2-way ANOVA, we compared the differences of ligand expression change between the middle dose of palbociclib, trametinib, and the combination treatment; this test did not reveal any significant results. Overall, these results suggest that combining the MEK inhibitor and CDK 4/6 inhibitor could be inducing an immunostimulatory tumor phenotype by slowing the inhibitory ligand upregulation (as seen with high doses of trametinib) while maintaining upregulation of death receptors and activating ligands.

We hypothesized that because the chemotherapeutics are cytostatic drugs, we would see a change in proliferation of A549 cells. We stained the cells with CFSE prior to treatments for the main purpose of tracking the tumor cells that directly received the full length/dose of treatment, as opposed to cells that were newly proliferating and exposed to only a fraction of the treatment, or outgrowing as resistant cells. When we analyzed the live tumor populations for CFSE fluorescence, our results revealed that CFSE diluted from 2 days to 8 days, signifying continued proliferation of the tumor cells (**Figure 3.10**). The comparison between high and low doses of either chemotherapies demonstrates higher CFSE remained in higher doses, signifying slower proliferation. Although the cell proliferation was slowed, cells remained, further supporting addition of NK cells to complete the killing of tumors.

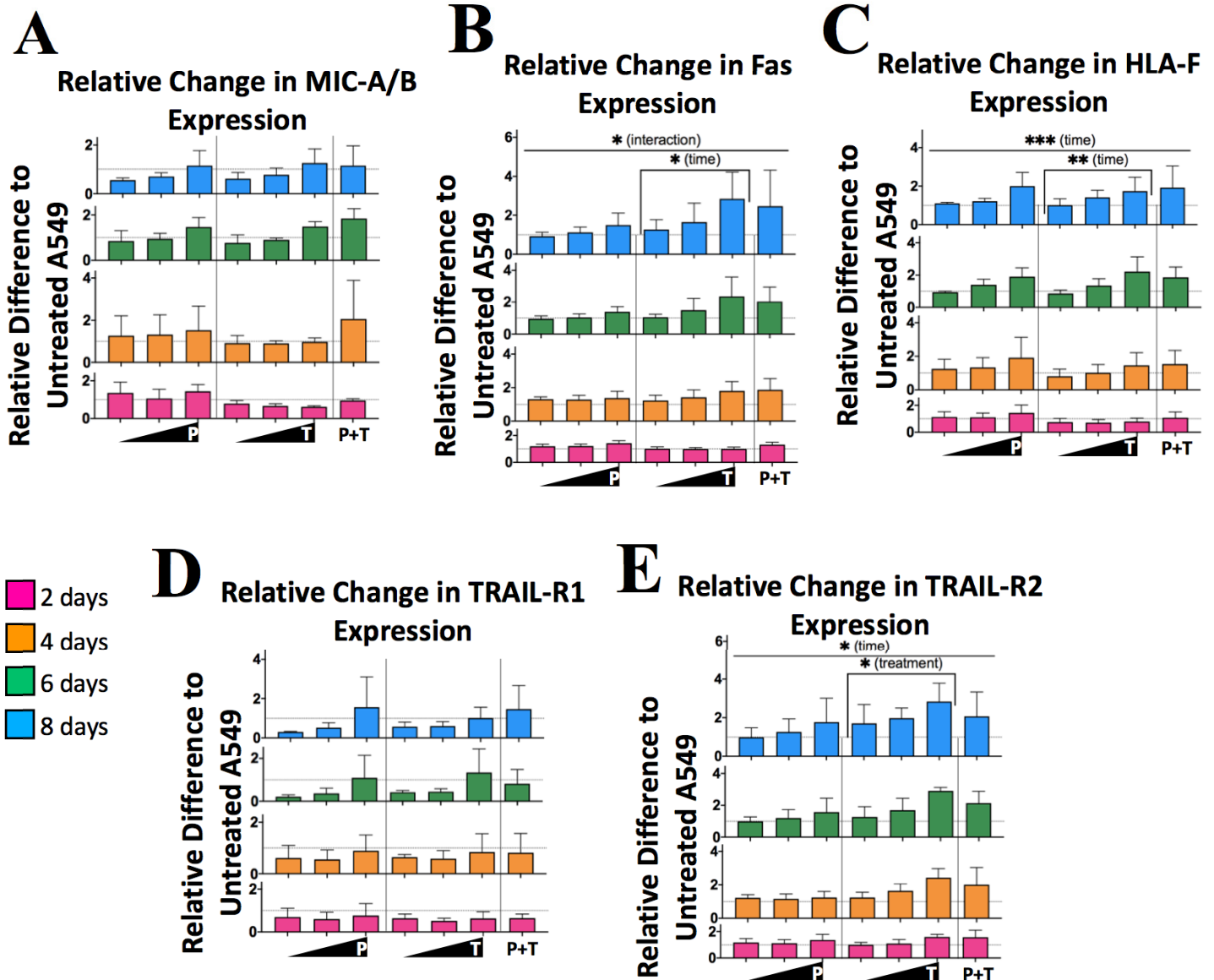


**Figure 3.8 Palbociclib (P) and Trametinib (T) chemotherapy treatments induce death receptor and activating ligand upregulation in a dose- and time-dependent manner.** (A-E) A549 cells were treated with either low, middle or high doses of either Trametinib (5 nM, 25 nM, 125 nM) or Palbociclib (100 nM, 500 nM, 1500 nM), or the middle dose of both drugs every two days. The cells were treated for either two, four, six or eight days, then stained for flow cytometry with Viability Dye eF1506, anti-MIC-A/B antibodies, anti-Fas antibodies, and anti-HLA-F antibodies, anti-TRAIL-R1 antibodies, and anti-TRAIL-R2 antibodies. The mean fluorescence intensities were normalized against untreated A549 cells to achieve the relative difference in tumor phenotypic evolution (n=3; n=2 for TRAIL-R1). RM 2-way ANOVAs were performed comparing the tumor ligand changes to untreated A549 cells within all treatment groups, and within Palbociclib doses alone, Trametinib doses alone, or the combination alone. \* = significantly different from baseline as indicated by the line at y=1 (\*, p<0.05; \*\*, p<0.01; \*\*\*, p<0.001; \*\*\*\*, p<0.0001).

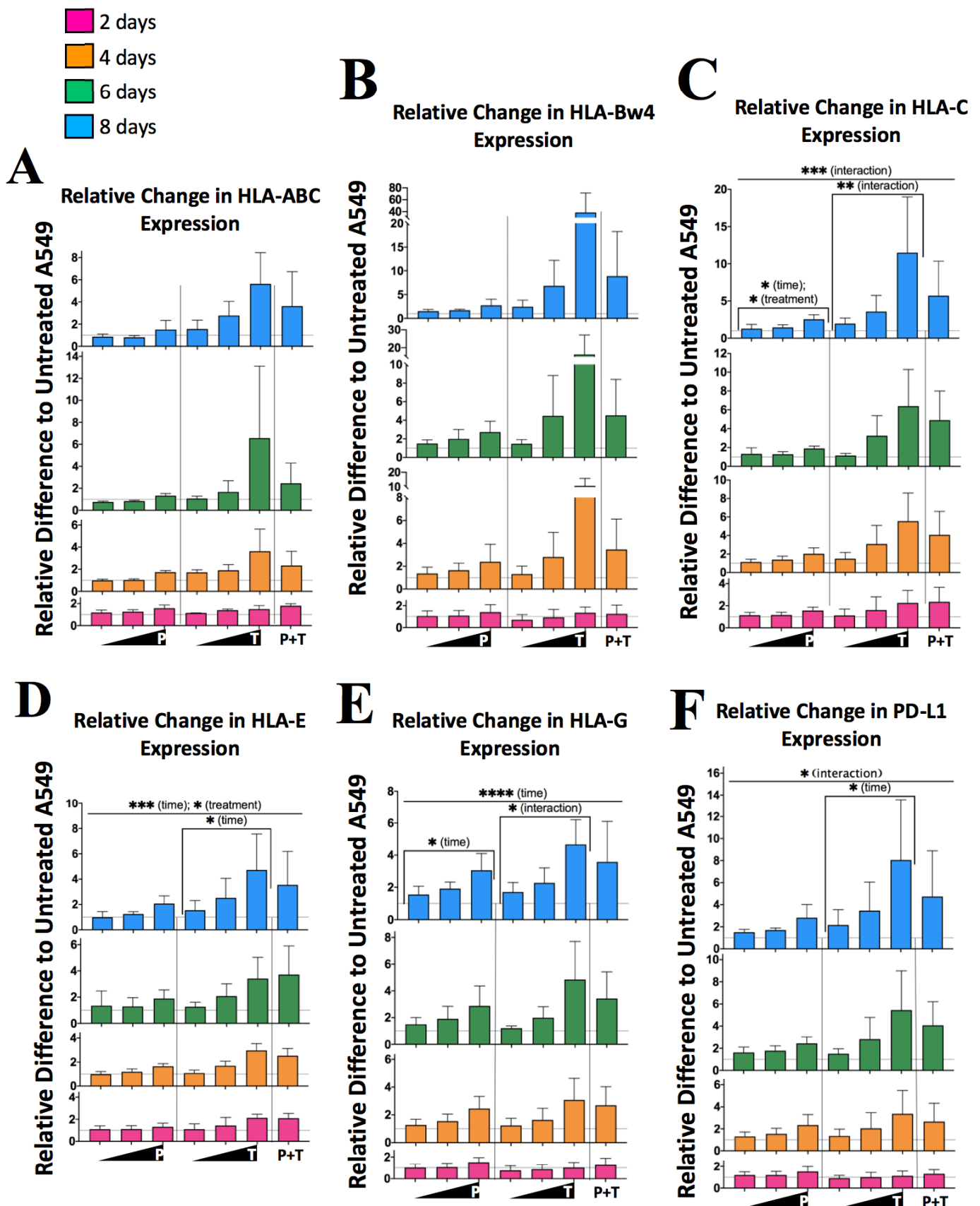
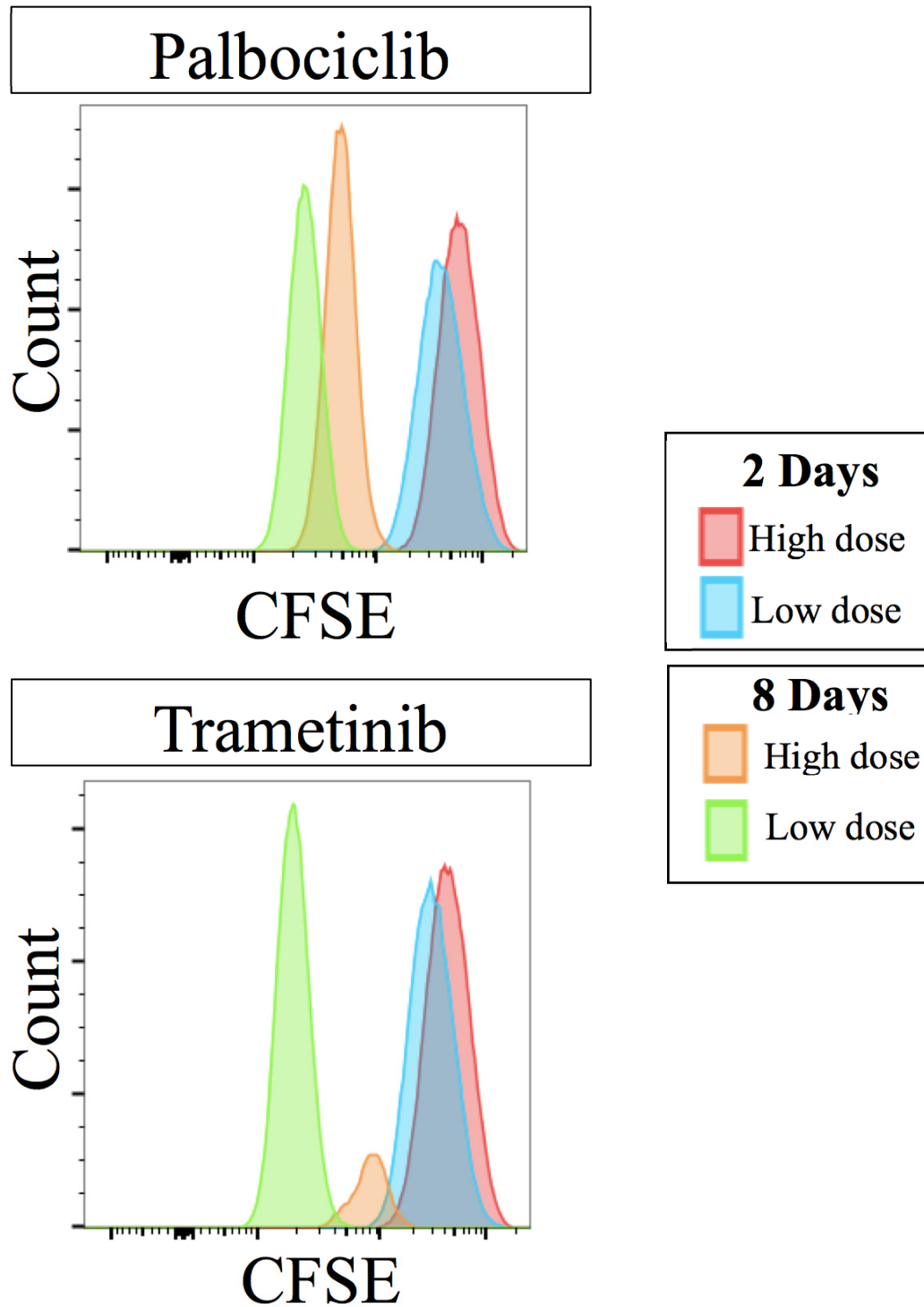


Figure 3.9 Palbociclib (P) and Trametinib (T) chemotherapy treatments induce inhibitory ligand upregulation in a dose- and time-dependent manner.

**Figure 3.9 Palbociclib (P) and Trametinib (T) chemotherapy treatments induce inhibitory ligand upregulation in a dose- and time-dependent manner.** (A-F) A549 cells were treated with either low, middle or high doses of either Trametinib (5 nM, 25 nM, 125 nM) or Palbociclib (100 nM, 500 nM, 1500 nM), or the middle dose of both drugs every two days. The cells were treated for either two, four, six or eight days, then stained for flow cytometry with Viability Dye eFl506, anti-HLA-ABC antibodies, anti-HLA-Bw4 antibodies, anti-HLA-C antibodies, anti-HLA-E antibodies, anti-HLA-G antibodies, anti-PD-L1 antibodies. The mean fluorescence intensities were normalized against untreated A549 cells to achieve the relative difference in tumor phenotypic evolution (n=3; n=2 for HLA-ABC). RM 2-way ANOVAs were performed comparing the tumor ligand changes to untreated A549 cells within all treatment groups, and within Palbociclib doses alone, Trametinib doses alone, or the combination alone. \* = significantly different from baseline as indicated by the line at y=1 (\*, p<0.05; \*\*, p<0.01; \*\*\*, p<0.001; \*\*\*\*, p<0.0001).



**Figure 3.10 Palbociclib and trametinib treatments slow A549 proliferation.** A549 cells were stained with CFSE, then treated with either low or high doses of either Trametinib (5 nM, 125 nM) or Palbociclib (100 nM, 1500 nM). The cells were treated for either two or eight days, then stained for flow cytometry with Viability Dye eFl506. The live cells were gated on, and the CFSE histograms were overlaid.



### *3.1.5 Irradiation treatment induces death receptors and upregulation of activating and inhibitory ligands in a dose-dependent manner*

Based on the current understanding of low dose radiation (LDR) inducing an “immunostimulatory” phenotype, we hypothesized that low dose treatments would induce upregulation of the activating ligands and death receptors that interact with NK cells. By subjecting the tumor cells to four different doses of irradiation then leaving them to rest for either 1, 3 or 5 days, we were able to assess how the tumor cell changes differ with increasing time after irradiation. The impact of longer exposure and different irradiation doses was assessed by separate repeated measures (RM) 2-way ANOVA after 1 day, 3 days, and 5 days. Normal distribution could not be assumed for TRAIL-R1 (1 and 3 days), and larger sample sizes are required to perform Wilcoxon matched-pairs signed rank test.

One day post-treatment, our results revealed a significant dose-dependent upregulation of Fas (n=4, p=0.0006 [interaction]), HLA-F (n=4, p=0.0011 [interaction]), and TRAIL-R2 (n=4, p=0.0246 [interaction]; **Figure 3.11B, C, E**), and PD-L1 (n=4, p=0.0139 [interaction]; **Figure 3.12F**). Three days post-treatment, we observed a significant dose-dependent upregulation of Fas (n=3, p=0.0108 [interaction]), HLA-F (n=3, p=0.0155 [interaction]), PD-L1 (n=3, p=0.0094 [interaction]), and HLA-ABC (n=3, p=0.0183 [interaction]; **Figure 3.12A**). Five days post-treatment, the only ligand that was significantly upregulated in a dose-dependent manner was HLA-F (n=3, p=0.0276 [interaction]). Compared to untreated cells, the death receptors that were upregulated with irradiation treatment include TRAIL-R1 (1 day; **Figure 3.11D**), Fas (5 days), and TRAIL-R2 (5 days). Similarly, the inhibitory ligands upregulated with irradiation treatment in comparison to untreated cells include HLA-Bw4 (1 day), HLA-G (1 day), HLA-C (5 days; **Figure 3.12B, C, E**), and PD-L1 (5 days). Overall, these results suggest that low “immunostimulatory” doses of irradiation induce activating ligands and death receptors to upregulate on tumor cells during the days following treatment. Therefore, these findings present an opportunity for NK cells to become activated by their cognate receptors and kill the tumor cells shortly after irradiation treatment, and before inhibitory ligands are upregulated.

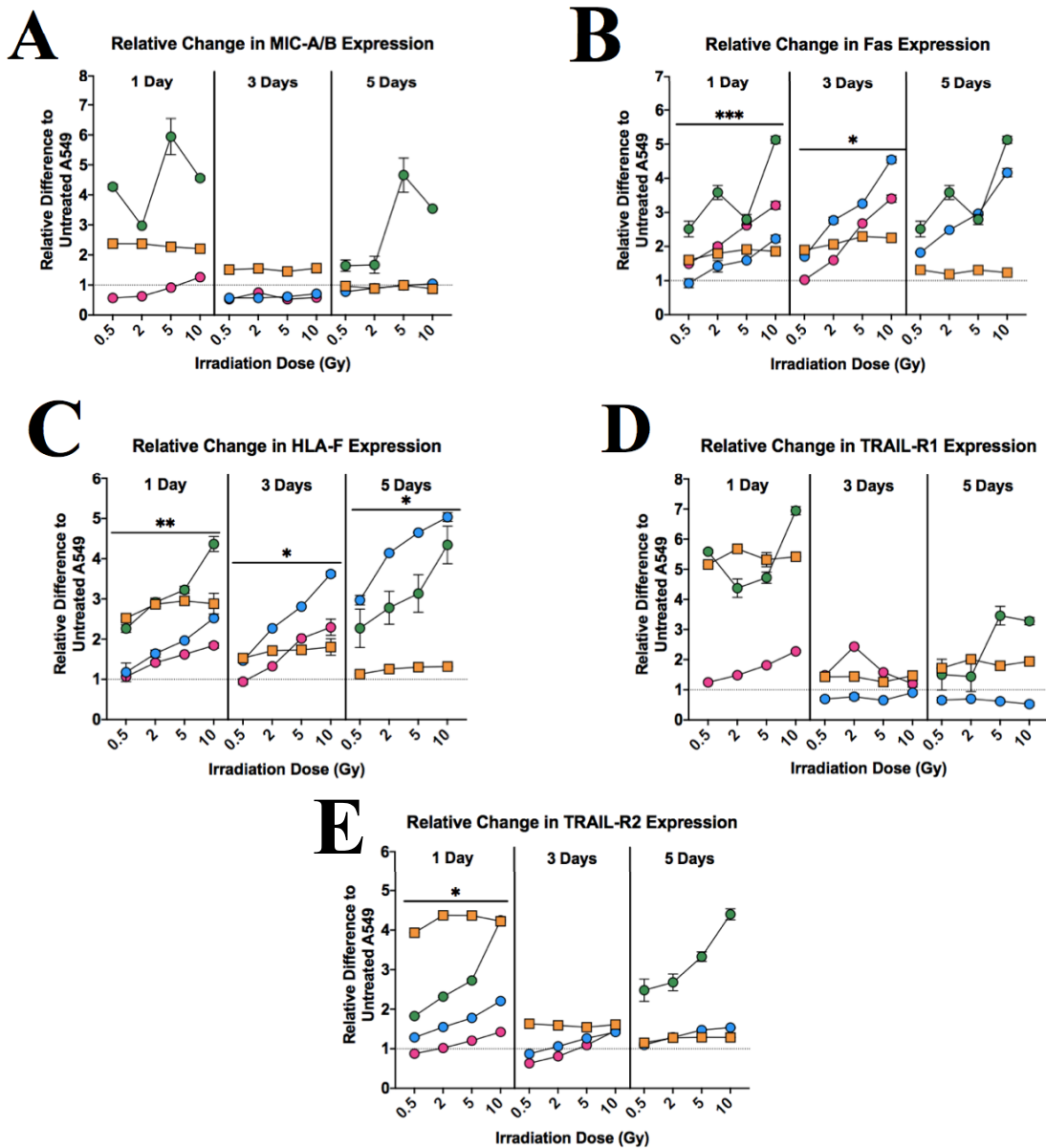


**Figure 3.11 Irradiation treatment induces dose-dependent upregulation of death receptors and activating ligands.** (A-E) A549 cells were subjected to varying doses of radiation on either the Varian TrueBeam Linear Accelerator (circles) or the Gamma Cell Irradiator (squares). The cells were left to rest for either one, three, or five days, then stained for flow cytometry with Viability Dye eFl506, anti-MIC-A/B antibodies, anti-Fas antibodies, and anti-HLA-F antibodies, anti-TRAIL-R1 antibodies, and anti-TRAIL-R2 antibodies. The mean fluorescence intensities were normalized against untreated A549 cells to achieve the relative difference in tumor phenotypic evolution (n=2-4). RM 2-way ANOVA were performed within each time point group (if n=3) comparing the tumor ligand changes to untreated A549 cells. \* = significantly different from baseline as indicated by the line at y=1 (\*, p<0.05; \*\*, p<0.01; \*\*\*, p<0.001; \*\*\*\*, p<0.0001). Each colour represents a different experiment, and the experiments were completed in replicates, as indicated by the error bars.

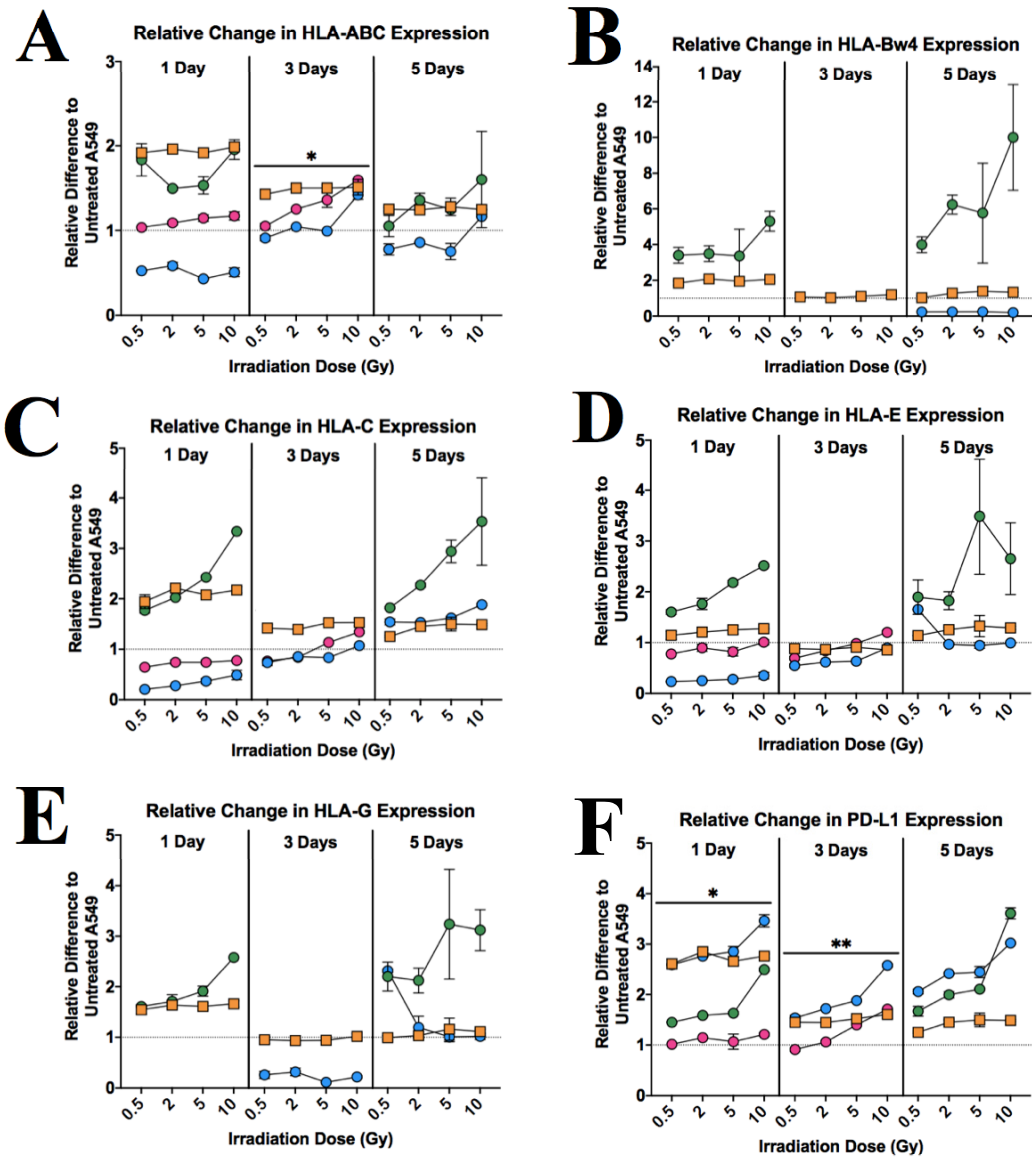


**Figure 3.12 Irradiation treatment induces dose-dependent upregulation of inhibitory ligands.** (A-F) A549 cells were subjected to varying doses of radiation on either the Varian TrueBeam Linear Accelerator (circles) or the Gamma Cell Irradiator (squares). The cells were left to rest for either one, three, or five days, then stained for flow cytometry with Viability Dye eF1506, anti-HLA-ABC antibodies, anti-HLA-C antibodies, anti-HLA-E antibodies, anti-HLA-G antibodies, anti-PD-L1 antibodies. The mean fluorescence intensities were normalized against untreated A549 cells to achieve the relative difference in tumor phenotypic evolution (n=2-4). RM 2-way ANOVA were performed within each time point group (if n=3) comparing the tumor ligand changes to untreated A549 cells. \* = significantly different from baseline as indicated by the line at y=1 (\*, p<0.05; \*\*, p<0.01; \*\*\*, p<0.001; \*\*\*\*, p<0.0001). Each colour represents a different experiment, and the experiments were completed in replicates, as indicated by the error bars.

### *3.1.6 Death receptors and activating and inhibitory ligands on A549 cells rapidly evolve depending on different treatment pressures*

Our results indicate that the tumor is highly dynamic, with changes to its phenotype potentially impacting the subset(s) of NK cells with which it would be expected to interact. This highlights a need to consider how therapies and NK cells interact, but also opens the possibility to create compounding NK cell-based therapies that could be combined with therapy to provide the best targeting of changing tumors. To summarize the phenotypic tumor evolution, the relative expression changes of the analyzed ligands compared to untreated A549 cells were assessed using in a heat map (**Figure 3.13**). This overview allows for a simplified visualization of when inhibitory ligands are upregulated, and therefore are expected to inhibit more NK cells, compared to when activating ligands are upregulated, which will promote NK cell cytotoxic activity.

Stimulation with IFN- $\gamma$ , which represents an inflammatory environment, results in the greatest upregulation of almost all inhibitory ligands after three days of treatment, except for HLA-E, which is highest after day one. The death receptors and activating ligands respond more dissimilarly, as some are most upregulated on day three (HLA-F, Fas), while others are downregulated with IFN- $\gamma$  in comparison to unstimulated conditions (MIC-A/B, TRAIL-R1). The stimulation generally results in persistence of these expression changes, demonstrated by the death receptors and ligands continuing to be mostly upregulated compared to untreated cells over three days.

Stimulation with PBMCs, without IFN- $\gamma$  treatment, consistently resulted in the greatest upregulation of inhibitory ligands after 10 hours of a co-culture, and the death receptors and activating ligands reached the greatest upregulation after 5 or 10 hours. When the cells are treated with IFN- $\gamma$  first, the PBMC co-culture induces upregulation of inhibitory ligands across all hours in the time-course, suggesting that the addition of PBMCs has a less consequential effect than the inflammatory stimuli in this experiment. HLA-G was the only inhibitory ligand that steadily upregulated with longer co-cultures compared to untreated cells. The death receptors and activating ligands that result in greater expression with longer PBMC stimulation follow similar trends with and without IFN- $\gamma$  (MIC-A/B, HLA-F, TRAIL-R1). When comparing these effects of PBMC pressure to NK cells specifically, the relative change in both activating and inhibitory ligands and

death receptors is similar among effector groups. Almost all ligands and receptors revealed greater upregulation with the effectors when the cells were treated with IFN- $\gamma$  first, except for MIC-A/B and TRAIL-R2. This suggests that if the NK cells are inducing changes on tumor cell surfaces, it is likely occurring additively with IFN- $\gamma$ -induced changes. The trends reflect upregulation of MIC-A/B, TRAIL-R2, and HLA-G with effector cells in the conditions without IFN- $\gamma$ , therefore suggesting NK cells alone are particularly impacting those changes to ligand and receptor expressions.

Stimulation with chemotherapies resulted in consistent changes in inhibitory ligands: the greatest upregulations occurred with the highest dose of trametinib, followed by less intense changes in the combination treatment. The activating ligands had the greatest relative expression change with either palbociclib (MIC-A/B, HLA-F, TRAIL-R1) or trametinib (TRAIL-R2, Fas), though importantly, these upregulations were maintained in the combination treatment.

Stimulation with an immunosensitizing dose of irradiation (5 Gy) induced the greatest upregulation of inhibitory ligands generally 5-7 days after treatment. The greatest relative change for death receptors and activating ligands was again diverse among the ligands: MIC-A/B and TRAIL-R1 at day 1, Fas at day 3, HLA-F at day 5, and TRAIL-R2 at day 7. Overall, the death receptors and activating ligands upregulated more rapidly post-irradiation treatment than the inhibitory ligands. This contrast reveals an opportunity to target irradiated tumor cells in the days soon after treatment, prior to upregulation of many of the inhibitory ligands. However, it is promising that different death receptors and activating ligands upregulate on various days post-treatment because it cultivates immunostimulatory tumor phenotypes that can be targeted by diverse NK cells after irradiation.

In conclusion, our first aim has illuminated how various treatment pressures induce NSCLC phenotypic evolution of the death receptors and activating and inhibitory ligands that interact with NK cells. These results reflect diverse changes in the receptors and ligands, however, the trends help identify time points and conditions that can promote activating interactions between tumor cells and NK cells. As HLA ligands and PD-L1 were often upregulated in response to IFN- $\gamma$  and clinical treatments, we expect that blocking these inhibitory interactions will promote NK cell activation.

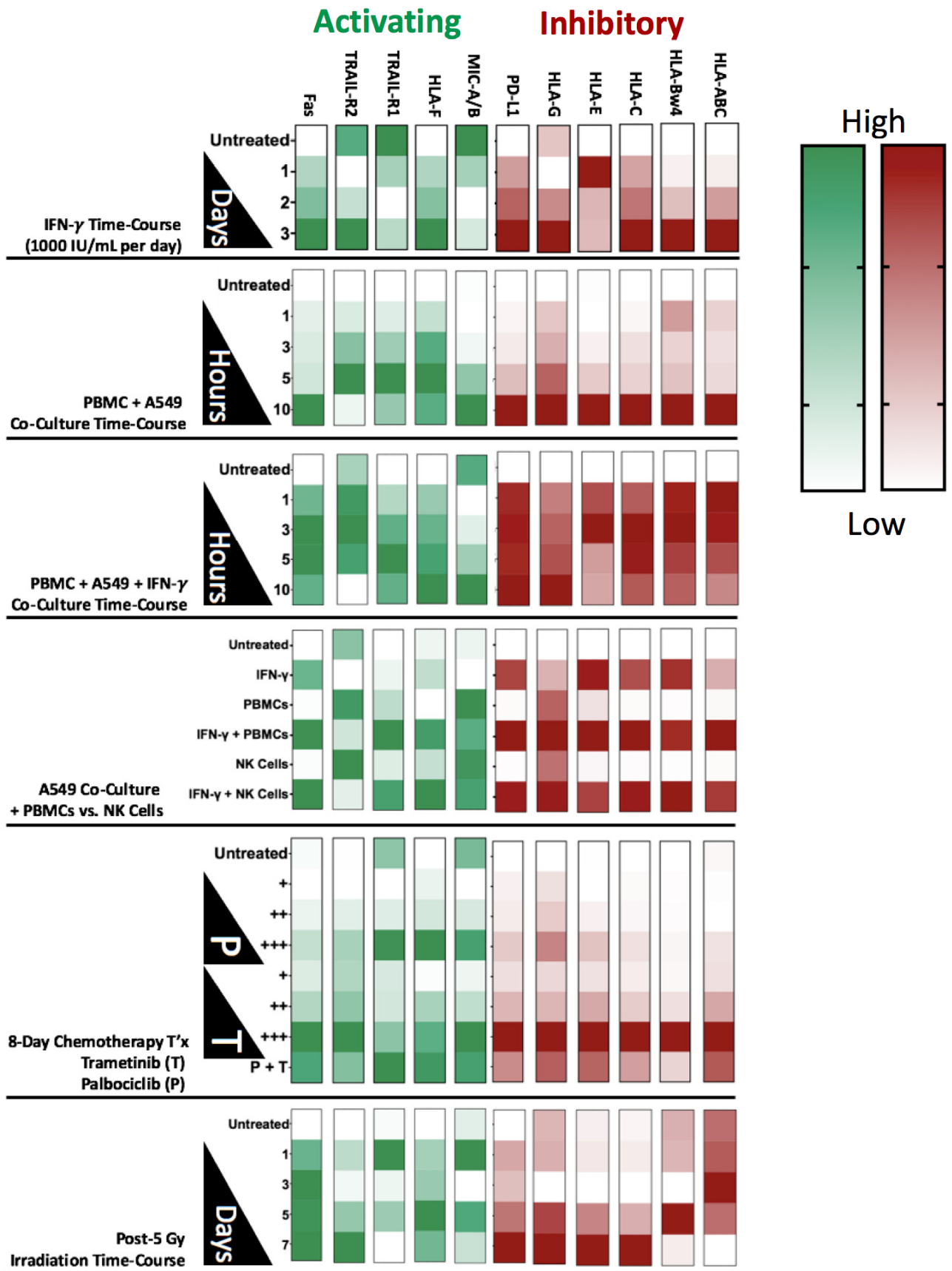


Figure 3.13 Death receptors and activating and inhibitory ligands on A549 cells rapidly evolve depending on different treatment pressures.

**Figure 3.13 Death receptors and activating and inhibitory ligands on A549 cells rapidly evolve depending on different treatment pressures.** A549 cells were subjected to various treatment conditions (as outlined in previous figures), then stained for flow cytometry with Viability Dye eFl506, anti-MIC-A/B antibodies, anti-Fas antibodies, and anti-HLA-F antibodies, anti-TRAIL-R1 antibodies, anti-TRAIL-R2 antibodies, anti-HLA-ABC antibodies, anti-HLA-Bw4 antibodies, anti-HLA-C antibodies, anti-HLA-E antibodies, anti-HLA-G antibodies, anti-PD-L1 antibodies, anti-TRAIL-R2 antibodies, anti-TRAIL-R1 antibodies, anti-MIC-A/B antibodies, anti-HLA-F antibodies, and anti-Fas antibodies. The mean fluorescence intensities were normalized against untreated A549 cells to achieve the relative difference in tumor phenotypic evolution within each treatment condition. The relative difference in expressions were graphed in heat maps, with the colours indicating the gradient between high (activating: green; inhibitory: red) and low (white) relative expression change.

### 3.2 NK cell response is rescued with inhibitory ligand blockade

As demonstrated in 3.1, HLA ligands and PD-L1 were often upregulated in response to IFN- $\gamma$  and clinical treatments. This is expected inhibit the NK cells that express the cognate inhibitory receptors, even though our results demonstrate that IFN- $\gamma$  and clinical treatments simultaneously induce the upregulation of activating ligands. We hypothesized that blocking inhibitory interactions between NK cells and A549 cells could reduce the inhibition and rescue the NK cell response.

#### *3.2.1 HLA ligands' blockade on A549 cells induces greater response of cognate receptor-positive NK cells*

We hypothesized that blocking HLA-C, which inhibits KIR2DL2/L3<sup>+</sup> NK cells, would rescue reactivity among them; and that using W6/32, which blocks HLA-A, -B, -C, and -E, would result in an even greater rescue of response within KIR<sup>+</sup> and NKG2A<sup>+</sup> NK cells. The impact of the blocking antibody treatments was assessed by RM 1-way ANOVAs with prior IFN- $\gamma$  treatment, and tests for linear trends. In comparison to the unstimulated, the NK cells expressing KIR2DL2/L3, KIR3DL1 and NKG2A had greater activation when the HLA ligands were blocked (**Figure 3.14A-D**). This trend was revealed to be significant for the NKG2A<sup>+</sup> KIR<sup>-</sup> NK cells as more HLA ligands were blocked from inhibiting the NK cells (n=3, p=0.0195 [linear trend]). Overall, these results demonstrate that inhibitory interactions prompted by HLA ligands are potent features in the NK-tumor interaction.



○ IFN- $\gamma$ <sup>-</sup>  
 □ IFN- $\gamma$ <sup>+</sup>

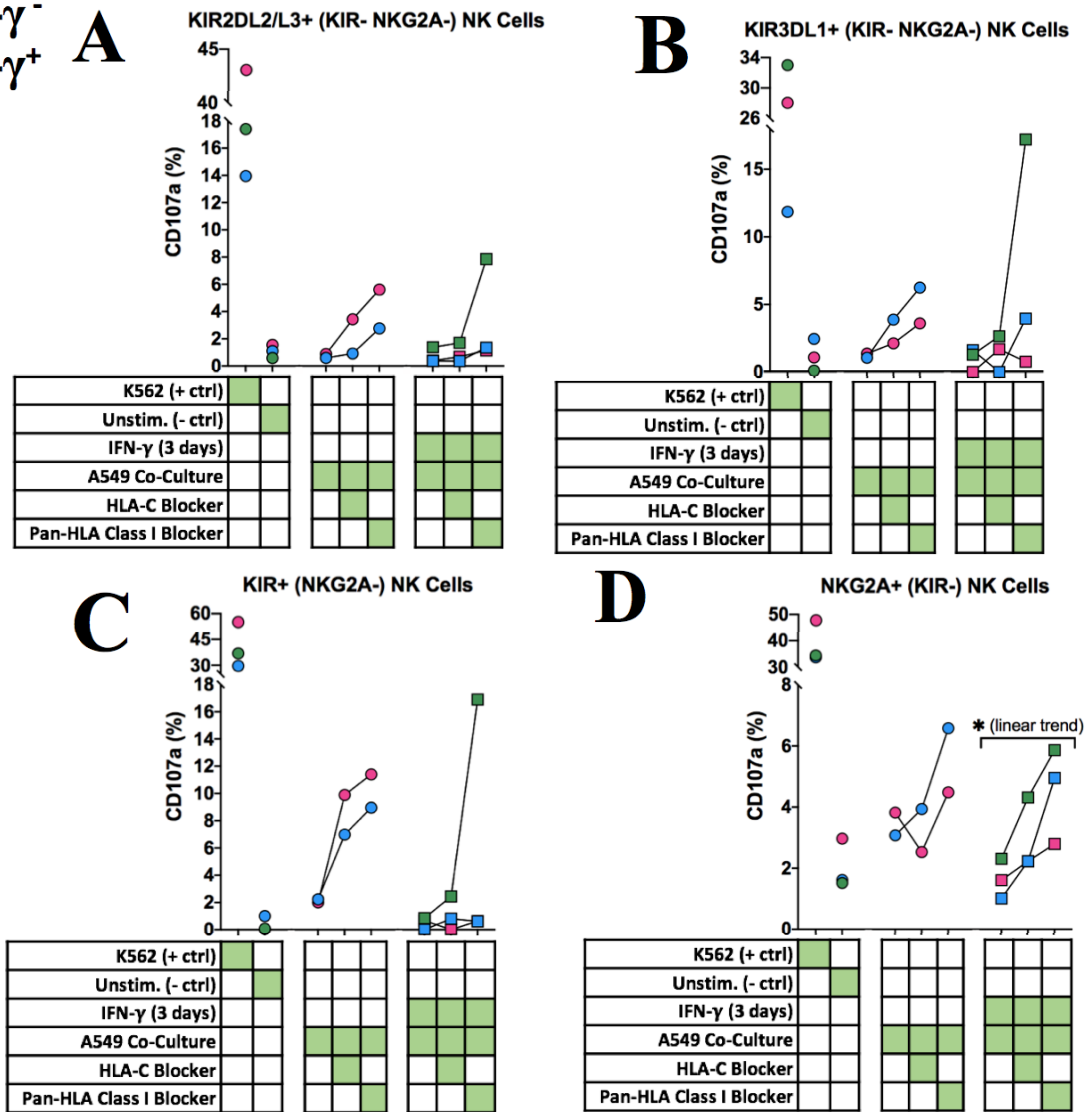


**Figure 3.14 Blocking HLA ligands on A549 cell surfaces induces greater response of cognate receptor-positive NK cells.** (A-D) A549 cells were treated with or without IFN- $\gamma$  (1000 IU/mL) once per day for 3 days. The cells were incubated for 30 minutes with either an HLA-C blocking antibody (DT9, 2  $\mu$ g/ $\mu$ l) or W6/32 (an HLA class I blocking antibody, 2  $\mu$ g/ $\mu$ l). With both antibodies, an Fc block was added (0.5  $\mu$ g/ $\mu$ L). The antibodies were washed off, then the cells were co-cultured with PBMCs for 5 hours, separated, and stained for flow cytometry. The PBMCs were stained with Viability Dye eF1506, anti-CD107a antibodies, anti-CD3 antibodies, anti-CD56 antibodies, anti-KIR2DL2/L3 antibodies, anti-KIR3DL1 antibodies, anti-KIR3DL1/S1 antibodies, and anti-NKG2A antibodies. The single inhibitory receptor-positive NK cell populations were gated on, and the percent of responding cells was determined by the frequency of CD107a<sup>+</sup> cells in the population. RM 1-way ANOVA and tests for linear trends were performed for the NK cells challenging A549 cells treated with IFN- $\gamma$ , comparing the change in activation with the blocking antibodies (n=3; \*, p<0.05; \*\*, p<0.01; \*\*\*, p<0.001; \*\*\*\*, p<0.0001). The colours represent different PBMC donors.

### *3.2.2 Blocking the PD-1/PD-L1 axis induces greater response of PD-1<sup>+</sup> NK cells*

We hypothesized that blocking the PD-1/PD-L1 immune checkpoint pathway would induce greater activation of PD-1<sup>+</sup> NK cells. We inhibited this axis using an anti-PD-1 blocking antibody for the NK cells, and an anti-PD-L1 blocking antibody (atezolizumab) for the tumor cells. The impact of the blocking antibody treatments was assessed by RM 1-way ANOVAs with prior IFN- $\gamma$  treatment, with Tukey's multiple comparison tests and tests for linear trends. In comparison to the unstimulated, the NK cells expressing PD-1 (KIR<sup>-</sup> NKG2A<sup>-</sup>) were significantly more activated with the combination of both blocking antibodies (n=3, p=0.0338; **Figure 3.15A**). The results revealed a significant linear trend with the addition of anti-PD-1, to anti-PD-L1, to the combination (n=3, p=0.0101 [linear trend]). Similarly, the PD-1<sup>+</sup> NKG2D<sup>+</sup> (KIR<sup>-</sup> NKG2A<sup>-</sup>) NK cells were significantly more activated with more blocking antibodies (n=3, p=0.0109 [linear trend]; **Figure 3.15B**). As expected, there were limited changes in the non-IFN- $\gamma$  treated conditions, as results from 3.1 demonstrated that PD-L1 is upregulated with stimulation from IFN- $\gamma$  or other treatments. Overall, these results support the use of anti-PD-1 and anti-PD-L1 blocking antibodies to induce a greater response of PD-1<sup>+</sup> NK cells, especially those that also express activating receptors, and reveal an important subpopulation of NK cells that is impaired during treatment.

○ IFN- $\gamma$ <sup>-</sup>  
 □ IFN- $\gamma$ <sup>+</sup>

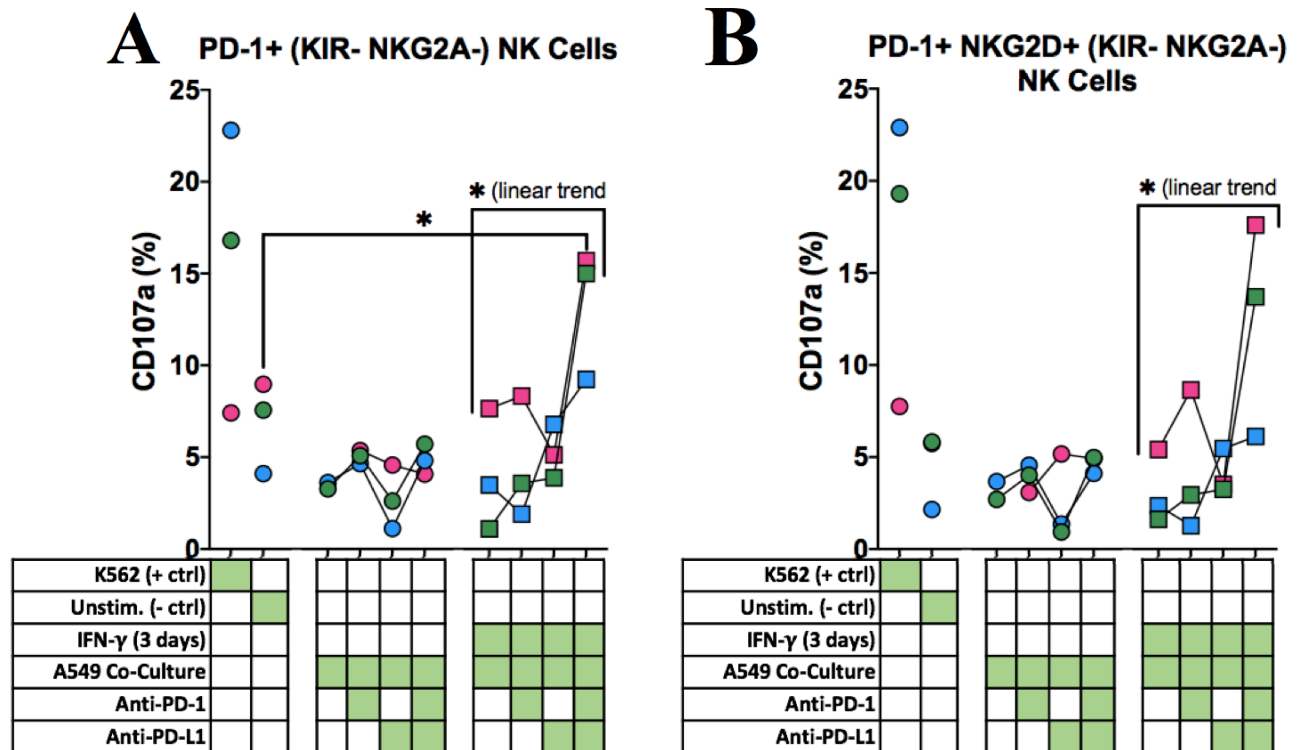


**Figure 3.15 Blocking the PD-1/PD-L1 axis induces greater response of PD-1<sup>+</sup> NK cells.** (A-B) A549 cells were treated with or without IFN- $\gamma$  (1000 IU/mL) once per day for 3 days. The A549 cells were incubated with an anti-PD-L1 blocking antibody (atezolizumab, 2  $\mu$ g/mL), and the PBMCs were incubated with an anti-PD-1 blocking antibody (6  $\mu$ g/mL). After 30 minutes, the antibodies were washed off, then the cells were co-cultured with PBMCs for 5 hours, separated, and stained for flow cytometry. The PBMCs were stained with Viability Dye eFl506, anti-CD107a antibodies, anti-CD3 antibodies, anti-CD56 antibodies, anti-KIR2DL2/L3 antibodies, anti-KIR3DL1 antibodies, anti-KIR3DL1/S1 antibodies, anti-NKG2A antibodies, and anti-PD-1 antibodies. The NK cell populations expressing inhibitory receptors (KIR3DL1, KIR3DL1/S1, KIR2DL2/L3 and NKG2A) were excluded, and the PD-1<sup>+</sup> and PD-1<sup>+</sup> NKG2D<sup>+</sup> populations were gated on. The percent of responding cells was determined by the frequency of CD107a<sup>+</sup> cells in each population. RM 1-way ANOVA, Tukey's multiple comparisons tests, and tests for linear trend were performed for the NK cells challenging A549 cells treated with IFN- $\gamma$ , comparing the change in activation with the blocking antibodies (n=3; \*, p<0.05; \*\*, p<0.01; \*\*\*, p<0.001; \*\*\*\*, p<0.0001). The colours represent different PBMC donors.

### 3.3 NK cell response to tumors post-treatment

#### 3.3.1 *The subset of NK cells responding to a tumor can be predicted by the tumor cell phenotype post-chemotherapy*

Our results from 3.1.4 demonstrated tumor cells phenotypically evolving with palbociclib and trametinib. We therefore hypothesized that the NK cell populations responding to the A549 cells will change with different treatments. First, we examined the changing activation of NK cell populations against tumor cells treated at each of the three doses of palbociclib or trametinib, and the combination treatment of the two small molecules. When analyzing the NK cells expressing KIR2DL2/L3 that were negative for KIR2DL1, KIR3DL1, KIR3DL1/S1, and NKG2A, our results revealed the activation of this population drops when the cognate inhibitory ligand, HLA-C, was upregulated (**Figure 3.16**). This is observed specifically at the highest dose of trametinib and the combination treatment. Similarly, the percent of degranulating NK cells positive for KIR3DL1 that were negative for KIR2DL1, KIR2DL2/L3, and NKG2A dropped when the cognate inhibitory receptor HLA-Bw4 was upregulated with the highest dose of trametinib (**Figure 3.17**). Our results further revealed that PD-1<sup>+</sup> NK cells had greater activation when the cells were negative for KIR2DL1, KIR2DL2/L3, KIR3DL1, and KIR3DL1/S1 (**Figure 3.18**). For the activating interactions between TRAIL on NK cells and TRAIL-R1 and TRAIL-R2 on tumor cells, our results revealed the similar observation that TRAIL<sup>+</sup> NK cells had greater activation when the cells were negative for KIR2DL1, KIR2DL2/L3, KIR3DL1, and KIR3DL1/S1 (**Figure 3.19**). We observed a similar result for NKG2D<sup>+</sup> NK cells (**Figure 3.20**) and FasL<sup>+</sup> NK cells (**Figure 3.21**). Furthermore, the activation of TRAIL<sup>+</sup> NK cells and FasL<sup>+</sup> NK cells increased with the upregulation of their cognate activating ligands, specifically in the combination treatment. Overall, analyzing the changing tumor phenotype with the responding NK cell populations revealed that chemotherapy will strongly influence tumor-NK interactions. Our results demonstrated the importance of KIRs for repressing NK cell activation, because degranulation of KIR-negative NK cells was higher than their KIR-expressing counterparts against HLA-expressing tumor cells.

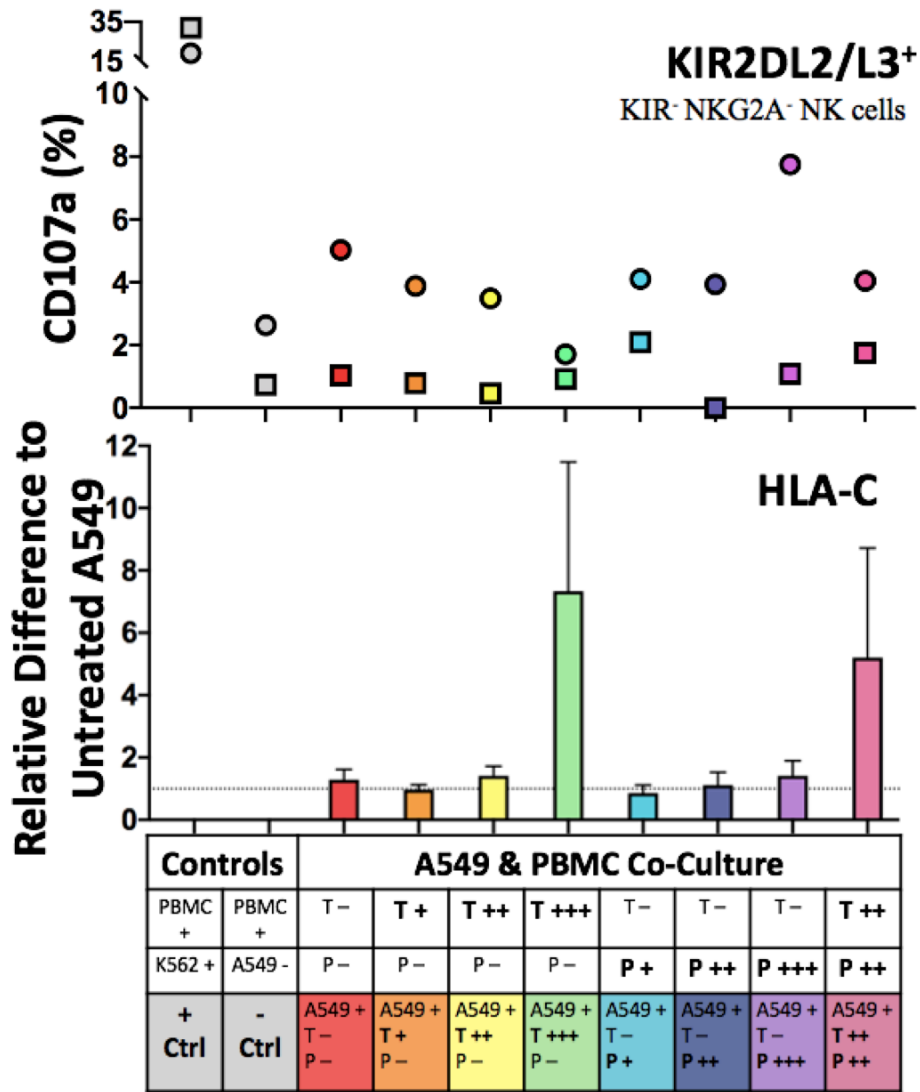


**Figure 3.16 Activation of KIR2DL2/L3<sup>+</sup> NK cells drops when chemotherapy treatment induces HLA-C upregulation.** A549 cells were treated with either low (+), middle (++) or high (+++) doses of either trametinib (5 nM, 25 nM, 125 nM) or palbociclib (100 nM, 500 nM, 1500 nM), or the middle dose of both drugs every 2 days for 8 days. The cells were then co-cultured with PBMCs for 5 hours, separated, and stained for flow cytometry. The PBMCs were stained with Viability Dye eF1506, anti-CD3 antibodies, anti-CD56 antibodies, anti-CD107a antibodies, anti-KIR2DL1 antibodies, anti- KIR2DL2/L3 antibodies, KIR3DL1 antibodies, anti-KIR3DL1/S1 antibodies, and anti-NKG2A antibodies. The single KIR2DL2/L3<sup>+</sup> NK cells were gated on (KIR2DL1<sup>-</sup> KIR3DL1<sup>-</sup> KIR3DL1/S1<sup>-</sup> NKG2A<sup>-</sup>), and the percent of responding cells was determined by the frequency of CD107a<sup>+</sup> cells in the population. The tumor cells were stained with Viability Dye eF1506 and anti-HLA-C antibodies. Each symbol represents a different PBMC donor (n=2). For the tumor cells, the mean fluorescence intensities were normalized against untreated A549 cells to achieve the relative difference in tumor phenotypic evolution (n=2).

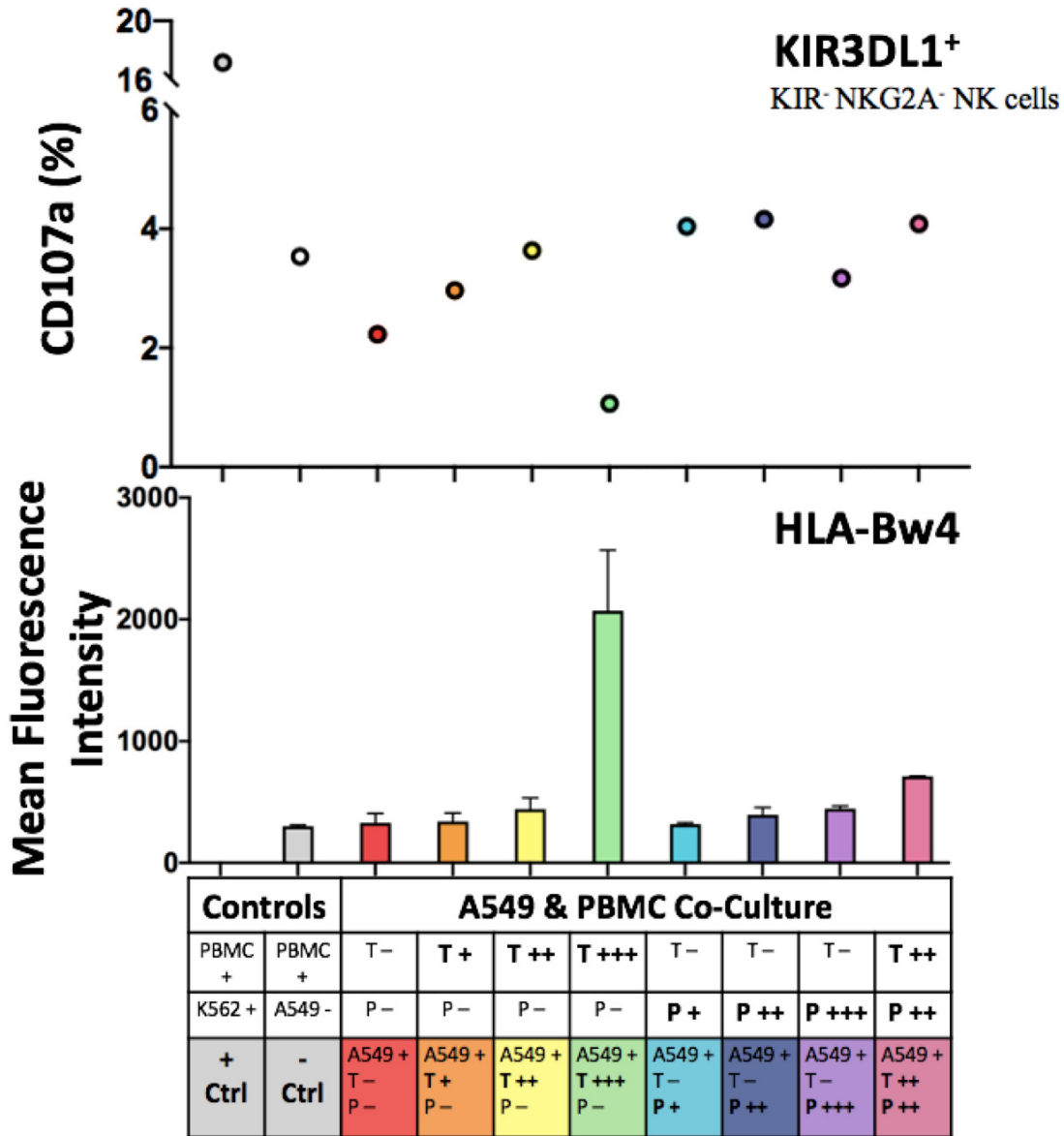


**Figure 3.17 Activation of KIR3DL1<sup>+</sup> NK cells drops when chemotherapy treatment induces HLA-Bw4 upregulation.** A549 cells were treated with either low (+), middle (++) or high (+++) doses of either trametinib (5 nM, 25 nM, 125 nM) or palbociclib (100 nM, 500 nM, 1500 nM), or the middle dose of both drugs every 2 days for 8 days. The cells were then co-cultured with PBMCs for 5 hours, separated, and stained for flow cytometry. The PBMCs were stained with Viability Dye eF1506, anti-CD3 antibodies, anti-CD56 antibodies, anti-CD107a antibodies, anti-KIR2DL1 antibodies, anti-KIR2DL2/L3 antibodies, KIR3DL1 antibodies, and anti-NKG2A antibodies. The single KIR3DL1<sup>+</sup> NK cells were gated on (KIR2DL1<sup>-</sup> KIR2DL2/L3<sup>-</sup> NKG2A<sup>-</sup>), and the percent of responding cells was determined by the frequency of CD107a<sup>+</sup> cells in the population. The tumor cells were stained with Viability Dye eF1506 and anti-HLA-Bw4 antibodies. The experiment was repeated in replicates, as indicated by the error bars (n=1).

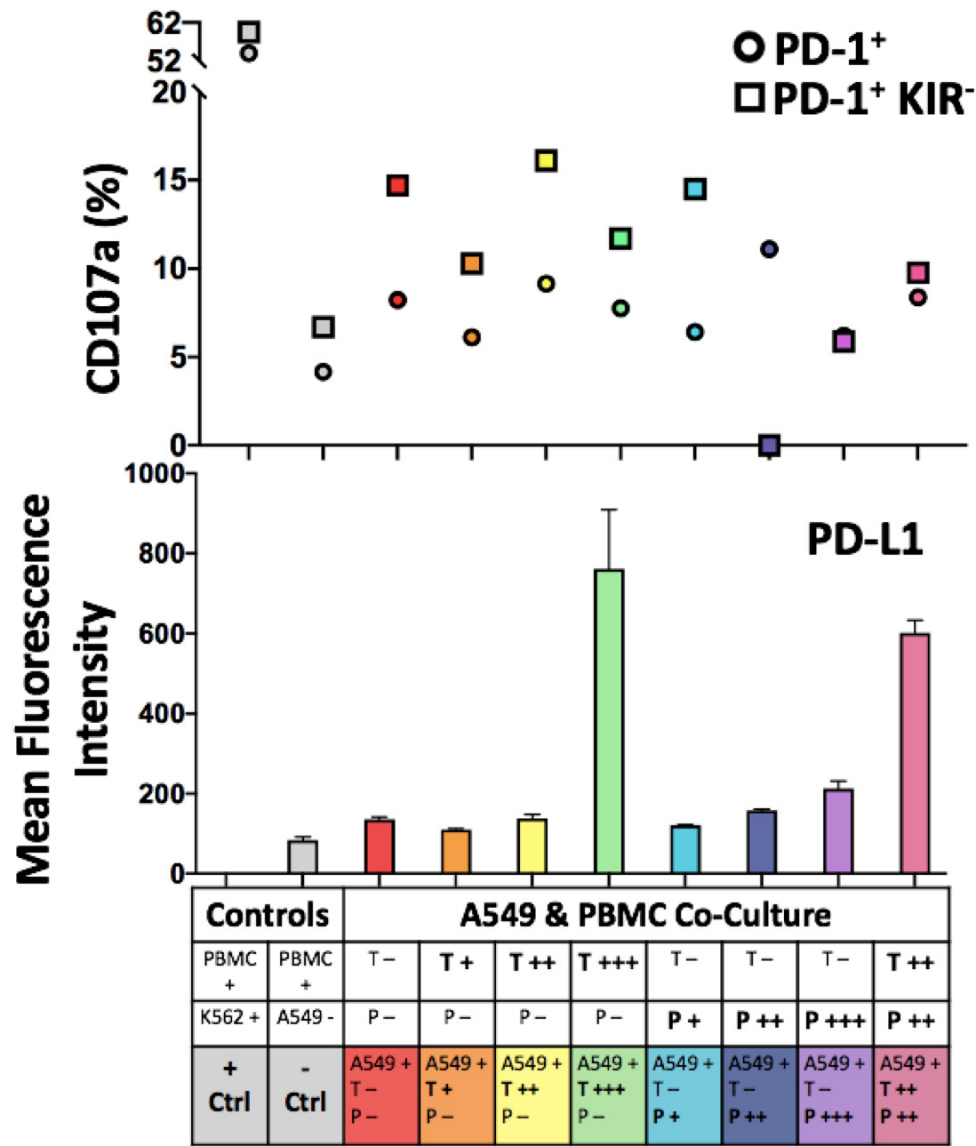


**Figure 3.18 Activation of PD-1<sup>+</sup> NK cells increases against chemotherapy-treated A549 cells when excluding KIR<sup>+</sup> NK cells.** A549 cells were treated with either low (+), middle (++) or high (+++) doses of either trametinib (5 nM, 25 nM, 125 nM) or palbociclib (100 nM, 500 nM, 1500 nM), or the middle dose of both drugs every 2 days for 8 days. The cells were then co-cultured with PBMCs for 5 hours, separated, and stained for flow cytometry. The PBMCs were stained with Viability Dye eF1506, anti-CD3 antibodies, anti-CD56 antibodies, anti-CD107a antibodies, anti-KIR2DL1 antibodies, anti-KIR2DL2/L3 antibodies, KIR3DL1 antibodies, anti-KIR3DL1/S1 antibodies, anti-NKG2A antibodies, and anti-PD-1 antibodies. The PD-1<sup>+</sup> NK cells (circles) and single PD-1<sup>+</sup> NK cells (KIR2DL1<sup>-</sup> KIR2DL2/L3<sup>-</sup> KIR3DL1<sup>-</sup> KIR3DL1/S1<sup>-</sup>; squares) were gated on, and the percent of responding cells was determined by the frequency of CD107a<sup>+</sup> cells in the population. The tumor cells were stained with Viability Dye eF1506 and anti-PD-L1 antibodies. The experiment was repeated in replicates, as indicated by the error bars (n=1). Data is representative of two trials.

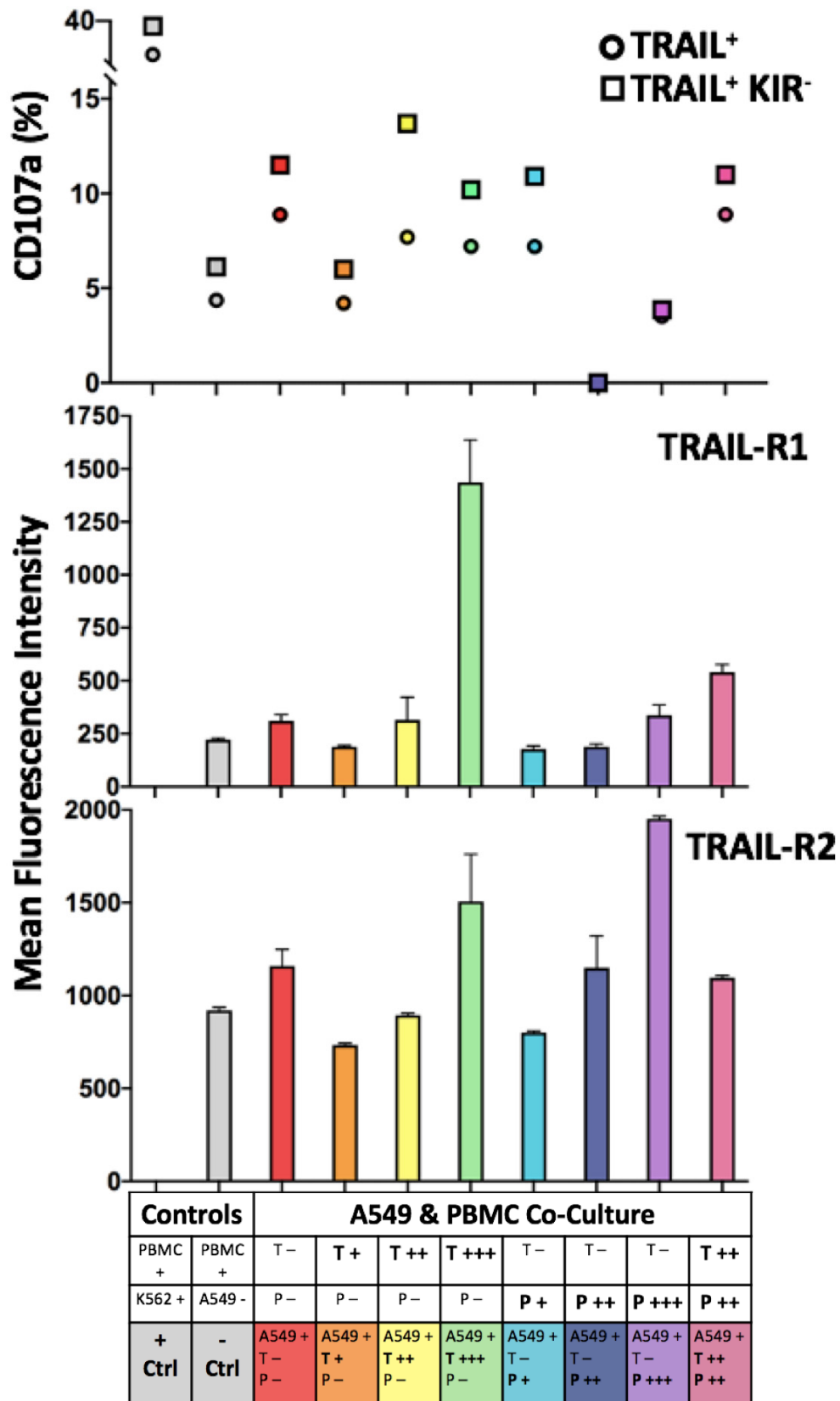
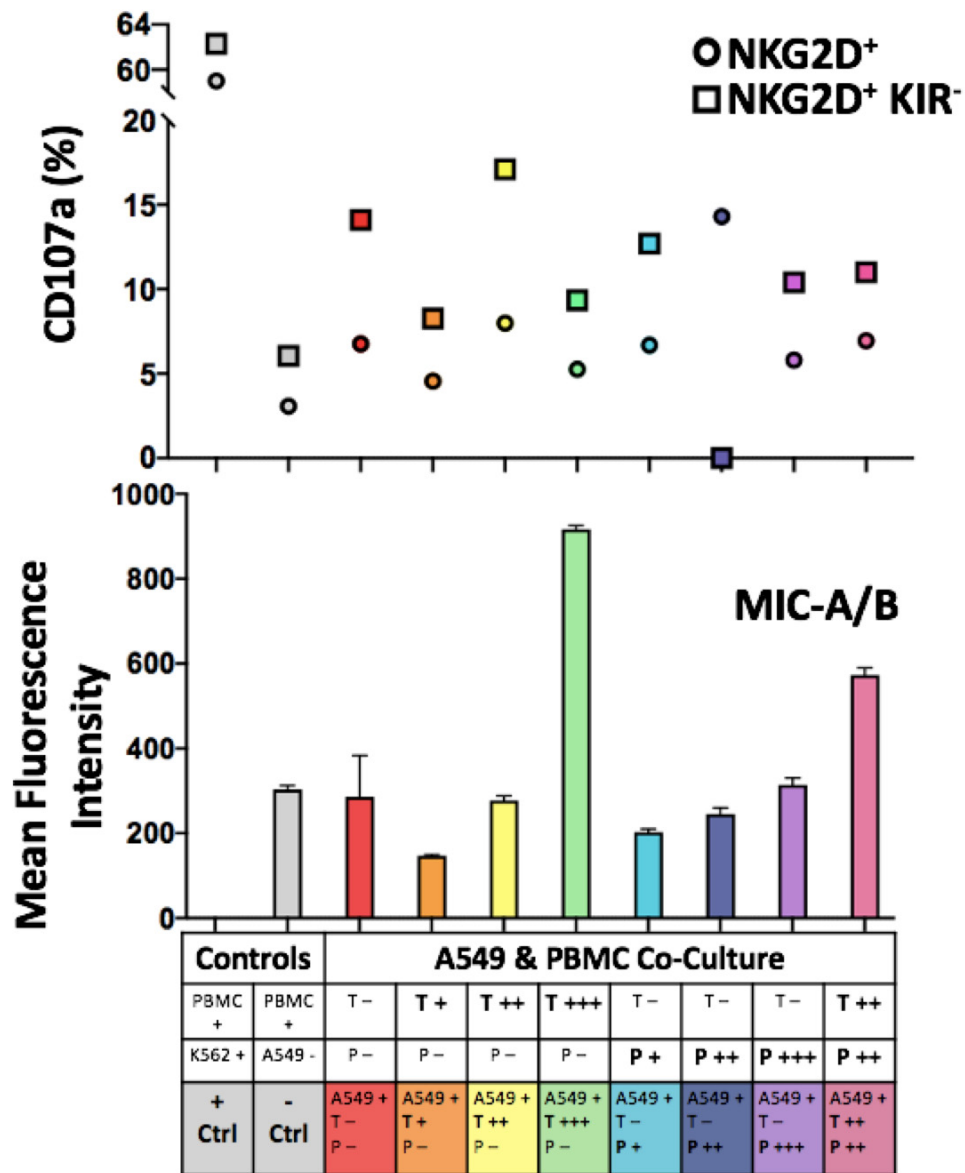


Figure 3.19 Activation of TRAIL<sup>+</sup> NK cells increases against chemotherapy-treated A549 cells when excluding KIR<sup>+</sup> NK cells.



**Figure 3.19 Activation of TRAIL<sup>+</sup> NK cells increases against chemotherapy-treated A549 cells when excluding KIR<sup>+</sup> NK cells.** A549 cells were treated with either low (+), middle (++) or high (+++) doses of either trametinib (5 nM, 25 nM, 125 nM) or palbociclib (100 nM, 500 nM, 1500 nM), or the middle dose of both drugs every 2 days for 8 days. The cells were then co-cultured with PBMCs for 5 hours, separated, and stained for flow cytometry. The PBMCs were stained with Viability Dye eF1506, anti-CD3 antibodies, anti-CD56 antibodies, anti-CD107a antibodies, anti-KIR2DL1 antibodies, anti- KIR2DL2/L3 antibodies, KIR3DL1 antibodies, anti-KIR3DL1/S1 antibodies, anti-NKG2A antibodies, and anti-TRAIL antibodies. The TRAIL<sup>+</sup> NK cells (circles) and single TRAIL<sup>+</sup> NK cells (KIR2DL1<sup>-</sup> KIR2DL2/L3<sup>-</sup> KIR3DL1<sup>-</sup> KIR3DL1/S1<sup>-</sup>; squares) were gated on, and the percent of responding cells was determined by the frequency of CD107a<sup>+</sup> cells in the population. The tumor cells were stained with Viability Dye eF1506, anti-TRAIL-R1 antibodies, and anti-TRAIL-R2 antibodies. The experiment was repeated in replicates, as indicated by the error bars (n=1). Data is representative of two trials.



**Figure 3.20 Activation of NKG2D<sup>+</sup> NK cells increases against chemotherapy-treated A549 cells when excluding KIR<sup>+</sup> NK cells.** A549 cells were treated with either low (+), middle (++) or high (+++) doses of either trametinib (5 nM, 25 nM, 125 nM) or palbociclib (100 nM, 500 nM, 1500 nM), or the middle dose of both drugs every 2 days for 8 days. The cells were then co-cultured with PBMCs for 5 hours, separated, and stained for flow cytometry. The PBMCs were stained with Viability Dye eF1506, anti-CD3 antibodies, anti-CD56 antibodies, anti-CD107a antibodies, anti-KIR2DL1 antibodies, anti- KIR2DL2/L3 antibodies, KIR3DL1 antibodies, anti-KIR3DL1/S1 antibodies, anti-NKG2A antibodies, and anti-NKG2D antibodies. The NKG2D<sup>+</sup> NK cells (circles) and single NKG2D<sup>+</sup> NK cells (KIR2DL1<sup>-</sup> KIR2DL2/L3<sup>-</sup> KIR3DL1<sup>-</sup> KIR3DL1/S1<sup>-</sup>; squares) were gated on, and the percent of responding cells was determined by the frequency of CD107a<sup>+</sup> cells in the population. The tumor cells were stained with Viability Dye eF1506 and anti-MIC-A/B antibodies. The experiment was repeated in replicates, as indicated by the error bars (n=1).

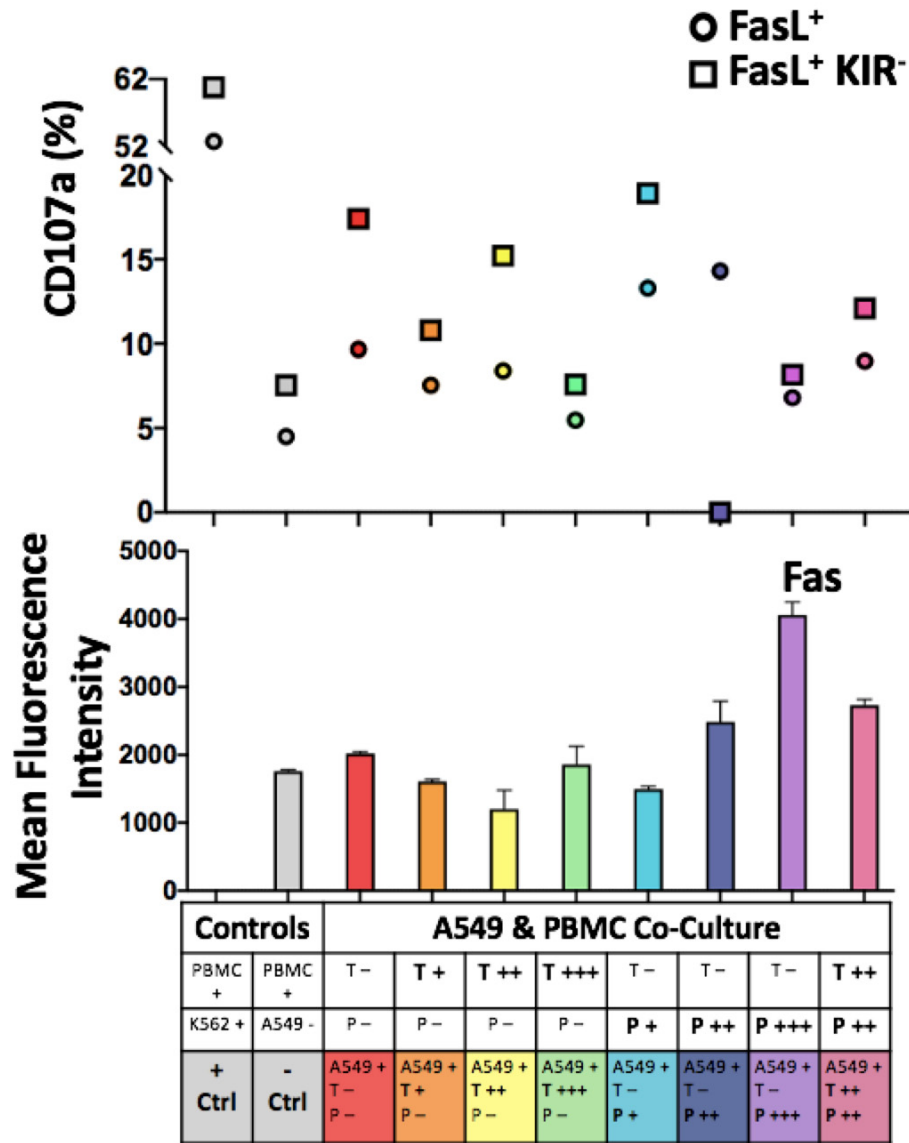


**Figure 3.21 Activation of Fas<sup>+</sup> NK cells increases when chemotherapy treatment induces Fas upregulation.** A549 cells were treated with either low (+), middle (++) or high (+++) doses of either trametinib (5 nM, 25 nM, 125 nM) or palbociclib (100 nM, 500 nM, 1500 nM), or the middle dose of both drugs every 2 days for 8 days. The cells were then co-cultured with PBMCs for 5 hours, separated, and stained for flow cytometry. The PBMCs were stained with Viability Dye eF1506, anti-CD3 antibodies, anti-CD56 antibodies, anti-CD107a antibodies, anti-KIR2DL1 antibodies, anti-KIR2DL2/L3 antibodies, KIR3DL1 antibodies, anti-KIR3DL1/S1 antibodies, anti-NKG2A antibodies, and anti-Fas antibodies. The Fas<sup>+</sup> NK cells (circles) and single Fas<sup>+</sup> NK cells (KIR2DL1<sup>-</sup> KIR2DL2/L3<sup>-</sup> KIR3DL1<sup>-</sup> KIR3DL1/S1<sup>-</sup>; squares) were gated on, and the percent of responding cells was determined by the frequency of CD107a<sup>+</sup> cells in the population. The tumor cells were stained with Viability Dye eF1506 and anti-Fas antibodies. The experiment was repeated in replicates, as indicated by the error bars (n=1).

We further analyzed the impact of a five-hour PBMC co-culture on the relative tumor ligand expression of A549 cells treated with no chemotherapy, the middle doses of palbociclib and trametinib, and the combination of the two. The impact of different therapies and 8-day exposure was assessed by RM 2-way ANOVAs. For the death receptors and activating ligands, our results revealed a significant upregulation in comparison to untreated A549 cells for MIC-A/B (n=7, p<0.0001 [time]), Fas (n=7, p<0.0001 [time]), HLA-F (n=7, p<0.0001 [time]), TRAIL-R1 (n=5, p<0.0001 [time]), and TRAIL-R2 (n=7, p<0.0001 [time]; **Figure 3.22A-E**). In comparison to the PBMC co-culture without prior chemotherapy treatment, TRAIL-R2 expression was lower when treated with trametinib. For the inhibitory ligands, our results revealed a significant upregulation in comparison to untreated A549 cells for HLA-ABC (n=7, p=0.0005 [time]), HLA-Bw4 (n=5, p=0.0103 [time]), HLA-C (n=7, p=0.0011 [time]), HLA-E (n=5, p=0.0003 [time]), HLA-G (n=7, p<0.0001 [time]), and PD-L1 (n=7, p<0.0001 [time]; **Figure 3.23A-F**). Sidak's multiple comparison tests revealed that in comparison to untreated, specific treatment groups significantly upregulated expression of MIC-A/B (PBMC only, p=0.0318; trametinib, p=0.0040; combination, p=0.0047), HLA-F (trametinib, p=0.0444; combination, p=0.0143), TRAIL-R1 (PBMC only, p=0.0247; trametinib, p=0.0054; combination, p=0.0089), TRAIL-R2 (PBMC only, p=0.0284, combination, p=0.0381), Fas (combination, p=0.0049), HLA-ABC (trametinib, p=0.0424), HLA-E (combination, p=0.0302), HLA-G (trametinib, p=0.0385; combination, p=0.0009), and PD-L1 (combination, p=0.0302). Overall, these results reflect that the tumor ligand and receptor upregulations occurring with chemotherapy treatments either persist or potentially upregulate further with the addition of PBMCs.

With unpaired t-tests, we analyzed the impact of the PBMC pressure within a treatment group, and our results revealed a significant upregulation of MIC-A/B with effector cells compared to without effector cells when treated with trametinib (n=5, p=0.0413). When considering only the CFSE<sup>+</sup> population, however, we found that HLA-G, within the trametinib treatment group, was significantly upregulated with the addition of PBMCs (n=4, p=0.0190). This result likely reflects that when analyzing all A549 cells after 8 days of chemotherapy, many of the original cells will have died and the cells remaining represent those that proliferated after the therapy initiation, and therefore that

did not receive the full 8-day treatment. Overall, the upregulation of MIC-A/B and HLA-G on trametinib-treated A549 cells with the addition of PBMC co-cultures supports our findings from 3.1.3, which demonstrated that NK cells independently induce the upregulation of these two ligands.

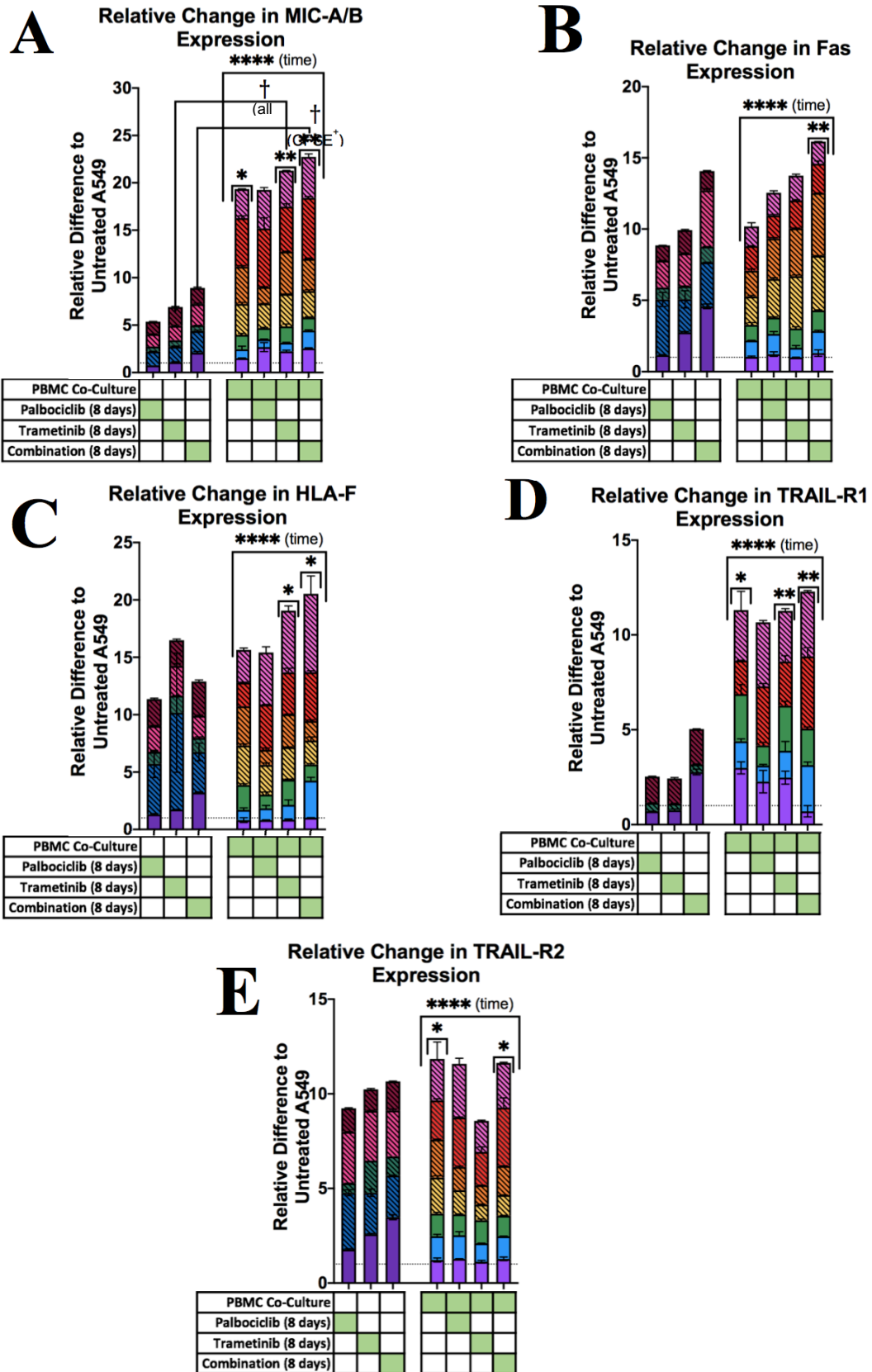


Figure 3.22 Chemotherapy and PBMC co-cultures induce death receptor and activating ligand upregulation.

**Figure 3.22 Chemotherapy and PBMC co-cultures induce death receptor and activating ligand upregulation.** A549 cells were treated with either trametinib (25 nM), palbociclib (500 nM), or both every 2 days for 8 days. The cells were then either stained for flow cytometry, or co-cultured with PBMCs for 5 hours, separated, and then stained for flow cytometry. A549 cells were stained with Viability Dye eFl506, anti-MIC-A/B antibodies, anti-Fas antibodies, and anti-HLA-F antibodies, anti-TRAIL-R1 antibodies, and anti-TRAIL-R2 antibodies. The bars labelled with slashes signify CFSE<sup>+</sup> cells (n=7 with CFSE labelling, n=4 without CFSE labelling). The mean fluorescence intensities were normalized against untreated A549 cells to achieve the relative difference in tumor phenotypic evolution. RM 2-way ANOVA were performed of the groups challenged with PBMC co-culture comparing the tumor ligand changes to untreated A549 cells. Sidak's (\*) multiple comparisons tests were completed, and unpaired t-tests (†) were performed within chemotherapy conditions of all cells and CFSE<sup>+</sup> cells, comparing cells treated with and without the PBMC co-culture. \* = significantly different from baseline as indicated by the line at y=1 (\*, p<0.05; \*\*, p<0.01; \*\*\*, p<0.001; \*\*\*\*, p<0.0001). Each colour represents a different experiment, and the experiments were completed in replicates, as indicated by the error bars.

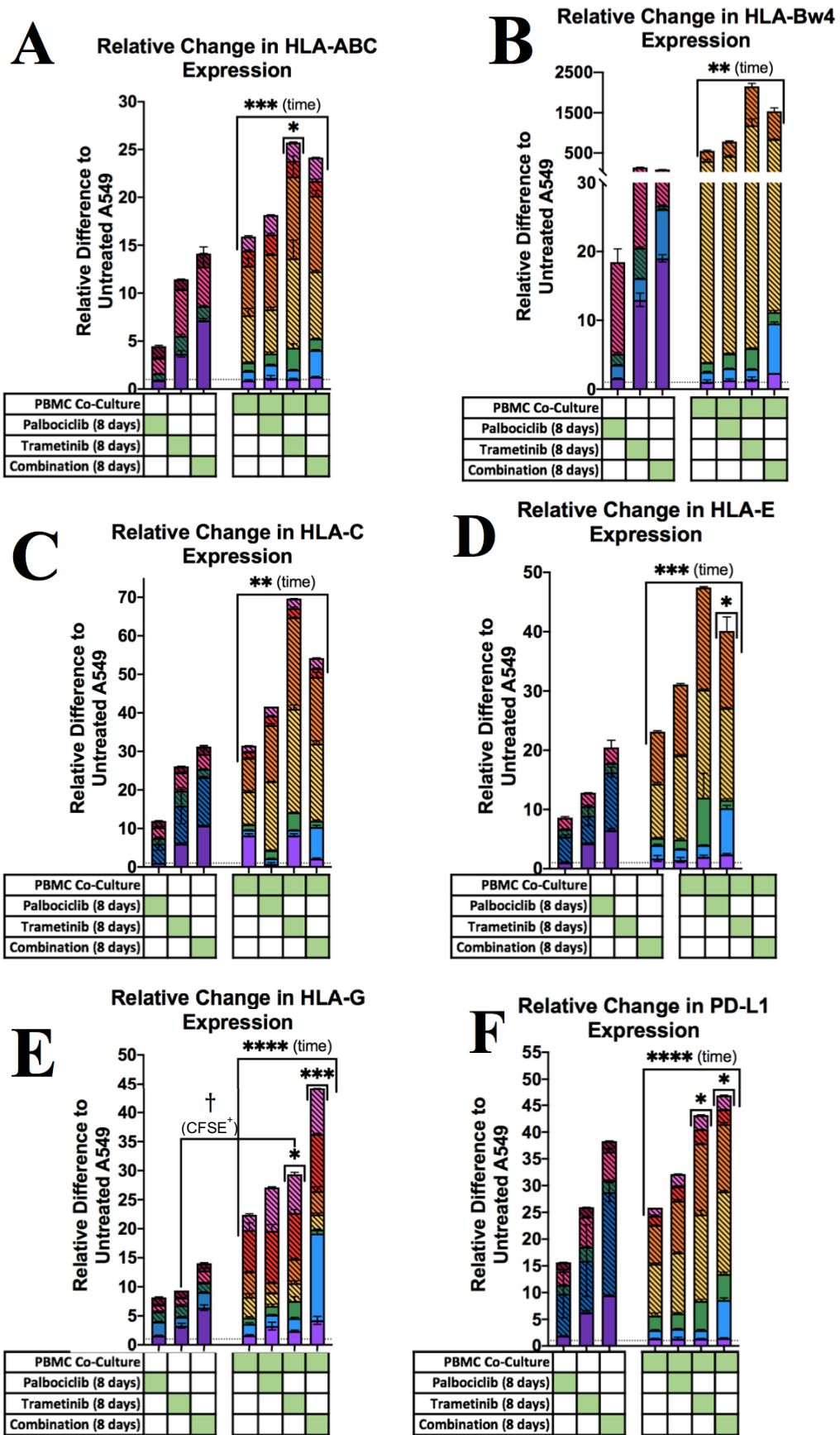


Figure 3.23 Chemotherapy and PBMC co-cultures induce death receptor and activating ligand upregulation.



**Figure 3.23 Chemotherapy and PBMC co-cultures induce inhibitory ligand upregulation.** A549 cells were treated with either trametinib (25 nM), palbociclib (500 nM), or both every 2 days for 8 days. The cells were then either stained for flow cytometry, or co-cultured with PBMCs for 5 hours, separated, and then stained for flow cytometry. A549 cells were stained with Viability Dye eFl506, anti-HLA-ABC antibodies, anti-HLA-C antibodies, anti-HLA-E antibodies, anti-HLA-G antibodies, anti-PD-L1 antibodies. The bars labelled with slashes signify CFSE<sup>+</sup> cells (n=7 with CFSE labelling, n=4 without CFSE labelling). The mean fluorescence intensities were normalized against untreated A549 cells to achieve the relative difference in tumor phenotypic evolution. RM 2-way ANOVA were performed of the groups challenged with PBMC co-culture comparing the tumor ligand changes to untreated A549 cells. Sidak's (\*) multiple comparisons tests were completed, and unpaired t-tests (†) were performed within chemotherapy conditions of CFSE<sup>+</sup> cells, comparing cells treated with and without the PBMC co-culture. \* = significantly different from baseline as indicated by the line at y=1 (\*, p<0.05; \*\*, p<0.01; \*\*\*, p<0.001; \*\*\*\*, p<0.0001). Each colour represents a different experiment, and the experiments were completed in replicates, as indicated by the error bars.

We next investigated which NK cell populations were killing the chemotherapy-treated tumor cells. The populations analyzed included: 1) activating receptor/ligand negative (NKG2D<sup>-</sup> TRAIL<sup>-</sup> FasL<sup>-</sup>), 2) activating receptor/ligand positive (individually and triple positive) and KIR<sup>+</sup> (KIR2DL2/L3<sup>+</sup> KIR3DL1<sup>+</sup>), and 3) activating receptor/ligand positive (individually and triple positive) and KIR<sup>-</sup> (KIR2DL2/L3<sup>-</sup> KIR3DL1<sup>-</sup>). We selected these populations because we wanted to examine the balance of activation by inhibitory KIRs and activating receptor/ligands. The change in degranulation between populations was assessed by RM 1-way ANOVAs and tests for linear trends within each treatment group. NK cells that did not express activating ligands or receptors had limited activation against all treatment groups (**Figure 3.24**). The NK cell activation increased as the populations expressed activating receptor/ligands, and even more so when the inhibitory KIRs were excluded. This trend was found to be significant among the unstimulated NK cells (n=4, p<0.0001 [linear trend]), the NK cells against palbociclib-treated tumor cells (n=4, p=0.0039 [linear trend]), the NK cells against trametinib-treated tumor cells (n=4, p<0.0001 [linear trend]), and the NK cells against the tumor cells treated with both chemotherapies (n=4, p<0.0001 [linear trend]). These results are consistent with our findings that chemotherapies induce the upregulation of HLA-C, the inhibitory ligand for KIR2DL2/L3, and HLA-Bw4, the inhibitory ligand for KIR3DL1. As expected, when these inhibitory interactions are eliminated by analyzing NK cells that are negative for both KIRs, the percent degranulation increases. This further supports our findings from **Figures 3.16-3.21**, which demonstrated the importance of KIRs for repressing NK cell activation against chemotherapy-treated A549 cells.

Generally, NK cells expressing all three activating receptor/ligands (green bars) demonstrated the greatest activation. When comparing between the three, the results reveal interdonor variation, and Tukey's multiple comparisons tests did not reveal any significant differences (sufficient power was not reached for every condition; see **Appendix Table 2**). By visualization, we observed a general trend of the greatest activation among FasL<sup>+</sup> NK cells, followed by TRAIL<sup>+</sup> NK cells, then lastly the NKG2D<sup>+</sup> NK cells. This trend was particularly clear amongst the unstimulated NK cells and in the combination treatment group. In the palbociclib treatment group, NKG2D<sup>+</sup> NK

cells were generally more activated. However, in the trametinib treatment group, the FasL<sup>+</sup> NK cells were more activated as expected since the effects of trametinib were significant for Fas upregulation, whereas the impact of palbociclib was non-significant for Fas (**Figure 3.8**). Within the donors, the combination treatment generally activated the activating receptor/ligand positive KIR<sup>-</sup> cells more than the palbociclib treatment. These results reflect the phenotypic changes occurring to death receptors and activating ligands on chemotherapy-treated tumor cells also impact the phenotype of the responding NK cell populations.

Overall, the results from 3.2.1 demonstrate that as chemotherapies induce phenotypic changes to A549 cells, the phenotype of the activated NK cells differs. Different therapies result in greater upregulation of different activating or inhibitory ligands, and in turn the NK cells are more, or less, activated. The strongest NK cells against all chemotherapy-treated tumor cells were triple positive for activating FasL, TRAIL, and NKG2D, and negative for inhibitory KIRs.

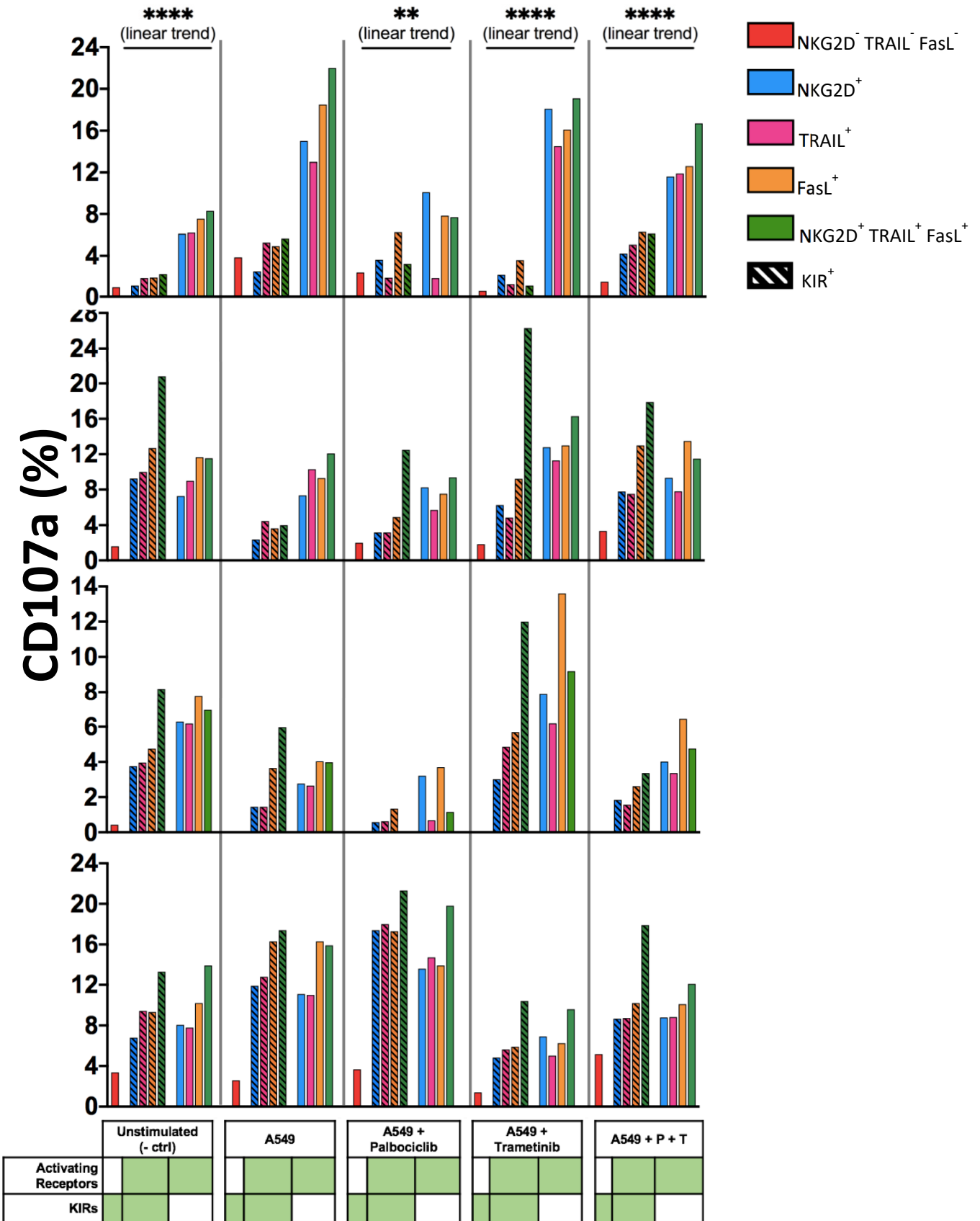
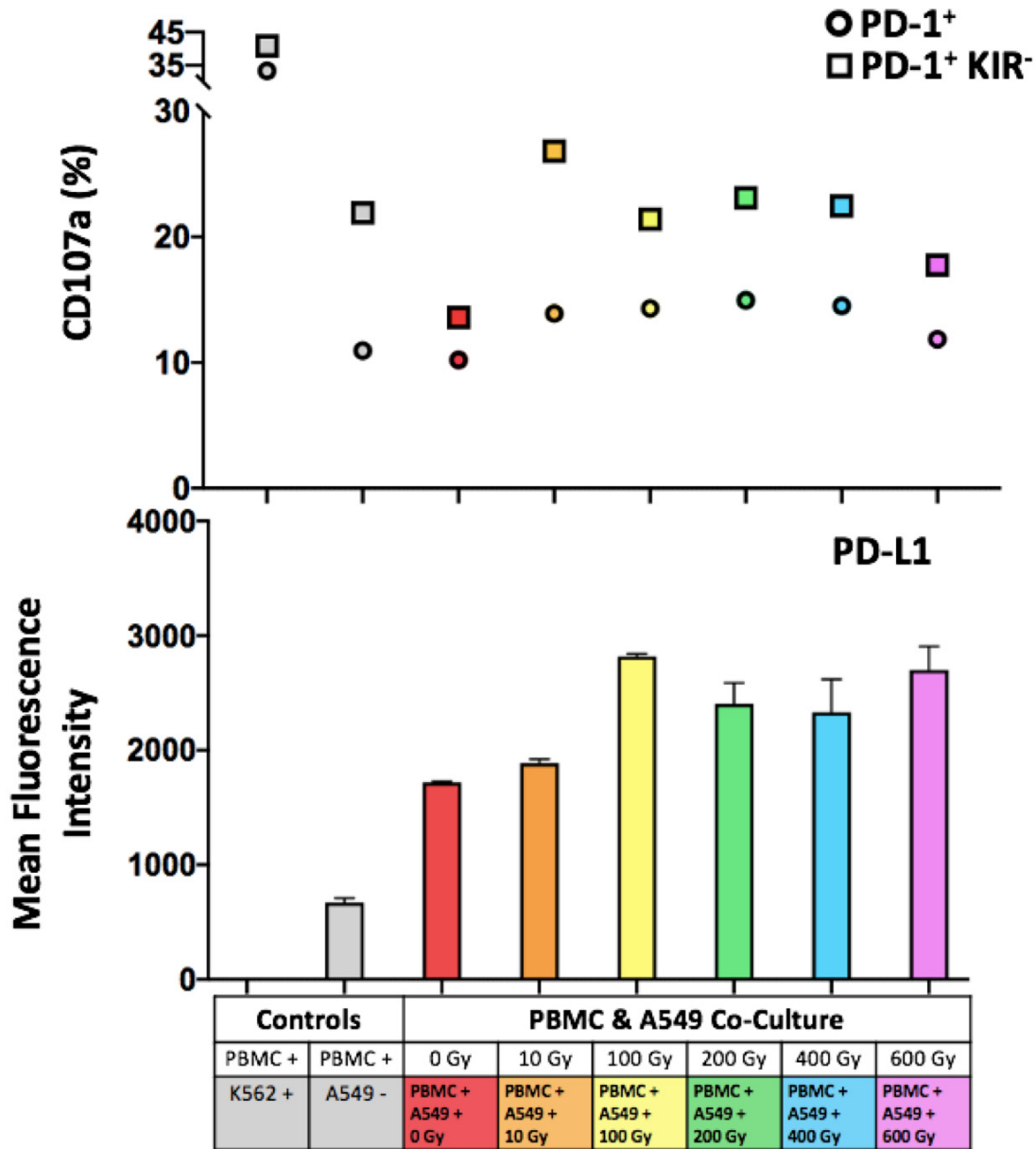


Figure 3.24 Activation of NK cells against chemotherapy-treated tumor cells depends on the expression of inhibitory KIRs.

**Figure 3.24 Activation of NK cells against chemotherapy-treated tumor cells depends on the expression of inhibitory KIRs.** A549 cells were treated with either trametinib (25 nM), palbociclib (500 nM), or both every 2 days for 8 days. The cells were then co-cultured with PBMCs for 5 hours, separated, and then stained for flow cytometry. PBMCs were stained with Viability Dye eFl506, anti-CD107a antibodies, anti-CD3 antibodies, anti-CD56 antibodies, anti-KIR2DL2/L3 antibodies, anti-KIR3DL1 antibodies, anti-FasL antibodies, anti-TRAIL antibodies, and anti-NKG2D antibodies. Within each treatment group, the NK cell populations gated on were either activating receptor<sup>-</sup> (NKG2D<sup>-</sup> TRAIL<sup>-</sup> FasL<sup>-</sup>, red bars) or activating receptor<sup>+</sup> (NKG2D<sup>+</sup>, blue bars; TRAIL<sup>+</sup>, pink bars; FasL<sup>+</sup>, orange bars; NKG2D<sup>+</sup> TRAIL<sup>+</sup> FasL<sup>+</sup>, green bars). The activating receptor<sup>+</sup> populations were further divided as KIR<sup>+</sup> (KIR2DL2/L3<sup>+</sup> KIR3DL1<sup>+</sup>) or KIR<sup>-</sup> (KIR2DL2/L3<sup>-</sup> KIR3DL1<sup>-</sup>). The percent of responding cells was determined by the frequency of CD107a<sup>+</sup> cells in the population. Each graph in a row represents one donor (n=4). RM 1-way ANOVA and tests for linear trends were performed for the NK cells within each treatment group (columns), comparing the change in activation between NK cell populations (\*, p<0.05; \*\*, p<0.01; \*\*\*, p<0.001; \*\*\*\*, p<0.0001). Wilcoxon tests were completed for the A549 treatment group as normal distribution could not be assumed.

### *3.3.2 The subset of NK cells responding to a tumor can be predicted by the tumor cell phenotype after irradiation treatment*

The tumor phenotyping results from 3.1.5 demonstrated that tumor cells, post irradiation, upregulate death receptors and activating and inhibitory ligands in a dose-dependent manner. We therefore hypothesized that the NK cell populations responding to A549 cells will change with different doses of irradiation. We treated A549 cells with increasing doses on the Gamma Cell Irradiator, then co-cultured them with PBMCs after 72 hours. When analyzing the NK cells expressing PD-1, our results revealed the activation of this population drops when the cognate inhibitory ligand, PD-L1, was upregulated, particularly at the highest dose (**Figure 3.25**). This decrease in activation is more emphasized when the population excludes KIR2DL2/L3 and KIR3DL1. Furthermore, the activation of PD-1<sup>+</sup> NK cells is greater when the population is KIR<sup>-</sup>. When analyzing the activating pairings, we observed the activation of FasL<sup>+</sup> NK cells increases as the cognate death receptor Fas is upregulated (**Figure 3.26**). Similarly, the activation is greater when the FasL<sup>+</sup> NK cells are KIR<sup>-</sup>. This trend is observed again with the NKG2D<sup>+</sup> cells (**Figure 3.27**) and the TRAIL<sup>+</sup> cells (**Figure 3.28**). The percent of degranulation of TRAIL<sup>+</sup> NK cells decreases at the higher doses, which follows the cognate tumor death receptors TRAIL-R1 and TRAIL-R2, which upregulate with as doses increase and then the expression goes back down at the highest doses. Overall, these results signify the control that KIRs have on repressing NK cell activation, and that the responding population to irradiated tumor cells will reflect how the tumor cells evolve.



**Figure 3.25 Activation of PD-1<sup>+</sup> NK cells increases against irradiated A549 cells when excluding KIR<sup>+</sup> NK cells.** A549 cells were subjected to varying doses of irradiation on the Gamma Cell Irradiator, and were left to rest for 72 hours. The cells were then co-cultured with PBMCs for 5 hours, separated, and stained for flow cytometry. The PBMCs were stained with Viability Dye eFl506, anti-CD3 antibodies, anti-CD56 antibodies, anti-CD107a antibodies, anti- KIR2DL2/L3 antibodies, KIR3DL1 antibodies, and anti-PD-1 antibodies. The PD-1<sup>+</sup> NK cells (circles) and single PD-1<sup>+</sup> NK cells (KIR2DL2/L3<sup>-</sup> KIR3DL1<sup>-</sup>; squares) were gated on, and the percent of responding cells was determined by the frequency of CD107a<sup>+</sup> cells in the population. The tumor cells were stained with Viability Dye eFl506 and anti-PD-L1 antibodies. The experiment was repeated in replicates, as indicated by the error bars (n=1).

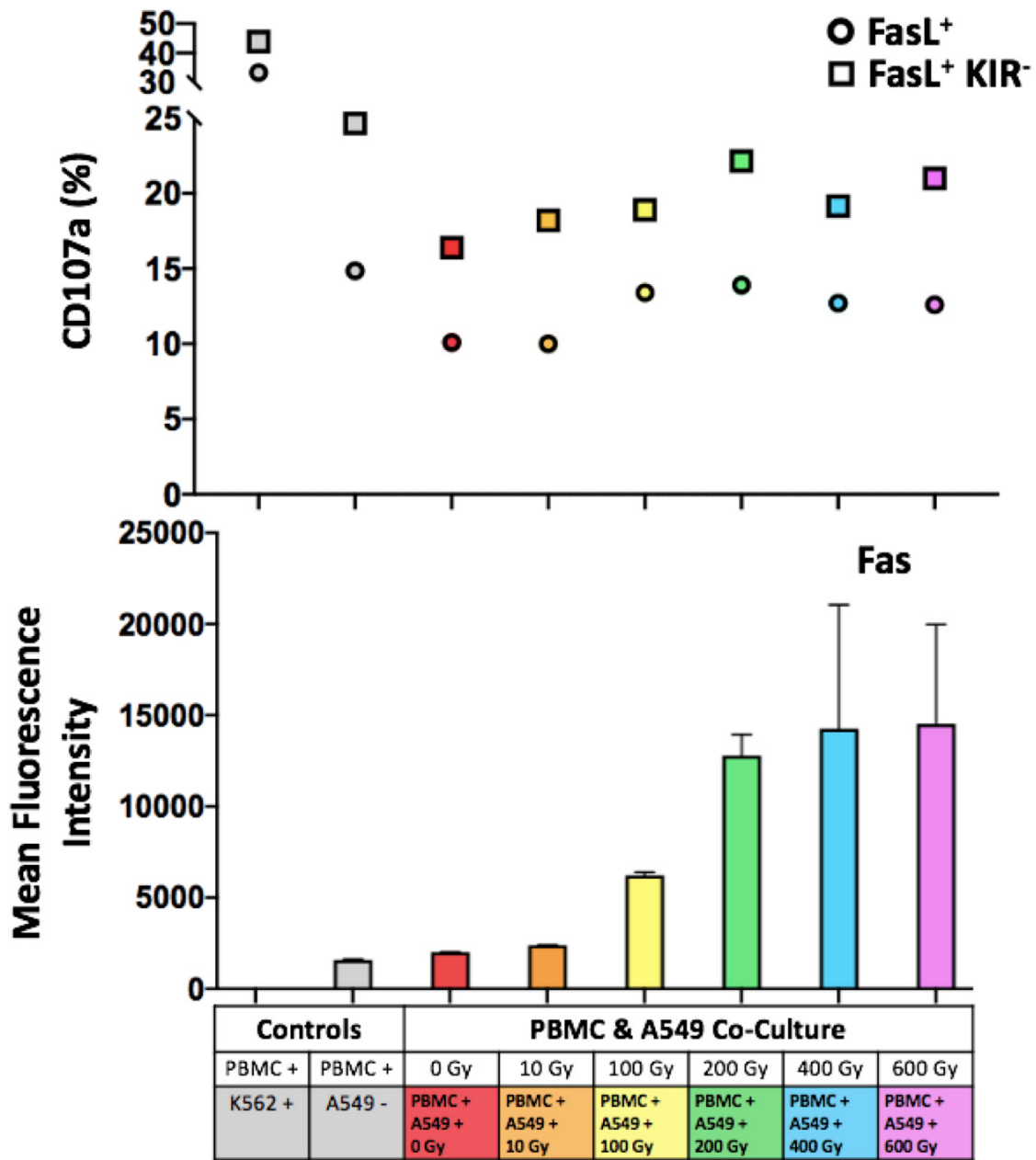


**Figure 3.26 Activation of FasL<sup>+</sup> NK cells increases as irradiation induces Fas upregulation on A549 cells.** A549 cells were subjected to varying doses of irradiation on the Gamma Cell Irradiator, and were left to rest for 72 hours. The cells were then co-cultured with PBMCs for 5 hours, separated, and stained for flow cytometry. The PBMCs were stained with Viability Dye eFl506, anti-CD3 antibodies, anti-CD56 antibodies, anti-CD107a antibodies, anti- KIR2DL2/L3 antibodies, KIR3DL1 antibodies, and anti-FasL antibodies. The FasL<sup>+</sup> NK cells (circles) and FasL<sup>+</sup> KIR<sup>-</sup> NK cells (KIR2DL2/L3<sup>-</sup> KIR3DL1<sup>-</sup>; squares) were gated on, and the percent of responding cells was determined by the frequency of CD107a<sup>+</sup> cells in the population. The tumor cells were stained with Viability Dye eFl506 and anti-Fas antibodies. The experiment was repeated in replicates, as indicated by the error bars (n=1).



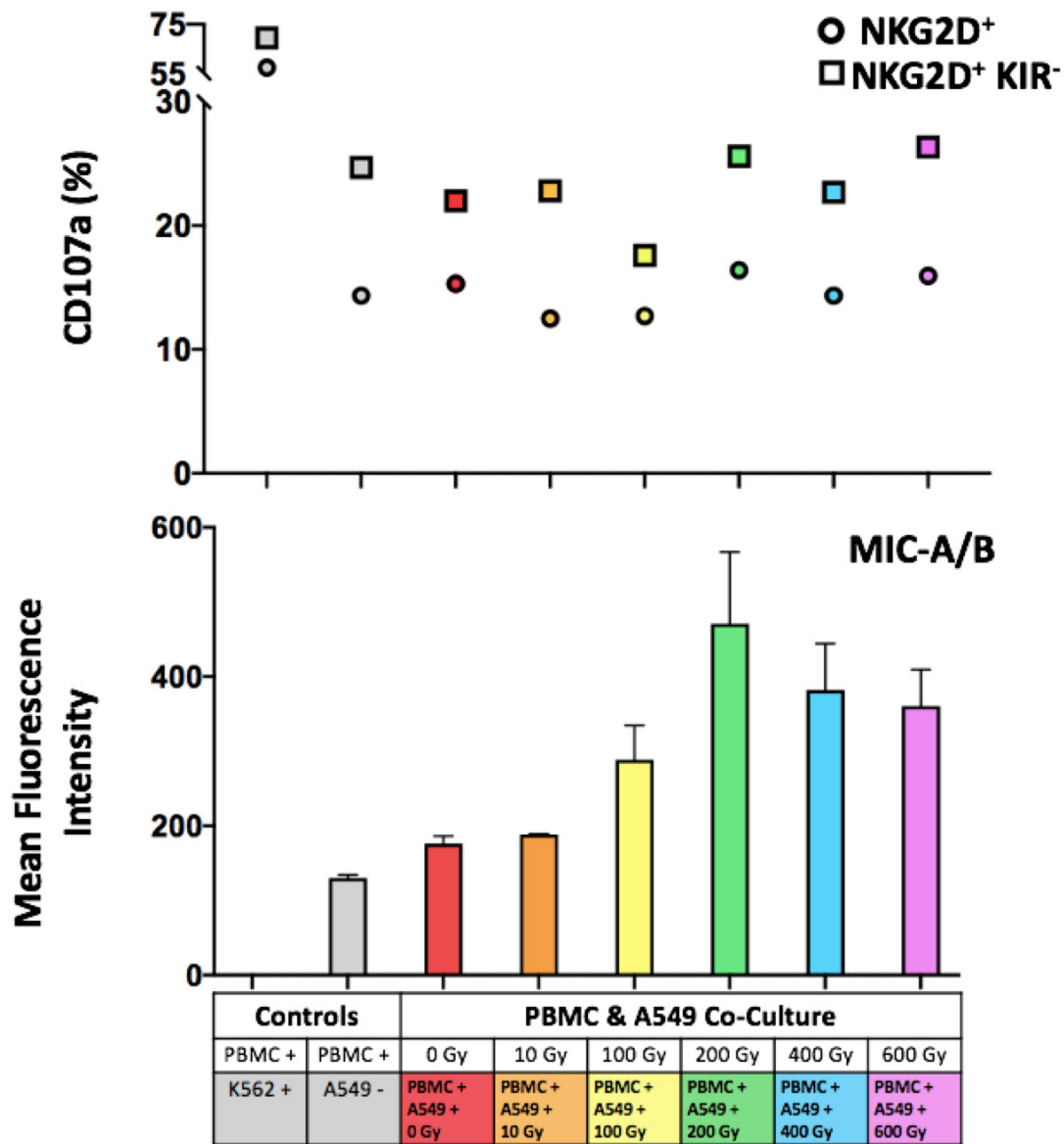


**Figure 3.27 Activation of NKG2D<sup>+</sup> NK cells increases against irradiated A549 cells when excluding KIR<sup>+</sup> NK cells.** A549 cells were subjected to varying doses of irradiation on the Gamma Cell Irradiator, and were left to rest for 72 hours. The cells were then co-cultured with PBMCs for 5 hours, separated, and stained for flow cytometry. The PBMCs were stained with Viability Dye eF1506, anti-CD3 antibodies, anti-CD56 antibodies, anti-CD107a antibodies, anti- KIR2DL2/L3 antibodies, KIR3DL1 antibodies, and anti-NKG2D antibodies. The NKG2D<sup>+</sup> NK cells (circles) and NKG2D<sup>+</sup> KIR<sup>-</sup> NK cells (KIR2DL2/L3<sup>-</sup> KIR3DL1<sup>-</sup>; squares) were gated on, and the percent of responding cells was determined by the frequency of CD107a<sup>+</sup> cells in the population. The tumor cells were stained with Viability Dye eF1506 and anti-MIC-A/B antibodies. The experiment was repeated in replicates, as indicated by the error bars (n=1).

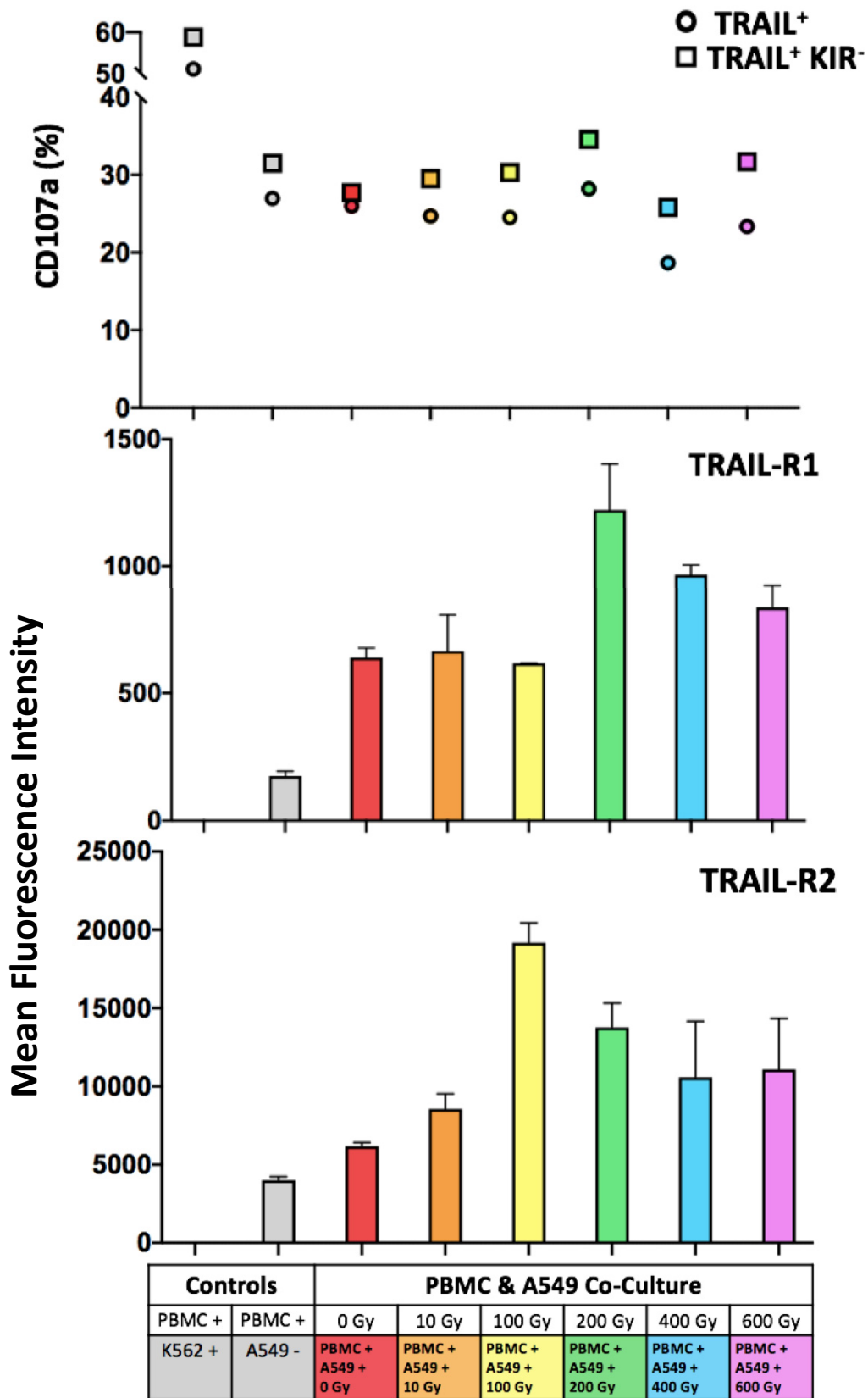


Figure 3.28 Activation of TRAIL<sup>+</sup> NK cells increases against irradiated A549 cells when excluding KIR<sup>+</sup> NK cells.

**Figure 3.28 Activation of TRAIL<sup>+</sup> NK cells increases against irradiated A549 cells when excluding KIR<sup>+</sup> NK cells.** A549 cells were subjected to varying doses of irradiation on the Gamma Cell Irradiator, and were left to rest for 72 hours. The cells were then co-cultured with PBMCs for 5 hours, separated, and stained for flow cytometry. The PBMCs were stained with Viability Dye eF1506, anti-CD3 antibodies, anti-CD56 antibodies, anti-CD107a antibodies, anti- KIR2DL2/L3 antibodies, KIR3DL1 antibodies, and anti-TRAIL antibodies. The TRAIL<sup>+</sup> NK cells (circles) and TRAIL<sup>+</sup> KIR<sup>-</sup> NK cells (KIR2DL2/L3<sup>-</sup> KIR3DL1<sup>-</sup>; squares) were gated on, and the percent of responding cells was determined by the frequency of CD107a<sup>+</sup> cells in the population. The tumor cells were stained with Viability Dye eF1506, anti-TRAIL-R1 antibodies and anti-TRAIL-R2 antibodies. The experiment was repeated in replicates, as indicated by the error bars (n=1).

### **3.4 Impact of inhibitory ligand blockade on the NK cell response to tumors post-treatment**

#### *3.4.1 Inhibitory ligand blockade rescues the inhibitory receptor-positive NK cells against chemotherapy-treated A549 cells*

Our results from 3.3.1 revealed that the responding NK cell populations to chemotherapy-treated tumor cells are impacted by the rapidly evolving tumor ligands and receptors, as demonstrated in 3.1.4. As the cognate inhibitory ligands are upregulated, the expression of KIRs and PD-1 on NK cell surfaces induce inhibition. The upregulation of death receptors and activating ligands with chemotherapy induced cognate receptor/ligand-expressing NK cells to become activated, and NK cells triple expressing FasL, TRAIL, and NKG2D were the strongest responders. As demonstrated in 3.2.1 and 3.2.2, when the inhibitory interactions are blocked with antibodies, the KIR and PD-1 expressing NK cells can become further activated. Therefore, we hypothesized that we could enhance NK cell cytotoxic killing of chemotherapy-treated A549 cells by blocking these interactions. We treated A549 cells with the middle dose of palbociclib, trametinib, and a combination of the two for 8 days, then blocked the inhibitory ligands with either an anti-PD-L1 blocking antibody (atezolizumab), W6/32 (blocks HLA-A, -B, -C, and -E), or both. We co-cultured the cells with PBMCs for 5 hours, and analyzed the changes in activation of NK cell populations that were KIR<sup>+</sup> (KIR2DL2/L3<sup>+</sup> KIR3DL1<sup>+</sup>) PD-1<sup>+</sup> and expressed activating receptor/ligands. The populations analyzed were either positive for one activating receptor/ligand, single positive for one activating receptor/ligand (i.e. excluded the other two), or triple positive.

Without any blocking antibodies, these inhibitory receptor positive populations, even while expressing activating receptors, had the lowest activation against trametinib-treated A549 cells, followed by the cells treated with combination chemotherapy (**Figure 3.29**). These results support our findings in **Figure 3.9**, which demonstrated significant upregulation of HLA ligands and PD-L1 with trametinib and the combination treatment. Interestingly, the activation of the NK cells against palbociclib-treated A549 cells remained relatively high in comparison to the other chemotherapy-treated groups. This again supports our results from **Figure 3.9** in that palbociclib did not induce the upregulation of inhibitory ligands as much as trametinib and the combination treatment.

When the blocking antibodies were added, the activation of the KIR<sup>+</sup> PD-1<sup>+</sup> NK cells was rescued, particularly against trametinib-treated A549 cells. The rescue, determined by increase in degranulation, remained relatively consistent between the FasL<sup>+</sup>, NKG2D<sup>+</sup>, TRAIL<sup>+</sup> and triple activating receptor/ligands positive populations. Similarly, the blocking antibodies rescued the response of these NK cell populations against A549 cells treated with the chemotherapy combination. These results support our findings from **Figure 3.24**, which demonstrate the activation ability of FasL<sup>+</sup>, NKG2D<sup>+</sup>, and TRAIL<sup>+</sup> NK cell populations against chemotherapy-treated tumor cells when they are less likely to be inhibited (i.e. do not express KIR2DL2/L3 or KIR3DL1). Importantly, the activation rescue ability of each individual activating receptor/ligand demonstrates that all three are contributing to NK cell tumor cell killing.

When comparing the individual activating receptor/ligand positive populations and the triple positive populations, the FasL<sup>+</sup> NKG2D<sup>+</sup> TRAIL<sup>+</sup> NK cells had higher percent activation, particularly in the blocking antibody treatment conditions. This again supports our findings from **Figure 3.24**, where we observed the triple positive NK cell populations to have greater activation than the populations expressing one activating receptor/ligand. When the single activating receptor/ligand positive NK cells are gated to exclude the remaining two receptor/ligands, the activation within treatment groups changes. Single TRAIL<sup>+</sup> and NKG2D<sup>+</sup> populations exhibited diminished activation, whereas single FasL<sup>+</sup> activation remained relatively consistent. This suggests that the increased activation of TRAIL<sup>+</sup> or NKG2D<sup>+</sup> populations, particularly in the trametinib condition, was likely contributed to by the NK cells that co-expressed FasL. Overall, these results support the use of inhibitory interaction blocking antibodies with chemotherapy in patients, as it will increase the activation and cytotoxic killing of NK cells that express both activating and inhibitory receptors.

# Activating Receptor<sup>+</sup> NK Cell Response

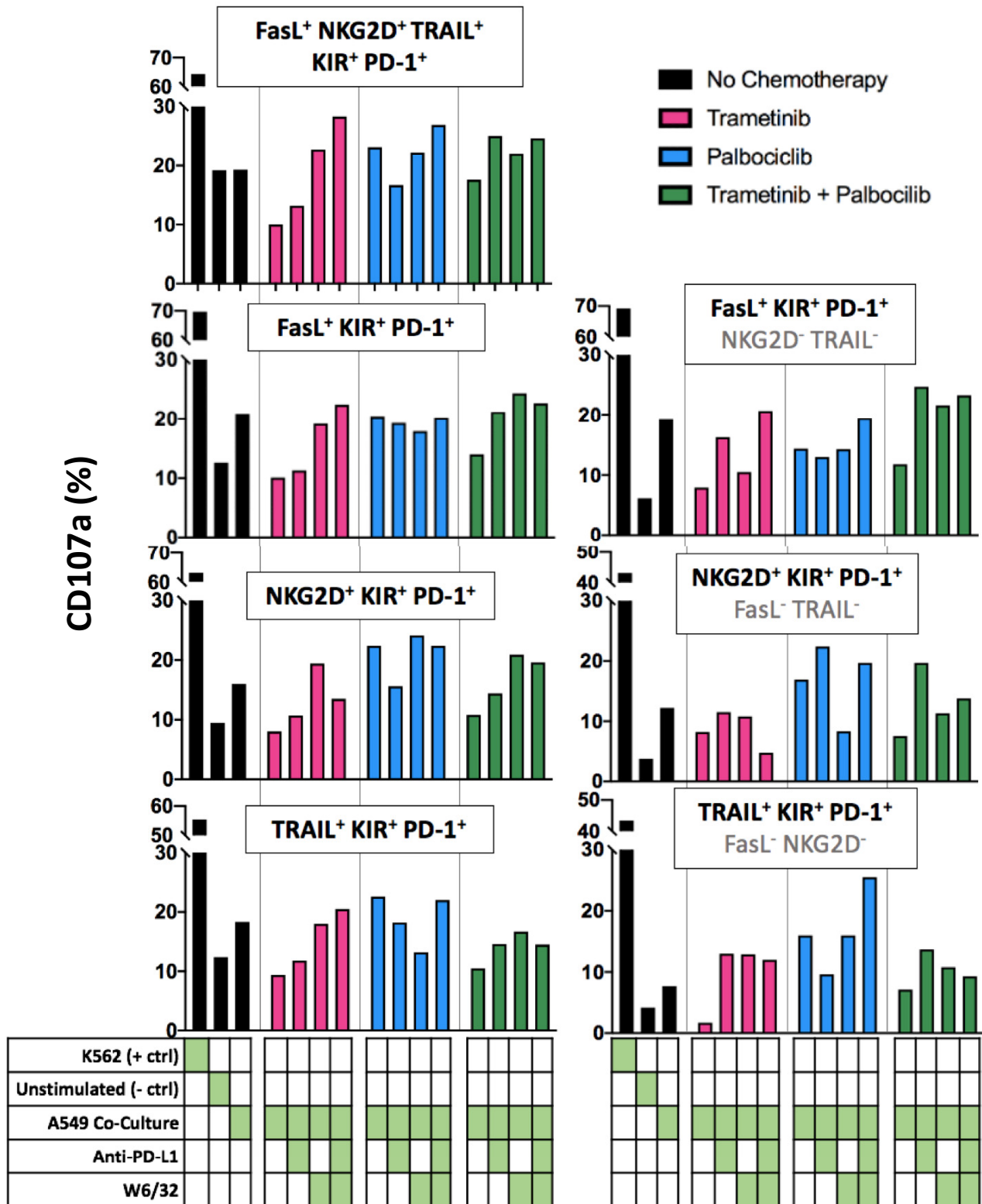


Figure 3.29 Blocking inhibitory interactions rescues the inhibitory receptor-positive NK cell response against chemotherapy-treated A549 cells.

**Figure 3.29 Blocking inhibitory interactions rescues the inhibitory receptor-positive NK cell response against chemotherapy-treated A549 cells.** A549 cells were treated with either trametinib (25 nM, pink bars), palbociclib (500 nM, blue bars), or both (green bars) every 2 days for 8 days. The tumor cells were incubated for 30 minutes with either an anti-PD-L1 blocking antibody (atezolizumab, 2  $\mu\text{g}/\text{mL}$ ), W6/32 (HLA class I inhibitor, 6  $\mu\text{g}/\mu\text{L}$ ) or a combination of both. The blocking antibodies were washed off, then the A549 cells were co-cultured with PBMCs for 5 hours, separated, and then stained for flow cytometry. PBMCs were stained with Viability Dye eFl506, anti-CD107a antibodies, anti-CD3 antibodies, anti-CD56 antibodies, anti-KIR2DL2/L3 antibodies, anti-KIR3DL1 antibodies, anti-PD-1 antibodies, anti-FasL antibodies, anti-NKG2D antibodies, and anti-TRAIL-antibodies. The NK cell populations gated on were KIR2DL2/L3<sup>+</sup>, KIR3DL1<sup>+</sup>, PD-1<sup>+</sup>, and either express all three activating receptor/ligands (FasL<sup>+</sup>, TRAIL<sup>+</sup>, or NKG2D<sup>+</sup>), or one. Those populations were further gated to exclude the remaining two activating receptor/ligands. The percent of responding cells was determined by the frequency of CD107a<sup>+</sup> cells in each population. This experiment was completed in replicates, indicated by the error bars (n=1)

### *3.4.2 Inhibitory ligand blockade rescues the inhibitory receptor-positive NK cells against irradiated A549 cells*

Our results from 3.1.5 demonstrated that irradiation induces changes in expression of ligands for NK cells, which in turn impacted which NK cell populations responds (3.3.2). Similar to 3.4.1, we hypothesized that the use of inhibitory ligand blockade would rescue the response of inhibitory receptor-positive NK cells against irradiated tumor cells. We irradiated A549 cells on the Varian TrueBeam Linear Accelerator at 5 Gy, then left the cells to rest for either 1 or 5 days. The tumor cells were incubated with either the anti-HLA-C blocking antibody DT9, W6/32, an anti-PD-1 blocking antibody, atezolizumab, or a combination of the latter three.

When comparing all the NK cells to those that are KIR<sup>+</sup> or KIR<sup>+</sup> PD-1<sup>+</sup>, our results revealed that, as expected, it is the NK cell populations expressing the cognate inhibitory receptors that increase in activation in the presence of blocking antibodies (**Figure 3.30**). This is particularly seen against the tumor cells that were left to rest for 5 days rather than 1 day, with the greatest upregulation occurring in the conditions treated with the anti-PD-L1 blocking antibody, atezolizumab. We further examined the activating receptor positive populations that were either KIR<sup>-</sup> (uneducated) or KIR<sup>+</sup> (educated). As previously seen, the activation of the cells that express KIRs was increased with the blocking antibodies (**Figure 3.31**). This greater percent of activation was higher than the uneducated NK cells, even though they express all three activating receptor/ligands (FasL, TRAIL, NKG2D). This suggests that the strongest NK cell populations against irradiated tumor cells are KIR<sup>+</sup>, and blocking the inhibition is crucial to unleashing their cytotoxic activity. We compared the differences in the three activating receptor/ligands on educated NK cells, and observed the greatest response among the FasL<sup>+</sup> populations (**Figure 3.32**). Overall, these results suggest that the NK cells best able to attack irradiated tumor cells are those that are educated, FasL<sup>+</sup>, and with the inhibitory interactions blocked.

In sum, our results reveal that tumor cells' expression of ligands and receptors for NK cells is dynamic, and influences interactions with and killing by NK cells. Therefore, the features of tumor cell phenotypes and NK cell functions could reveal opportunities to



intervene within the existing SOC therapies to maximize NK cell function and contributions in tumor cell control and killing.

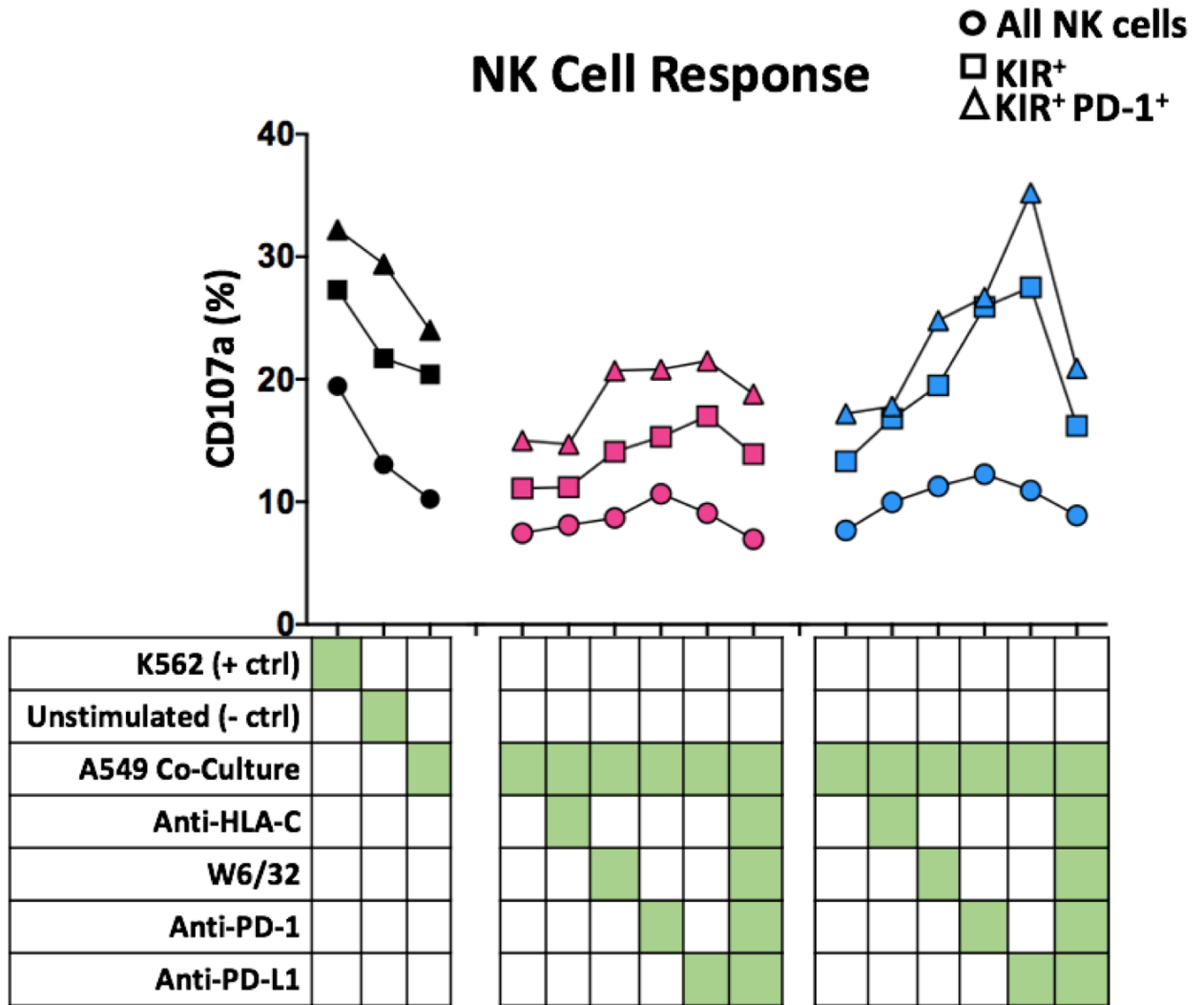


**Figure 3.30 Blocking inhibitory interactions rescues the inhibitory receptor-positive NK against irradiated A549 cells, particularly after 5 days.** A549 cells were irradiated at 5 Gy, then left to rest for either 1 day (pink) or 5 days (blue). PBMCs were incubated with an anti-PD-1 blocking antibody (6 $\mu$ g/mL), and the tumor cells were incubated with either an anti-HLA-C blocking antibody (DT9, 6  $\mu$ g/ $\mu$ L), W6/32 (HLA class I inhibitor, 6  $\mu$ g/ $\mu$ L), an anti-PD-L1 blocking antibody (atezolizumab, 2  $\mu$ g/mL), or a combination of the latter two. After 30 minutes, the blocking antibodies were washed off, then the A549 cells were co-cultured with PBMCs for 5 hours, separated, and then stained for flow cytometry. The PBMCs were stained with Viability Dye eF1506, anti-CD107a antibodies, anti-CD3 antibodies, anti-CD56 antibodies, anti-KIR2DL2/L3 antibodies, anti-KIR3DL1 antibodies, and anti-PD-1 antibodies. The NK cells were gated on (circles), and the populations further gated were KIR2DL2/L3<sup>+</sup> and KIR3DL1<sup>+</sup> (squares) or KIR2DL2/L3<sup>+</sup> KIR3DL1<sup>+</sup> PD-1<sup>+</sup> (triangles). The percent of responding cells was determined by the frequency of CD107a<sup>+</sup> cells in each population (n=1).

## NK Cell Response

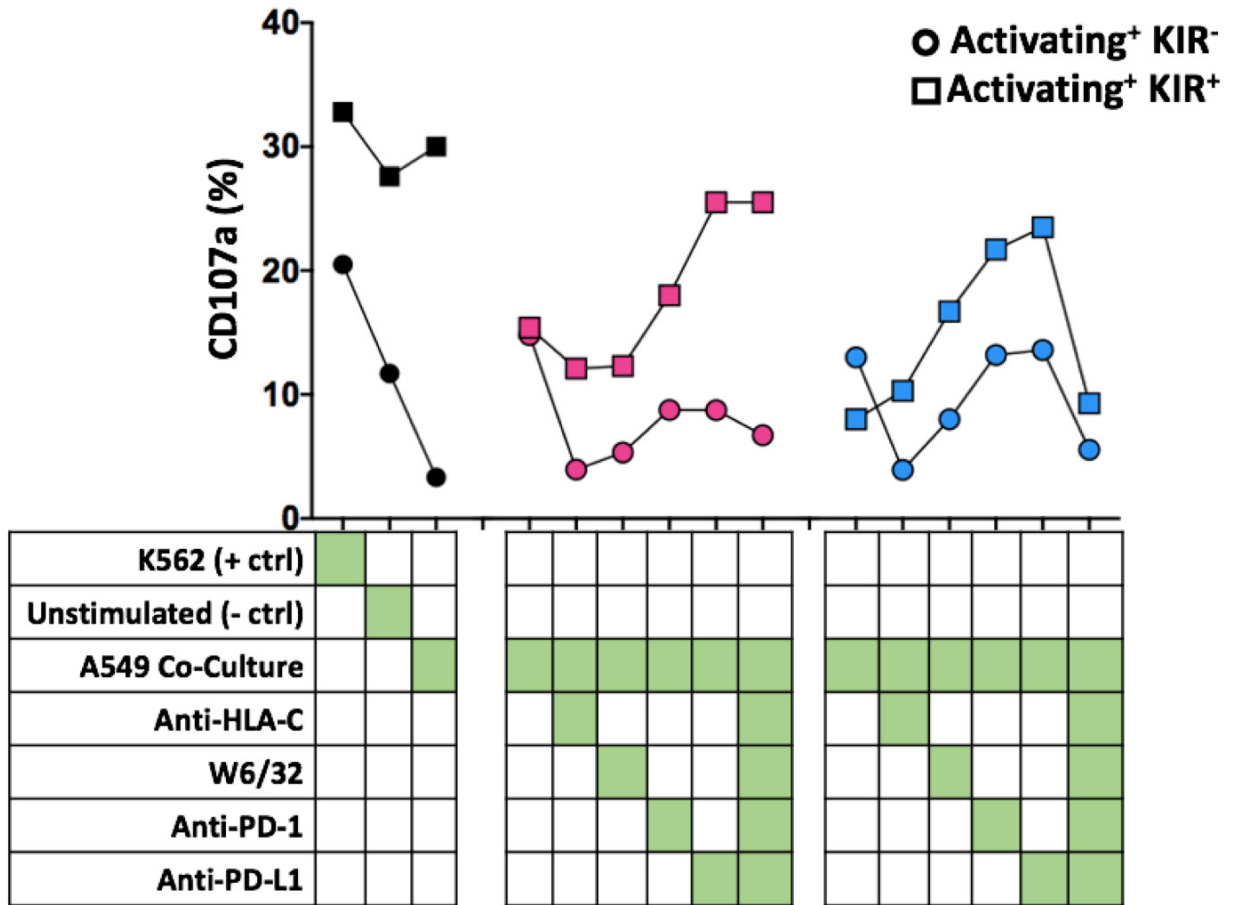


**Figure 3.31 Activation of educated activating receptor/ligand-positive NK cells increases against irradiated A549 cells as inhibitory interactions are blocked.** A549 cells were irradiated at 5 Gy, then left to rest for either 1 day (pink) or 5 days (blue). PBMCs were incubated with an anti-PD-1 blocking antibody (6 $\mu$ g/mL), and the tumor cells were incubated with either an anti-HLA-C blocking antibody (DT9, 6  $\mu$ g/ $\mu$ L), W6/32 (HLA class I inhibitor, 6  $\mu$ g/ $\mu$ L), an anti-PD-L1 blocking antibody (atezolizumab, 2  $\mu$ g/mL), or a combination of the latter two. After 30 minutes, the blocking antibodies were washed off, then the A549 cells were co-cultured with PBMCs for 5 hours, separated, and then stained for flow cytometry. The PBMCs were stained with Viability Dye eF1506, anti-CD107a antibodies, anti-CD3 antibodies, anti-CD56 antibodies, anti-KIR2DL2/L3 antibodies, anti-KIR3DL1 antibodies, anti-FasL antibodies, anti-TRAIL antibodies, and anti-NKG2D antibodies. The NK cells gated on were expressing activating ligand/receptors (FasL<sup>+</sup>, TRAIL<sup>+</sup>, NKG2D<sup>+</sup>) and were either positive (squares) or negative (circles) for KIR2DL2/L3<sup>+</sup> and KIR3DL1<sup>+</sup>. The percent of responding cells was determined by the frequency of CD107a<sup>+</sup> cells in each population (n=1).

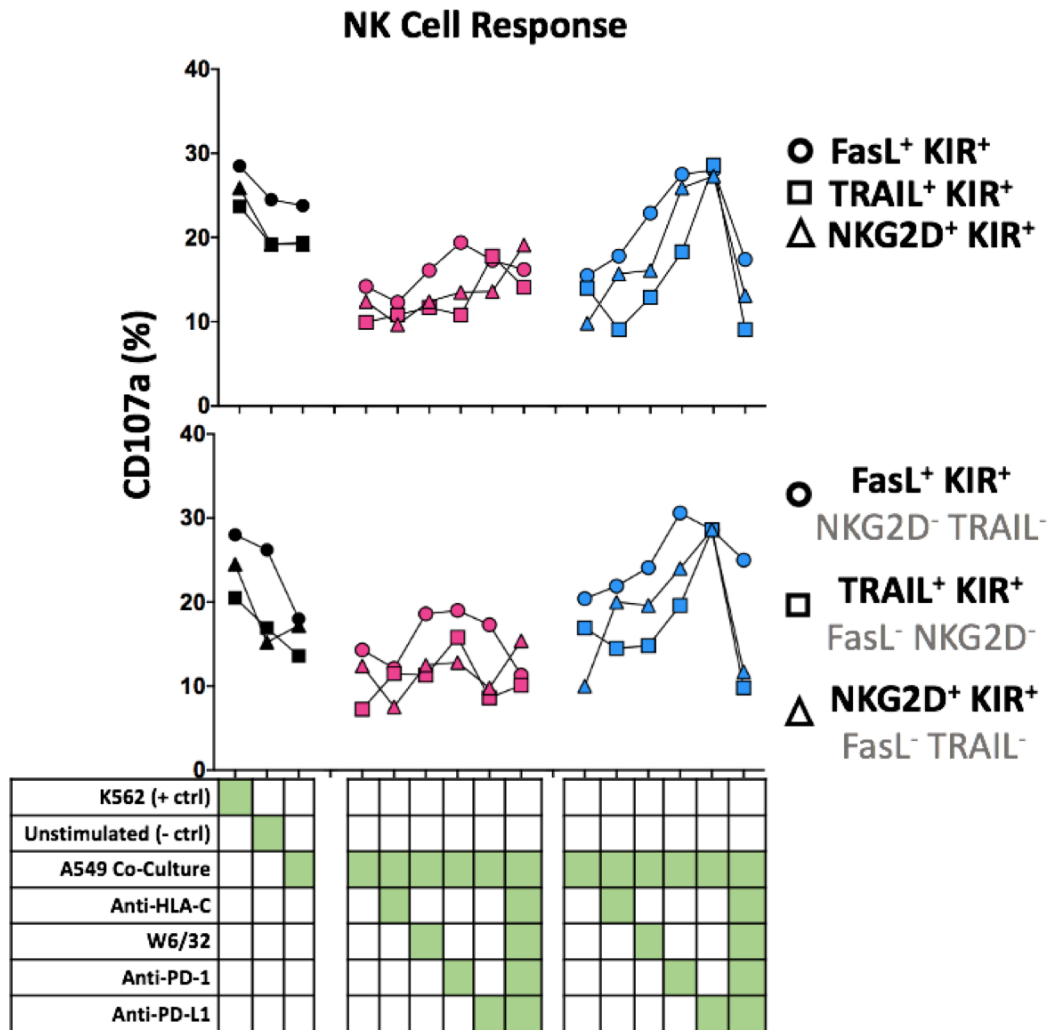


**Figure 3.32 FasL<sup>+</sup> NK cells were more activated against irradiated A549 cells than TRAIL<sup>+</sup> and NKG2D<sup>+</sup> NK cells.** A549 cells were irradiated at 5 Gy, then left to rest for either 1 day (pink) or 5 days (blue). PBMCs were incubated with an anti-PD-1 blocking antibody (6µg/mL), and the tumor cells were incubated with either an anti-HLA-C blocking antibody (DT9, 6 µg/µL), W6/32 (HLA class I inhibitor, 6 µg/µL), an anti-PD-L1 blocking antibody (atezolizumab, 2 µg/mL), or a combination of the latter two. After 30 minutes, the blocking antibodies were washed off, then the A549 cells were co-cultured with PBMCs for 5 hours, separated, and then stained for flow cytometry. The PBMCs were stained with Viability Dye eF1506, anti-CD107a antibodies, anti-CD3 antibodies, anti-CD56 antibodies, anti-KIR2DL2/L3 antibodies, anti-KIR3DL1 antibodies, anti-FasL antibodies, anti-TRAIL antibodies, and anti-NKG2D antibodies. The NK cells gated on were KIR2DL2/L3<sup>+</sup> and KIR3DL1<sup>+</sup>, and expressed FasL (circles), TRAIL (squares), or NKG2D (triangles; top graph). Those populations were further gated to exclude the remaining two activating receptor/ligands (bottom graph). The percent of responding cells was determined by the frequency of CD107a<sup>+</sup> cells in each population (n=1).

## **CHAPTER 4: DISCUSSION**

NK cells bear powerful anti-tumor functions, and understanding how to strengthen their response to evolving NSCLC phenotypes with treatment is crucial to enhancing patient outcomes. We hypothesized that NK cells, as dynamic and durable effectors with phenotypic and functional diversity, can be selected against rapidly evolving NSCLC tumors. We approached this goal by studying the phenotypic changes to NSCLC during inflammation, interaction with immune cells, chemotherapy and radiation, and how these change interactions with NK cell subsets. Tumor phenotyping data provided insight in how the tumors evolve, and allowed us to predict which NK cell populations would be the most efficient tumor killers in different conditions (summarized in **Figure 4.1**).

Although the dynamics of NK ligands were different for each condition tested, we overall observed transient changes that would implicate different subsets of NK cells as the ideal anticancer effectors. Hence, we conclude that there is a window of opportunity during which NK cell function could best support anticancer immunity with clinical treatments. We recommend simultaneous or combinatorial therapies aimed at supporting NK cell function during these clinical treatments.

NSCLC is a difficult cancer to cure because it's often diagnosed at late stages, therefore the cancer has become metastatic and spread through the body (Canadian Cancer Society, 2020). The interaction between the immune system and tumors leads to three dynamic stages of cancer immunosurveillance: the elimination phase, where immune cells kill tumors; the equilibrium phase, where immune cells suppress net tumor growth; and the escape phase, where tumors evolve to avoid immune recognition and grow uncontrollably (Dunn et al., 2004). NK cells have proven to be strong anticancer effectors, and their phenotypic diversity provides an opportunity to leverage certain populations to treat tumor cells at all stages, including the escape phase (Shin et al., 2020).

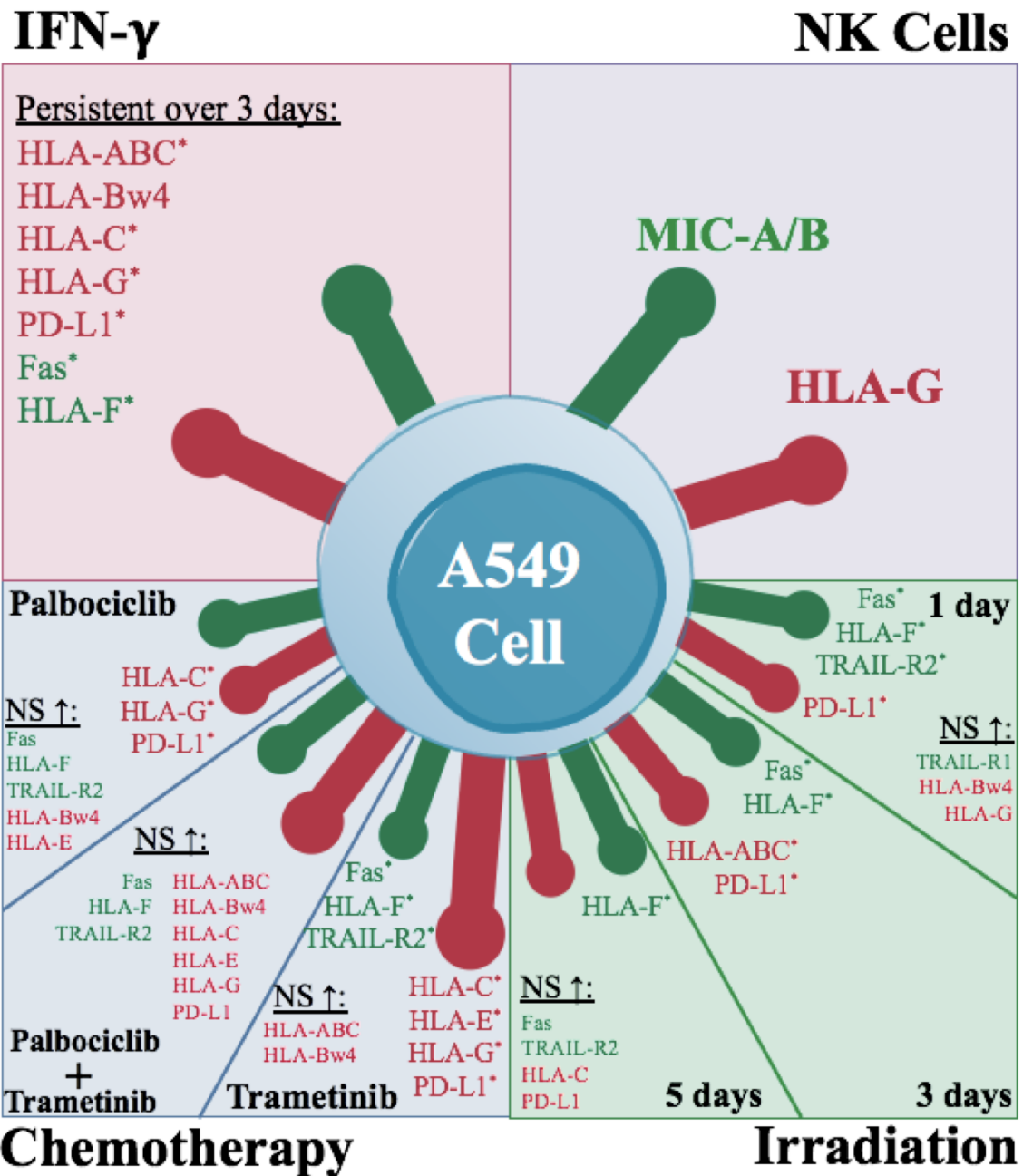


**Figure 4.1 Summary of stimulation-induced phenotypic changes observed on A549 cells.** A549 cells stimulated with IFN- $\gamma$ , NK cells, small molecule chemotherapy (palbociclib and trametinib) and irradiation. The important changes within each condition are highlighted in their respective quadrant. Red signifies inhibitory receptors, and green signifies activating receptors. \* signifies significant phenotypic changes. In the chemotherapy quadrant, the size of the receptor is relative to the intensity of the ligand expression change.

## 4.1 Phenotypic evolution of NSCLC death receptors and inhibitory and activating ligands within the TME

### 4.1.1 HLA class I regulation on tumor cells

Expression of HLA class I molecules is important for both innate and adaptive anticancer immunity. For an activated T cell response, tumor antigen specific T cells must interact with presented antigens on HLA molecules (Waldman et al., 2020). Conversely, NK cells that express cognate KIRs to the HLA class I ligands become inhibited from their interaction (Kannan et al., 2017). Due to these opposing effects, a strong anti-tumor immune response will leverage both T cells and NK cells, and understanding how HLA class I expression is regulated is key to unleashing their response. As part of the tumor escape phase, tumor cells can downregulate HLA class I molecules to “hide” from CD8<sup>+</sup> T cells, while concurrently removing an important inhibitory signal for NK cells (Kersh et al., 2016). When the surface expression is only partially lost in comparison to tumors that are negative for HLA class I or high-expressing, a tumor may escape both T and NK cell responses; a precedent for this has been observed in colorectal tumors (Watson et al., 2006).

HLA class I expression is regulated at several levels transcriptionally and epigenetically. Changes in HLA class I expression can be divided into reversible, regulatory defects and irreversible, structural defects. **Irreversible downregulation** include loss of heterozygosity (in chromosome 6 [*HLA-ABC* genes] or 15 [*β2m* gene]); HLA allelic loss (due to mutations, deletions, and somatic recombination); mutations in antigen processing and presentation machinery (APM); and resistance to IFN- $\gamma$ -mediated upregulation (due to JAK-STAT pathway defects; F. Garrido et al., 2010). Resistance to ICB is associated with these irreversible changes, such as the *JAK1/2* IFN- $\gamma$  signalling pathway defects (Shin et al., 2017) and loss of antigen processing and presentation genes (Gettinger et al., 2017). In the absence of HLA expression or presentation, effector T cells are unable to become activated, but the “missing self” capabilities of NKs might be leveraged in this context. Our results have demonstrated the ability of KIR- and PD-1-expressing NK cells to target NSCLC when administered with ICB and HLA blocking antibodies (i.e. comparative to irreversible loss of HLA class I molecules). This finding is supported by a HLA class I-deficient lymphoma mouse model that revealed PD-1

blockade enhanced NK cell anti-tumor functions, and tumor control relied on NK cells rather than T cells (Hsu et al., 2018).

**Reversible downregulation** involve defects in the regulation of HLA class I genes, including components of the APM, the *HLA class I heavy genes*, and  $\beta 2m$  gene (F. Garrido et al., 2010). This can occur as a result of downregulating key transcription factors by epigenetic changes or mutations, such as NLRC5 and IRF2 (Dhatchinamoorthy et al., 2021). These represent temporary changes that can be reversed by stimulation with IFN- $\gamma$  or other cytokines (F. Garrido et al., 2010; Méndez et al., 2008). This can reflect the dynamic changes occurring within the TME, which involves cross-talk through cytokines between immune cells and tumor cells (J. Wang et al., 2019). For example, macrophages are key regulators of inflammation through cytokines, which in turn induce further cytokine release from other immune cells that can influence HLA expression on tumor cells (F. Garrido et al., 2010; J. Wang et al., 2019). Induction of HLA class I molecules by IFN- $\gamma$  stimulation is caused by the upregulated expression of the transcription factors IRF1, STAT1, and NLRC5; our results consistently demonstrated this upregulation with IFN- $\gamma$  treatment (Der et al., 1998).

Overall, understanding the mechanisms for HLA class I regulation provides insight into the processes occurring during tumor evolution post-stimulation. Educated NK cells bear strong cytotoxic functions and lower threshold for activation, therefore are competent effectors against HLA-mismatched or HLA-downregulated/lost tumors (Boudreau & Hsu, 2018). However, as increased inflammation within the TME restores the HLA class I expression, these educated NK cell populations will be shut down. Uneducated NK cells require stronger stimuli for activation, however can still be important effectors against HLA-expressing tumor cells (Boudreau & Hsu, 2018). Hence, predicting the expression of HLA on a tumor directly informs the characteristics of an ideal NK cell effector.

#### *4.1.2 Impact of IFN- $\gamma$*

Within the TME, IFN- $\gamma$  supports both pro-tumor and anti-tumor immunity (Jorgovanovic et al., 2020). When bound by proinflammatory cytokines (such as IL-12, IL-15, IL-18, IL-21), IFN- $\gamma$  producing cells (NK cells, natural killer T cells, and CD8<sup>+</sup> and CD4<sup>+</sup> T



cells) are stimulated and transcriptional elements for IFN- $\gamma$  are activated (Jorgovanovic et al., 2020). Release of IFN- $\gamma$  induces a positive feedback loop, as its binding to APCs can stimulate release of proinflammatory cytokines, including more IFN- $\gamma$  (Garris et al., 2018). An inflammatory environment can acutely benefit the immune response to eliminate tumor cells, however chronic inflammation can promote tumorigenesis (J. Wang et al., 2019)

**Anti-tumor functions of IFN- $\gamma$**  involve both interactions with immune cells and tumor cells. IFN- $\gamma$  stimulation on macrophages contributes to reprogramming the cells to a M1 proinflammatory phenotype (Müller et al., 2017). M1 macrophages gain increased tumoricidal activity and expression of proinflammatory molecules (ex. TNF, IL-12; Jorgovanovic et al., 2020; Müller et al., 2017). IFN- $\gamma$  stimulates further anti-tumor immunity through DC maturation and induced co-stimulatory molecule expression, T helper (Th) 1 polarization, and enhanced T effector cell activity and proliferation (Jorgovanovic et al., 2020). Tumor impacts of IFN- $\gamma$  include the upregulation of activating ligands and death receptors such as Fas, which can stimulate the immune response (Aquino-López et al., 2017; Xu et al., 1998). Moreover, IFN- $\gamma$  induces tumor cell apoptosis via JAK1-STAT1-caspase pathway (Y. Liu et al., 2017; Song et al., 2019).

**Pro-tumor functions of IFN- $\gamma$**  contribute to cancer immunoediting. IFN- $\gamma$  promotes tumor escape through inducing the upregulation of inhibitory ligands such as HLA class I molecules and PD-L1, and the enzyme indoleamine-2,3-dioxygenase (IDO) on tumor cell surfaces (Aquino-López et al., 2017; Jorgovanovic et al., 2020; Ribas, 2015). IDO has anti-immune effects, such as suppression of NK and T cell responses (A. Park et al., 2019; Puccetti & Grohmann, 2007). Furthermore, IFN- $\gamma$  aids tumorigenesis by inducing cancer stem cells to become highly metastatic (H. Chen et al., 2011).

In our experiments, IFN- $\gamma$  similarly supports both inhibition (pro-tumor) and activation (anti-tumor) activities of NK cells. IFN- $\gamma$  led to persistent upregulation of all inhibitory ligands except for HLA-E, which was briefly upregulated but the expression change did not persist after two or three days. The activating surface proteins that persisted were death receptor Fas and activating ligand HLA-F. While the activating interactions can promote NK cell cytotoxic functions, the upregulated inhibitory ligands will suppress NK cell activation. Hence, strategies to maximize NK cell functions may be

beneficial, such as blocking KIRs or adoptive transfer of allogeneic KIR-mismatched NK cells. As demonstrated in our results, the impact of HLA class I blocking antibodies increased the degranulation of NK cells when the tumors were pre-treated with IFN- $\gamma$ . The upregulated HLA molecules will contribute to T cell activation, and the two populations may work concurrently to eliminate cancer.

Our results and others' suggest that PD-1/PD-L1 ICB can be beneficial in an IFN- $\gamma$ -rich TME. PD-1 blockade will rescue PD-1<sup>+</sup> NK cells that co-express activating ligands and receptors to the cognate upregulated tumor proteins (i.e. FasL/Fas). Clinical trials with IFN- $\gamma$  are currently ongoing to examine its combinatorial use with nivolumab (anti-PD-1; NCT02614456) and pembrolizumab (anti-PD-1; NCT03063632). Overall, our results with IFN- $\gamma$  treatment support previous findings of induced phenotypic changes to tumor cells (F. Garrido et al., 2010; Méndez et al., 2008; Yano et al., 2000). The limited NK cell response we observed with inhibitory ligand blockade in the absence of prior IFN- $\gamma$  stimulation further supports the use ICB in IFN- $\gamma$ -rich tumors. Those inflamed tumors are infiltrated by immune cells, which further impact the cancer's ability to develop and persist.

#### *4.1.3 Effector cells*

The immune contexture of a TME can be defined as “hot”, which are highly infiltrated, or “cold”, which are tumors that are not infiltrated (Galon & Bruni, 2019). Cold tumors therefore can be described as immunologically naïve, meaning the induced changes from immunoediting or released cytokines typically seen in inflamed, infiltrated tumors are less frequent (Galon & Bruni, 2019). We sought to better understand the NK-tumor interactions, and how they contribute to tumor elimination or tumor escape. During PBMC co-cultures in the absence of IFN- $\gamma$ , there was limited expression changes of the inhibitory ligands, HLA-F, and Fas until 5 or 10 hours of PBMC pressure. Combinatorial IFN- $\gamma$  pre-treatment with PBMC pressure resulted in upregulation of inhibitory ligands after 1 hour, which decreased towards baseline levels over the subsequent 9 hours of PBMC co-culture. MIC-A/B and HLA-G were upregulated with longer exposure to PBMCs both with and without prior IFN- $\gamma$  stimulation, and these expression changes

were determined to be induced independently by NK cells. NK cells may be contributing additively with IFN- $\gamma$  to induce upregulation of the other receptor and ligand expressions.

NK cells became more activated with longer co-cultures, correlating to when tumor surface proteins were upregulated in the conditions without IFN- $\gamma$  pre-treatment. One possible mechanism is increased IFN- $\gamma$  production by the activated NK cells at the later time points, which contributed to the phenotypic tumor changes. The release of IFN- $\gamma$  could activate T cells, which then kill tumor cells presenting HLA class I ligands. This may be reflected in the decrease in expression at later time points of the IFN- $\gamma$ -treated cells. To confirm this, we could analyze the supernatants from the co-cultures via enzyme-linked immunosorbent assays (ELISAs) to quantify the IFN- $\gamma$  production, or block IFN- $\gamma$  in the co-cultures with a monoclonal antibody. Through flow cytometry, the tumor cells could be stained with a cell tracker (either cell trace violet or CFSE) to compare the number of dying cells, and the effector T cell activation could be specifically analyzed by staining for CD8, CD25 (the IL-2 receptor) and CD28 (the costimulatory receptor). Another possible mechanism is that as NK cells became more activated they released other cytokines that promoted phenotypic changes, such as TNF, which can induce HLA class I expression (Lu et al., 2001). The interactions between tumor cells and NK cells could have encouraged tumor immunoediting. HLA<sup>+</sup> cells don't get killed as quickly as HLA<sup>-</sup> cells, therefore the HLA<sup>+</sup> tumor cells could emerge as the dominant population after 10 hours with NK cell effectors.

**Upregulation of MIC-A/B** was observed with PBMC and NK cell pressure, both with and without prior IFN- $\gamma$  treatment. MIC-A and MIC-B are NKG2D ligands (NKG2DLs), and their expression is regulated at the transcriptional and post-transcriptional levels in response to DNA damage and cellular stress (Duan et al., 2019; Gasser et al., 2005). Other NKG2DLs are related to cellular stress and inflammation, and are important in immunosurveillance (Raulet et al., 2013). The NKG2D receptor is also expressed on  $\gamma\delta$  T cells, CD8<sup>+</sup> T cells, and some CD4<sup>+</sup> T cells; therefore the upregulation of NKG2DLs facilitate various immune cell targeted killing (Duan et al., 2019). In cancer settings, the upregulation of MIC-A and MIC-B is associated with the hyperproliferative state (via E2F transcription factors activation), the heat shock stress pathway, and the DNA damage response (DDR). The NK cell pressure induced MIC-A/B upregulation

may be attributed to tumor cell stress from the NK cell attack, induced apoptosis, or released cytokines. To test this, we could analyze the soluble factors via ELISAs, or stain the tumor populations with Annexin V to detect cells undergoing cellular apoptosis to compare MIC-A/B fluorescence.

**Soluble NKG2DLs** can block NKG2D receptors and therefore inhibit the immune interactions with tumor cells; this represents a putative immune escape mechanism (Raulet et al., 2013). Some studies demonstrated soluble NKG2DLs reduce expression of NKG2D on CD8<sup>+</sup> T cells,  $\gamma\delta$  T cells and NK cells, however further investigation is required due conflicting results (Groh et al., 2002; Helmut Salih & Rammensee, 2021; Raulet et al., 2013). Inconsistencies in the literature may be attributed to the nature of excreted ligands (i.e. monovalent vs multivalent) or the soluble NKG2DLs blocking the epitope that NKG2D-specific antibodies bind (Raulet et al., 2013). To test if MIC-A and MIC-B were released from tumor cell surfaces in our experiments, we could analyze the supernatants after the PBMC co-culture time-course experiments; we did not observe a downregulation of NKG2D on NK cell surfaces over the 10 hours (data not shown).

**Upregulation of HLA-G** was observed with PBMC and NK cell pressure, and the expression changes were further additive with IFN- $\gamma$ . HLA-G is a non-classical HLA class Ib molecule that inhibits T cells and NK cell lytic functions by binding KIR2DL4 (Rodríguez, 2017). There is low cell surface expression of HLA-G on healthy cells, aside from the fetal-maternal interface, but HLA-G is often upregulated on tumor cells (Yie et al., 2007). Of 106 NSCLC primary tissue samples, 75% expressed aberrant levels of HLA-G; this expression was associated with poorer prognosis (Yie et al., 2007). HLA-G expression has also been correlated with loss of classical HLA class I molecules and increased IL-10 expression, and other anti-immune functions in cancer include inhibiting: T cell proliferation and cytotoxic functions, B cell maturation and antibody production, immune cell chemotaxis, neutrophil phagocytosis, and maturation and function of DCs (Loustau et al., 2020; Urosevic et al., 2001). Furthermore, trogocytosis, which is a mechanism of membrane fragments transfer initiated by cell-to-cell contact, has been demonstrated to transfer HLA-G from tumor cells to the surface of activated NK cells (Caumartin et al., 2007). These NK cells temporarily stop proliferating and behave as

suppressor cells rather than their cytotoxic functions (Caumartin et al., 2007). Therefore, since HLA-G suppresses both innate and adaptive immunity and is limited on healthy cells, it holds promise as targetable immune checkpoint, especially as our results demonstrate induced expression with NK cell pressure (Krijgsman et al., 2020). Future studies are required to understand HLA-G's regulation and whether blocking antibodies could be beneficial to patient outcomes (Krijgsman et al., 2020).

Overall, effector cells are contributing to the changing tumor phenotypes, which demonstrates the potential impacts of NK cell interactions within the TME. Strategizing NK-centric immunotherapies against NSCLC is benefited by understanding how NK cell pressure shapes cancer immunoediting. Our results suggest NKG2D<sup>+</sup> KIR2DL4<sup>-</sup> cells would be the greater tumor killers due to enhanced activation via MIC-A and MIC-B, and limited suppression via HLA-G.

## **4.2 Impact of clinical treatments on NSCLC evolution and NK cell response**

### *4.2.1 Chemotherapy-induced phenotypic changes on NSCLC*

SOC chemotherapeutics for NSCLC are generally platinum-based, but we elected to examine small molecule palbociclib and trametinib because they demonstrated increased activation of NK cells, cellular senescence and tumor regression in *KRAS*-mutant lung tumor models (Ruscetti et al., 2018). The *KRAS* oncogene, mutated in ~25% NSCLC tumors, is extremely difficult to treat and has limited targeted therapeutic options (Forsythe et al., 2020). Our phenotyping data revealed dose- and time-dependent changes in NK cell ligand expression on tumor cells after treatment with the cytostatic small molecule chemotherapies, and impaired tumor cell proliferation at higher doses. Combination of palbociclib and trametinib resulted in continued upregulation of death receptors and activating ligands (as seen with individual treatments), while limiting the inhibitory ligand upregulations demonstrated with high doses of trametinib.

**Palbociclib** selectively inhibits CDK4 and CDK6, and is currently approved for use in combination with letrozole, an aromatase inhibitor, against estrogen-receptor positive, human epidermal receptor 2-negative advanced breast cancer (Ma & Sparano, 2021). CDK4/6 inhibitors block the phosphorylation of retinoblastoma protein, a tumor suppressor; thus, CDK4/6 inhibitors stop the transition of G<sub>1</sub>-to-S cell growth cycle (Finn

et al., 2015). Our analysis on the impact of palbociclib for NSCLC evolution revealed the upregulation of death receptors (Fas, TRAIL-R2), classical and nonclassical HLA class I ligands, and PD-L1.

Chemotherapies generally act on rapidly proliferating cells to induce senescence or invoke their death. Their mechanism of actions introduce genotoxic or cellular stress, which initiates a program of responsiveness within the tumor cells (Chircop & Speidel, 2014). This response can manifest as increased expression of death receptors, therefore sensitizing the tumor cells to apoptotic-induced death by NK cells (Elrod & Sun, 2008). In agreement with this, we find that palbociclib induces upregulation of Fas and TRAIL-R2. Furthermore, these responses from platinum-based chemotherapies in NSCLC have demonstrated the downregulation of HLA class I molecules (Okita et al., 2016). While we expected to see HLA class I downregulation in our chemotherapy experiments, the inverse response of upregulation may be specific to palbociclib (see possible trametinib mechanisms below). Upregulation of HLA in response to palbociclib reveals an opportunity for T and NK cell therapies to work collaboratively.

CDK4 directly regulates expression of PD-L1 via proteasome-mediated degradation (Fouad et al., 2019). Briefly, the substrates selected for ubiquitination are controlled by E3 enzymes, which form multiple subunit ligases with cullin scaffold proteins and adaptor proteins, such as Speckle-type POZ protein (SPOP; Fouad et al., 2019; Tan et al., 2017; X. Zhou & Sun, 2021). Cullin3-SPOP E3 ligase targets PD-L1 for ubiquitination, and CDK4 mediates this event by phosphorylating SPOP (Zhang et al., 2018). Blocking CDK4-mediated phosphorylation *in vivo* with breast cancer, colon adenocarcinoma, and melanoma models leads to SPOP degradation, and consequently increased expression of PD-L1 (Zhang et al., 2018). Combining CDK4/6 inhibitors with anti-PD-1 enhanced tumor regression, improved OS, and rescued levels of infiltrating immune cells from a decrease induced by palbociclib alone (Yu et al., 2019). In patients with advanced melanoma, palbociclib similarly induced expression of PD-L1 (Yu et al., 2019). Whole genome sequencing of these patients revealed that copy-number gains of *CDK4* significantly associated with no clinical benefit from anti-PD-1 therapy (Yu et al., 2019). To our knowledge, there are no studies assessing the combination of palbociclib and PD-1/PD-L1 blockade in NSCLC; understanding the mechanistic impact of CDK4/6

inhibitors on PD-L1 abundance suggests this combinatorial strategy warrants investigation.

CDK4/6 inhibitors also suppress proliferation of Tregs (Goel et al., 2017), and increase effector T cell infiltration and activation (J. Deng et al., 2018). Our novel observation that palbociclib induces upregulation of Fas and TRAIL-R2 suggests that these immune benefits might also include activation of NK cells. In advanced NSCLC, CDK4/6 inhibitors as monotherapy demonstrate limited overall curative effect and tumors can acquire resistance, but the changes induced in tumor cells by palbociclib may nevertheless condition NSCLC for susceptibility to other interventions. Indeed, their use is being studied in combination with other anticancer agents, such as trametinib (Garutti et al., 2021; Goldman et al., 2018; Ruscetti et al., 2018; Scagliotti et al., 2018).

**Trametinib**, a selective allosteric inhibitor of MEK1 and MEK2, is currently approved for use in melanoma and NSCLC in combination with dabrafenib, a BRAF inhibitor (Weart et al., 2018). By targeting the MAPK signalling pathway, trametinib inhibits cell growth and induces apoptosis (Lugowska et al., 2015). When we treated NSCLC cells with trametinib, our results revealed an even greater upregulation of inhibitory ligands (HLA class I molecules and PD-L1) than observed with palbociclib. We similarly observed the upregulation of death receptors, as expected with anticancer agent stimulation (Elrod & Sun, 2008).

HLA class Ia and Ib expression has similarly been induced with MEK inhibitors *in vitro* and *in vivo*, which resulted in improved killing by effector T cells (Brea et al., 2016; Dummer et al., 2017; L. Liu et al., 2015). Potential mechanisms for the role of the MAPK pathway in upregulating HLA class I molecules include NF- $\kappa$ B regulation at the mRNA level and JAK/STAT pathways inducing TNF and IFN- $\gamma$  (Brea et al., 2016). However, there are inconclusive results in the literature on the regulation of PD-L1 by the MAPK pathway. Some studies have observed decreased expression PD-L1 with MEK inhibitors (Della Corte et al., 2019; Stutvoet et al., 2019), while others have observed PD-L1 upregulation (Kang et al., 2019). While further studies are required to elucidate the mechanistic action of trametinib on PD-L1 regulation, it is important to note that combining MEK inhibitors with PD-1/PD-L1 blockade in melanoma, head and neck squamous cell carcinoma, and colon carcinoma has resulted in significantly delayed

tumor growth, and increased infiltrating CD8<sup>+</sup> T cells (Hu-Lieskovan et al., 2015; Kang et al., 2019; L. Liu et al., 2015).

Trametinib is currently being assessed in studies and clinical trials, however, its inability to target other downstream RAS pathways provides a rationale for combining with other anticancer agents. Promising results in NSCLC have been found when combining trametinib with navitoclax, a BCL-XL/BCL-2 inhibitor (Corcoran et al., 2013); or with momelotinib, a JAK2 and TBK1 inhibitor; (Barbie et al., 2018). Several clinical trials are examining the use of various MEK inhibitors with pemetrexed and cisplatin (NCT02964689), with erlotinib (EGFR inhibitor; NCT01859026), with pembrolizumab (anti-PD-1; NCT03299088), with carboplatin and pemetrexed (NCT02185690), and with palbociclib (NCT03170206; Salgia et al., 2021).

We investigated the combination of palbociclib and trametinib, which had been reported to induce NK cell activation by an unidentified mechanism (Ruscetti et al., 2018). Combining the two cytostatic small molecules resulted in the continued upregulation of death receptors and activating ligands, identifying a mode of activation for the NK cells. We hypothesize these changes were attributed to the cellular stress and apoptosis induction from chemotherapy treatments. Interestingly, the inhibitory ligand upregulation in the combined therapy was limited compared to high doses of trametinib; this controlled response may contribute to the activation of NK cells.

Overall, the phenotyping of A549 cells treated with palbociclib, trametinib and the combination provided insight on how the tumors evolve and what potential interactions may arise when NK cells are present. Indeed, we now demonstrated that the subset of responding NK cells can be predicted and triaged based on the ligands expressed on tumor cells in different conditions (discussed in 4.2.3). Our results strongly indicate that the tumor prior to chemotherapy is phenotypically different than during or temporarily after treatment. While the phenotypic changes with palbociclib are similar to those in the combination treatment, the strategy of combining the two drugs would assist in controlling for acquired resistance and tumor escape. As mentioned, PD-L1 in NSCLC has been observed to downregulate in response to MEK inhibitors, therefore the combination with palbociclib would likely support PD-L1 upregulation. PD-L1 expression is a predictor of successful ICB, and studies have demonstrated both



palbociclib and trametinib to be beneficial in tumor control when combined with an anti-PD-1 or anti-PD-L1 agent.

#### *4.2.2 Irradiation-induced phenotypic changes on NSCLC*

Radiation treatment can be broadly divided into stereotactic body radiation therapy (SBRT), conventionally fractionated radiation therapy (CFRT), and low-dose (immunosensitizing) radiation (LDR). SBRT is used with curative intent in early NSCLC, as it has been demonstrated to have better patient outcomes compared to CFRT at stage I (Haque et al., 2018; Nyman et al., 2016). CFRT, which is used with curative intent for patients with advanced disease, delivers high doses of irradiation that can negatively impact immune function. High doses of irradiation increases the expression of PD-L1 and HLA class I molecules (Chiriva-Internati et al., 2006; B. Park et al., 2014; Santin et al., 1996). Conversely, LDR can be “immunosensitizing”; it has been observed to kill tumor cells while maintaining survival of normal cells (Yang et al., 2016), to induce an immunostimulatory cytokine profile (Yang et al., 2016), to enhance activation of NK cells and DCs while lessening immunoregulatory Treg populations (L. Zhou et al., 2018), and to induce expression of stress ligands that further activate the immune system (Gasser et al., 2005; Yang et al., 2014). Therefore, we sought to phenotype NSCLC cells in the days post-immunosensitizing irradiation to understand how the surface level expression changes may influence the immune activation.

**Death receptors and activating ligands** were upregulated in our experiments at 1, 3, and 5 days post treatment. Different activating surface proteins were upregulated greater on different days; this is important because it provides an opportunity for various NK cell populations to become activated and perform cytotoxic functions at different time points. It also implies that one static population of NK cells is unlikely to be continuously responsive throughout the course of treatment, and polyfactorial NK cell cocktails should be supported, primed or transferred. As there was consistently at least one targetable activating ligand or death receptor at each day analyzed, our results revealed that NK cells can be used in combination with lower radiation doses to kill the tumor cells that survived the initial radiotherapy. Because the activating surface protein

changes are prolonged, the window for NK cell intervention is wide, which enhances the practicality of delivering combination treatments of NK cells and radiotherapy.

Our observed upregulated activating cell surface proteins was congruent with the literature. In colorectal cancer cells, 5 Gy irradiation treatment induced upregulation of Fas, TRAIL-R1 and TRAIL-R2 (Cacan et al., 2015). Another colorectal cancer study treated tumor cells at 2.5 Gy, 5 Gy, and 10 Gy, and observed upregulated expression of Fas, and TRAIL-R1 and TRAIL-R2 which both persisted to 7 days post-treatment (Ifeadi & Garnett-Benson, 2012). In p53 wild-type breast cancer and osteosarcoma cells, irradiation treatment induced Fas upregulation and arrested growth at G<sub>1</sub> cell cycle phase (Sheard et al., 1997). However, in p53-mutant or p53-null breast cancer, osteosarcoma, leiomyosarcoma, and fibrosarcoma cells, irradiation did not impact arrestment of cell cycles or upregulate Fas (Sheard et al., 1997). These results suggest that p53, a tumor suppressor gene, is important for irradiation-induced Fas expression; since p53 is activated after DNA double stranded breaks, irradiation may induce a p53-dependent pathway that promotes stress ligand upregulation (Sheard et al., 1997). Irradiation is known to induce the DDR, therefore this pathway likely contributes to activating ligand upregulations (Gasser et al., 2005). Other possible contributing mechanisms for these expression changes include low dose radiation increasing the histone acetylation at their promoter regions, therefore making the genes more accessible for transcription, and the decreased binding of the histone deacetylase HDAC2 to specifically the Fas promoter region (Cacan et al., 2015).

**HLA class I molecules** were upregulated with lower doses of irradiation at various time-points (specifically HLA-ABC, HLA-Bw4, HLA-C, HLA-G). When we analyzed the relative tumor change expressions for 5 Gy irradiation at 1, 3, 5 and 7 days (**Figure 3.12**), the results revealed a trend of greater expression changes at day 5 and 7 compared to earlier post-treatment. This suggests an opportunity for T cells and NK cells to work in collaboration. In the initial days post irradiation, NK cells can be activated due to lower levels of HLA class I and upregulated death receptors and activating ligands. As HLA class I molecules are upregulated, uneducated NK cells, with sufficient pro-activation signals, can participate in killing HLA<sup>+</sup> tumor cells. As well, T cells can potentially become activated and continue killing tumor cells that were not eliminated by

radiotherapy. Although T cells with anticancer activity are naturally primed in many cancers, in light of this further strategies to ensure priming of a T cell response could be beneficial, such as oncolytic virotherapy to induce antigen release and epitope spreading, or via cancer vaccination (Roy et al., 2021). Non-apoptotic death pathways, such as immunogenic cell death, release antigens from destroyed cells, which can further support T cell immune activation and inflammation (Minute et al., 2020). Moreover, NSCLC tumors often experience irreversible loss of HLA class I molecules (described in 4.1.1), therefore these tumors are predicted to be targetable by NK cells with LDR even after 5 or 7 days (McGranahan et al., 2017).

**PD-L1** expression was upregulated at all timepoints assessed post-treatment, which is likely attributed to irradiation-induced DNA double-stranded breaks initiating the DDR. Our results are supported by findings in the literature, which demonstrate PD-L1 upregulation with LDR (Dovedi et al., 2014), and in an ATM/ATR/Chk1-dependent manner (therefore DDR-dependent; Sato et al., 2017). These results suggest that radiation, both at low and high doses, will induce PD-L1 and inhibit PD-1<sup>+</sup> immune cells from attacking the tumor. This is evidence for combining radiotherapy with PD-1/PD-L1 ICB, and studies have demonstrated the combination resulted in improved OS and tumor control *in vivo* (L. Deng et al., 2014; Dovedi et al., 2014) and in patients with NSCLC (Shaverdian et al., 2017). There are currently ongoing clinical trials assessing the PD-1 blockade for patients with NSCLC at stage I with SBRT (NCT03110978, NCT02599454, NCT03050554, NCT03148327, NCT03446911, NCT03383302), at stage III with CFRT (NCT03245177), and at stage IV with hypofractionated radiation (NCT02463994, NCT03035890, NCT03176173).

Understanding how both chemotherapies and irradiation impact NSCLC phenotypes can help us develop therapies to improve NK cell anti-tumor functions. We next analyzed the responding populations to clinically treated-A549 cells, and how the addition of ICB affected those responses.

#### *4.2.3 NK cell populations responding to NSCLC post-clinical therapy*

Activation of NK cell populations against both chemotherapy-treated and irradiated A549 cells was highly dependent on the phenotype of those evolved tumor cells. Upregulation

of inhibitory ligands, specifically HLA-C, HLA-Bw4, and PD-L1, resulted in less activation of NK cells expressing KIR2DL2/L3, KIR3DL1, and PD-1, respectively. To further support this, NK cells expressing activating receptor/ligands that were KIR2DL2/L3<sup>-</sup> and KIR3DL1<sup>-</sup> had greater degranulation levels than their KIR-expressing counterparts against HLA-expressing tumor cells. This confirms what is understood in the literature: the presence of activating stimuli is generally not enough to overcome KIR-HLA inhibition (Long et al., 2013).

We expected that the **inhibition driven via KIR-HLA interactions** would dominantly inhibit NK cells. Indeed, when we blocked these interactions with antibodies, NK cell degranulation increased, especially among NK cells bearing cognate KIR. This confirmed KIR-HLA driven NK cell inhibition. NK effector functions are linked to cytoskeletal machinery, and activating and inhibitory pathways induce different cytoskeleton rearrangements (Ben-Shmuel et al., 2021). The immunological synapse between NK cells and their targets is dependent on actin rearrangements to ensure stability and longevity in the contact, to assemble signalling complexes, and to mediate killing (Ben-Shmuel et al., 2021). How the cytoskeletal machinery and the immunological synapse influence NK cell activation versus inhibition is complex and under constant investigation; studies have found that receptors form clusters, and the size of those signalling clusters then impacts the strength of that signal (Ben-Shmuel et al., 2021; Oszmiana et al., 2016). Clustering of activating receptors and ligands has been shown to be abolished when KIRs bind to HLA (Ben-Shmuel et al., 2021). Overall, the KIR-HLA interactions are important considerations when choosing to target cells with NK cells, as the expression of activating ligands and death receptors on target cell surfaces is unlikely to overcome the inhibition from expressed cognate HLA class I molecules.

We expected that the **activation driven via activating interactions** promoted NK cell degranulation when inhibitory interactions were lessened. As chemotherapy-treated or irradiated A549 cells expressed activating ligands and death receptors, the NK cell populations that do not express KIR and PD-1 were activated when they expressed cognate activating receptor/ligands. We analyzed FasL, TRAIL, and NKG2D; however there are substantially more activating receptors that were likely contributing to the NK

cell responses that were not included in this study. We compared the activation between NK cell populations that expressed one receptor/ligand and those that expressed all three FasL, TRAIL, and NKG2D. Our analysis revealed the greatest activation when the NK cells were triple positive, therefore suggesting synergy among the co-activating pathways.

**Synergy of co-activating receptors and ligands** on NK cells has been studied to some extent, especially in the context of NK cell-based immunotherapy; however more research is required. Studies are suggesting that NK cell activation is due to combinatorial synergy from multiple activating signals (Chester et al., 2015; Long et al., 2013). For example, NKG2D has been observed to work synergistically with other activating receptors, such as 2B4 and NKp46 (Bryceson et al., 2006), and NKp46 demonstrates synergy with 2B4 (Zamai et al., 2020). Understanding the importance of different NK cell activating signals is crucial to determining ideal NK cell populations for targeting cancer to maximize NK cell tumor killing. Our results demonstrate that synergistic effects with NK cell activating receptor/ligands warrants further investigation, especially in the context of clinical treatments that upregulate activating tumor surface proteins.

**PD-1 and PD-L1 blocking antibodies** rescued the response of PD-1<sup>+</sup> NK cells against PD-L1-expressing tumor cells (induced with IFN- $\gamma$ , chemotherapy, or irradiation). Interestingly, we observed the greatest rescue response of PD-1<sup>+</sup> NK cells with anti-PD-L1 against A549 cells on 5 days post-irradiation. However, our phenotyping data revealed that PD-L1 was similarly upregulated on day 1, though the same increase in degranulation was not observed in that condition. One hypothesis is that since the death receptors and activating ligands evolve to different degrees depending on how many days the tumor cells rested after irradiation, then potentially the activating interactions occurring on day 5 with the NK cells are more significant to the rescue response. As co-activating receptor/ligands demonstrated synergy, a possible explanation is that the activating interactions on day 5 induce greater synergy than those on day 1. This further supports our previous point that more research is required to understand the co-activating synergy for NK cells because they may influence greater activation with ICB.

**Combination of trametinib and palbociclib** was previously demonstrated to induce NK cell activation by an unidentified mechanism (Ruscetti et al., 2018). Our results revealed that compared to palbociclib alone, the combination treatment supported greater activation of NK cells expressing activating receptor/ligands (KIR<sup>-</sup> PD-1<sup>-</sup>). Addition of inhibitory ligand blockade resulted in relatively similar responses among treatment conditions. However, when we analyzed the single activating receptor/ligand populations, the FasL<sup>+</sup> (TRAIL<sup>-</sup> NKG2D<sup>-</sup>) NK cells were greater responders against combination treated A549 cells than either individual chemotherapy. This result is supported by our phenotyping data that revealed greater Fas expression in the combination treatment compared to the middle dose of either individual chemotherapy. This suggests that the Fas/FasL interaction may be critical to enhanced NK cell activation when combining CDK4/6 inhibitors and MEK inhibitors against *KRAS*-mutant NSCLC.

Overall, the use of NK cells against chemotherapy-treated or irradiated A549 cells has important anti-tumor functions, however NK cell populations able to respond will be strongly influenced by the ligands available on the tumor as it changes in response to therapy. As our phenotyping data demonstrates the consistent upregulation of PD-L1, the addition of blocking antibodies was important for inducing a response of PD-1<sup>+</sup> NK cells. Previous work demonstrated the indispensable role of NK cells with PD-1 blockade in an HLA class-I deficient lymphoma model (Hsu et al., 2018). KIR-expressing NK cells were consequential in inhibiting activation: they were rescued when inhibitory interactions were blocked, and inhibited when we looked at these KIR<sup>+</sup> populations via specific gating. Importantly, the activation of NK cells, even in the presence of inhibitory ligand blockade, still requires the activation stimuli from Fas and other activating interactions to mount a response. The co-activating receptor/ligands are working in synergy, and further research is required to maximize this synergy for NK-centric immunotherapies. Overall, this project has helped understand the role of individual receptor-ligand pairings between NK cells and NSCLC cells, specifically in the context of clinical treatment. It has provided insight on how NK cells can be utilized in combination with other anticancer agents.

### 4.3 Applications

We focused on NSCLC in this project, which continues to have high mortality rates and is in need for improved treatment options for patients with advanced disease (Brenner et al., 2020). Our first application of the results from this project come from the wide-ranging phenotyping data of A549 cells in various treatments. Clinical treatments are chosen partly based on the phenotype of the tumor prior to therapy; as our results have demonstrated, tumor cells evolve when stimulated with IFN- $\gamma$ , immune cells (specifically NK cells), small molecule chemotherapies, and immunosensitizing doses of irradiation. A common change was the upregulation of PD-L1, which was determined to be persistent in the various treatments. This encourages the use of PD-1 blockade in combination with other therapies, as the upregulated immune checkpoint molecule will inhibit activation from both the innate and adaptive immune system. While PD-1 blockade is already used in combination with chemotherapy or radiation in the clinic, our results provide novel insight into how NK cells are likely being recruited in these treatments.

The phenotyping data further helped identify the changes to tumor surface ligand expression that impact the subset of responding NK cells. If these are found to be consistent between tumors – in essence, if a specific chemotherapy or radiation regimen leads to a predictable phenotype – we could design “off-the-shelf” NK cells that could be given in adoptive therapy. Allogeneic NK cell adoptive transfer has had limited success in solid tumors, and current work is aiming to improve trafficking into TME and in combination with other immunostimulatory agents (Shin et al., 2020). These previous studies have not employed a selection for specific NK cell phenotypes or cells with specific characteristics. In that light, perhaps it is unsurprising that they have yielded heterogeneous results. Our data demonstrates that the phenotype of the NK cell has an immense impact on if the effector will be able to mount a cytotoxic response. Therefore, we hypothesize that the current limitations to adoptive therapy are partly due to incompatibility between donor NK cells and tumor cells. The KIR-HLA interactions induce substantial inhibition to the NK cells, and we have demonstrated that HLA class I molecules are often upregulated after stimulation. As well, upregulation PD-L1 will induce further NK cell inhibition. Even if the NK cells express activating receptor/ligands

that are known to be upregulated on the tumor cells, if the inhibitory interactions are still present, the anti-tumor functions of NK cells cannot be exploited.

Our results provide evidence into how NK cells can target *KRAS*-mutant tumors, which is a common mutation for NSCLC with only one approved targetable therapy option for *KRAS*-G12C isoform (Salgia et al., 2021; Sequist & Neal, 2021). We demonstrated that combination of two small molecules, trametinib and palbociclib, induces a phenotype that can be targeted by FasL<sup>+</sup> NK cells with the addition of PD-1/PD-L1 blockade. The interactions between upregulated HLA class I molecules and KIRs are important in NK targeting, again highlighting the importance of researching how chemotherapies influence tumor cells to inhibit immune cells. Understanding the phenotypic changes *in vitro* and *in vivo* can help us predict what will occur in a patient, and therefore influence what NK cell populations will be most responsive. The upregulation with HLA class I ligands as well suggests that strategies to complement T cell activation (such as priming anti-cancer T cell responses) might enhance the overall efficacy of therapies by providing a secondary effector cell that is equipped to respond to the escape mechanisms of a tumor. Rather than considering these immune populations as independent effectors, our results indicate their different activation capabilities can be used to an advantage and in parallel when targeting tumors.

Lastly, we suggested the importance of timing the NK cell targeting with ongoing clinical treatments. For irradiated NSCLC cells, the phenotypic changes vary depending on the number of days post-treatment. Our analysis revealed that earlier time points creates a more targetable phenotype due to NK cell interactions, therefore suggesting a temporary window that NK cells can be given as an adoptive therapy. Similarly with the chemotherapy treatment, the phenotypic changes were more induced with longer exposure; to promote NK cell activation against chemotherapy-treated tumor cells, the adoptive transfer could be timed with expected phenotypic changes that induce the upregulation of Fas and other important death receptors and activating ligands. Hence, we conclude that there is a window of opportunity during which NK cell function could best support anticancer immunity with chemotherapy and radiotherapy.



#### 4.5 Critique and Limitations

A major limitation to this project was the limited access to the lab due to the COVID-19 pandemic. No experiments occurred during the research shutdown from March, 2020 to July 2020, and there was limited access to the lab space due to social distancing requirements for the remainder of the project. Consequently, I was unable to get trained for the Fortessa, therefore I had to rely on others to run my flow cytometry samples. The pandemic impacted ordering and shipments, hence we suffered supply chain issues. This project initially included other aims, such as cloning defects in HLA processing and presentation into the A549 genome to investigate how these alterations impact interactions with NK cells and resistance to ICB. As a novice to molecular subcloning, I would have required training to complete this aspect of my project, which was impractical given heavily restricted lab access. Recognizing the limited access that would continue for the remainder of my project, we chose to focus on the aims presented in this thesis as they were already underway and had established protocols. Noteworthy, time that I could not spend working in the laboratory as usual was spent analyzing my results, and contributing as co-first author to a published manuscript (Nersesian, Schwartz et al., 2021).

The entirety of this project was completed *in vitro*, which fosters a base understanding of how immune cells and tumor cells function and interact. However, there are many limitations that come with *in vitro* work: the TME is a complex network of cells and soluble factors interacting, and cytotoxic assays between PBMCs and tumor cell lines are unable to represent this complexity. Cell-to-cell communications within the TME impact both immune and tumor phenotypes that our analysis does not capture.

This project only included one cell line, a *KRAS*-mutant human lung adenocarcinoma (A549). We initially planned on repeating the important treatment conditions and time-points in other *KRAS*-mutant cell lines, specifically HOP-62, HCC-1355, and Calu-6. Again our time was limited due to the research shutdown and we faced supply chain issues. This limits the strength of our findings as we have not yet demonstrated its reproducibility in other NSCLC cell lines.

The panels chosen to analyze the phenotype of A549 cells and the responding NK cells are limited in that many important markers were not included. This was a

consequence of ensuring there was no fluorochrome spill on the Fortessa. We designed our panel based on published literature and receptor-ligand pairs expected to be relevant for NK cell function in NSCLC, but many other pairs have not yet been investigated in this context and could be relevant. A PhD student in our lab, Stacey Lee, has now established (Winter 2020) an effector panel and tumor panel that each include 28 markers; these designed panels will be beneficial in the future as they will allow for a more comprehensive analysis of phenotypic changes on tumors post-treatment, as well as the phenotype of responding NK cells. Furthermore, the panels were expanded as the project continued, therefore experiments completed earlier in the degree did not include all the final markers analyzed in this thesis. Therefore this occasionally limited the ability to complete statistical tests for the tumor ligands and receptors that did not reach  $n=3$ .

#### **4.6 Future Directions**

We have many future directions to this project to further understand the treatment-induced evolution of NSCLC and the ideal NK cell populations for targeting lung cancer. As mentioned throughout the discussion, we aim to examine the supernatant of tumor and PBMC co-cultures by ELISAs to identify the soluble factors that may be influencing tumor evolution and immune interactions. As described, tumors can shed proteins, such as MIC-A and MIC-B, which influence NK cell activity. Analysis by ELISAs could inform if this is occurring in our co-cultures, and under what conditions is the shedding being induced. To gain a better understanding of the mechanism behind tumor evolution, we aim to analyze tumor samples pre- and post-treatment by qPCR. This method will help gain insight on if the upregulation of tumor proteins occurs from pre-transcribed genes, or if the treatment pressure is inducing transcription.

We empirically tested the anti-PD-1 antibody for ADCC by assessing the NK viability when the antibody was added. This antibody was only incubated with NK cells, then washed off prior to co-culture with tumor cells. Therefore, the only likely ADCC that could occur is NK cells killing other NK cells, though we did not see a decreased viability. However, we would like to confirm this by staining our NK cells with CD16 and examine if the expression remains constant, and if it is overrepresented in the responding cell populations.

We aim to confirm our hypothesis that we can select for ideal NK cell populations to target evolved NSCLC. Through the use of the BD FACS Aria III cell sorter, we can isolate NK cell populations that we expect to be the most efficient killers against chemotherapy-treated and irradiated NSCLC cell lines. This experiment will confirm our findings that certain populations, examined by FlowJo gating, will become more activated. Here, we aim to examine FasL<sup>+</sup> NK cells in comparison to FasL<sup>+</sup> NKG2D<sup>+</sup> TRAIL<sup>+</sup> NK cells to elucidate if synergy of all three receptors results in greater activation than single activating receptor/ligand positive effectors. These sorted NK cells will exclude the inhibitory receptors that our results deemed crucial for inhibition (KIR2DL2/L3, KIR3DL1, and PD-1).

Lastly, we hope to move our *in vitro* findings to an *in vivo* model. With the help of Stacey Lee, we have established that our humanized mouse models can grow A549 tumors, and the addition of NK cells at higher densities resulted in greater control of tumor growth. This project would entail examining how the tumors change after irradiation and chemotherapies, and whether tumor growth is more controlled with NK cell populations that we expect to be more efficient killers.

#### **4.8 Concluding Remarks**

With this project, we have demonstrated that NSCLC rapidly evolves after pressure from IFN- $\gamma$ , NK cells, small molecule chemotherapies, and low doses of irradiation. These timely changes to the tumor cell surfaces interact with NK cells, and change which populations are best able to respond. As NSCLC remains a difficult cancer to treat, more clinical treatments are aiming to stimulate the immune system to strengthen other anticancer agents' abilities of controlling tumor growth. Tumor escape and resistance to therapy remains a challenge for NSCLC treatment, therefore our project's findings of the ideal NK phenotypes can help with tumor elimination. If we can target tumors with a few NK cell populations that are able to not only kill the resting tumor but as well the evolved tumor, then we expect to limit tumor escape. Further investigation into these ideal effector populations is warranted, along with a greater understanding of how the clinical treatments induce different NSCLC tumors to evolve. Overall, NK cells hold great promise in the treatment of rapidly evolving NSCLC, and we look forward to seeing how

future research capitalizes on their phenotypic and functional diversity to improve patient outcomes.

## **REFERENCES**

- Ansell, S. M., Lesokhin, A. M., Borrello, I., Halwani, A., Scott, E. C., Gutierrez, M., Schuster, S. J., Millenson, M. M., Cattry, D., Freeman, G. J., Rodig, S. J., Chapuy, B., Ligon, A. H., Zhu, L., Grosso, J. F., Kim, S. Y., Timmerman, J. M., Shipp, M. A., & Armand, P. (2015). PD-1 Blockade with Nivolumab in Relapsed or Refractory Hodgkin's Lymphoma. *New England Journal of Medicine*, *372*(4), 311–319. <https://doi.org/10.1056/nejmoa1411087>
- Antonia, S. J., Borghaei, H., Ramalingam, S. S., Horn, L., De Castro Carpeño, J., Pluzanski, A., Burgio, M. A., Garassino, M., Chow, L. Q. M., Gettinger, S., Crinò, L., Planchard, D., Butts, C., Drilon, A., Wojcik-Tomaszewska, J., Otterson, G. A., Agrawal, S., Li, A., Penrod, J. R., & Brahmer, J. (2019). Four-year survival with nivolumab in patients with previously treated advanced non-small-cell lung cancer: a pooled analysis. *The Lancet Oncology*, *20*(10), 1395–1408. [https://doi.org/10.1016/S1470-2045\(19\)30407-3](https://doi.org/10.1016/S1470-2045(19)30407-3)
- Aquino-López, A., Senyukov, V. V., Vlastic, Z., Kleinerman, E. S., & Lee, D. A. (2017). Interferon gamma induces changes in Natural Killer (NK) cell ligand expression and alters NK cell-mediated lysis of pediatric cancer cell lines. *Frontiers in Immunology*, *8*(APR), 391. <https://doi.org/10.3389/fimmu.2017.00391>
- Barbie, D. A., Spira, A., Kelly, K., Humeniuk, R., Kawashima, J., Kong, S., & Koczywas, M. (2018). Phase 1B Study of Mometinib Combined With Trametinib in Metastatic, Kirsten Rat Sarcoma Viral Oncogene Homolog-Mutated Non-Small-Cell Lung Cancer After Platinum-Based Chemotherapy Treatment Failure. *Clinical Lung Cancer*, *19*(6), e853–e859. <https://doi.org/10.1016/j.clcc.2018.07.004>
- Barnes, J. L., Zubair, M., John, K., Poirier, M. C., & Martin, F. L. (2018). Carcinogens and DNA damage. In *Biochemical Society Transactions* (Vol. 46, Issue 5, pp. 1213–1224). Portland Press Ltd. <https://doi.org/10.1042/BST20180519>
- Beldi-Ferchiou, A., & Caillat-Zucman, S. (2017). Control of NK cell activation by immune checkpoint molecules. In *International Journal of Molecular Sciences* (Vol. 18, Issue 10). MDPI AG. <https://doi.org/10.3390/ijms18102129>

- Ben-Shmuel, A., Sabag, B., Biber, G., & Barda-Saad, M. (2021). The Role of the Cytoskeleton in Regulating the Natural Killer Cell Immune Response in Health and Disease: From Signaling Dynamics to Function. In *Frontiers in Cell and Developmental Biology* (Vol. 9, p. 95). Frontiers Media S.A. <https://doi.org/10.3389/fcell.2021.609532>
- Borghaei, H., Paz-Ares, L., Horn, L., Spigel, D. R., Steins, M., Ready, N. E., Chow, L. Q., Vokes, E. E., Felip, E., Holgado, E., Barlesi, F., Kohlhäufel, M., Arrieta, O., Burgio, M. A., Fayette, J., Lena, H., Poddubskaya, E., Gerber, D. E., Gettinger, S. N., ... Brahmer, J. R. (2015). Nivolumab versus Docetaxel in Advanced Nonsquamous Non–Small-Cell Lung Cancer. *New England Journal of Medicine*, 373(17), 1627–1639. <https://doi.org/10.1056/nejmoa1507643>
- Boudreau, J. E., & Hsu, K. C. (2018). Natural Killer Cell Education and the Response to Infection and Cancer Therapy: Stay Tuned. In *Trends in Immunology* (Vol. 39, Issue 3, pp. 222–239). Elsevier Ltd. <https://doi.org/10.1016/j.it.2017.12.001>
- Brahmer, J., Reckamp, K. L., Baas, P., Crinò, L., Eberhardt, W. E. E., Poddubskaya, E., Antonia, S., Pluzanski, A., Vokes, E. E., Holgado, E., Waterhouse, D., Ready, N., Gainor, J., Arén Frontera, O., Havel, L., Steins, M., Garassino, M. C., Aerts, J. G., Domine, M., ... Spigel, D. R. (2015). Nivolumab versus Docetaxel in Advanced Squamous-Cell Non–Small-Cell Lung Cancer. *New England Journal of Medicine*, 373(2), 123–135. <https://doi.org/10.1056/nejmoa1504627>
- Brea, E. J., Oh, C. Y., Manchado, E., Budhu, S., Gejman, R. S., Mo, G., Mondello, P., Han, J. E., Jarvis, C. A., Ulmert, D., Xiang, Q., Chang, A. Y., Garippa, R. J., Merghoub, T., Wolchok, J. D., Rosen, N., Lowe, S. W., & Scheinberg, D. A. (2016). Kinase regulation of human MHC class I molecule expression on cancer cells. *Cancer Immunology Research*, 4(11), 936–947. <https://doi.org/10.1158/2326-6066.CIR-16-0177>
- Breglio, A. M., Rusheen, A. E., Shide, E. D., Fernandez, K. A., Spielbauer, K. K., McLachlin, K. M., Hall, M. D., Amable, L., & Cunningham, L. L. (2017). Cisplatin is retained in the cochlea indefinitely following chemotherapy. *Nature*

- Communications*, 8(1), 1–9. <https://doi.org/10.1038/s41467-017-01837-1>
- Brenner, D. R., Weir, H. K., Demers, A. A., Ellison, L. F., Louzado, C., Shaw, A., Turner, D., Woods, R. R., & Smith, L. M. (2020). Projected estimates of cancer in Canada in 2020. *CMAJ*, 192(9), E199–E205. <https://doi.org/10.1503/cmaj.191292>
- Bryceson, Y. T., March, M. E., Ljunggren, H. G., & Long, E. O. (2006). Synergy among receptors on resting NK cells for the activation of natural cytotoxicity and cytokine secretion. *Blood*, 107(1), 159–166. <https://doi.org/10.1182/blood-2005-04-1351>
- Burke, J. D., & Young, H. A. (2019). IFN- $\Gamma$ : A cytokine at the right time, is in the right place. In *Seminars in Immunology* (Vol. 43, p. 101280). Academic Press. <https://doi.org/10.1016/j.smim.2019.05.002>
- Cacan, E., Greer, S. F., & Garnett-Benson, C. (2015). Radiation-induced modulation of immunogenic genes in tumor cells is regulated by both histone deacetylases and DNA methyltransferases. *International Journal of Oncology*, 47(6), 2264–2275. <https://doi.org/10.3892/ijo.2015.3192>
- Campoli, M., & Ferrone, S. (2011). HLA antigen and NK cell activating ligand expression in malignant cells: a story of loss or acquisition. In *Seminars in immunopathology* (Vol. 33, Issue 4, pp. 321–334). NIH Public Access. <https://doi.org/10.1007/s00281-011-0270-z>
- Canadian Cancer Society. (2020). *Lung cancer statistics*. <https://www.cancer.ca/en/cancer-information/cancer-type/lung/statistics/?region=on>
- Canadian Cancer Society. (2021a). *Immunotherapy for lung cancer*. <https://www.cancer.ca/en/cancer-information/cancer-type/lung/treatment/immunotherapy/?region=on>
- Canadian Cancer Society. (2021b). *Treatments for non–small cell lung cancer*. <https://www.cancer.ca/en/cancer-information/cancer-type/lung/treatment/?region=on>
- Canadian Cancer Statistics Advisory Committee. (2020). Canadian Cancer Statistics: A 2020 special report on lung cancer. In *Health Promotion and Chronic Disease Prevention in Canada* (Vol. 40, Issue 10). <https://doi.org/10.24095/hpcdp.40.10.05>

- Caumartin, J., Favier, B., Daouya, M., Guillard, C., Moreau, P., Carosella, E. D., & LeMaoult, J. (2007). Trogocytosis-based generation of suppressive NK cells. *EMBO Journal*, *26*(5), 1423–1433. <https://doi.org/10.1038/sj.emboj.7601570>
- Chen, H. C., Chou, A. S. Bin, Liu, Y. C., Hsieh, C. H., Kang, C. C., Pang, S. T., Yeh, C. T., Liu, H. P., & Liao, S. K. (2011). Induction of metastatic cancer stem cells from the NK/LAK-resistant floating, but not adherent, subset of the UP-LN1 carcinoma cell line by IFN- $\gamma$ . *Laboratory Investigation*, *91*(10), 1502–1513. <https://doi.org/10.1038/labinvest.2011.91>
- Chen, R., Manochakian, R., James, L., Azzouqa, A. G., Shi, H., Zhang, Y., Zhao, Y., Zhou, K., & Lou, Y. (2020). Emerging therapeutic agents for advanced non-small cell lung cancer. In *Journal of Hematology and Oncology* (Vol. 13, Issue 1, pp. 1–23). BioMed Central Ltd. <https://doi.org/10.1186/s13045-020-00881-7>
- Chen, S., Crabill, G. A., Pritchard, T. S., McMiller, T. L., Wei, P., Pardoll, D. M., Pan, F., & Topalian, S. L. (2019). Mechanisms regulating PD-L1 expression on tumor and immune cells. *Journal for ImmunoTherapy of Cancer*, *7*(1), 1–12. <https://doi.org/10.1186/s40425-019-0770-2>
- Chester, C., Fritsch, K., & Kohrt, H. E. (2015). Natural killer cell immunomodulation: Targeting activating, inhibitory, and co-stimulatory receptor signaling for cancer immunotherapy. In *Frontiers in Immunology* (Vol. 6, Issue DEC, p. 601). Frontiers Research Foundation. <https://doi.org/10.3389/fimmu.2015.00601>
- Chircop, M., & Speidel, D. (2014). Cellular stress responses in cancer and cancer therapy. *Frontiers in Oncology*, *4*(OCT). <https://doi.org/10.3389/fonc.2014.00304>
- Chiriva-Internati, M., Grizzi, F., Pinkston, J., Morrow, K. J., D’Cunha, N., Frezza, E. E., Muzzio, P. C., Kast, W. M., & Cobos, E. (2006a). Gamma-radiation upregulates MHC class I/II and ICAM-I molecules in multiple myeloma cell lines and primary tumors. *In Vitro Cellular and Developmental Biology - Animal*, *42*(3–4), 89–95. <https://doi.org/10.1290/0508054.1>
- Chiriva-Internati, M., Grizzi, F., Pinkston, J., Morrow, K. J., D’Cunha, N., Frezza, E. E.,



- Muzzio, P. C., Kast, W. M., & Cobos, E. (2006b). Gamma-radiation upregulates MHC class I/II and ICAM-I molecules in multiple myeloma cell lines and primary tumors. *In Vitro Cellular and Developmental Biology - Animal*, 42(3–4), 89–95. <https://doi.org/10.1290/0508054.1>
- Cohen, R. B., Bauman, J. R., Salas, S., Colevas, A. D., Even, C., Cupissol, D., Posner, M. R., Lefebvre, G., Saada-Bouزيد, E., Bernadach, M., Seiwert, T. Y., Pearson, A. T., Calmels, F., Zerbib, R., Andre, P., Rotolo, F., Boyer-chammard, A., & Fayette, J. (2020). Combination of monalizumab and cetuximab in recurrent or metastatic head and neck cancer patients previously treated with platinum-based chemotherapy and PD-(L)1 inhibitors. *Journal of Clinical Oncology*, 38(15\_suppl), 6516–6516. [https://doi.org/10.1200/jco.2020.38.15\\_suppl.6516](https://doi.org/10.1200/jco.2020.38.15_suppl.6516)
- Corcoran, R. B., Cheng, K. A., Hata, A. N., Faber, A. C., Ebi, H., Coffee, E. M., Greninger, P., Brown, R. D., Godfrey, J. T., Cohoon, T. J., Song, Y., Lifshits, E., Hung, K. E., Shioda, T., Dias-Santagata, D., Singh, A., Settleman, J., Benes, C. H., Mino-Kenudson, M., ... Engelman, J. A. (2013). Synthetic Lethal Interaction of Combined BCL-XL and MEK Inhibition Promotes Tumor Regressions in KRAS Mutant Cancer Models. *Cancer Cell*, 23(1), 121–128. <https://doi.org/10.1016/j.ccr.2012.11.007>
- D’Addario, G., Pintilie, M., Leighl, N. B., Feld, R., Cerny, T., & Shepherd, F. A. (2005). Platinum-based versus non-platinum-based chemotherapy in advanced non-small-cell lung cancer: A meta-analysis of the published literature. *Journal of Clinical Oncology*, 23(13), 2926–2936. <https://doi.org/10.1200/JCO.2005.03.045>
- Daud, A. I., Wolchok, J. D., Robert, C., Hwu, W. J., Weber, J. S., Ribas, A., Hodi, F. S., Joshua, A. M., Kefford, R., Hersey, P., Joseph, R., Gangadhar, T. C., Dronca, R., Patnaik, A., Zarour, H., Roach, C., Toland, G., Lunceford, J. K., Li, X. N., ... Hamid, O. (2016). Programmed death-ligand 1 expression and response to the anti-programmed death 1 antibody pembrolizumab in melanoma. *Journal of Clinical Oncology*, 34(34), 4102–4109. <https://doi.org/10.1200/JCO.2016.67.2477>
- De Sousa, V. M. L., & Carvalho, L. (2018). Heterogeneity in Lung Cancer.

*Pathobiology*, 85(1–2), 96–107. <https://doi.org/10.1159/000487440>

Della Corte, C. M., Barra, G., Ciaramella, V., Di Liello, R., Vicidomini, G., Zappavigna, S., Luce, A., Abate, M., Fiorelli, A., Caraglia, M., Santini, M., Martinelli, E., Troiani, T., Ciardiello, F., & Morgillo, F. (2019). Antitumor activity of dual blockade of PD-L1 and MEK in NSCLC patients derived three-dimensional spheroid cultures. *Journal of Experimental and Clinical Cancer Research*, 38(1), 1–12. <https://doi.org/10.1186/s13046-019-1257-1>

Deng, J., Wang, E. S., Jenkins, R. W., Li, S., Dries, R., Yates, K., Chhabra, S., Huang, W., Liu, H., Aref, A. R., Ivanova, E., Paweletz, C. P., Bowden, M., Zhou, C. W., Herter-Sprue, G. S., Sorrentino, J. A., Bisi, J. E., Lizotte, P. H., Merlino, A. A., ... Wong, K. K. (2018). CDK4/6 inhibition augments antitumor immunity by enhancing T-cell activation. *Cancer Discovery*, 8(2), 216–233. <https://doi.org/10.1158/2159-8290.CD-17-0915>

Deng, L., Liang, H., Burnette, B., Beckett, M., Darga, T., Weichselbaum, R. R., & Fu, Y. X. (2014). Irradiation and anti-PD-L1 treatment synergistically promote antitumor immunity in mice. *Journal of Clinical Investigation*, 124(2), 687–695. <https://doi.org/10.1172/JCI67313>

Der, S. D., Zhou, A., Williams, B. R. G., & Silverman, R. H. (1998). Identification of genes differentially regulated by interferon  $\alpha$ ,  $\beta$ , or  $\gamma$  using oligonucleotide arrays. *Proceedings of the National Academy of Sciences of the United States of America*, 95(26), 15623–15628. <https://doi.org/10.1073/pnas.95.26.15623>

Devarakonda, S., Rotolo, F., Tsao, M. S., Lanc, I., Brambilla, E., Masood, A., Olausson, K. A., Fulton, R., Sakashita, S., McLeer-Florin, A., Ding, K., Le Teuff, G., Shepherd, F. A., Pignon, J. P., Graziano, S. L., Kratzke, R., Soria, J. C., Seymour, L., Govindan, R., & Michiels, S. (2018). Tumor mutation burden as a biomarker in resected non-small-cell lung cancer. *Journal of Clinical Oncology*, 36(30), 2995–3006. <https://doi.org/10.1200/JCO.2018.78.1963>

Dhatchinamoorthy, K., Colbert, J. D., & Rock, K. L. (2021). Cancer Immune Evasion Through Loss of MHC Class I Antigen Presentation. In *Frontiers in Immunology*

- (Vol. 12, p. 636568). Frontiers Media S.A.  
<https://doi.org/10.3389/fimmu.2021.636568>
- Dobosz, P., & Dzieciatkowski, T. (2019). The Intriguing History of Cancer Immunotherapy. In *Frontiers in Immunology* (Vol. 10, p. 2965). Frontiers Media S.A. <https://doi.org/10.3389/fimmu.2019.02965>
- Dovedi, S. J., Adlard, A. L., Lipowska-Bhalla, G., McKenna, C., Jones, S., Cheadle, E. J., Stratford, I. J., Poon, E., Morrow, M., Stewart, R., Jones, H., Wilkinson, R. W., Honeychurch, J., & Illidge, T. M. (2014). Acquired resistance to fractionated radiotherapy can be overcome by concurrent PD-L1 blockade. *Cancer Research*, 74(19), 5458–5468. <https://doi.org/10.1158/0008-5472.CAN-14-1258>
- Duan, S., Guo, W., Xu, Z., He, Y., Liang, C., Mo, Y., Wang, Y., Xiong, F., Guo, C., Li, Y., Li, X., Li, G., Zeng, Z., Xiong, W., & Wang, F. (2019). Natural killer group 2D receptor and its ligands in cancer immune escape. In *Molecular Cancer* (Vol. 18, Issue 1, pp. 1–14). BioMed Central Ltd. <https://doi.org/10.1186/s12943-019-0956-8>
- Dummer, R., Ramelyte, E., Schindler, S., Thürigen, O., Levesque, M. P., & Koelblinger, P. (2017). MEK inhibition and immune responses in advanced melanoma. *OncImmunity*, 6(8). <https://doi.org/10.1080/2162402X.2017.1335843>
- Dunn, G. P., Old, L. J., & Schreiber, R. D. (2004). The three Es of cancer immunoediting. In *Annual Review of Immunology* (Vol. 22, pp. 329–360). Annu Rev Immunol. <https://doi.org/10.1146/annurev.immunol.22.012703.104803>
- Elkrief, A., Joubert, P., Florescu, M., Tehfe, M., Blais, N., & Routy, B. (2020). Therapeutic landscape of metastatic non-small-cell lung cancer in Canada in 2020. *Current Oncology*, 27(1), 52–60. <https://doi.org/10.3747/co.27.5953>
- Elrod, H. A., & Sun, S.-Y. (2008). *Modulation of death receptors by cancer therapeutic agents inducing ligand (TRAIL) (i.e., DR4 and DR5) selectively kills cancer cells via induction of apoptosis while sparing normal cells. Thus, soluble recombinant TRAIL and agonistic antibodies to DR4 or DR5 have progressed to phase I and phase II clinical trials. Many cancer therapeutic drugs including chemotherapeutic agents.*

<https://doi.org/10.4161/cbt.7.2.5335>

- Ferlay, J., Colombet, M., Soerjomataram, I., Mathers, C., Parkin, D. M., Piñeros, M., Znaor, A., & Bray, F. (2019). Estimating the global cancer incidence and mortality in 2018: GLOBOCAN sources and methods. In *International Journal of Cancer* (Vol. 144, Issue 8, pp. 1941–1953). Wiley-Liss Inc.  
<https://doi.org/10.1002/ijc.31937>
- Finn, R. S., Crown, J. P., Lang, I., Boer, K., Bondarenko, I. M., Kulyk, S. O., Ettl, J., Patel, R., Pinter, T., Schmidt, M., Shparyk, Y., Thummala, A. R., Voytko, N. L., Fowst, C., Huang, X., Kim, S. T., Randolph, S., & Slamon, D. J. (2015). The cyclin-dependent kinase 4/6 inhibitor palbociclib in combination with letrozole versus letrozole alone as first-line treatment of oestrogen receptor-positive, HER2-negative, advanced breast cancer (PALOMA-1/TRIO-18): A randomised phase 2 study. *The Lancet Oncology*, *16*(1), 25–35. [https://doi.org/10.1016/S1470-2045\(14\)71159-3](https://doi.org/10.1016/S1470-2045(14)71159-3)
- Ford, C. (2015). *Understanding Q-Q Plots* | University of Virginia Library Research Data Services + Sciences. <https://data.library.virginia.edu/understanding-q-q-plots/>
- Forsythe, M. L., Alwithenani, A., Bethune, D., Castonguay, M., Drucker, A., Flowerdew, G., French, D., Fris, J., Greer, W., Henteleff, H., MacNeil, M., Marignani, P., Morzycki, W., Plourde, M., Snow, S., & Xu, Z. (2020). Molecular profiling of non-small cell lung cancer. *PLoS ONE*, *15*(8 August 2020).  
<https://doi.org/10.1371/journal.pone.0236580>
- Fouad, S., Wells, O. S., Hill, M. A., & D'Angiolella, V. (2019). Cullin Ring Ubiquitin Ligases (CRLs) in Cancer: Responses to Ionizing Radiation (IR) Treatment. In *Frontiers in Physiology* (Vol. 10, p. 1144). Frontiers Media S.A.  
<https://doi.org/10.3389/fphys.2019.01144>
- Galon, J., & Bruni, D. (2019). Approaches to treat immune hot, altered and cold tumours with combination immunotherapies. In *Nature Reviews Drug Discovery* (Vol. 18, Issue 3, pp. 197–218). Nature Publishing Group. <https://doi.org/10.1038/s41573-018-0007-y>

- Garcia-Beltran, W. F., Hölzemer, A., Martrus, G., Chung, A. W., Pacheco, Y., Simoneau, C. R., Rucevic, M., Lamothe-Molina, P. A., Pertel, T., Kim, T. E., Dugan, H., Alter, G., Dechanet-Merville, J., Jost, S., Carrington, M., & Altfeld, M. (2016). Open conformers of HLA-F are high-affinity ligands of the activating NK-cell receptor KIR3DS1. *Nature Immunology*, *17*(9), 1067–1074. <https://doi.org/10.1038/ni.3513>
- Garrido, F., Cabrera, T., & Aptsiauri, N. (2010). “Hard” and “soft” lesions underlying the HLA class I alterations in cancer cells: Implications for immunotherapy. In *International Journal of Cancer* (Vol. 127, Issue 2, pp. 249–256). John Wiley & Sons, Ltd. <https://doi.org/10.1002/ijc.25270>
- Garrido, G., Rabasa, A., Garrido, C., Chao, L., Garrido, F., García-Lora, ángel M., & Sánchez-Ramírez, B. (2017). Upregulation of HLA Class I Expression on Tumor Cells by the Anti-EGFR Antibody Nimotuzumab. *Frontiers in Pharmacology*, *8*(OCT), 595. <https://doi.org/10.3389/fphar.2017.00595>
- Garris, C. S., Arlauckas, S. P., Kohler, R. H., Trefny, M. P., Garren, S., Piot, C., Engblom, C., Pfirschke, C., Siwicki, M., Gungabeesoon, J., Freeman, G. J., Warren, S. E., Ong, S. F., Browning, E., Twitty, C. G., Pierce, R. H., Le, M. H., Algazi, A. P., Daud, A. I., ... Pittet, M. J. (2018). Successful Anti-PD-1 Cancer Immunotherapy Requires T Cell-Dendritic Cell Crosstalk Involving the Cytokines IFN- $\gamma$  and IL-12. *Immunity*, *49*(6), 1148-1161.e7. <https://doi.org/10.1016/j.immuni.2018.09.024>
- Garutti, M., Targato, G., Buriolla, S., Palmero, L., Minisini, A. M., & Puglisi, F. (2021). CDK4/6 Inhibitors in Melanoma: A Comprehensive Review. *Cells*, *10*(6), 1334. <https://doi.org/10.3390/cells10061334>
- Gasser, S., Orsulic, S., Brown, E. J., & Raulet, D. H. (2005). The DNA damage pathway regulates innate immune system ligands of the NKG2D receptor. *Nature*, *436*(7054), 1186–1190. <https://doi.org/10.1038/nature03884>
- Gettinger, S., Choi, J., Hastings, K., Truini, A., Datar, I., Sowell, R., Wurtz, A., Dong, W., Cai, G., Melnick, M. A., Du, V. Y., Schlessinger, J., Goldberg, S. B., Chiang, A., Sanmamed, M. F., Melero, I., Agorreta, J., Montuenga, L. M., Lifton, R., ...

- Politi, K. (2017). Impaired HLA class I antigen processing and presentation as a mechanism of acquired resistance to immune checkpoint inhibitors in lung cancer. *Cancer Discovery*, 7(12), 1420–1435. <https://doi.org/10.1158/2159-8290.CD-17-0593>
- Goel, S., Decristo, M. J., Watt, A. C., Brinjones, H., Sceneay, J., Li, B. B., Khan, N., Ubellacker, J. M., Xie, S., Metzger-Filho, O., Hoog, J., Ellis, M. J., Ma, C. X., Ramm, S., Krop, I. E., Winer, E. P., Roberts, T. M., Kim, H. J., McAllister, S. S., & Zhao, J. J. (2017). CDK4/6 inhibition triggers anti-tumour immunity. *Nature*, 548(7668), 471–475. <https://doi.org/10.1038/nature23465>
- Goldman, J. W., Mazieres, J., Barlesi, F., Koczywas, M., Dragnev, K. H., Göksel, T., Cortot, A. B., Girard, N., Wessler, C., Bischoff, H., Nadal, E., Park, K., Lu, S., Taus, A., Cobo, M., Hurt, K., Chiang, A., Hossain, A., John, W. J., & Paz-Ares, L. G. (2018). A randomized phase 3 study of abemaciclib versus erlotinib in previously treated patients with stage IV NSCLC with KRAS mutation: JUNIPER. *Journal of Clinical Oncology*, 36(15\_suppl), 9025–9025. [https://doi.org/10.1200/jco.2018.36.15\\_suppl.9025](https://doi.org/10.1200/jco.2018.36.15_suppl.9025)
- Gong, X., Li, X., Jiang, T., Xie, H., Zhu, Z., Zhou, F., & Zhou, C. (2017). Combined Radiotherapy and Anti-PD-L1 Antibody Synergistically Enhances Antitumor Effect in Non-Small Cell Lung Cancer. *Journal of Thoracic Oncology*, 12(7), 1085–1097. <https://doi.org/10.1016/j.jtho.2017.04.014>
- Grégoire, C., Chasson, L., Luci, C., Tomasello, E., Geissmann, F., Vivier, E., & Walzer, T. (2007). The trafficking of natural killer cells. In *Immunological Reviews* (Vol. 220, Issue 1, pp. 169–182). John Wiley & Sons, Ltd. <https://doi.org/10.1111/j.1600-065X.2007.00563.x>
- Groh, V., Wu, J., Yee, C., & Spies, T. (2002). Tumour-derived soluble MIC ligands impair expression of NKG2D and T-cell activation. *Nature*, 419(6908), 734–738. <https://doi.org/10.1038/nature01112>
- Gwozdowicz, S., Nestorowicz, K., Graczyk-Pol, E., Szlendak, U., Rogatko-Koros, M., Mika-Witkowska, R., Pawliczak, D., Zubala, M., Malinowska, A., Witkowska, A.,

- & Nowak, J. (2019). KIR specificity and avidity of standard and unusual C1, C2, Bw4, Bw6 and A3/11 amino acid motifs at entire HLA:KIR interface between NK and target cells, the functional and evolutionary classification of HLA class I molecules. In *International Journal of Immunogenetics* (Vol. 46, Issue 4, pp. 217–231). Blackwell Publishing Ltd. <https://doi.org/10.1111/iji.12433>
- Haines, E., Chen, T., Kommajosyula, N., Chen, Z., Herter-Sprie, G. S., Cornell, L., Wong, K. K., & Shapiro, G. I. (2018). Palbociclib resistance confers dependence on an FGFR-MAP kinase-mTOR-driven pathway in KRAS-mutant non-small cell lung cancer. *Oncotarget*, *9*(60), 31572–31589. <https://doi.org/10.18632/oncotarget.25803>
- Haque, W., Verma, V., Polamraju, P., Farach, A., Butler, E. B., & Teh, B. S. (2018). Stereotactic body radiation therapy versus conventionally fractionated radiation therapy for early stage non-small cell lung cancer. *Radiotherapy and Oncology*, *129*(2), 264–269. <https://doi.org/10.1016/j.radonc.2018.07.008>
- Hellmann, M. D., Paz-Ares, L., Bernabe Caro, R., Zurawski, B., Kim, S.-W., Carcereny Costa, E., Park, K., Alexandru, A., Lupinacci, L., de la Mora Jimenez, E., Sakai, H., Albert, I., Vergnenegre, A., Peters, S., Syrigos, K., Barlesi, F., Reck, M., Borghaei, H., Brahmer, J. R., ... Ramalingam, S. S. (2019). Nivolumab plus Ipilimumab in Advanced Non-Small-Cell Lung Cancer. *New England Journal of Medicine*, *381*(21), 2020–2031. <https://doi.org/10.1056/nejmoa1910231>
- Hellmann, M., & West, H. (2021). *Management of advanced non-small cell lung cancer lacking a driver mutation: Immunotherapy - UpToDate*. [https://www.uptodate.com/contents/management-of-advanced-non-small-cell-lung-cancer-lacking-a-driver-mutation-immunotherapy?search=non-small-cell-lung-cancer&topicRef=4607&source=see\\_link](https://www.uptodate.com/contents/management-of-advanced-non-small-cell-lung-cancer-lacking-a-driver-mutation-immunotherapy?search=non-small-cell-lung-cancer&topicRef=4607&source=see_link)
- Helmut Salih, S. R., & Rammensee, H.-G. (2021). Human Tumors by Proteolytic Shedding Cutting Edge: Down-Regulation of MICA on. *J Immunol References*, *169*, 4098–4102. <https://doi.org/10.4049/jimmunol.169.8.4098>
- Herbst, R. S., Soria, J. C., Kowanetz, M., Fine, G. D., Hamid, O., Gordon, M. S., Sosman, J. A., McDermott, D. F., Powderly, J. D., Gettinger, S. N., Kohrt, H. E. K.,

- Horn, L., Lawrence, D. P., Rost, S., Leabman, M., Xiao, Y., Mokattrin, A., Koeppen, H., Hegde, P. S., ... Hodi, F. S. (2014). Predictive correlates of response to the anti-PD-L1 antibody MPDL3280A in cancer patients. *Nature*, *515*(7528), 563–567.  
<https://doi.org/10.1038/nature14011>
- Hong, H. A., Loubser, A. S., de Assis Rosa, D., Naranbhai, V., Carr, W., Paximadis, M., Lewis, D. A., Tiemessen, C. T., & Gray, C. M. (2011). Killer-cell immunoglobulin-like receptor genotyping and HLA killer-cell immunoglobulin-like receptor-ligand identification by real-time polymerase chain reaction. *Tissue Antigens*, *78*(3), 185–194. <https://doi.org/10.1111/j.1399-0039.2011.01749.x>
- Horowitz, A., Strauss-Albee, D. M., Leipold, M., Kubo, J., Nemat-Gorgani, N., Dogan, O. C., Dekker, C. L., Mackey, S., Maecker, H., Swan, G. E., Davis, M. M., Norman, P. J., Guethlein, L. A., Desai, M., Parham, P., & Blish, C. A. (2013). Genetic and environmental determinants of human NK cell diversity revealed by mass cytometry. *Science Translational Medicine*, *5*(208), 208ra145.  
<https://doi.org/10.1126/scitranslmed.3006702>
- Hsu, J., Hodgins, J. J., Marathe, M., Nicolai, C. J., Bourgeois-Daigneault, M. C., Trevino, T. N., Azimi, C. S., Scheer, A. K., Randolph, H. E., Thompson, T. W., Zhang, L., Iannello, A., Mathur, N., Jardine, K. E., Kirn, G. A., Bell, J. C., McBurney, M. W., Raulat, D. H., & Ardolino, M. (2018). Contribution of NK cells to immunotherapy mediated by PD-1/PD-L1 blockade. *Journal of Clinical Investigation*, *128*(10), 4654–4668. <https://doi.org/10.1172/JCI99317>
- Hsu, K. C., & Dupont, B. (2005). Natural killer cell receptors: Regulating innate immune responses to hematologic malignancy. *Seminars in Hematology*, *42*(2).  
<https://doi.org/10.1053/j.seminhematol.2005.01.010>
- Hsu, K. C., Liu, X.-R., Selvakumar, A., Mickelson, E., O'Reilly, R. J., & Dupont, B. (2002). Killer Ig-Like Receptor Haplotype Analysis by Gene Content: Evidence for Genomic Diversity with a Minimum of Six Basic Framework Haplotypes, Each with Multiple Subsets. *The Journal of Immunology*, *169*(9), 5118–5129.  
<https://doi.org/10.4049/jimmunol.169.9.5118>



- Hu-Lieskovan, S., Mok, S., Homet Moreno, B., Tsoi, J., Robert, L., Goedert, L., Pinheiro, E. M., Koya, R. C., Graeber, T. G., Comin-Anduix, B., & Ribas, A. (2015). Improved antitumor activity of immunotherapy with BRAF and MEK inhibitors in BRAFV600E melanoma. *Science Translational Medicine*, 7(279).  
<https://doi.org/10.1126/scitranslmed.aaa4691>
- Hu, W., Wang, G., Huang, D., Sui, M., & Xu, Y. (2019). Cancer immunotherapy based on natural killer cells: Current progress and new opportunities. In *Frontiers in Immunology* (Vol. 10, Issue MAY, p. 1205). Frontiers Media S.A.  
<https://doi.org/10.3389/fimmu.2019.01205>
- Ifeadi, V., & Garnett-Benson, C. (2012). Sub-lethal irradiation of human colorectal tumor cells imparts enhanced and sustained susceptibility to multiple death receptor signaling pathways. *PLoS ONE*, 7(2), e31762.  
<https://doi.org/10.1371/journal.pone.0031762>
- InvivoGen. (n.d.). *Anti-PD-L1 hIgG1 N298A antibody | Atezolizumab-based*. Retrieved May 30, 2021, from <https://www.invivogen.com/anti-hpd11-higg1n298a>
- Ivarsson, M. A., Michaëlsson, J., & Fauriat, C. (2014). Activating killer cell Ig-like receptors in health and disease. In *Frontiers in Immunology* (Vol. 5, Issue APR, p. 184). Frontiers Research Foundation. <https://doi.org/10.3389/fimmu.2014.00184>
- Jonges, L. E., Giezeman-Smits, K. M., Van Vlierberghe, R. L. E., Ensink, N. G., Hagens, M., Joly, É., Eggermont, A. M. M., Van de Velde, C. J. H., Fleuren, G. J., & Kuppen, P. J. K. (2000). NK cells modulate MHC class I expression on tumor cells and their susceptibility to lysis. *Immunobiology*, 202(4), 326–338.  
[https://doi.org/10.1016/S0171-2985\(00\)80037-6](https://doi.org/10.1016/S0171-2985(00)80037-6)
- Jorgovanovic, D., Song, M., Wang, L., & Zhang, Y. (2020). Roles of IFN- $\gamma$  in tumor progression and regression: A review. In *Biomarker Research* (Vol. 8, Issue 1, pp. 1–16). BioMed Central Ltd. <https://doi.org/10.1186/s40364-020-00228-x>
- Kamiya, T., Seow, S. V., Wong, D., Robinson, M., & Campana, D. (2019). Blocking expression of inhibitory receptor NKG2A overcomes tumor resistance to NK cells.

*Journal of Clinical Investigation*, 129(5), 2094–2106.

<https://doi.org/10.1172/JCI123955>

Kamphorst, A. O., Pillai, R. N., Yang, S., Nasti, T. H., Akondy, R. S., Wieland, A., Sica, G. L., Yu, K., Koenig, L., Patel, N. T., Behera, M., Wu, H., McCausland, M., Chen, Z., Zhang, C., Khuri, F. R., Owonikoko, T. K., Ahmed, R., & Ramalingam, S. S. (2017). Proliferation of PD-1+ CD8 T cells in peripheral blood after PD-1-targeted therapy in lung cancer patients. *Proceedings of the National Academy of Sciences of the United States of America*, 114(19), 4993–4998.

<https://doi.org/10.1073/pnas.1705327114>

Kang, S. H., Keam, B., Ahn, Y. O., Park, H. R., Kim, M., Kim, T. M., Kim, D. W., & Heo, D. S. (2019). Inhibition of MEK with trametinib enhances the efficacy of anti-PD-L1 inhibitor by regulating anti-tumor immunity in head and neck squamous cell carcinoma. *OncImmunity*, 8(1).

<https://doi.org/10.1080/2162402X.2018.1515057>

Kannan, G. S., Aquino-Lopez, A., & Lee, D. A. (2017). Natural killer cells in malignant hematology: A primer for the non-immunologist. In *Blood Reviews* (Vol. 31, Issue 2, pp. 1–10). Churchill Livingstone. <https://doi.org/10.1016/j.blre.2016.08.007>

Kersh, A. E., Sasaki, M., Cooper, L. A., Kissick, H. T., & Pollack, B. P. (2016). Understanding the impact of ErbB activating events and signal transduction on antigen processing and presentation: MHC expression as a model. In *Frontiers in Pharmacology* (Vol. 7, Issue SEP). Frontiers Media S.A.

<https://doi.org/10.3389/fphar.2016.00327>

Knorr, D. A., Ni, Z., Hermanson, D., Hexum, M. K., Bendzick, L., Cooper, L. J. N., Lee, D. A., & Kaufman, D. S. (2013). Clinical-Scale Derivation of Natural Killer Cells From Human Pluripotent Stem Cells for Cancer Therapy. *STEM CELLS Translational Medicine*, 2(4), 274–283. <https://doi.org/10.5966/sctm.2012-0084>

Konjević, G. M., Vuletić, A. M., Mirjačić Martinović, K. M., Larsen, A. K., & Jurišić, V. B. (2019). The role of cytokines in the regulation of NK cells in the tumor environment. In *Cytokine* (Vol. 117, pp. 30–40). Academic Press.

<https://doi.org/10.1016/j.cyto.2019.02.001>

- Krijgsman, D., Roelands, J., Hendrickx, W., Bedognetti, D., & Kuppen, P. J. K. (2020). Hla-G: A new immune checkpoint in cancer? *International Journal of Molecular Sciences*, *21*(12), 1–11. <https://doi.org/10.3390/ijms21124528>
- Lanier, L. L., Corliss, B., Wu, J., & Phillips, J. H. (1998). Association of DAP12 with activating CD94/NKG2C NK cell receptors. *Immunity*, *8*(6), 693–701. [https://doi.org/10.1016/S1074-7613\(00\)80574-9](https://doi.org/10.1016/S1074-7613(00)80574-9)
- Lee, A. J., & Ashkar, A. A. (2018). The dual nature of type I and type II interferons. In *Frontiers in Immunology* (Vol. 9, Issue SEP, p. 2061). Frontiers Media S.A. <https://doi.org/10.3389/fimmu.2018.02061>
- Li, Y., Hermanson, D. L., Moriarity, B. S., & Kaufman, D. S. (2018). Human iPSC-Derived Natural Killer Cells Engineered with Chimeric Antigen Receptors Enhance Anti-tumor Activity. *Cell Stem Cell*, *23*(2), 181-192.e5. <https://doi.org/10.1016/j.stem.2018.06.002>
- Lin, C., Shi, X., Zhao, J., He, Q., Fan, Y., Xu, W., Shao, Y., Yu, X., & Jin, Y. (2020). Tumor Mutation Burden Correlates With Efficacy of Chemotherapy/Targeted Therapy in Advanced Non–Small Cell Lung Cancer. *Frontiers in Oncology*, *10*, 480. <https://doi.org/10.3389/fonc.2020.00480>
- Lin, M., Luo, H., Liang, S., Chen, J., Liu, A., Niu, L., & Jiang, Y. (2020). Pembrolizumab plus allogeneic NK cells in advanced non-small cell lung cancer patients. *Journal of Clinical Investigation*, *130*(5), 2560–2569. <https://doi.org/10.1172/JCI132712>
- Liu, C., Zheng, S., Jin, R., Wang, X., Wang, F., Zang, R., Xu, H., Lu, Z., Huang, J., Lei, Y., Mao, S., Wang, Y., Feng, X., Sun, N., Wang, Y., & He, J. (2020). The superior efficacy of anti-PD-1/PD-L1 immunotherapy in KRAS-mutant non-small cell lung cancer that correlates with an inflammatory phenotype and increased immunogenicity. *Cancer Letters*, *470*, 95–105. <https://doi.org/10.1016/j.canlet.2019.10.027>

- Liu, E., Marin, D., Banerjee, P., Macapinlac, H. A., Thompson, P., Basar, R., Nassif Kerbauy, L., Overman, B., Thall, P., Kaplan, M., Nandivada, V., Kaur, I., Nunez Cortes, A., Cao, K., Daher, M., Hosing, C., Cohen, E. N., Kebriaei, P., Mehta, R., ... Rezvani, K. (2020). Use of CAR-Transduced Natural Killer Cells in CD19-Positive Lymphoid Tumors. *New England Journal of Medicine*, 382(6), 545–553. <https://doi.org/10.1056/nejmoa1910607>
- Liu, L., Mayes, P. A., Eastman, S., Shi, H., Yadavilli, S., Zhang, T., Yang, J., Seestaller-Wehr, L., Zhang, S. Y., Hopson, C., Tsvetkov, L., Jing, J., Zhang, S., Smothers, J., & Hoos, A. (2015). The BRAF and MEK inhibitors dabrafenib and trametinib: Effects on immune function and in combination with immunomodulatory antibodies targeting PD-1, PD-L1, and CTLA-4. *Clinical Cancer Research*, 21(7), 1639–1651. <https://doi.org/10.1158/1078-0432.CCR-14-2339>
- Liu, Y., Liang, X., Yin, X., Lv, J., Tang, K., Ma, J., Ji, T., Zhang, H., Dong, W., Jin, X., Chen, D., Li, Y., Zhang, S., Xie, H. Q., Zhao, B., Zhao, T., Lu, J., Hu, Z. W., Cao, X., ... Huang, B. (2017). Blockade of IDO-kynurenine-AhR metabolic circuitry abrogates IFN- $\gamma$ -induced immunologic dormancy of tumor-repopulating cells. *Nature Communications*, 8(1), 1–15. <https://doi.org/10.1038/ncomms15207>
- Lo Nigro, C., Macagno, M., Sangiolo, D., Bertolaccini, L., Aglietta, M., & Merlano, M. C. (2019). NK-mediated antibody-dependent cell-mediated cytotoxicity in solid tumors: biological evidence and clinical perspectives. *Annals of Translational Medicine*, 7(5), 105–105. <https://doi.org/10.21037/atm.2019.01.42>
- Long, E. O., Sik Kim, H., Liu, D., Peterson, M. E., & Rajagopalan, S. (2013). Controlling natural killer cell responses: Integration of signals for activation and inhibition. In *Annual Review of Immunology* (Vol. 31, pp. 227–258). NIH Public Access. <https://doi.org/10.1146/annurev-immunol-020711-075005>
- Loustau, M., Anna, F., Dréan, R., Lecomte, M., Langlade-Demoyen, P., & Caumartin, J. (2020). HLA-G Neo-Expression on Tumors. *Frontiers in Immunology*, 11, 1685. <https://doi.org/10.3389/fimmu.2020.01685>
- Lu, Y., Yamauchi, N., Koshita, Y., Fujiwara, H., Sato, Y., Fujii, S., Takahashi, M., Sato,

- T., Kato, J., Yamagishi, H., & Niitsu, Y. (2001). Administration of sub-tumor regression dosage of TNF- $\alpha$  to mice with pre-existing parental tumors augments the vaccination effect of TNF gene-modified tumor through the induction of MHC class I molecule. *Gene Therapy*, 8(7), 499–507. <https://doi.org/10.1038/sj.gt.3301429>
- Lugowska, I., Kosela-Paterczyk, H., Kozak, K., & Rutkowski, P. (2015). Trametinib: A MEK inhibitor for management of metastatic melanoma. In *Oncotargets and Therapy* (Vol. 8, pp. 2251–2259). Dove Medical Press Ltd. <https://doi.org/10.2147/OTT.S72951>
- Ma, C. X., & Sparano, J. A. (2021). *Treatment approach to metastatic hormone receptor-positive, HER2-negative breast cancer: Endocrine therapy and targeted agents - UpToDate*. [https://www.uptodate.com/contents/treatment-approach-to-metastatic-hormone-receptor-positive-her2-negative-breast-cancer-endocrine-therapy-and-targeted-agents?search=palbociclib&source=search\\_result&selectedTitle=2~24&usage\\_type=default&display\\_rank=1](https://www.uptodate.com/contents/treatment-approach-to-metastatic-hormone-receptor-positive-her2-negative-breast-cancer-endocrine-therapy-and-targeted-agents?search=palbociclib&source=search_result&selectedTitle=2~24&usage_type=default&display_rank=1)
- McGranahan, N., Rosenthal, R., Hiley, C. T., Rowan, A. J., Watkins, T. B. K., Wilson, G. A., Birkbak, N. J., Veeriah, S., Van Loo, P., Herrero, J., Swanton, C., Jamal-Hanjani, M., Shafi, S., Czyzewska-Khan, J., Johnson, D., Laycock, J., Bosshard-Carter, L., Gorman, P., Hynds, R. E., ... Dessimoz, C. (2017). Allele-Specific HLA Loss and Immune Escape in Lung Cancer Evolution. *Cell*, 171(6), 1259-1271.e11. <https://doi.org/10.1016/j.cell.2017.10.001>
- Méndez, R., Rodríguez, T., Campo, A. Del, Monge, E., Maleno, I., Aptsiauri, N., Jiménez, P., Pedrinaci, S., Pawelec, G., Ruiz-Cabello, F., & Garrido, F. (2008). Characterization of HLA class I altered phenotypes in a panel of human melanoma cell lines. *Cancer Immunol Immunother*, 57, 719–729. <https://doi.org/10.1007/s00262-007-0411-3>
- Middleton, D., & Gonzelez, F. (2010). The extensive polymorphism of KIR genes. In *Immunology* (Vol. 129, Issue 1, pp. 8–19). Wiley-Blackwell. <https://doi.org/10.1111/j.1365-2567.2009.03208.x>

- Midthun, D. E. (2021). *Overview of the initial treatment and prognosis of lung cancer - UpToDate*. [https://www.uptodate.com/contents/overview-of-the-initial-treatment-and-prognosis-of-lung-cancer?search=non-small-cell-lung-cancer&source=search\\_result&selectedTitle=1~150&usage\\_type=default&display\\_rank=1#H4](https://www.uptodate.com/contents/overview-of-the-initial-treatment-and-prognosis-of-lung-cancer?search=non-small-cell-lung-cancer&source=search_result&selectedTitle=1~150&usage_type=default&display_rank=1#H4)
- Miller, J. S., Soignier, Y., Panoskaltsis-Mortari, A., McNearney, S. A., Yun, G. H., Fautsch, S. K., McKenna, D., Le, C., Defor, T. E., Burns, L. J., Orchard, P. J., Blazar, B. R., Wagner, J. E., Slungaard, A., Weisdorf, D. J., Okazaki, I. J., & McGlave, P. B. (2005). Successful adoptive transfer and in vivo expansion of human haploidentical NK cells in patients with cancer. *Blood*, *105*(8), 3051–3057. <https://doi.org/10.1182/blood-2004-07-2974>
- Minute, L., Teijeira, A., Sanchez-Paulete, A. R., Ochoa, M. C., Alvarez, M., Otano, I., Etxeberrria, I., Bolaños, E., Azpilikueta, A., Garasa, S., Casares, N., Luis Perez Gracia, J., Rodriguez-Ruiz, M. E., Berraondo, P., & Melero, I. (2020). Cellular cytotoxicity is a form of immunogenic cell death. *Journal for ImmunoTherapy of Cancer*, *8*(1), 325. <https://doi.org/10.1136/jitc-2019-000325>
- Mody, C. H., Ogbomo, H., Xiang, R. F., Kyei, S. K., Feehan, D., Islam, A., & Li, S. S. (2019). Microbial killing by NK cells. In *Journal of Leukocyte Biology* (Vol. 105, Issue 6, pp. 1285–1296). John Wiley and Sons Inc. <https://doi.org/10.1002/JLB.MR0718-298R>
- Mok, T. S. K., Wu, Y. L., Kudaba, I., Kowalski, D. M., Cho, B. C., Turna, H. Z., Castro, G., Srimuninnimit, V., Laktionov, K. K., Bondarenko, I., Kubota, K., Lubiniecki, G. M., Zhang, J., Kush, D., Lopes, G., Gomez Aubin, G., Fein, L., Kaen, D., Kowalyszyn, R., ... Kubota, K. (2019). Pembrolizumab versus chemotherapy for previously untreated, PD-L1-expressing, locally advanced or metastatic non-small-cell lung cancer (KEYNOTE-042): a randomised, open-label, controlled, phase 3 trial. *The Lancet*, *393*(10183), 1819–1830. [https://doi.org/10.1016/S0140-6736\(18\)32409-7](https://doi.org/10.1016/S0140-6736(18)32409-7)
- Montfort, A., Colacios, C., Levade, T., Andrieu-Abadie, N., Meyer, N., & Ségui, B.

- (2019). The TNF paradox in cancer progression and immunotherapy. In *Frontiers in Immunology* (Vol. 10, Issue JULY, p. 1818). Frontiers Media S.A.  
<https://doi.org/10.3389/fimmu.2019.01818>
- Moore, A. R., Rosenberg, S. C., McCormick, F., & Malek, S. (2021). Switch-II pocket Sotorasib (AMG 510) 2C07 Switch-II groove SOS interface Dimer interface RBD interface 90° 135° RAS-targeted therapies Clinical development of potential therapies for RAS-mutant tumours RAS mutational spectrum. In *Nature Reviews Drug Discovery*. <https://doi.org/10.1038/s41573-021-00220-6>
- Moradi, S., Stankovic, S., O'Connor, G. M., Pymm, P., MacLachlan, B. J., Faoro, C., Retière, C., Sullivan, L. C., Saunders, P. M., Widjaja, J., Cox-Livingstone, S., Rossjohn, J., Brooks, A. G., & Vivian, J. P. (2021). Structural plasticity of KIR2DL2 and KIR2DL3 enables altered docking geometries atop HLA-C. *Nature Communications*, *12*(1), 1–11. <https://doi.org/10.1038/s41467-021-22359-x>
- Müller, E., Christopoulos, P. F., Halder, S., Lunde, A., Beraki, K., Speth, M., Øynebråten, I., & Corthay, A. (2017). Toll-like receptor ligands and interferon- $\gamma$  synergize for induction of antitumor M1 macrophages. *Frontiers in Immunology*, *8*(OCT), 1383. <https://doi.org/10.3389/fimmu.2017.01383>
- Nersesian, S., Schwartz, S. L., Grantham, S. R., MacLean, L. K., Lee, S. N., Pugh-Toole, M., & Boudreau, J. E. (2021). NK cell infiltration is associated with improved overall survival in solid cancers: A systematic review and meta-analysis. *Translational Oncology*, *14*(1), 100930.  
<https://doi.org/10.1016/j.tranon.2020.100930>
- Nyman, J., Hallqvist, A., Lund, J. Å., Brustugun, O. T., Bergman, B., Bergström, P., Friesland, S., Lewensohn, R., Holmberg, E., & Lax, I. (2016). SPACE – A randomized study of SBRT vs conventional fractionated radiotherapy in medically inoperable stage I NSCLC. *Radiotherapy and Oncology*, *121*(1), 1–8.  
<https://doi.org/10.1016/j.radonc.2016.08.015>
- O'Donnell, J. S., L Teng, M. W., & Smyth, M. J. (2019). Cancer immunoediting and resistance to T cell-based immunotherapy. *Nature Reviews Clinical Oncology*,

16(3), 151–167. <https://doi.org/10.1038/s41571-018-0142-8>

- Ohri, N. (2017). Radiotherapy dosing for locally advanced non-small cell lung carcinoma: “MTD” or “ALARA”? In *Frontiers in Oncology* (Vol. 7, Issue SEP). Frontiers Media S.A. <https://doi.org/10.3389/fonc.2017.00205>
- Okita, R., Yukawa, T., Nojima, Y., Maeda, A., Saisho, S., Shimizu, K., & Nakata, M. (2016). MHC class I chain-related molecule A and B expression is upregulated by cisplatin and associated with good prognosis in patients with non-small cell lung cancer. *Cancer Immunology, Immunotherapy*, 65(5), 499–509. <https://doi.org/10.1007/s00262-016-1814-9>
- Orange, J. S. (2008). Formation and function of the lytic NK-cell immunological synapse. *Nature Reviews Immunology*, 8(9), 713–725. <https://doi.org/10.1038/nri2381>
- Oszmiana, A., Williamson, D. J., Cordoba, S. P., Morgan, D. J., Kennedy, P. R., Stacey, K., & Davis, D. M. (2016). The Size of Activating and Inhibitory Killer Ig-like Receptor Nanoclusters Is Controlled by the Transmembrane Sequence and Affects Signaling. *Cell Reports*, 15(9), 1957–1972. <https://doi.org/10.1016/j.celrep.2016.04.075>
- Oyer, J. L., Gitto, S. B., Altomare, D. A., & Copik, A. J. (2018). PD-L1 blockade enhances anti-tumor efficacy of NK cells. *OncImmunology*, 7(11). <https://doi.org/10.1080/2162402X.2018.1509819>
- Parham, P., Barnstable, C. J., & Bodmer, W. F. (1979). Use of a Monoclonal Antibody (W6/32) in Structural Studies of HLA-A,B,C Antigens. *The Journal of Immunology*, 123(1).
- Park, A., Yang, Y., Lee, Y., Kim, M. S., Park, Y.-J., Jung, H., Kim, T.-D., Lee, H. G., Choi, I., & Yoon, S. R. (2019). Indoleamine-2,3-Dioxygenase in Thyroid Cancer Cells Suppresses Natural Killer Cell Function by Inhibiting NKG2D and NKp46 Expression via STAT Signaling Pathways. *Journal of Clinical Medicine*, 8(6), 842. <https://doi.org/10.3390/jcm8060842>



- Park, B., Yee, C., & Lee, K. M. (2014). The effect of radiation on the immune response to cancers. In *International Journal of Molecular Sciences* (Vol. 15, Issue 1, pp. 927–943). Multidisciplinary Digital Publishing Institute (MDPI).  
<https://doi.org/10.3390/ijms15010927>
- Paul, S., & Lal, G. (2017). The molecular mechanism of natural killer cells function and its importance in cancer immunotherapy. In *Frontiers in Immunology* (Vol. 8, Issue SEP, p. 1). Frontiers Media S.A. <https://doi.org/10.3389/fimmu.2017.01124>
- Penault-Llorca, F., & Radošević-Robin, N. (2018). Tumor mutational burden in non-small cell lung cancer—the pathologist’s point of view. In *Translational Lung Cancer Research* (Vol. 7, Issue 6, pp. 716–721). AME Publishing Company.  
<https://doi.org/10.21037/tlcr.2018.09.26>
- Pende, D., Falco, M., Vitale, M., Cantoni, C., Vitale, C., Munari, E., Bertaina, A., Moretta, F., Del Zotto, G., Pietra, G., Mingari, M. C., Locatelli, F., & Moretta, L. (2019). Killer Ig-like receptors (KIRs): Their role in NK cell modulation and developments leading to their clinical exploitation. In *Frontiers in Immunology* (Vol. 10, Issue MAY, p. 1179). Frontiers Media S.A.  
<https://doi.org/10.3389/fimmu.2019.01179>
- Perea, F., Sánchez-Palencia, A., Gómez-Morales, M., Bernal, M., Concha, Á., García, M. M., González-Ramírez, A. R., Kerick, M., Martín, J., Garrido, F., Ruiz-Cabello, F., & Aptsiauri, N. (2018). HLA class I loss and PD-L1 expression in lung cancer: Impact on T-cell infiltration and immune escape. *Oncotarget*, 9(3), 4120–4133.  
<https://doi.org/10.18632/oncotarget.23469>
- Pesce, S., Greppi, M., Grossi, F., Del Zotto, G., Moretta, L., Sivori, S., Genova, C., & Marcenaro, E. (2019). PD/1-PD-Ls checkpoint: Insight on the potential role of NK cells. In *Frontiers in Immunology* (Vol. 10, Issue JUN, p. 1242). Frontiers Media S.A. <https://doi.org/10.3389/fimmu.2019.01242>
- Puccetti, P., & Grohmann, U. (2007). IDO and regulatory T cells: A role for reverse signalling and non-canonical NF- $\kappa$ B activation. In *Nature Reviews Immunology* (Vol. 7, Issue 10, pp. 817–823). Nature Publishing Group.

<https://doi.org/10.1038/nri2163>

- Ramnath, N., Tan, D., Li, Q., Hylander, B. L., Bogner, P., Ryes, L., & Ferrone, S. (2006). Is downregulation of MHC class I antigen expression in human non-small cell lung cancer associated with prolonged survival? *Cancer Immunology, Immunotherapy*, 55(8), 891–899. <https://doi.org/10.1007/s00262-005-0085-7>
- Raulet, D. H., Gasser, S., Gowen, B. G., Deng, W., & Jung, H. (2013). *Regulation of Ligands for the NKG2D Activating Receptor*. <https://doi.org/10.1146/annurev-immunol-032712-095951>
- Reits, E. A., Hodge, J. W., Herberts, C. A., Groothuis, T. A., Chakraborty, M., Wansley, E. K., Camphausen, K., Luiten, R. M., De Ru, A. H., Neijssen, J., Griekspoor, A., Mesman, E., Verreck, F. A., Spits, H., Schlom, J., Van Veelen, P., & Neefjes, J. J. (2006). Radiation modulates the peptide repertoire, enhances MHC class I expression, and induces successful antitumor immunotherapy. *Journal of Experimental Medicine*, 203(5), 1259–1271. <https://doi.org/10.1084/jem.20052494>
- Rezvani, K., & Rouce, R. H. (2015). The application of natural killer cell immunotherapy for the treatment of cancer. In *Frontiers in Immunology* (Vol. 6, Issue NOV, p. 1). Frontiers Research Foundation. <https://doi.org/10.3389/fimmu.2015.00578>
- Ribas, A. (2015). Adaptive immune resistance: How cancer protects from immune attack. In *Cancer Discovery* (Vol. 5, Issue 9, pp. 915–919). American Association for Cancer Research Inc. <https://doi.org/10.1158/2159-8290.CD-15-0563>
- Rodríguez, J. A. (2017). HLA-mediated tumor escape mechanisms that may impair immunotherapy clinical outcomes via T-cell activation (Review). In *Oncology Letters* (Vol. 14, Issue 4, pp. 4415–4427). Spandidos Publications. <https://doi.org/10.3892/ol.2017.6784>
- Roy, D. G., Geoffroy, K., Marguerie, M., Khan, S. T., Martin, N. T., Kmiecik, J., Bobbala, D., Aitken, A. S., de Souza, C. T., Stephenson, K. B., Lichty, B. D., Auer, R. C., Stojdl, D. F., Bell, J. C., & Bourgeois-Daigneault, M. C. (2021). Adjuvant oncolytic virotherapy for personalized anti-cancer vaccination. *Nature*

*Communications*, 12(1), 1–11. <https://doi.org/10.1038/s41467-021-22929-z>

Rubnitz, J. E., Inaba, H., Ribeiro, R. C., Pounds, S., Rooney, B., Bell, T., Pui, C. H., & Leung, W. (2010). NKAML: A pilot study to determine the safety and feasibility of haploidentical natural killer cell transplantation in childhood acute myeloid leukemia. *Journal of Clinical Oncology*, 28(6), 955–959. <https://doi.org/10.1200/JCO.2009.24.4590>

Ruggeri, L., Capanni, M., Urbani, E., Perruccio, K., Shlomchik, W. D., Tosti, A., Posati, S., Rogaia, D., Frassoni, F., Aversa, F., Martelli, M. F., & Velardi, A. (2002). Effectiveness of donor natural killer cell alloreactivity in mismatched hematopoietic transplants. *Science*, 295(5562), 2097–2100. <https://doi.org/10.1126/science.1068440>

Ruscetti, M., Leibold, J., Bott, M. J., Fennell, M., Kulick, A., Salgado, N. R., Chen, C. C., Ho, Y. jui, Sanchez-Rivera, F. J., Feucht, J., Baslan, T., Tian, S., Chen, H. A., Romesser, P. B., Poirier, J. T., Rudin, C. M., De Stanchina, E., Manchado, E., Sherr, C. J., & Lowe, S. W. (2018). NK cell–mediated cytotoxicity contributes to tumor control by a cytostatic drug combination. *Science*, 362(6421), 1416–1422. <https://doi.org/10.1126/science.aas9090>

Salgia, R., Pharaon, R., Mambetsariev, I., Nam, A., & Sattler, M. (2021). *The improbable targeted therapy: KRAS as an emerging target in non-small cell lung cancer (NSCLC)*. <https://doi.org/10.1016/j.xcrm.2020.100186>

Samatar, A. A., & Poulikakos, P. I. (2014). Targeting RAS-ERK signalling in cancer: Promises and challenges. In *Nature Reviews Drug Discovery* (Vol. 13, Issue 12, pp. 928–942). Nature Publishing Group. <https://doi.org/10.1038/nrd4281>

Santin, A. D., Hiserodt, J. C., Fruehauf, J., DiSaia, P. J., Pecorelli, S., & Granger, G. A. (1996). Effects of irradiation on the expression of surface antigens in human ovarian cancer. *Gynecologic Oncology*, 60(3), 468–474. <https://doi.org/10.1006/gyno.1996.0075>

Sato, H., Niimi, A., Yasuhara, T., Permata, T. B. M., Hagiwara, Y., Isono, M., Nuryadi,

- E., Sekine, R., Oike, T., Kakoti, S., Yoshimoto, Y., Held, K. D., Suzuki, Y., Kono, K., Miyagawa, K., Nakano, T., & Shibata, A. (2017). DNA double-strand break repair pathway regulates PD-L1 expression in cancer cells. *Nature Communications*, 8(1). <https://doi.org/10.1038/s41467-017-01883-9>
- Scagliotti, G. V., Bondarenko, I., Ciuleanu, T.-E., Bryl, M., Fülöp, A., Vicente, D., Bischoff, H., Hurt, K., Lu, Y., Estrem, S., Wijayawardana, S. R., Chiang, A., & Govindan, R. (2018). A randomized phase 2 study of abemaciclib versus docetaxel in patients with stage IV squamous non-small cell lung cancer (sqNSCLC) previously treated with platinum-based chemotherapy. *Journal of Clinical Oncology*, 36(15\_suppl), 9059–9059. [https://doi.org/10.1200/jco.2018.36.15\\_suppl.9059](https://doi.org/10.1200/jco.2018.36.15_suppl.9059)
- Sebastian, N. T., Xu-Welliver, M., & Williams, T. M. (2018). Stereotactic body radiation therapy (SBRT) for early stage nonsmall cell lung cancer (NSCLC): Contemporary insights and advances. In *Journal of Thoracic Disease* (Vol. 10, Issue Suppl 21, pp. S2451–S2464). AME Publishing Company. <https://doi.org/10.21037/jtd.2018.04.52>
- Sequist, L. V., & Neal, J. W. (2021). *Sotorasib: Drug information - UpToDate*. [https://www.uptodate.com/contents/sotorasib-drug-information?search=nsclc&topicRef=16538&source=see\\_link](https://www.uptodate.com/contents/sotorasib-drug-information?search=nsclc&topicRef=16538&source=see_link)
- Shaver, K. A., Croom-Perez, T. J., & Copik, A. J. (2021). Natural Killer Cells: The Linchpin for Successful Cancer Immunotherapy. *Frontiers in Immunology*, 12, 1446. <https://doi.org/10.3389/fimmu.2021.679117>
- Shaverdian, N., Lisberg, A. E., Bornazyan, K., Veruttipong, D., Goldman, J. W., Formenti, S. C., Garon, E. B., & Lee, P. (2017). Previous radiotherapy and the clinical activity and toxicity of pembrolizumab in the treatment of non-small-cell lung cancer: a secondary analysis of the KEYNOTE-001 phase 1 trial. *The Lancet Oncology*, 18(7), 895–903. [https://doi.org/10.1016/S1470-2045\(17\)30380-7](https://doi.org/10.1016/S1470-2045(17)30380-7)
- Sheard, M. A., Vojtesek Borek, Janakova Libuse, Kovarik Jan, & Zaloudik Jan. (1997). Up-regulation of Fas (CD95) in human p53 wild-type cancer cells treated with ionizing radiation. *Int. J. Cancer*, 73, 757–762.

<https://onlinelibrary.wiley.com/doi/epdf/10.1002/%28SICI%291097-0215%2819971127%2973%3A5%3C757%3A%3AAID-IJC24%3E3.0.CO%3B2-1>

Sherr, C. J., Beach, D., & Shapiro, G. I. (2016). Targeting CDK4 and CDK6: From discovery to therapy. In *Cancer Discovery* (Vol. 6, Issue 4, pp. 353–367). American Association for Cancer Research Inc. <https://doi.org/10.1158/2159-8290.CD-15-0894>

Shin, D. S., Zaretsky, J. M., Escuin-Ordinas, H., Garcia-Diaz, A., Hu-Lieskovan, S., Kalbasi, A., Grasso, C. S., Hugo, W., Sandoval, S., Torrejon, D. Y., Palaskas, N., Abril-Rodriguez, G., Parisi, G., Azhdam, A., Chmielowski, B., Cherry, G., Seja, E., Berent-Maoz, B., Shintaku, I. P., ... Ribas, A. (2017). Primary resistance to PD-1 blockade mediated by JAK1/2 mutations. *Cancer Discovery*, 7(2), 188–201. <https://doi.org/10.1158/2159-8290.CD-16-1223>

Shin, M. H., Kim, J., Lim, S. A., Kim, J., Kim, S. J., & Lee, K. M. (2020). NK cell-based immunotherapies in cancer. In *Immune Network* (Vol. 20, Issue 2). Korean Association of Immunologists. <https://doi.org/10.4110/in.2020.20.e14>

Smyth, M. J., Cretney, E., Kelly, J. M., Westwood, J. A., Street, S. E. A., Yagita, H., Takeda, K., Dommelen, S. L. H. V., Degli-Esposti, M. A., & Hayakawa, Y. (2005). Activation of NK cell cytotoxicity. In *Molecular Immunology* (Vol. 42, Issue 4 SPEC. ISS., pp. 501–510). Elsevier Ltd. <https://doi.org/10.1016/j.molimm.2004.07.034>

Song, M., Ping, Y., Zhang, K., Yang, L., Li, F., Zhang, C., Cheng, S., Yue, D., Maimela, N. R., Qu, J., Liu, S., Sun, T., Li, Z., Xia, J., Zhang, B., Wang, L., & Zhang, Y. (2019). Low-dose IFN $\gamma$  induces tumor cell stemness in tumor microenvironment of non-small cell lung cancer. *Cancer Research*, 79(14), 3737–3748. <https://doi.org/10.1158/0008-5472.CAN-19-0596>

Soriani, A., Zingoni, A., Cerboni, C., Lannitto, M. L., Ricciardi, M. R., Gialleonardo, V. Di, Cippitelli, M., Fionda, C., Petrucci, M. T., Guarini, A., Foà, R., & Santoni, A. (2009). ATM-ATR-dependent up-regulation of DNAM-1 and NKG2D ligands on multiple myeloma cells by therapeutic agents results in enhanced NK-cell

- susceptibility and is associated with a senescent phenotype. *Blood*, 113(15), 3503–3511. <https://doi.org/10.1182/blood-2008-08-173914>
- Spel, L., Boelens, J. J., Van Der Steen, D. M., Blokland, N. J. G., van Noesel, M. M., Molenaar, J. J., Heemskerk, M. H. M., Boes, M., & Nierkens, S. (2015). Natural killer cells facilitate PRAME-specific T-cell reactivity against neuroblastoma. *Oncotarget*, 6(34), 35770–35781. <https://doi.org/10.18632/oncotarget.5657>
- Stutvoet, T. S., Kol, A., de Vries, E. G. E., de Bruyn, M., Fehrmann, R. S. N., Terwisscha van Scheltinga, A. G. T., & de Jong, S. (2019). MAPK pathway activity plays a key role in PD-L1 expression of lung adenocarcinoma cells. *Journal of Pathology*, 249(1), 52–64. <https://doi.org/10.1002/path.5280>
- Tan, Y., Ci, Y., Dai, X., Wu, F., Guo, J., Liu, D., North, B. J., Huo, J., & Zhang, J. (2017). Cullin 3SPOP ubiquitin E3 ligase promotes the poly-ubiquitination and degradation of HDAC6. *Oncotarget*, 8(29), 47890–47901. <https://doi.org/10.18632/oncotarget.18141>
- Taube, J. M., Klein, A., Brahmer, J. R., Xu, H., Pan, X., Kim, J. H., Chen, L., Pardoll, D. M., Topalian, S. L., & Anders, R. A. (2014). Association of PD-1, PD-1 ligands, and other features of the tumor immune microenvironment with response to anti-PD-1 therapy. *Clinical Cancer Research*, 20(19), 5064–5074. <https://doi.org/10.1158/1078-0432.CCR-13-3271>
- Tomasetti, C., & Vogelstein, B. (2015). Variation in cancer risk among tissues can be explained by the number of stem cell divisions. *Science*, 347(6217), 78–81. <https://doi.org/10.1126/science.1260825>
- Tremante, E., Lo Monaco, E., Ingegnere, T., Sampaoli, C., Fraioli, R., & Giacomini, P. (2015). Monoclonal antibodies to HLA-E bind epitopes carried by unfolded  $\beta$ 2m-free heavy chains. *European Journal of Immunology*, 45(8), 2356–2364. <https://doi.org/10.1002/eji.201545446>
- Ueda, T., Kumagai, A., Iriguchi, S., Yasui, Y., Miyasaka, T., Nakagoshi, K., Nakane, K., Saito, K., Takahashi, M., Sasaki, A., Yoshida, S., Takasu, N., Seno, H., Uemura, Y.,

- Tamada, K., Nakatsura, T., & Kaneko, S. (2020). Non-clinical efficacy, safety and stable clinical cell processing of induced pluripotent stem cell-derived anti-glypican-3 chimeric antigen receptor-expressing natural killer/innate lymphoid cells. *Cancer Science*, *111*(5), 1478–1490. <https://doi.org/10.1111/cas.14374>
- Urosevic, M., Kurrer, M. O., Kamarashev, J., Mueller, B., Weder, W., Burg, G., Stahel, R. A., Dummer, R., & Trojan, A. (2001). Human leukocyte antigen G up-regulation in lung cancer associates with high-grade histology, human leukocyte antigen class I loss and interleukin-10 production. *American Journal of Pathology*, *159*(3), 817–824. [https://doi.org/10.1016/S0002-9440\(10\)61756-7](https://doi.org/10.1016/S0002-9440(10)61756-7)
- Vey, N., Karlin, L., Sadot-Lebouvier, S., Broussais, F., Berton-Rigaud, D., Rey, J., Charbonnier, A., Marie, D., André, P., Paturel, C., Zerbib, R., Bennouna, J., Salles, G., & Gonçalves, A. (2018). A phase 1 study of lirilumab (antibody against killer immunoglobulinlike receptor antibody KIR2D; IPH2102) in patients with solid tumors and hematologic malignancies. *Oncotarget*, *9*(25), 17675–17688. <https://doi.org/10.18632/oncotarget.24832>
- Vigliar, E., Malapelle, U., Iaccarino, A., Acanfora, G., Pisapia, P., Clery, E., De Luca, C., Bellevicine, C., & Troncone, G. (2019). PD-L1 expression on routine samples of non-small cell lung cancer: Results and critical issues from a 1-year experience of a centralised laboratory. *Journal of Clinical Pathology*, *72*(6), 412–417. <https://doi.org/10.1136/jclinpath-2019-205732>
- Vilches, C., Castaño, J., Gómez-Lozano, N., & Estefanía, E. (2007). Facilitation of KIR genotyping by a PCR-SSP method that amplifies short DNA fragments. *Tissue Antigens*, *70*(5). <https://doi.org/10.1111/J.1399-0039.2007.00923.X>
- Vivier, E., Raulet, D. H., Moretta, A., Caligiuri, M. A., Zitvogel, L., Lanier, L. L., Yokoyama, W. M., & Ugolini, S. (2011). Innate or adaptive immunity? The example of natural killer cells. In *Science* (Vol. 331, Issue 6013, pp. 44–49). NIH Public Access. <https://doi.org/10.1126/science.1198687>
- Waldman, A. D., Fritz, J. M., & Lenardo, M. J. (2020). A guide to cancer immunotherapy: from T cell basic science to clinical practice. In *Nature Reviews*

- Immunology* (Vol. 20, Issue 11, pp. 651–668). Nature Research.  
<https://doi.org/10.1038/s41577-020-0306-5>
- Wang, F., Wang, S., & Zhou, Q. (2020). The Resistance Mechanisms of Lung Cancer Immunotherapy. In *Frontiers in Oncology* (Vol. 10, p. 568059). Frontiers Media S.A. <https://doi.org/10.3389/fonc.2020.568059>
- Wang, J., Li, D., Cang, H., & Guo, B. (2019). Crosstalk between cancer and immune cells: Role of tumor-associated macrophages in the tumor microenvironment. In *Cancer Medicine* (Vol. 8, Issue 10, pp. 4709–4721). Blackwell Publishing Ltd.  
<https://doi.org/10.1002/cam4.2327>
- Watson, N. F. S., Ramage, J. M., Madjd, Z., Spendlove, I., Ellis, I. O., Scholefield, J. H., & Durrant, L. G. (2006). Immunosurveillance is active in colorectal cancer as downregulation but not complete loss of MHC class I expression correlates with a poor prognosis. *International Journal of Cancer*, *118*(1), 6–10.  
<https://doi.org/10.1002/ijc.21303>
- Weart, T. C., Miller, K. D., & Simone, C. B. (2018). Spotlight on dabrafenib/trametinib in the treatment of non-small-cell lung cancer: Place in therapy. In *Cancer Management and Research* (Vol. 10, pp. 647–652). Dove Medical Press Ltd.  
<https://doi.org/10.2147/CMAR.S142269>
- Wu, H.-X., Wang, Z.-X., Zhao, Q., Chen, D.-L., He, M.-M., Yang, L.-P., Wang, Y.-N., Jin, Y., Ren, C., Luo, H.-Y., Wang, Z.-Q., & Wang, F. (2019). Tumor mutational and indel burden: a systematic pan-cancer evaluation as prognostic biomarkers. *Annals of Translational Medicine*, *7*(22), 640–640.  
<https://doi.org/10.21037/atm.2019.10.116>
- Wu, J., Cherwinski, H., Spies, T., Phillips, J. H., & Lanier, L. L. (2000). DAP10 and DAP12 form distinct, but functionally cooperative, receptor complexes in natural killer cells. *Journal of Experimental Medicine*, *192*(7), 1059–1067.  
<https://doi.org/10.1084/jem.192.7.1059>
- Xu, X., Fu, X.-Y., Plate, J., & Chong, A. S.-F. (1998). IFN- $\gamma$  Induces Cell Growth



Inhibition by Fas-mediated Apoptosis: Requirement of STAT1 Protein for Up-Regulation of Fas and FasL Expression. *Cancer Research*, 58(13).

Yang, G., Kong, Q., Wang, G., Jin, H., Zhou, L., Yu, D., Niu, C., Han, W., Li, W., & Cui, J. (2014). Low-dose ionizing radiation induces direct activation of natural killer cells and provides a novel approach for adoptive cellular immunotherapy. *Cancer Biotherapy and Radiopharmaceuticals*, 29(10), 428–434.

<https://doi.org/10.1089/cbr.2014.1702>

Yang, G., Li, W., Jiang, H., Liang, X., Zhao, Y., Yu, D., Zhou, L., Wang, G., Tian, H., Han, F., Cai, L., & Cui, J. (2016). Low-dose radiation may be a novel approach to enhance the effectiveness of cancer therapeutics. In *International Journal of Cancer* (Vol. 139, Issue 10, pp. 2157–2168). Wiley-Liss Inc.

<https://doi.org/10.1002/ijc.30235>

Yano, T., Sugio, K., Yamazaki, K., Kase, S., Yamaguchi, M., Ondo, K., & Sugimachi, K. (2000). Direct IFN $\gamma$  influence of interferon- $\gamma$  on proliferation and cell-surface antigen expression of non-small cell lung cancer cells. *Lung Cancer*, 30(3), 169–174.

[https://doi.org/10.1016/S0169-5002\(00\)00136-7](https://doi.org/10.1016/S0169-5002(00)00136-7)

Yie, S. mian, Yang, H., Ye, S. rong, Li, K., Dong, D. dan, & Lin, X. mei. (2007). Expression of human leucocyte antigen G (HLA-G) is associated with prognosis in non-small cell lung cancer. *Lung Cancer*, 58(2), 267–274.

<https://doi.org/10.1016/j.lungcan.2007.06.011>

Yu, J., Yan, J., Guo, Q., Chi, Z., Tang, B., Zheng, B., Yu, J., Yin, T., Cheng, Z., Wu, X., Yu, H., Dai, J., Sheng, X., Si, L., Cui, C., Bai, X., Mao, L., Lian, B., Wang, X., ... Kong, Y. (2019). Genetic aberrations in the CDK4 pathway are associated with innate resistance to PD-1 blockade in Chinese patients with non-cutaneous melanoma. *Clinical Cancer Research*, 25(21), 6511–6523.

<https://doi.org/10.1158/1078-0432.CCR-19-0475>

Zamai, L., Del Zotto, G., Buccella, F., Gabrielli, S., Canonico, B., Artico, M., Ortolani, C., & Papa, S. (2020). Understanding the Synergy of NKp46 and Co-Activating Signals in Various NK Cell Subpopulations: Paving the Way for More Successful

- NK-Cell-Based Immunotherapy. *Cells*, 9(3). <https://doi.org/10.3390/cells9030753>
- Zhang, J., Bu, X., Wang, H., Zhu, Y., Geng, Y., Nihira, N. T., Tan, Y., Ci, Y., Wu, F., Dai, X., Guo, J., Huang, Y. H., Fan, C., Ren, S., Sun, Y., Freeman, G. J., Sicinski, P., & Wei, W. (2018). Cyclin D-CDK4 kinase destabilizes PD-L1 via cullin 3-SPOP to control cancer immune surveillance. *Nature*, 553(7686), 91–95. <https://doi.org/10.1038/nature25015>
- Zhou, L., Zhang, X., Li, H., Niu, C., Yu, D., Yang, G., Liang, X., Wen, X., Li, M., & Cui, J. (2018). Validating the pivotal role of the immune system in low-dose radiation-induced tumor inhibition in Lewis lung cancer-bearing mice. *Cancer Medicine*, 7(4), 1338–1348. <https://doi.org/10.1002/cam4.1344>
- Zhou, X., & Sun, S. C. (2021). Targeting ubiquitin signaling for cancer immunotherapy. In *Signal Transduction and Targeted Therapy* (Vol. 6, Issue 1, pp. 1–15). Springer Nature. <https://doi.org/10.1038/s41392-020-00421-2>